SEISMIC EVALUATION AND RETROFIT ASSESSMENT OF MULTI STOREY STRUCTURES USING PUSHOVER ANALYSIS (POA)

BY

MUHAMMAD AJMAL

A Thesis Presented to the
DEANSHIP OF GRADUATE STUDIES

KING FAHD UNIVERSITY OF PETROLEUM & MINERALS

DHAHRAN, SAUDI ARABIA

In Partial Fulfillment of the
Requirements for the Degree of

MASTER OF SCIENCE

In

CIVIL ENGINEERING

SEPTEMBER, 2012

KING FAHD UNIVERSITY OF PETROLEUM & MINERALS

DHAHRAN- 31261, SAUDI ARABIA

DEANSHIP OF GRADUATE STUDIES

This thesis, written by **MUHAMMAD AJMAL** under the direction his thesis advisor and approved by his thesis committee, has been presented and accepted by the Dean of Graduate Studies, in partial fulfillment of requirements for the degree of **MASTER OF SCIENCE IN CIVIL ENGINEERING.**

Dr. Mohammed H.Baluch
(Advisor)

Dr. Nedal A. Ratrout
Department Chairman
26 DEC 2012

for. Dr. Muhammad K.Rahman
(Co-Advisor) 26 DEC 2012

Dr. Salam A. Zummo
Dean of Graduate Studies

Dr. Ali H. Al-Gadhib
(Member)

30/12/12
Date

Dr. Hussain J. Al-Gahtani
(Member)

Dr. Al Farabi M. Sharif
(Member)

To my respected parents, teachers and friends whose utmost love, care and effort against all odds brought me to this height of knowledge and to those who always pray for my success in life and to those from whom I have learnt so much throughout my career with the blessings of Almighty Allah

ACKNOWLEDGMENTS

In the name of Almighty ALLAH, the Most Beneficent and the Most Merciful

First and the foremost, I thank Allah (subhana wataala) who has bestowed health, and knowledge to complete this study. Peace and blessing of Allah be upon His holy Prophet (Salallahu alahi wasallam). I acknowledge KFUPM for the support extended towards my research through its remarkable facilities and for providing me the opportunity to pursue graduate studies.

I acknowledge, with deep gratitude and appreciation, the inspiration, encouragement, valuable time and guidance given to me by Prof. M. H. Baluch, who served me as thesis advisor. This work was completed due to his guidance and personal involvement in this study. His valuable suggestions and useful discussions made this work interesting and raised my comfort and confidence level.

I am deeply indebted and grateful to Dr. Muhammad Kalimur Rahman, my co-advisor, for his extensive guidance, continuous support, and personal involvement throughout my study. I would have never accomplished this study without the valuable suggestions and the support given by him.

I am also grateful to my Committee Members, Dr. Ali H. Al-Gadhib, Dr. Hussain J. Al-Gahtani and Dr. Al-Farabi M. Sharif, for their constructive guidance, valuable advices and cooperation.

I would like to express my deepest gratitude to my beloved parents for having faith in me and all my family members for their love, moral support, prayers and encouragement throughout my life.

I am also thankful to my friend Danish Ahmed, Ahmed Zubair and all my friends for their encouragement, support and prayers.

Special thanks are due to Dr. Zekai Celep, Dr. Alper Ilki, Cem Demir, Mustafa Comert and all students at Istanbul Technical University (ITU) for their guidance and support during this study.

TABLE OF CONTENTS

LIST OF TABLES

LIST OF FIGURES

ABSTRACT

Full Name : Muhammad Ajmal

Thesis Title : Seismic Evaluation and Retrofit Assessment of Multi Storey Structures Using Pushover Analysis(POA)

Major Field : Civil Engineering (Structures)

Date of Degree : September,2012

Recent awareness of a potential seismic event in low to moderate seismicity regions of Saudi Arabia have led to concerns of safety and vulnerability of reinforced concrete buildings, in which ductile detailing has not been provided explicitly in the design process. Most of buildings design in Saudi Arabia are based on gravity load and wind load and their behavior may be non-ductile during a seismic activity which may cause damage to life as well as economy.

The aim of this study entitled, **'Seismic Evaluation And Retrofit Assessment Of Multi Storey Structures Using Pushover Analysis',** is to gain insight into the behavior of reinforced concrete frames designed without seismic consideration and subjected to moderate seismic action using pushover technique . The main objectives of this study were to investigate the behavior of non-seismically designed existing reinforced concrete frames and to assess the influence of different retrofitting schemes on seismic resistance using pushover analysis.

In this study, a typical existing reinforced concrete frame of building in Madinah was selected for which pushover analysis was carried out using nonlinear finite element

structural analysis and design software SAP2000. This study lead to estimate (1) the relation between the lateral forces and deformations during the inelastic behavior of the structure (2) estimation of the inter-storey drifts (3) formation of hinge and sequence of yielding of members (4) capacity of structure (5) estimation of base shear capacity and roof displacement. Based on the formation of hinges in a pushover analysis of typical existing RC frame, suitable retrofitting schemes were appended to the structure and parametric studies were conducted using pushover analysis.

ملخص الرسالة

الاسم الكامل: محمد أجمل

عنوان الرسالة: تقييم الزلزالي وتقييم الهياكل التحديثية ستوري موضوع باستخدام التحليل بالدفع المتتالي (POA)

الرئيسية الميدانية: الهندسة المدنية (الهياكل)

تاريخ الدرجة: سبتمبر، 2012

وقد أدت الوعي مؤخرا الحدث الزلزالي المحتملة في مناطق منخفضة إلى معتدلة الزلزالية للمملكة العربية السعودية مخاوف من سلامة المباني وضعف الخرسانة المسلحة، والتي لم يتم الدكتايل بالتفصيل المنصوص عليها صراحة في عملية التصميم. وتستند معظم المباني تصميم في المملكة العربية السعودية على تحميل الجاذبية والرياح وتحميل سلوكهم قد يكون غير قابل للسحب خلال النشاط الزلزالي الذي قد يسبب الضرر في الحياة وكذلك الاقتصاد.

والهدف من هذه الدراسة بعنوان "تقييم الزلزالي وتقييم الهياكل التحديثية ستوري موضوع استخدام تحليل المهمة اليسيرة، هو التبصر في سلوك إطارات مصممة الخرسانة المسلحة دون النظر الزلزالية وتعرض الى معتدلة العمل الزلزالية باستخدام تقنية مهمة سهلة. وكانت الأهداف الرئيسية لهذه الدراسة للتحقيق في سلوك غير مصممة زلزاليا إطارات المسلحة القائمة وملموسة لتقييم تأثير التعديل التحديثي مخططات مختلفة على مقاومة الزلازل باستخدام التحليل مهمة سهلة.

في هذه الدراسة، تم اختيار القائمة المسلحة نموذجية ملموسة لبناء الإطار في المدينة المنورة التي تم إجراء تحليل مهمة سهلة خارج باستخدام تحليل العناصر المحدودة غير الخطية وهيكلية تصميم البرمجيات SAP2000. هذا الاعلان الدراسة لتقدير (1) العلاقة بين القوى الجانبية وتشوهات خلال السلوك غير مرن للهيكل (2) تقدير الانجرافات بين الطوابق (3) تشكيل وتسلسل مفصل على إنتاج أفراد (4) قدرة هيكل (5) تقدير قدرة القص قاعدة والتشريد السطح. استنادا إلى تشكيل يتوقف في تحليل الإطار النموذجي للمهمة سهلة RC القائمة، وإلحاق خطط مناسبة لإعادة تجهيز هيكل وأجريت دراسات باستخدام التحليل حدودي مهمة سهلة.

CHAPTER 1

INTRODUCTION

1.1 Prologue

The seismic assessment and design of structures is required because of the occurrence of earthquakes. Earthquakes are caused by differential movements of the earth's crust (Kramer 1996).The result of these movements is the well-known 'ground shaking' that can lead to significant damage and/or collapse of buildings, infrastructure systems.

Recent destructive earthquakes such as the 1995 Hyogo-ken-Nanbu earthquake in Japan, the 1999 Kocaeli earthquake in Turkey, the 2005 Kashmir earthquake in Pakistan, the 2010 earthquake in Chile and Haiti have shown deficiency in structures. To tackle these deficiencies performance-based earthquake engineering has been introduced. In brief, performance based engineering deals with the estimation of quantities such as seismic capacity and seismic demands for different performance levels of the structure. Generally, the methods available to the design engineer to calculate seismic demands are either dynamic time history analyses or pushover analyses.

Dynamic time history analysis requires as much as possible detailed mathematical models of multi-degree-of-freedom systems, MDOF, i.e. structures, together with

information on ground motion characteristics, rendering it quite impractical for everyday use, especially when overly complex structures need to be considered. Additionally the response derived from such an analysis is generally very sensitive to the characteristics of the ground motions as well as the material models used.

A simpler option to assess the performance of structures is pushover analysis or simplified nonlinear static analysis, even though this also requires as much as possible detailed mathematical models of MDOF systems. The method's applicability is increasing continuously in practice because of its relative simplicity. This method assumes that the response of a structure can be predicted by the first, or the first few modes of vibration, which remain constant throughout its response time. It involves the incremental application of loading that follows some predetermined pattern, until the failure modes of the structure can be identified, thus producing a force-displacement relationship or capacity curve, which gives a clear indication of the nonlinear response. The resulting displacement demands from the preceding analysis are then checked and the structural performance of the elements is assessed.

Pushover analysis is included in different codes e.g. in USA (ATC-55, 2005; ASCE, 2007; FEMA, 2000), in Japan (BCJ, 2009), in Europe (CEN, 2004) and in Turkey (MPWS, 2007). Pushover analysis can excess real force acting on brittle elements, identify failure mechanism of the structure, estimate inter-storey drifts, formation of hinge and sequence of yielding of members, capacity of structure.

1.2 Seismicity of Saudi Arabia

The Arabian Peninsula is frequently strike by earthquake in past few years and the north, east and western border of this region is near to seismic active zone. The Arabian plate includes Yemen, some part of Iran, Syria and Gulf states strikes with the Turkish plate i.e. mountains of Anatolia and Iranian Plate i.e. Zagros mountains. This strike causes movement of Arabian plate by 2 centimeters every year which causes expansion in Red Sea and produces friction between two plates of Arabian plate in eastern region.

This is near the Afar Triple Junction as shown in Figure 1.1, which includes three divergent boundaries, one tearing the African continent apart, one moving the Saudi Peninsula away from Africa, and one moving the Indian Ocean and islands away from Africa. Jeddah is near the Red Sea fault which is right in the middle and rides along the Red Sea. Not too many strong earthquakes from the Red Sea fault do much damage in Jeddah, so their building codes are pretty slack.

Figure 1.1: Afar Triple Junctions

At the triple junction, the Earth's crust is slowly being ripped apart as shown in Figure 1.2. This causes continuous earthquakes and fissures hundreds of meters long and deep appearing in the ground.

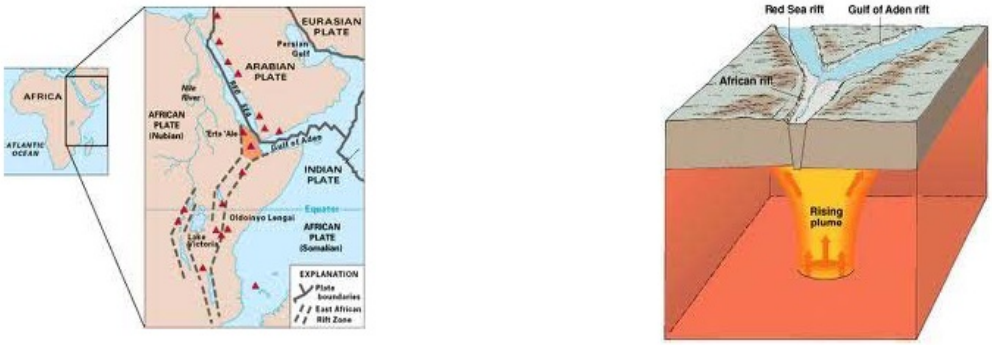

Figure 1.2: Triple Junction Ripped due to Earthquakes and Fissures

In late 2005, 163 earthquakes of magnitudes greater than 4 ML were recorded. The epicenter of the quake was right next to Jeddah about 70 kilometers off of the coast as shown in Figure 1.3.

Figure 1.3: Epicenter near Jeddah

The quake was only a 5.5 on the Richter scale, but it lasted for 2 minutes which is what caused all the destruction. The primary waves lasted the longest: 1 whole minute. The secondary waves and the surface waves each lasted 30 seconds.

In 2005 Saudi Geological Survey was assigned to monitor seismic activity in the region by Saudi cabinet. The Saudi Geological Survey includes the centers affiliated to King Abdul Aziz City for Science and Technology, King Saud University, King Abdul Aziz University, and King Fahd University for Petroleum and Minerals.

In 2007 Saudi Building code (SBC 301) committee decided to divide The Kingdom of Saudi Arabia into seven seismic regions as shown in Figure 1.4.

Figure 1.4: Seismic Zones of Saudi Arabia (SBC 301)

All large cities in western province which includes region 3 and 6 as well as eastern province which includes region 2 and 5 are located close to fault zones. As the population increases and new areas are developed, the seismic risk to human life and infrastructure increases in these region of Saudi Arabia.

1.3 Problem Statement

Recent awareness of a potential seismic events in low to moderate seismicity regions of Saudi Arabia such as Otaibah, Makkah (2005), Haradh, Eastern Province (2006) , Al-Hadama, Al-Amid, Al-Qarasa and Yanbu (2009), Eastern Province (August,2010) have led to concerns of safety and vulnerability of reinforced concrete buildings, in which ductile detailing has not been provided explicitly in the design process. Structures built majority in Saudi Arabia are designed primarily for combination of gravity and wind loads and are not able to resist seismic loading.

Gravity load designed (GLD) RC frames in Saudi Arabia have limited lateral load resistance and are susceptible to column-side sway or soft-story mechanisms under earthquake effects. In some cases, for relatively taller buildings in Saudi Arabia the design may have considered lateral forces due to wind loads, it is still important to carry out a complete seismic evaluation, since higher mode effects sometimes lead to soft-story mechanisms in the mid to upper levels of the building.

Also Non ductile detailing practice employed in these structures makes them prone to potential damage and failure during earthquake. Therefore during an unexpected seismic

activity the response of such structures inherited by the ductility and factor of safety provided. Hence the evaluation of seismic performance of the structures in Saudi Arabia is of interest.

This study has resulted in the development of a research collaboration between KFUPM and Istanbul Technical University (ITU) in Earthquake Engineering and it involves the study of non-linear behavior of the structures in Saudi Arabia when prone to moderate seismic earthquake using Pushover technique and focuses on the realistic demand of lateral forces and deformations required during inelastic behavior, estimation of the inter-storey drifts, formation of hinge and sequence of yielding of members, capacity of structure, estimation of base shear capacity and roof displacement.

1.4 Objectives

The main objective of this study is to gain insight into the behavior of typical detailed reinforced concrete frames constructed in a seismically active western region of Saudi Arabia subjected to moderate earthquake using pushover technique. It aims to encourage the inclusion of performance-based concepts in Saudi Arabia building code so that the current design practice consulting offices adopt pushover analysis on a regular basis. Basically, the objectives of this study are:

1. To assess the seismic vulnerability of an existing reinforced concrete building in Madinah, Saudi Arabia by selecting a typical shear wall frame using pushover analysis.

2. To identify the formation of plastic hinges and failure mechanism in the typical building under the expected design earthquake load.

3. To investigate various retrofitting schemes to enhance the seismic resisting capacity.

4. To propose various retrofitting strategies and investigate the performance by non-linear pushover analysis.

2. CHAPTER 2

LITERATURE REVIEW

2.1 Introduction

The static pushover analysis method, POA, has no strict theoretical base. It is mainly based on the assumption that the response of the structure is controlled by the first mode of vibration and mode shape, or by the first few modes of vibration, and that this shape remains constant throughout the elastic and inelastic response of the structure. This provides the basis for transforming a dynamic problem to a static problem.

Pushover analysis is included in different codes e.g. in USA (ATC-55, 2005; ASCE, 2007; FEMA, 2000), in Japan (BCJ, 2009), in Europe (CEN, 2004) and in Turkey (MPWS, 2007). Pushover analysis can excess real force acting on brittle elements, identify failure mechanism of the structure, estimate inter-storey drifts, formation of hinge and sequence of yielding of members, capacity of structure. Further explanation of pushover analysis, its development and research carried by researcher is explained in the following sections.

2.2 Pushover Analysis

Pushover analysis is an incremental static analysis used to determine the force-displacement relationship, or capacity curve for a structure or structural element. The analysis involves applying horizontal loads, in a prescribed pattern, to a structural model. The load is increased incrementally by pushing the structure. After few steps members start yielding. Then the structural model is modified according to nonlinear load deformation diagrams of members that results in a reduced global stiffness of the overall structure. The procedure is continued until the structure reaches a limit or collapse state. Then the structure capacity is determined by plotting roof displacement and base shear. Pushover curves as shown in Figure 2.1.

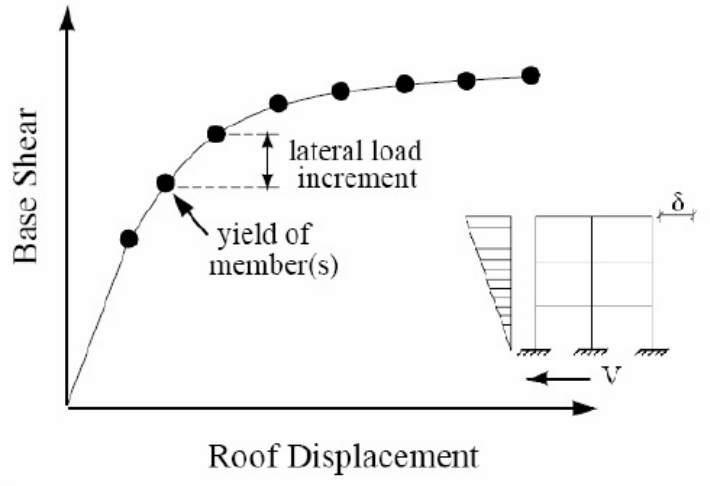

Figure 2.1: Typical Pushover Curve of a Structure

In the literature, two types of pushover analysis exist which are force controlled and displacement controlled. Force controlled pushover procedure should be used when the load is known such as gravity loading. On the other hand, pushover analysis is performed

as a displacement-controlled proposed by Allahabadi (1987). The magnitude of load combination is increased until control displacement reaches a specified value. All internal forces and deformations are computed at the target displacement level. Krawinkler and Seneviratna (1998) state that the pushover analysis is a very powerful tool to show the response of structure which cannot be visualized by elastic or dynamic analysis. Pushover analysis also exposes design weaknesses that may remain hidden in an elastic analysis [1].

Although pushover analysis has several advantages over elastic analysis procedures, this procedure has some limitations that affect the accuracy of results such as a torsional effect in buildings, estimate of target displacement, selection of lateral load patterns and identification of failure mechanisms due to higher modes of vibration.

In the pushover analysis, target displacement can be estimated as the displacement demand for the corresponding equivalent SDOF domain through the use of a shape vector and equation (Lawson et al 1994). The roof displacement at mass centre of the structure is used as target displacement. Moreover, hysteretic characteristics of MDOF systems should be incorporated into the equivalent SDOF model if displacement demand is affected from stiffness degradation or pinching, strength deterioration and P-Δ effects.

2.3 Conventional Pushover Analysis Methods

There are three Conventional POA methods which are adopted by FEMA. These methods are:

- Capacity spectrum Method
- Displacement Coefficient Method
- Modal Pushover Analysis

2.3.1 Capacity Spectrum Method

A nonlinear static analysis procedure that provides a graphical representation of the expected seismic performance of the existing or retrofitted structure by the intersection of the structure's capacity spectrum with a response spectrum (demand spectrum) representation of the earthquake's displacement demand on the structure. The intersection is the performance point and the displacement coordinate of the performance point is the estimated displacement demand on the structure for the specified level of seismic hazard [3, 5]. The proposed procedure consists of following steps:

1. Obtain pushover curve for MDOF system

2. Idealize the capacity curve as a bilinear.

3. Convert the idealized curve to acceleration displacement response spectrum (ADRS) format; obtain the capacity diagram as shown in Figure 2.2, by using Eqs. 2.1 and 2.2.

$$S_a = \frac{\left(\frac{V}{W}\right)}{\alpha_1} \tag{2.1}$$

where

S_a is spectral acceleration (m/s^2)

W is weight of the building

V is base shear (kN)

α_1 is the modal mass participation ratio for first mode

$$S_d = \frac{u_r}{\Gamma_1 \Phi_{r1}} \tag{2.2}$$

where

S_d is spectral displacement (m),Φ_{r1} is first mode shape function roof level amplitude value,Γ_1 is fundamental mode modal amplification factor and u_r is roof displacement (m)

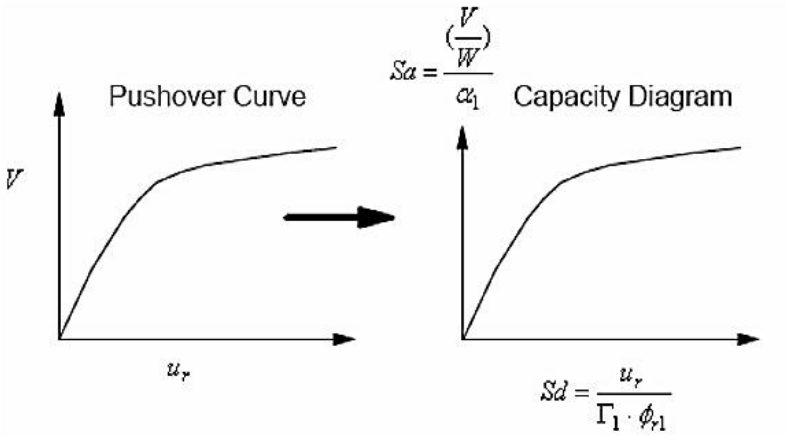

Figure 2.2: Capacity Spectrum obtained from Pushover curve

4. Obtain elastic and inelastic response spectra for 5% damping and various ductility levels in ADRS format as shown in Figure 2.3.

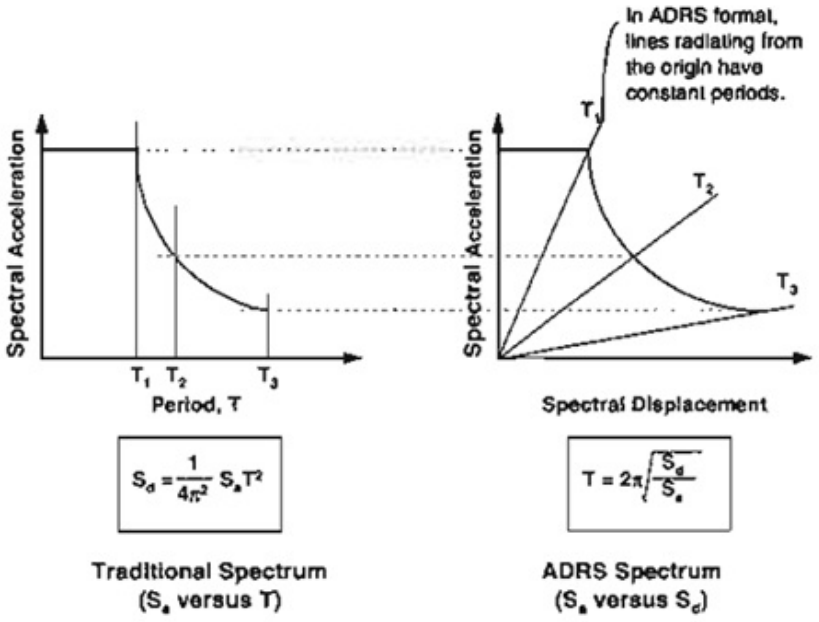

Figure 2.3: Conversion of Traditional Spectrum to ADRS Spectrum (ATC-40)

Then plot on the same graph capacity and demand curves as shown in Figure 2.4.

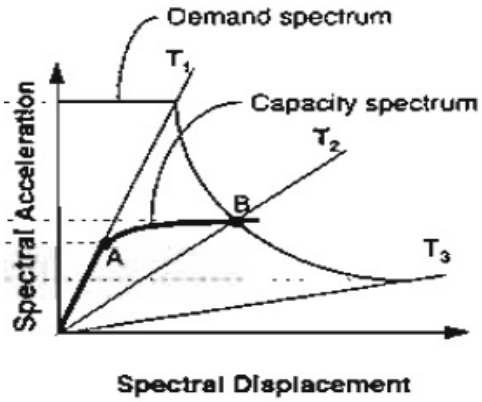

Figure 2.4: Capacity Spectrum and Demand Spectrum plotted on same graph (ATC-40)

5. Compute the ductility value at each intersection point on capacity and demand curves. When the calculated ductility is equal to the ductility of the inelastic demand curve, that intersection point also called performance point is selected as inelastic displacement demand of the equivalent SDOF system as shown in Figure 2.5.

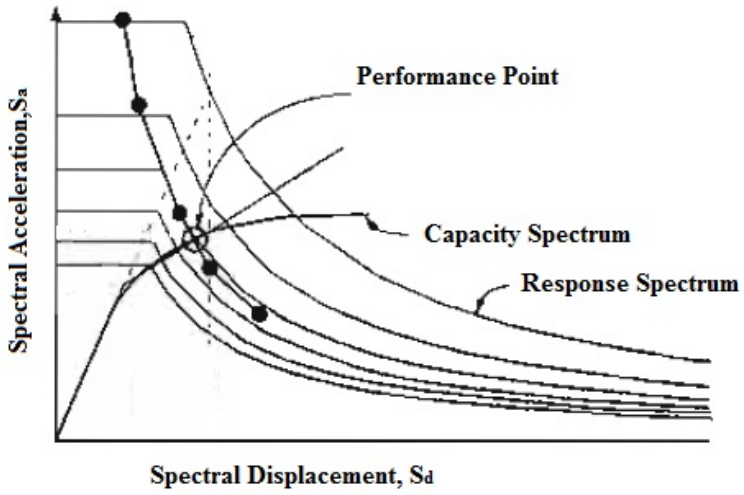

Figure 2.5: Performance point using Capacity Spectrum Method (ATC-40)

6. Convert the inelastic displacement demand of the equivalent SDOF system to response of MDOF system by using Eq.2.3.

$$u_r = S_d \Gamma_1 \Phi_{r1} \qquad (2.3)$$

2.3.2 Displacement Coefficient Method

The displacement coefficient method provides a direct numerical process for calculating the displacement demand. It does not require converting the capacity curve to spectral coordinates. The coefficient method is used for the calculation of target displacement, δ_t [3, 5]. Brief description of this procedure is given below.

1. Construct a bilinear representation of the capacity curve as shown in Figure 2.6.

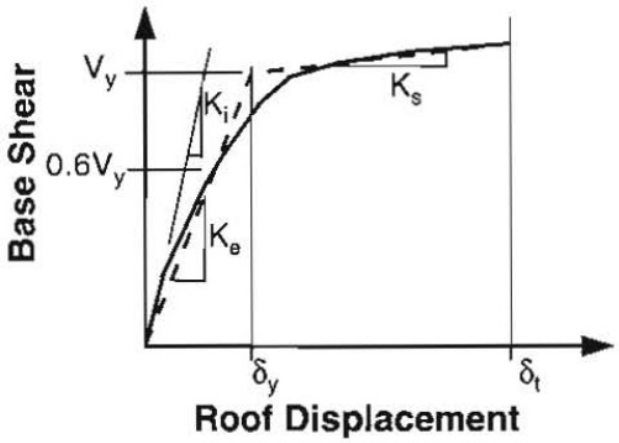

Figure 2.6: Bilinear Representation of Pushover curve (ATC-40)

2. Calculate the effective time period by using Eq.2.4

$$T_e = T_i\sqrt{\frac{K_i}{K_e}} \tag{2.4}$$

where,

T_e is the effective fundamental period (sec).

T_i is the elastic fundamental period (sec).

K_i is the elastic lateral stiffness of the structure.

K_e is the effective lateral stiffness of the structure.

3. Calculate the target displacement by using Eqs.2.5 and 2.6

$$\delta_t = C_0.C_1.C_2.C_3.S_d \tag{2.5}$$

$$S_d = \frac{S_a T_e^2 g}{4\pi^2} \tag{2.6}$$

In Equation 2.5, δ_t is the estimated maximum inelastic displacement of the control node. S_d is the elastic spectral displacement corresponding to the period T_e for the considered ground motion.

C_0, C_1, C_2 and C_3 are the coefficients that modify the elastic spectral displacement. These coefficients are explained below.

C_0: Modification factor to relate spectral displacement to the MDOF system control node displacement. Multiplication of first mode participation factor with the amplitude of the first mode vector at the control node level is used as C_0.

C_1: Modification factor to relate expected maximum inelastic displacements to displacements calculated from linear elastic spectral responses.

$$C_1 = \left(1.0 \text{ fo } T_e \geq T_s\right) \tag{2.7}$$

$$C_1 = \frac{1.0 + \frac{(R-1).T_s}{T_e}}{R} \text{ for } T_e < T_s \tag{2.8}$$

$$R = \frac{S_a C_m}{\left(\frac{V_y}{W}\right)} \tag{2.9}$$

where,

S_a is response spectrum acceleration, at the effective fundamental period and damping ratio of the system in the direction under consideration.

R is ratio of elastic strength demand to calculated yield strength.

T_s is the characteristic period of the response spectrum, defined as the period associated with the transition from the constant acceleration segment to constant velocity segment of the spectrum.

V_y is the yield strength calculated using the results of the nonlinear static procedure for idealized nonlinear force- deformation curve for the system.

C_m is the effective modal mass calculated for fundamental mode using Eigenvalues analysis.

W is the weight of the structure.

C_2: Modification factor to represent the effect of pinched hysteretic shape, stiffness degradation and strength degradation on maximum displacement response.

C_3: Modification factor to represent increased displacements due to P-Δ effects. C_3 is accepted as 1 in this study, since P-Δ effects are not considered.

$$C_3 = 1.0 + \frac{|\alpha|.(R-1)^{1.5}}{T_e} \tag{2.10}$$

where,

α is ratio of post yield stiffness to effective elastic stiffness as shown in Figure 2.7.

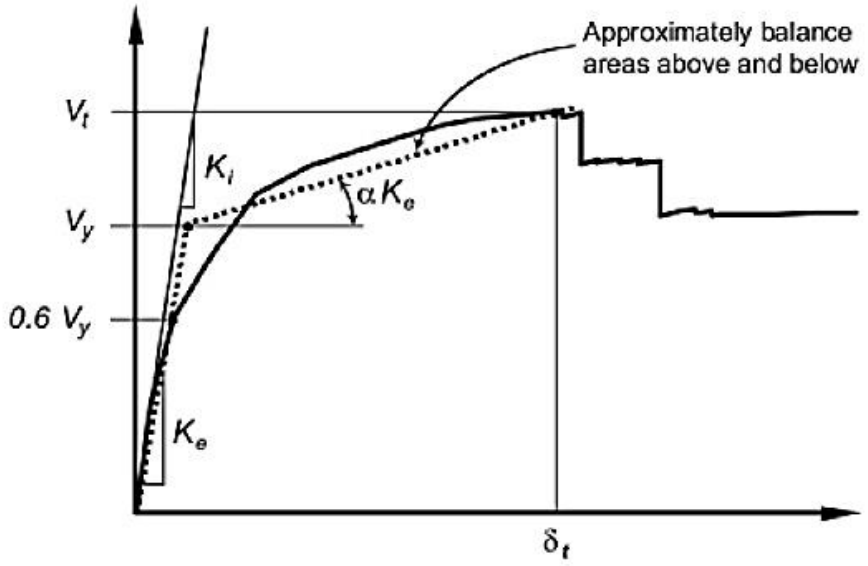

Figure 2.7: Idealization of Pushover Curve (FEMA-356)

2.3.3 Modal Pushover Analysis (MPA)

Modal Pushover Analysis (MPA) was proposed by Chopra and Goel in 2001. Their principle objective was to develop an improved analysis procedure based on the structural dynamics theory that has conceptual and computational simplicity with constant load pattern [3, 5]. The MPA procedure is summarized in a sequence of following steps:

1. First the natural frequencies, ω_n, and modes, Φ_n, for linear elastic analysis are computed.

2. Develop a pushover curve i.e. base shear (V_{bn}) and top displacement (u_{rn}) for the force distribution using obtained from Eq. 2.11.

$$S_n^* = \mathrm{m}.\Phi_n^i \tag{2.11}$$

where

m is the mass matrix.

Φ^i_n is the mode shape of i^{th} mode.

3. Apply force distribution S_n^* incrementally and record the base shears and associated roof displacements. The system should push beyond the target roof displacement in the selected mode.

4. Idealize the capacity curve as a bilinear curve using the FEMA-273 procedure.

5. Develop the (F_{sn} / L_n)-D_n relation by scaling the horizontal axis by $\Gamma_n\Phi_n$ and by scaling the vertical axis by M_n^* which is equal to $L_n\Gamma_n$ as shown in Figure 2.8.

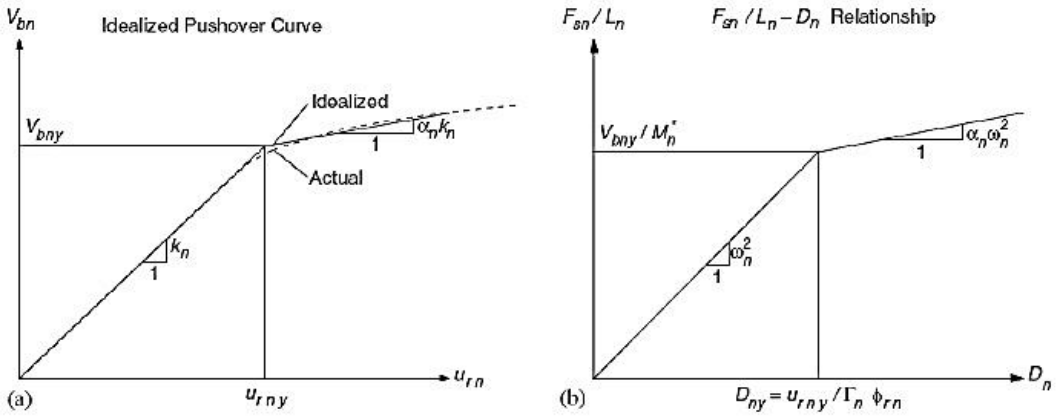

Figure 2.8: (a) Pushover Curve and (b) SDF-System Curve (Chopra and Goel, 2001)

Figure 2.9 shows the Idealization of pushover curve given by Chopra and Goel, 2001.

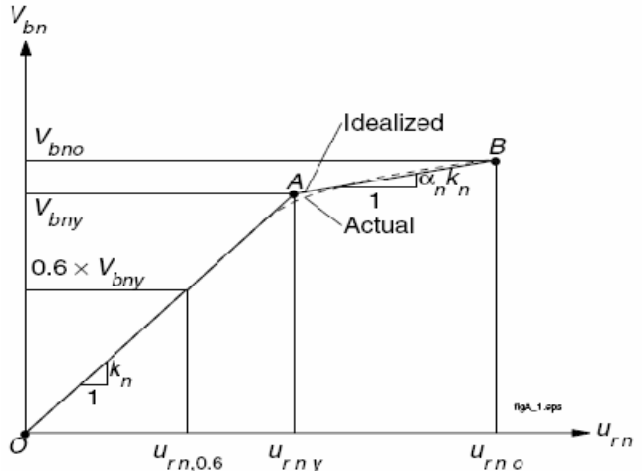

Figure 2.9: Idealization of Pushover Curve (Chopra and Goel, 2001)

6. Calculate the peak deformation of nth mode inelastic representative SDOF system under selected ground motion excitation, D_n.

7. Convert SDOF system result to MDOF form using Eq.2.12.

$$u_{mo} = \Gamma_n . \Phi^i_m . D_n \tag{2.12}$$

where

Γ_n is a modal amplification factor for nth mode.

Φ^i_m is shape factor at roof level.

D_n is the peak response of the representative SDOF system.

8. Take the results of MDOF responses from pushover database.

9. Repeat the procedure from step 2 to 8 for other modes. Usually first three modes are enough for obtaining required accuracy.

10. Determine the total response by combining the peak modal responses by using usually Square Root of the Sum of Squares (SRSS) or Complete Quadratic Combination (CQC) rule.

Figure 2.10 shows conceptual explanation of MPA of inelastic MDOF systems.

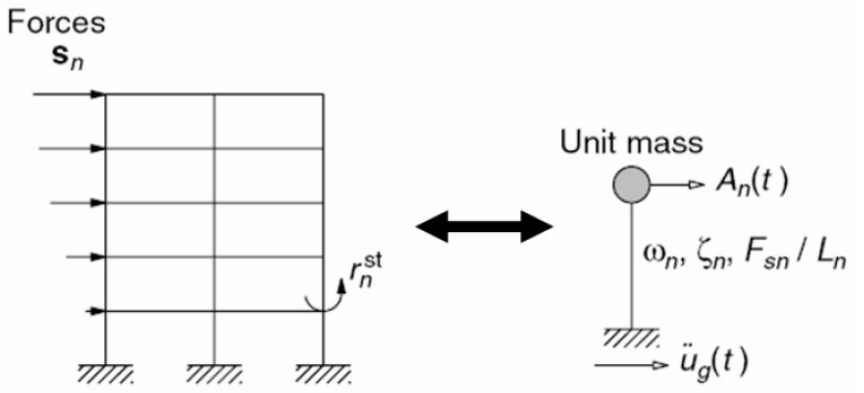

Figure 2.10: Conceptual explanation of MPA of inelastic MDOF systems (Chopra and Goel, 2001)

2.4 Recent Development in Pushover Analysis

The following review is concerned with studies of the development and application of pushover analysis. The findings of previous researchers are given in chronological order.

2.4.1 Adaptive Pushover Analysis (APA)

Adaptive pushover analysis (APA) is given by Elnashai in 2001. The Adaptive POA procedures are mostly concerned with an appropriate estimation of the force vector that is going to 'push' the structure at each static force increment. The monitoring in the change

of the incremental force vector could ensure that the stiffness degradation or strength deterioration of the structure is accounted for more realistically, than conventional nonlinear static analyses. When the new force vector has been determined, the remaining steps of the Adaptive POAs follow those of the Conventional POAs [6].

2.4.2 Method of Modal Combination (MMC)

Kalkan and Kunnath (2004) introduced Method of Modal combination. The author applied a number of load distributions based on the modal combination rule, to an eight-storey and a sixteen-storey reinforced concrete building. The pushover analyses results provided from the DCM method, were compared with those from nonlinear time-history analyses of a typical ground motion. These indicated quite good agreement in the estimation of the inter-storey drifts in the eight-storey building but inappropriate for the upper levels in the case of the sixteen-storey building [7].

2.4.3 Force-Based Adaptive Pushover (FAP)

This procedure is given by Antoniou and Pinho in 2004.They modified the adaptive pushover analysis propsed by Elnashai in 2001.In this procedure authors suggested to carry out Eigen value analysis at each step and accordingly lateral load is distributed on the structure [8].

2.4.4 Displacement-Based Adaptive Pushover (DAP)

This method is also introduced by Antoniou and Pinho in 2004. The method used monotonic lateral incremental displacements instead of monotonic lateral incremental forces to obtain the capacity curves. The authors applied it to twelve reinforced concrete buildings and compared the results with the force-based method and with nonlinear time-history analysis. It was concluded that the method was able to provide improved predictions of demands with respect to the conventional method. This was appointed to the static nature of the method that was used to the possible incorrect updating of the displacement vector [9, 10].

2.4.5 Multi-Modal Pushover Method

In 2005 Barros and Almeida introduced multi-modal pushover method. The load applied in this approach is based on the relative participation of each mode of vibration in the elastic response when structure subjected to earthquake. The method was tested on different structures and comparisons of the results were done with pushover and time history analysis [11].

2.4.6 Modified Modal Pushover Analysis (MMPA)

Aschehim et al. (2006) evaluated the Modified Modal Pushover analysis and energy-based pushover method by studying the behavior of five building models; a three-storey and eight-storey steel moment-resisting frames, a reinforced concrete wall building and

two weak storey variants of the steel frames. The results showed that the proposed method was in general satisfactory to approximate the target displacements and inter-storey drifts. Furthermore, it was pointed out that conventional pushover procedures tended to underestimate the roof displacements. Questionable estimates were obtained for the storey shears and the overturning moments. The authors prompted for more clarification of the cases where these methods could be reliable [12].

2.4.7 Factored Modal Combination (FMC)

Park et al. proposed factored modal combination method in 2007. In this method modal contribution were taken along with the directions. The author applied this method to 2D models and compared the results with conventional pushover methods [13].

2.5 Pushover Analysis of Existing Shear Wall Structures

Rana et al. (2004) conducted a pushover analysis of nineteen storeys, slender concrete tower building located in San Francisco with a gross area of 430,000 square feet. Lateral system of the building consists of shear walls with arrangement as shown in a typical floor plan in Figure 2.11. Typical shear walls are approximately 15 inches thick at the 15th storey and above, and 27 inches thick at the 14th storey and below, except for the transverse walls in the eastern half of the building where approximately 36 inches thick shear walls are present at the 6th storey and below. Typical floor plan is of rectangular shape and measures approximately 350 x 60 feet. An isometric view of the building is

shown in Figure 2.12, with some of the gravity beams and columns removed for clarity. The building was designed per 1997 Uniform Building Code (UBC) with an intended performance objective of Life Safety under design seismic event [14].

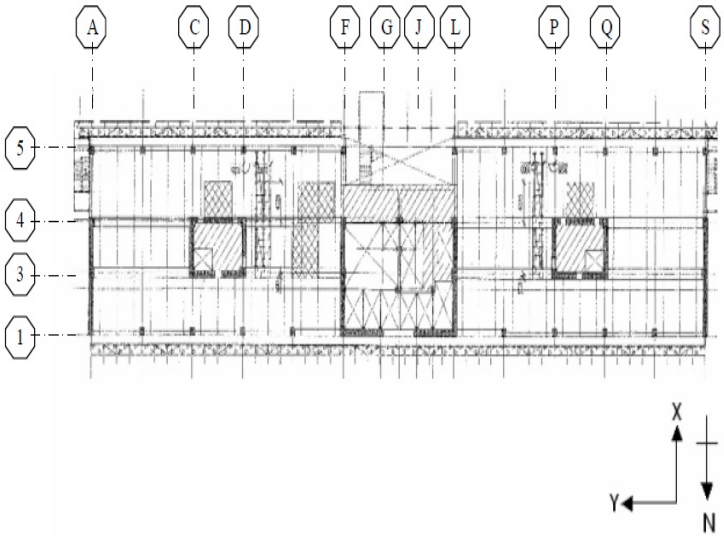

Figure 2.11: Typical Floor Plan and Wall Arrangement

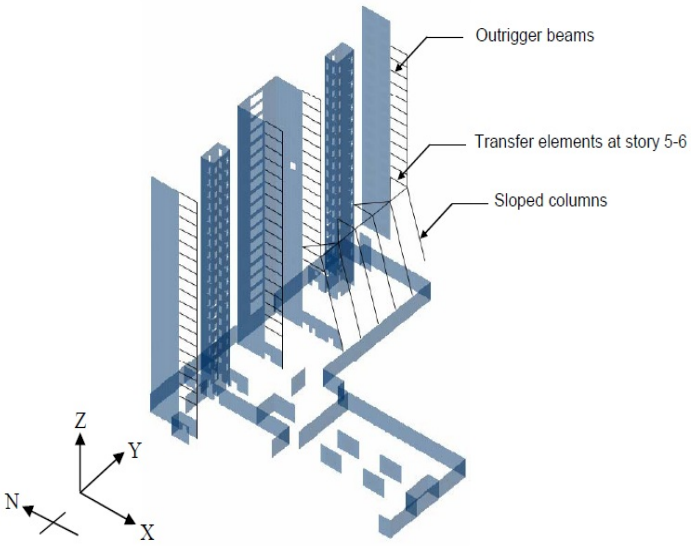

Figure 2.12: Isometric View of Analyzed Concrete Tower Building

Upon performing the various pushover runs shear hinges were found by Rana et al. at a few walls and spandrel locations which was considered undesirable for the performance objective. By performing trial runs with arbitrarily increased shear strength of the shear hinges at these locations, shear strengthening requirement was quantified as a factor of original shear strength. After strengthening the building; Rana et al found capacity curves to meet the demand curve by carrying out pushover analysis. The capacity curves and hinge formation are shown in Figs. 2.13 and 2.14.

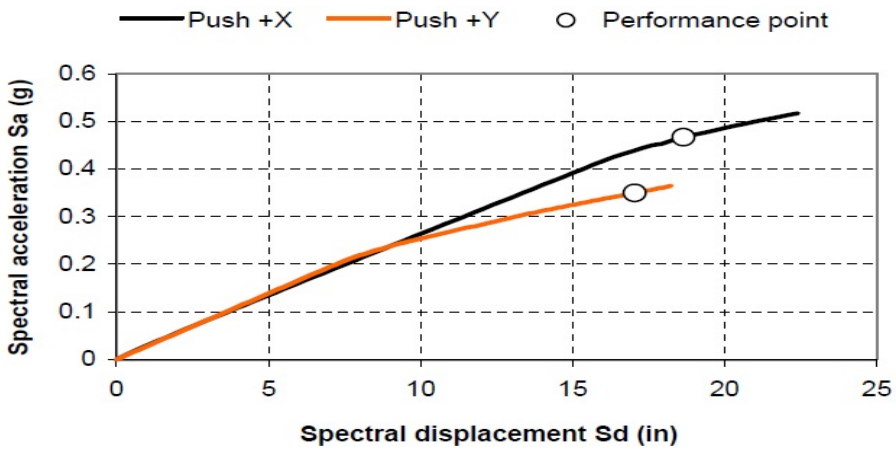

Figure 2.13: Pushover Capacity Curve and Performance Point

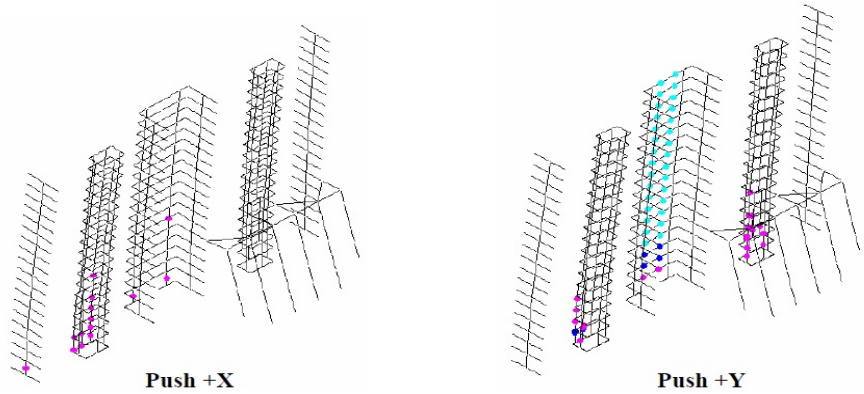

Figure 2.14: Building Deformation and Hinge Development at Performance Point

Goksu et al. (2006) performed a pushover analysis of typical RC building in Turkey. They investigated the behavior of existing and retrofitted building frame by RC or CFRP jackets. The building was constructed in 1970's and has all typical construction faults [15]. The typical plan of the building is shown in Figure 2.15.

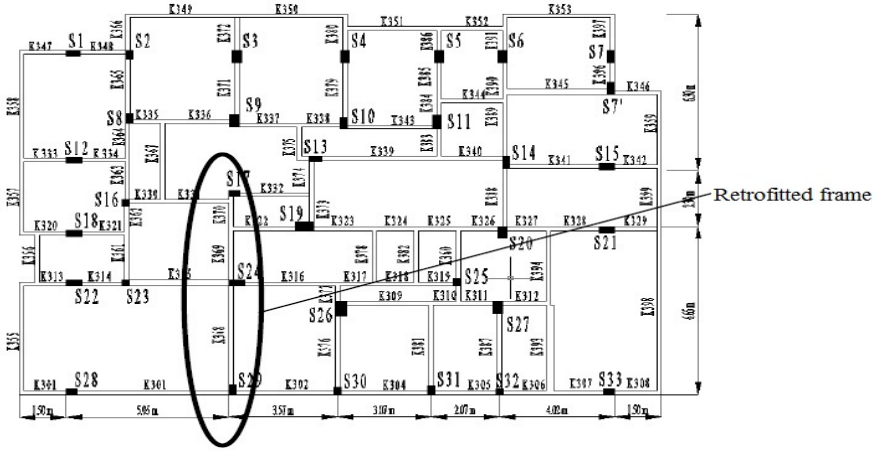

Figure 2.15: Typical Plan of the Building

The pushover curves for original and retrofitted structures in x and y directions are presented in Figure 2.16 for CFRP and reinforced concrete jacketing cases. Typical hinges formations are shown in Figure 2.17.

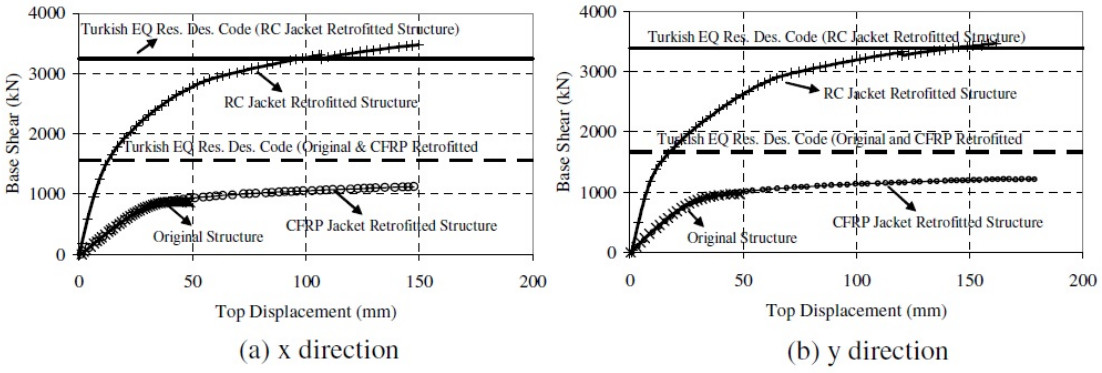

Figure 2.16: Pushover curves for Original and Retrofitted Structures

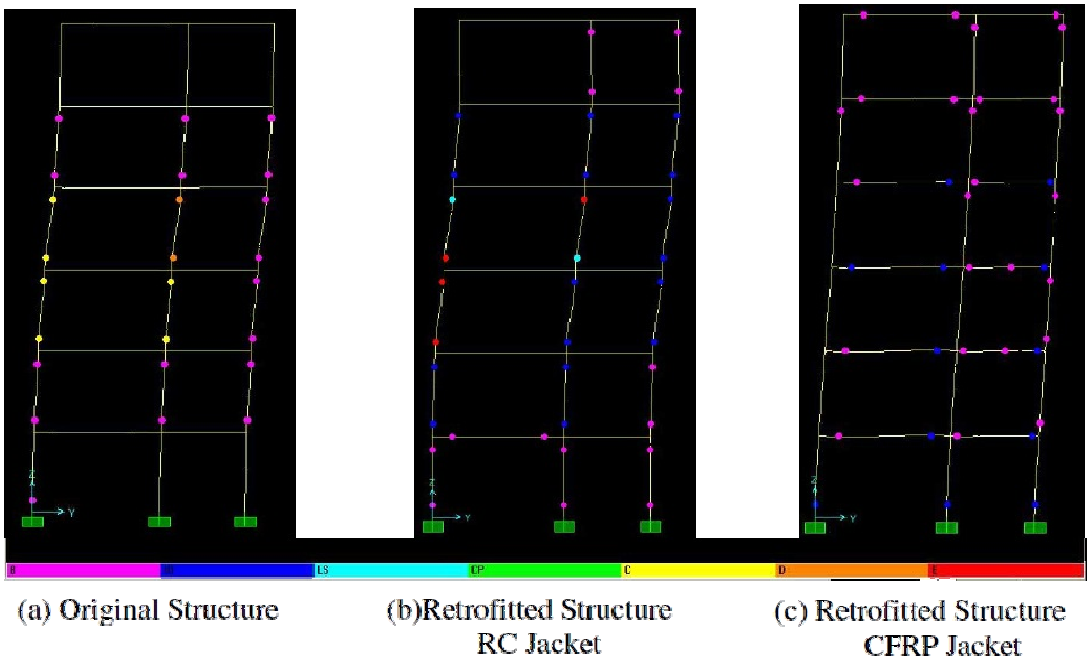

Figure 2.17: Hinge formations in Original and Retrofitted Structures

Phino et al. (2008) assessed the 3D Irregular Spear building with nonlinear static procedures. The applied four commonly available nonlinear static procedures (CSM, N2, MPA, and ACSM) to assess Spear building i.e. an irregular structure tested in full-scale under pseudo-dynamic conditions and subjected to bi-directional seismic loading. They compared the dynamic results with NSPs [16].

The building was built to full-scale and then tested within the European research project SPEAR (Fardis and Negro, 2006), so as to represent typical old constructions in Southern Europe without specific provisions for earthquake resistance. The typical plan of the building is shown in Figure 2.18.

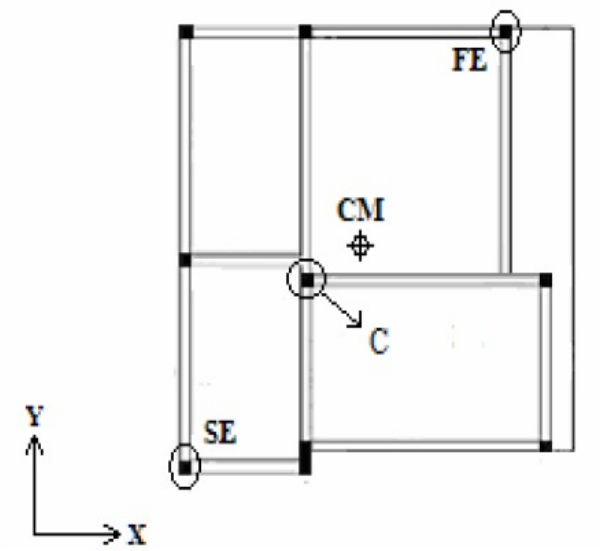

Figure 2.18: Typical Plan of Spear Building

After analysis Phino et al. plotted push over curves against dynamic results shown in Figure 2.19. The comparisons with the results obtained with nonlinear dynamic analysis of a verified model of the structure seemed to show that; overall, all NSPs tend to lead to reasonably satisfactory results.

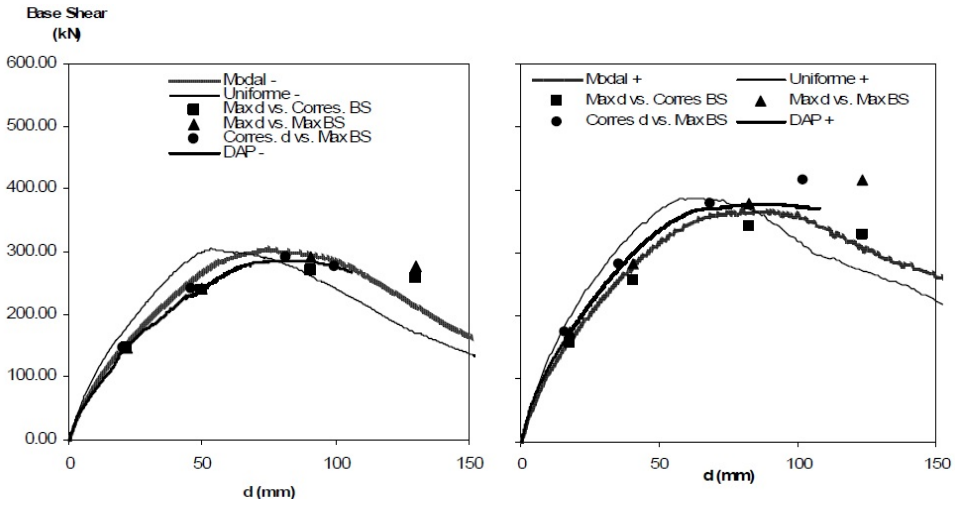

Figure 2.19: Pushover Curves in x and y directions

Fahjan et al. carried (2010) out Nonlinear static analysis of existing reinforced build with shear wall. They modeled shear walls by Mid-Pier and shell element method for existing school building [17]. The physical models are shown in Figure 2.20.

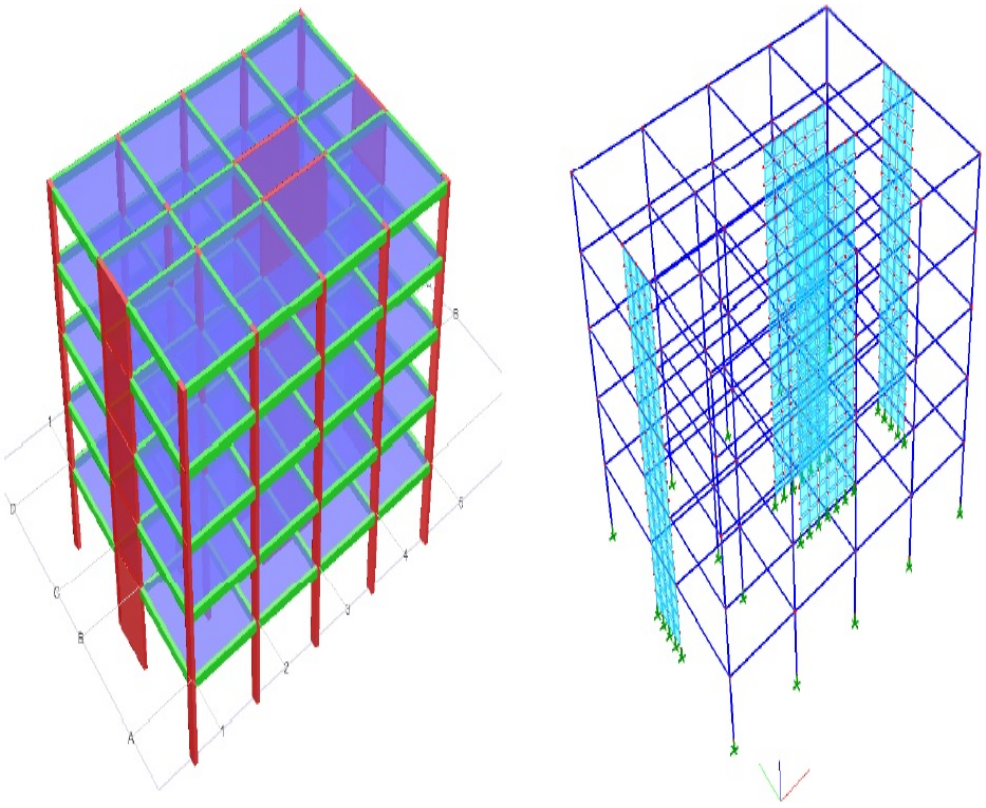

Figure 2.20: Existing School Building Model

Fahjan et al. concluded that the pushover analysis for FEM356 and Fiber approaches for the Mid-pier model showed same results. Mid-pier and shell element method gives approximately same results. Typical pushover curves and hinge formation are shown in Figs. 2.21 and 2.22

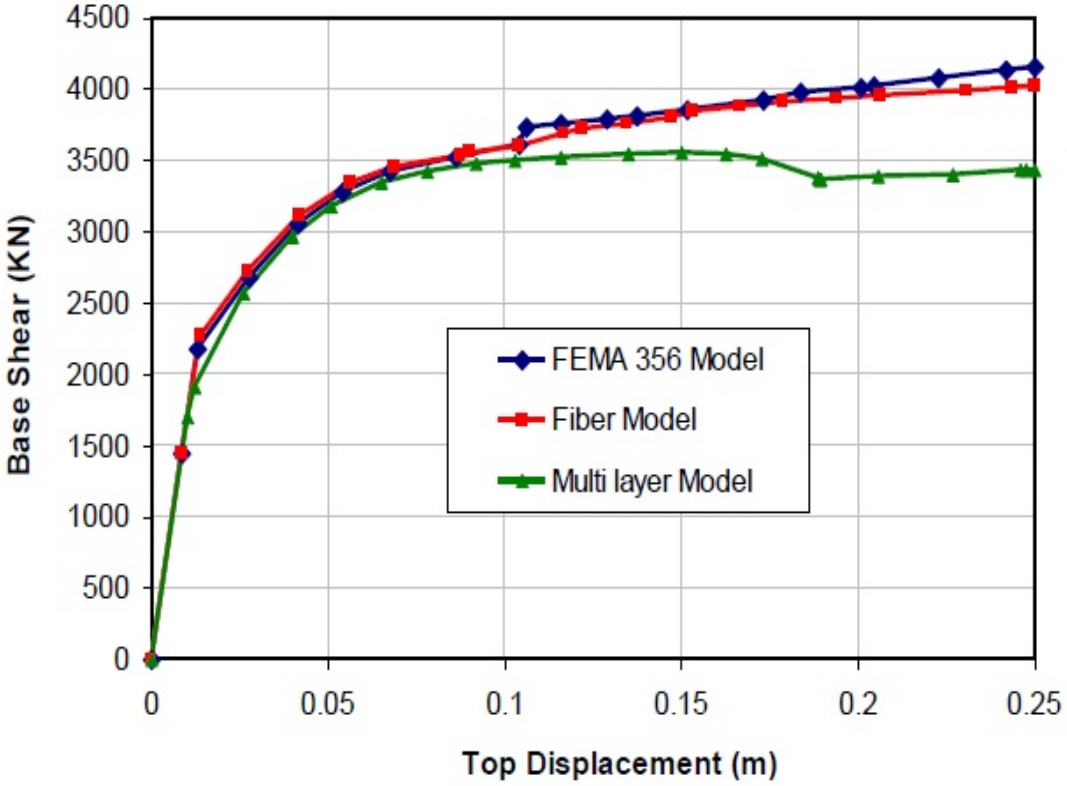

Figure 2.21: Pushover Curves for Existing School Buildings

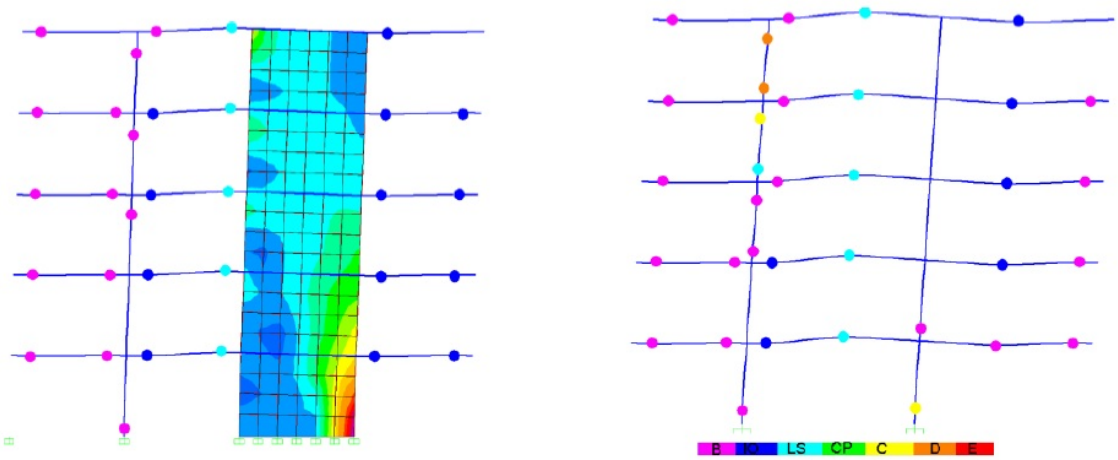

Multi layer shell Model

Mid-Pier Frame Model

Figure 2.22: Formation of hinge at performance point

2.6 Strengthening of Columns

2.6.1 Strengthening of the Column by FRP

The strengthening of existing column with FRP is very common technique. FRP increases the lateral confinement of the column and increase its axial load carrying capacity as well as some extent of ductility. FRP of column is done by wrapping, pre-fabricated shell jacketing and filament winding [18].

1. **Wrapping:** Column strengthening by FRP wrapping by FRP composites is common practice. FRP sheet is wrapped around the column with the use of polymer resins. Figure2.23 shows typical FRP wrapping methods for RC columns

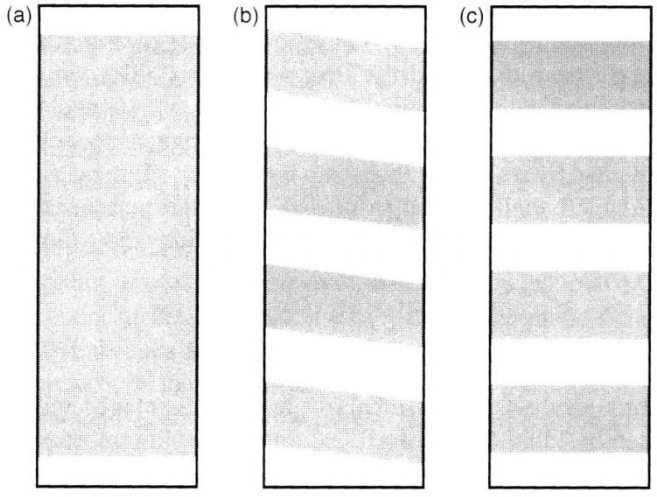

Figure 2.23: Typical FRP Wrapping Methods for RC Columns

2. **Filament Winding:** Filament winding principle is same as of wrapping only it has continuous fiber strands. Winding is done by computerized winding machine.
3. **Prefabricated shell Jacketing:** RC columns can be retrofitted by prefabricated FRP shells. The shells are produced using fibre sheets or strands with the impregnation of resins effected prior to field installation.

2.6.2 Strengthening of Column by Reinforced Concrete Jacketing

Reinforced concrete jacketing is one of the oldest techniques used to enhance the seismic capacity of the structural members .Reinforced jacketing is applied in cases of heavy damaged columns or in cases of insufficient column strength. RC jacketing is done depending on the space around the column. It can be done on one, two, three or four sides of the column. But it is recommended that columns should be jacketed on all sides. In order to achieve the best bond between new and existing concrete, four sided jacketing is best. Reinforced concrete jacketing improves column flexural strength and ductility. Closely spaced transverse reinforcement provided in the jacket improves the shear strength and ductility of the column. Figure 2.24 shows the typical strengthening of column by RC jacketing.

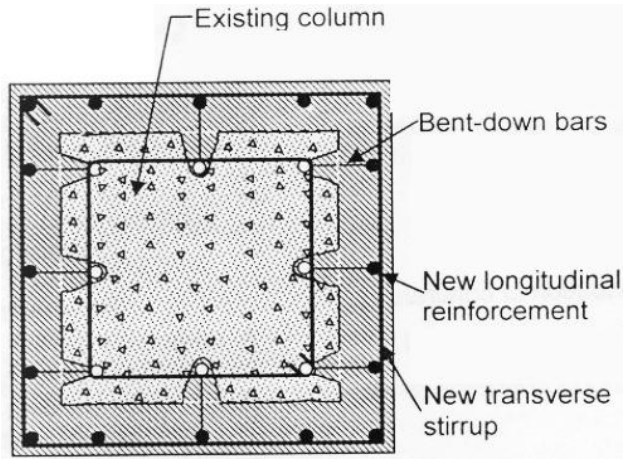

Figure 2.24: Typical strengthening of column by RC jacketing

In order to transfer the additional axial load from the old to the new longitudinal reinforcement, bent down bars are provided which are intermittent lap welded to bars of jacket and longitudinal bars in the existing column exposed for the purpose. Moreover, bent-down bars help in good anchorage between existing and new concrete. Figure 2.25 shows lap welded to bars of jacket and longitudinal bars.

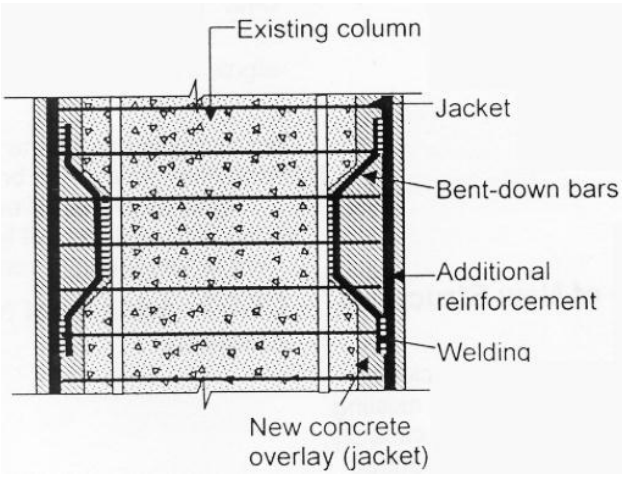

Figure 2.25: Lap welded to bars of Jacket and Longitudinal bars

2.6.3 Strengthening of Column by Steel Jacketing

Confining reinforced concrete column in steel jackets is one of the effective methods to improve the earthquake resistant capacity. As compared with conventional hoops or spirals, steel jacket has two more remarkable advantages

1) Easily provide a large amount of transverse steel, hence strong confinement to the compressed concrete.

2) Prevent spalling off of the shell concrete. Spalling of the shell concrete may be considered as the main reason for deterioration of bond and buckling of longitudinal bars of columns and is hardly prevented by conventional hoops.

Because of these advantages of the steel jacket, confining method utilizing steel jacket has been increasingly used to retrofit or strengthen the existing reinforced concrete columns without adequate detailing. Figure 2.26 shows typical strengthening of column by steel jacketing.

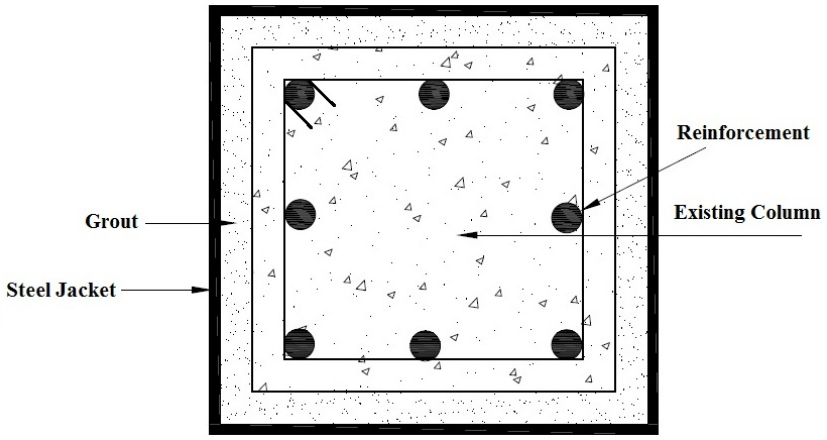

Figure 2.26: Typical strengthening of column by steel jacket

Some studies have shown that steel jacketing is an effective retrofit technique for seismically-deficient concrete columns. Based on satisfactory laboratory results, steel jackets have been employed to retrofit both circular and rectangular columns around the world. For circular columns, two half-circle steel shells, which have been rolled to a radius equal to the column radius plus ½ in. to 1 in. (13 mm to 25 mm) for clearance, are positioned over the portion of the column to be retrofitted, and the vertical seams are then welded. The space between the jacket and the column is flushed with water and then filled with a high-strength cement grout. To avoid any significant increase in the column flexural strength, a gap of approximately 2 in. (50 mm) is typically provided between the end of the jacket and any supporting member (e.g., footing, cap beam, or girders) since at large drift angles the jacket can act as a compression member as it bears against the supporting members.

CHAPTER 3

PUSHOVER ANALYSIS OF RC FRAME

3.1 Structural Analysis Using SAP2000

The structural analysis program SAP2000 is a software package from Computers and Structures, which is based on the finite element method for modeling and analysis. Also it has the capability of designing and optimizing building structures. Among the features introduced by the analysis engine of SAP2000 are Eigen value analysis, static and dynamic analysis, linear and nonlinear analysis, and pushover analysis. The analytical modeling used in this software is the member type model which means that beams or columns are modeled using single elements. The inelasticity formed in these single elements is assumed to be concentrated at the ends of the element, which is the case in the behavior of building elements during earthquake excitation. The hysteretic response of the concentrated plasticity at the ends of a member can be described by a moment curvature relationship.

SAP2000 can specify for each material one or more stress-strain curves that are used to generate nonlinear hinge properties in frame elements. The different curves can be used for different parts of a frame cross section. For example, in a RC material, SAP2000 can specify stress-strain curves for confined RC, unconfined RC, longitudinal reinforcing

steel, and hoop confinement reinforcing steel. For steel and other metal materials, SAP2000 typically only specify one stress-strain curve.

A variety of cross sections are available in SAP2000 element library. These sections include rectangular sections as used for modeling the beams and columns of the RC buildings. Also, the cross sections used for steel building are chosen from the built-in European sections included in the steel sections library.

SAP2000 is utilized in this study for pushover analysis because it provides the following features:

- Nonlinear static analysis procedures are specially designed in SAP2000 to handle the sharp drop-off in load carrying capacity of frame hinges used in pushover analysis.
- It allows displacement control nonlinear static analysis procedures, so that the structure can be pushed to a desired target displacement.
- Display capabilities in the graphical user interface to generate and plot pushover curves, including demand and capacity curves in spectral ordinates are very user friendly.
- Also it is capable to plot and get information about the state of every hinge formed at each step in the pushover analysis.

3.2 Element Description of SAP2000

3.2.1 Frame Element

Frame element is a prismatic or non-prismatic line element. Element can be divided into segments. The frame element has all six degrees of freedom at ends [19]. Element has its own local axis and the axes of this local system are denoted 1, 2and 3 as shown in Figure 3.1.

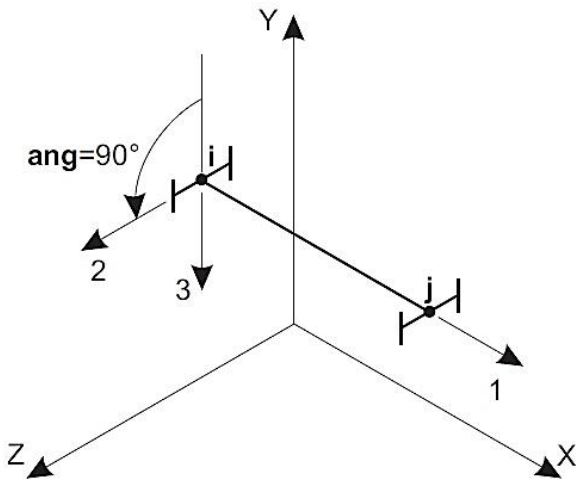

Figure 3.1: The Frame Element

3.2.2 Shell Element

The Shell element is a three or four node formulation that combines separate membrane and plate bending behavior. The four joint elements do not have to be planar. The Shell

elements have all six degrees of freedom at each end [19]. The four node quadrilateral and three node triangular shell element are shown in Figs. 3.2 and 3.3.

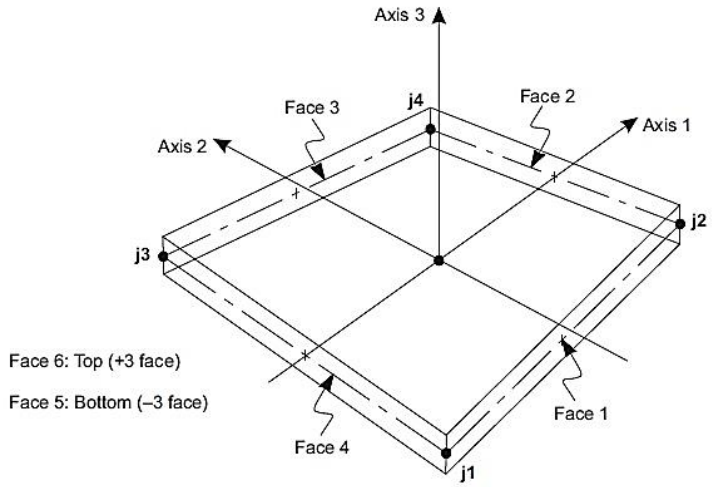

Figure 3.2: Four-node Quadrilateral Shell Element

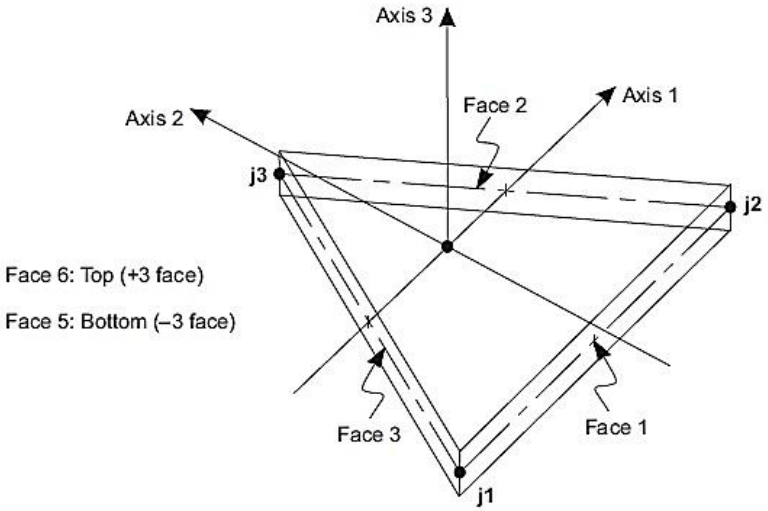

Figure 3.3: Three-node Triangular Shell Element

3.3 Frame Hinge Properties

SAP2000 introduces the capability of providing plastic hinges at discrete user defined hinges along the clear length of a frame element. The plastic hinge represents the post-yield behavior in one or more degree of freedom. Uncoupled moment, torsion, axial force and shear hinges are available to be modeled along the frame element. Also, P-M2-M3 hinge which yields based on the interaction of axial force and bending moments at the hinge location can be modeled. More than one type of hinge can exist at the same location, for example, the user might assign both M3 (moment) and V2 (shear) hinge to the same end of a frame element. Hinge properties can be assigned by available default hinges or either by user defined hinges. Default hinge properties are provided based on FEMA-356 criteria.

Hinge length is the distance over which the plastic strain or plastic curvature is integrated. Some guidelines like FEMA-356 give some recommendations for hinge length. Typically this length is taken as a fraction of the element length, and is often in the order of the depth of the section, particularly for moment-rotation hinges. Hinge length can be used to obtain full nonlinear behavior all over the total element length. This can be achieved by inserting a specified number of hinges each have a specified length such that the number of hinges times the hinge length gives the total length of the element. In this study, the potential plastic hinges are located at the ends of the element, since this is the location of the maximum straining actions for beams or columns during earthquake.

The plastic deformation curve is a force-displacement (moment-rotation) curve that gives the yield value and the plastic deformation following yield. This is done in terms of a curve with values at five points, A-B-C-D-E, as shown in Figure 3.4. The user can specify a symmetric curve, or one that differs in the positive and negative direction.

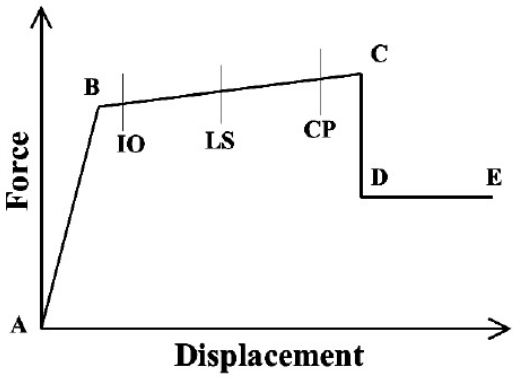

Figure 3.4: Force-Displacement or Moment-Rotation Curve for A Hinge Definition Used In Sap2000 (Plastic Deformation Curve)

The plastic deformation curve is characterized by the following points:

- Point A is origin.
- Point B is yielding state. No deformation occurs in the hinge up to point B, regardless of the deformation value specified for point B.
- Point C represents the ultimate capacity for pushover analysis.
- Point D represents the residual strength for pushover analysis.
- Point E represents total failure. Beyond point E the hinge will drop load down to point F (not shown) directly below point E on the horizontal axis. If the user does

not want the hinge to fail this way, a large value for the deformation at point E can be specified.

The user may specify additional deformation measures at points IO (immediate occupancy), LS (life safety), and CP (collapse prevention). These are informational measures that are reported in the analysis results and used for performance-based design. They do not have any effect on the behavior of the structure.

Prior to reaching point B, the deformation is linear and occurs in the frame element itself, not the hinge. Plastic deformation beyond point B occurs in the hinge in addition to any elastic deformation that may occur in the element. When the hinge unloads elastically, it does so without any plastic deformation, i.e., the unloading path is parallel to line A-B.

Curve scaling permits that the force-displacement (moment-rotation) curve of the hinge can be defined by entering normalized values and specify the required scale factor. Often, the normalized values are based on the yield force (moment) and yield displacement (rotation), so that the normalized values for point B on the curve would be (1,1). Any deformation given from A to B is not used. This means that the scale factor on deformation is actually used to scale the plastic deformation from point B to C, C to D, and D to E. However, it may still be convenient to use the yield deformation for scaling. When default hinge properties are used, the program automatically uses the yield values for scaling. These values are calculated based on the frame section properties and the yield stress provided for the element material.

In this study user defined hinge properties are utilized. Also, only two types of hinges are used to simulate the plastic hinge formation through the nonlinear behavior of the structure. The first is the coupled axial and moment hinge (PMM) which is assigned to the column elements. The hinge properties of this type are created based on the interaction surface that represents where yielding first occurs for different combinations of axial force, minor moment , and major moment acting on the section. The second type is the moment hinge (M-φ) which is assigned to the beam elements.

Interaction surface and moment rotation diagrams for column and beams are obtained using XTRACT fiber analysis software which is explained in section. For concrete Mander stress-strain relation is utilized and explained in section 3.7.1. For steel Kinematic nonlinear model is selected and explained in section 3.7.2. For CFRP strengthened member Lam and Teng Model (2003) is used for confined concrete by CFRP explained in section 3.7.3.

During the analysis, once a hinge yields for the first time, i.e., once the values of axial load and moment first reach the interaction surface, a net moment-rotation curve is interpolated to the yield point from the given curves. This curve is used for the rest of the analysis for that hinge. If the values of axial load and the moment change from the values used to interpolate the curve, the curve is adjusted to provide an energy equivalent moment-rotation curve. This means that the area under the moment rotation curve is held fixed, so that if the resultant moment is smaller, the ductility is larger. This is consistent with the underlying stress strain curves of axial fibers in the cross section.

3.4 Hinge Unloading Method

SAP2000 provides three different member unloading methods to redistribute load and remove load from hinge [19].

3.4.1 Unload Entire Structure Method

In the "Unload Entire Structure" option, when the hinge reaches point C on its force displacement diagram the software try to increase the base shear until the increase in lateral deformation otherwise base shear is reduced by reversing the lateral load till the force in that hinge is consistent with the value at point D on its force-displacement curve. All elements unload and lateral displacement is reduced since the base shear is reduced. After the hinge is fully unloaded, base shear is again increased, lateral displacement begins to increase and other elements of the structure start taking load that was released from the unloaded hinge. The method fails when two hinge compete in loading e.g. one hinge requires increase in applied load and second hinge require decrease in applied load. Pushover curve obtained by using member unloading method is shown in Figure 3.5.

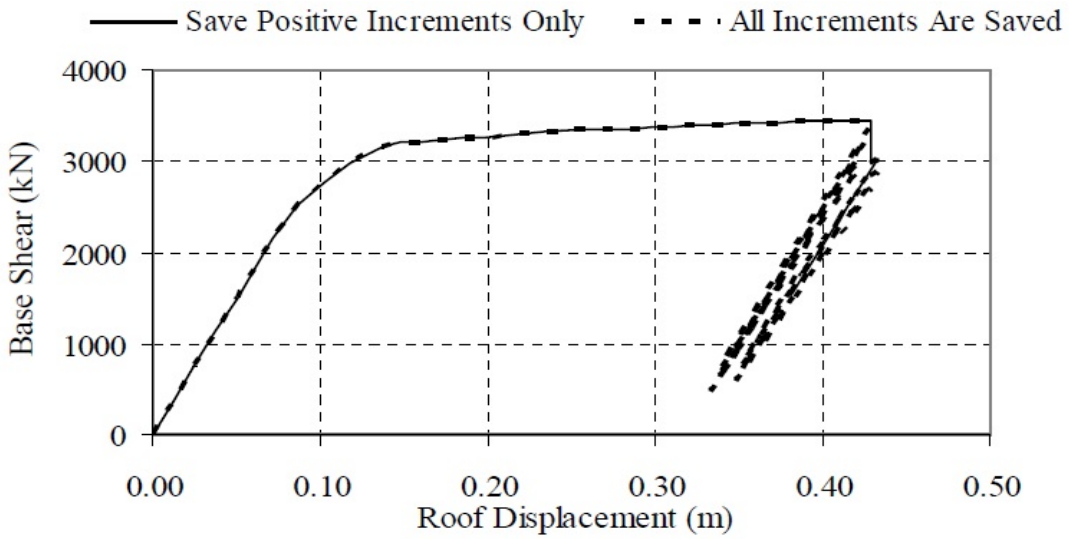

Figure 3.5: Pushover Curve by Unload Entire Structure Method

3.4.2 Apply Local Redistribution Method

In the "Apply Local Redistribution" option, only the element containing the hinge is unloaded instead of unloading the entire structure. If the program proceeds by reducing the base shear when a hinge reaches point C, the hinge unloading is performed by applying a temporary internal load that unloads the element. After unloading of hinge the applied temporary load is reversed and transfer to other members. Pushover curve obtained by using apply local redistribution method is shown in Figure 3.6.

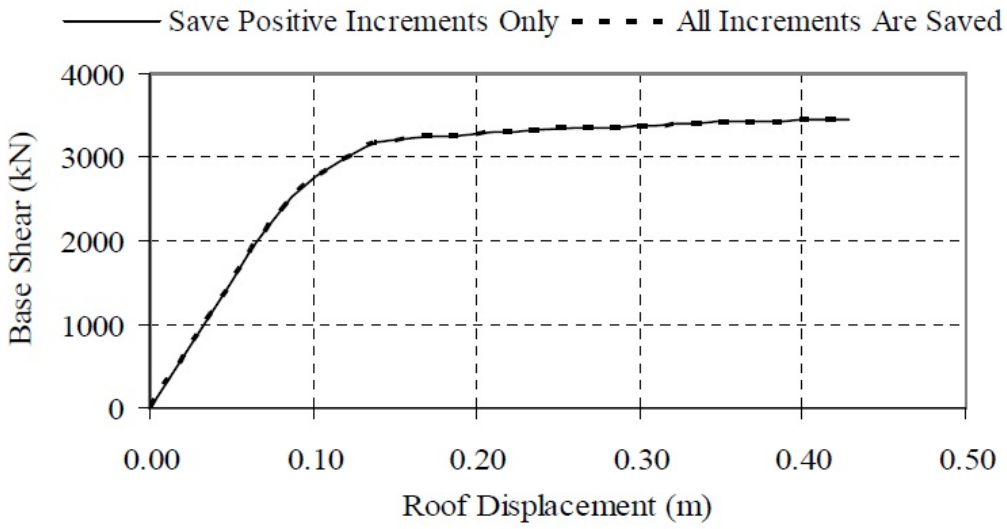

Figure 3.6: Pushover curve by Apply Local Redistribution method

3.4.3 Restart Using Secant Stiffness Method

In the "Restart Using Secant Stiffness" option, whenever any hinge reaches point C on a force - displacement curve, hinges are changed base on secant stiffness properties and then analysis is done. On the other hand, this method may also give solutions where the other two methods fail due to hinges with small (nearly horizontal) negative slopes. Pushover curve obtained by using restart using stiffness method is shown in Figure 3.7.

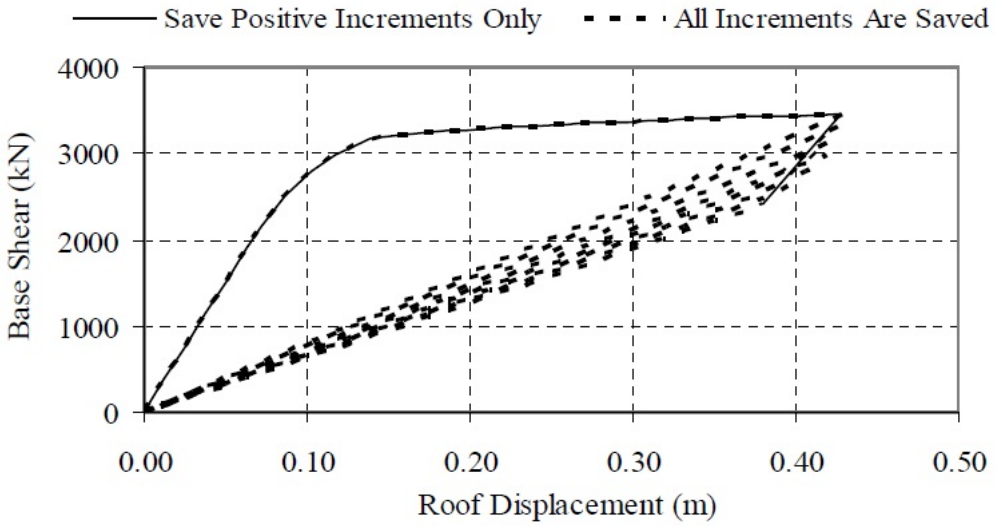

Figure 3.7: Pushover curve by Restart Using Secant Stiffness method

Although pushover curves obtained from each method have the same base shear capacity and maximum lateral displacement, pushover analysis is generally performed by using "Unload Entire Structure" unloading method with "Save Positive Increments Only" option because "Unload Entire Structure" is the most efficient method and uses a moderate number of total and null steps. However, "Apply Local Redistribution" requires a lot of very small steps and null steps that the unloading branch of pushover curve could not be observed usually. "Restart Loading Using Secant Stiffness" is the least efficient method.

3.5 Static Pushover Analysis in SAP2000

The following are the general sequence of steps involved in performing nonlinear static pushover analysis using SAP2000 in the present study:

1. The model of the structure is created.
2. Frame elements are adequately designed. For RC elements, the appropriate reinforcement ratios are provided for the assumed cross sections. For steel elements, the assumed sections are checked to be adequate.
3. Frame hinge properties are defined and assigned to the frame elements.
4. Load cases that are needed in the pushover analysis are defined, these loads cases includes:
    - Gravity loads and other loads that may be acting on the structure before the lateral seismic loads are applied.
    - Lateral loads that will be used to push the structure.
5. The nonlinear static analysis cases to be used for pushover analysis are defined, these cases includes:
    - A sequence of one or more cases that start from zero initial condition and apply gravity and other fixed loads using load control as shown in Figure 3.8.

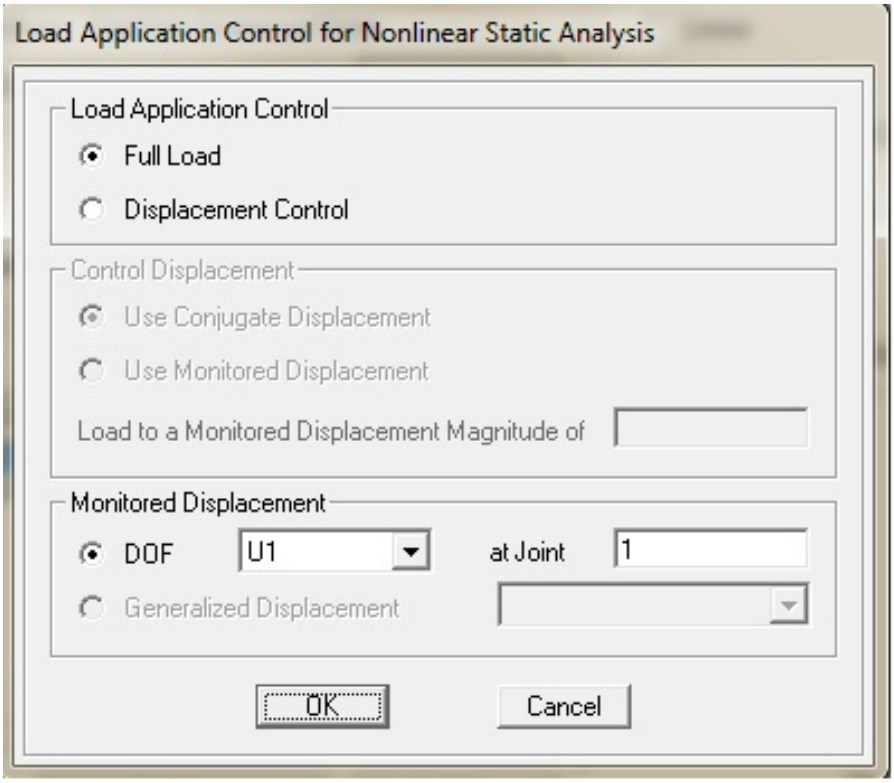

Figure 3.8: Force Control Option for Gravity Loads

- One or more pushover cases that start from previous cases loaded with gravity and fixed loads. These later pushover cases should be applied under displacement control. The monitored displacement is usually at the top of the structure and is used to plot the pushover curve as shown in Figure 3.9.

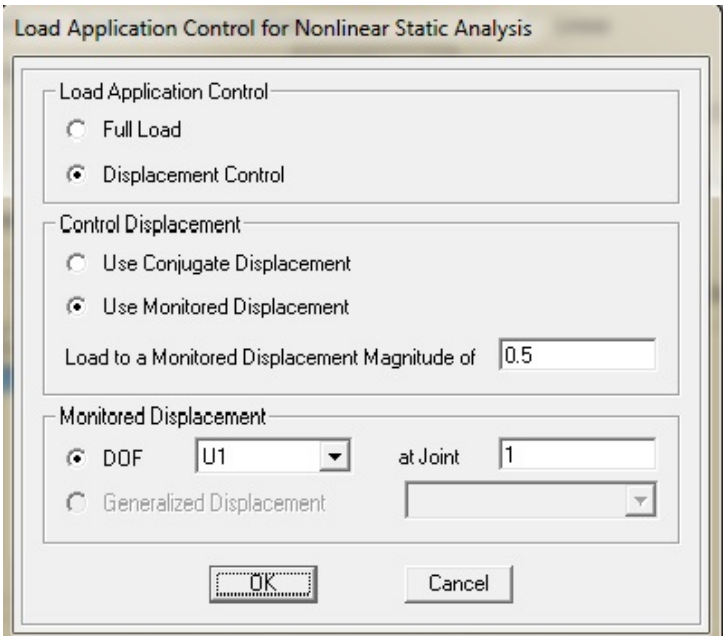

Figure 3.9: Displacement Control Option for Lateral Loads

6. Set the nonlinear parameter for pushover analysis as shown in Figure 3.10.

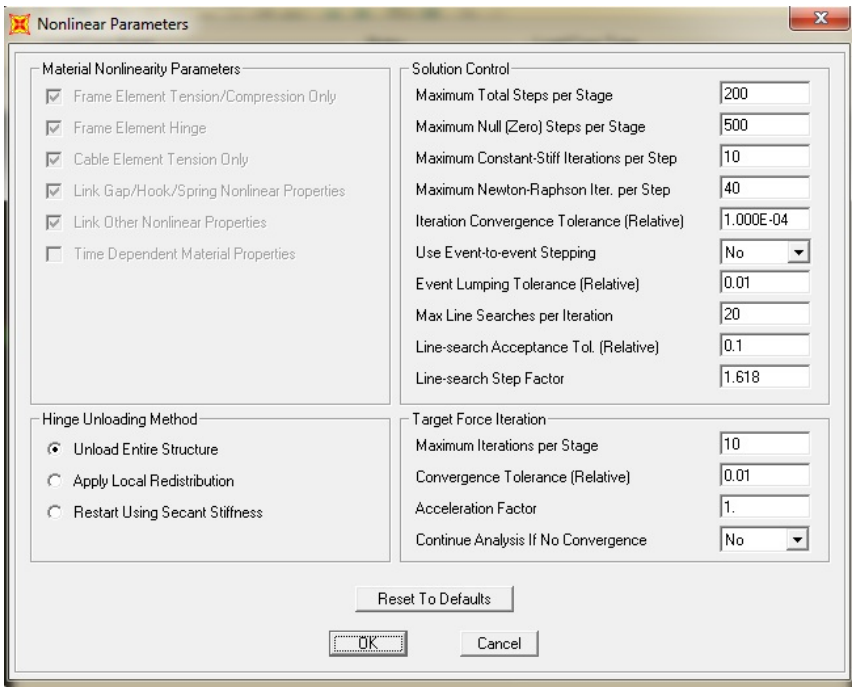

Figure 3.10: Nonlinear Parameters for Pushover Analysis

7. Pushover analysis cases are set to run.
8. At the last step, SAP2000 software plots the pushover curve, the deformed shape showing the hinge states, force and moment plots, and reports any other results needed.

3.6 Section Analysis Using XTRACT

XTRACT is a cross sectional analysis program. It can create Axial Force-Moment Interactions, Moment Curvatures and Moment-Moment Interactions.

XTRACT offers six material models. Unconfined and Confined concrete Mander model, Bilinear with Parabolic Strain Hardening, Bilinear Steel, Menegotto Pinto, and a User Defined. In this study Mander models for Unconfined and confined concrete Bilinear steel with parabolic strain hardening and user defined model for CFRP is used [20].

XTRACT is utilized in this study to obtain hinge properties for beams, columns and shear walls which were inserted in SAP2000. Following are the steps involve of modeling and analysis of sections.

1. Create a section using design templates available in XTRACT or by user can create any arbitrary section using section builder tools as shown in Figs. 3.11 and 3.12.

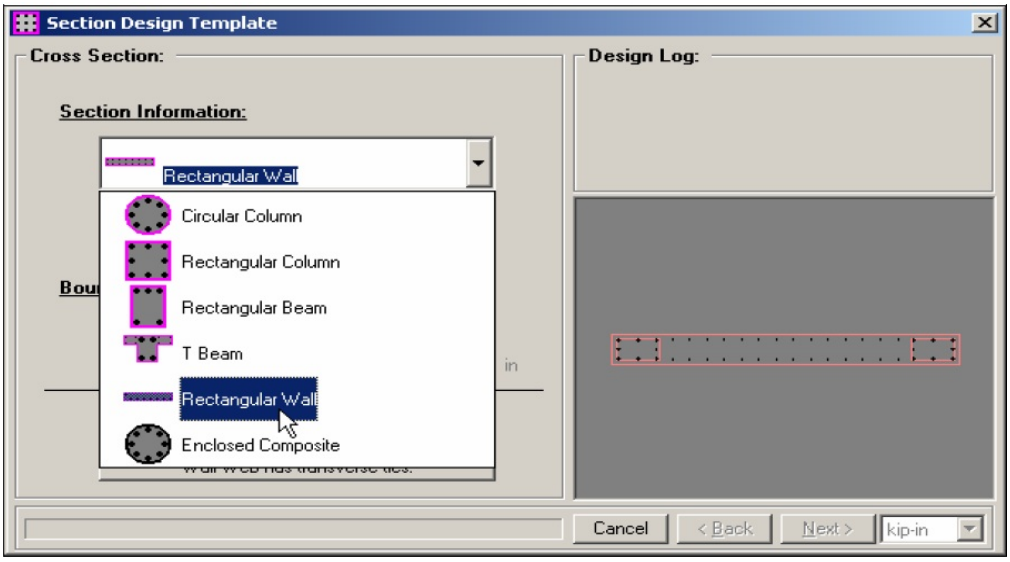

Figure 3.11: Built in Section Available in XTRACT

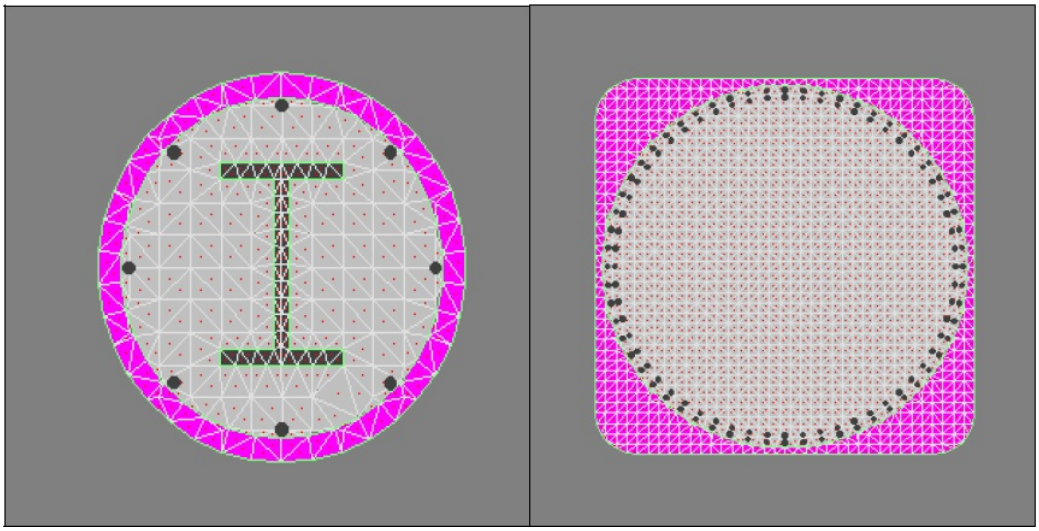

Figure 3.12: Non Standard Sections in XTRACT

2. Input the section properties as shown in Figure 3.13.

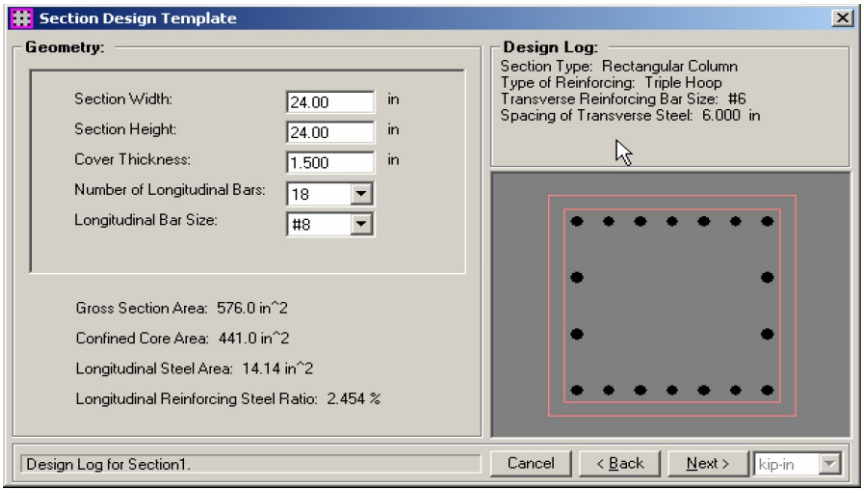

Figure 3.13: Section Properties Design Log

3. Input the parameters for unconfined concrete as shown in Figure 3.14.

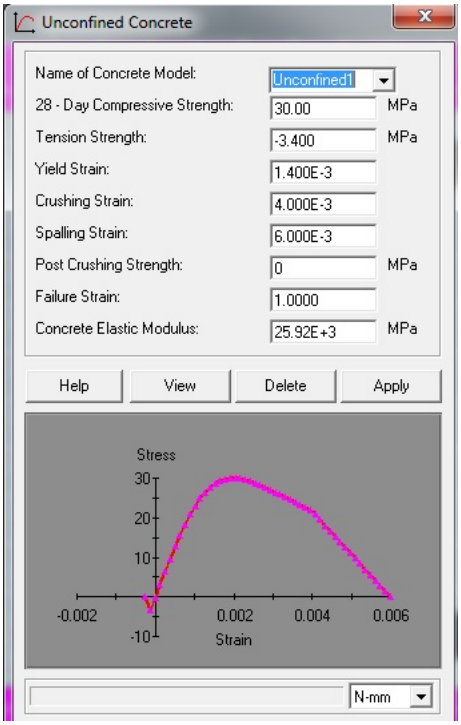

Figure 3.14: Input for Unconfined Concrete

4. Input Parameters for Confined concrete as shown in Figure 3.15.

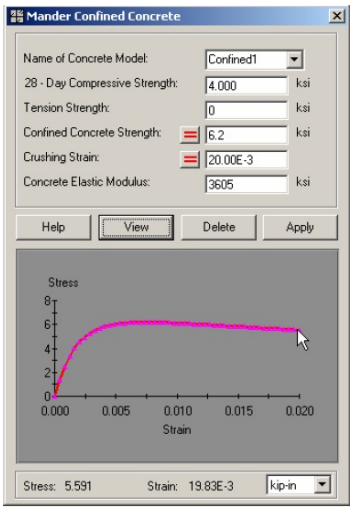

Figure 3.15: Input Parameters for Confined Concrete

5. Input parameters for Steel as shown in Figure 3.16.

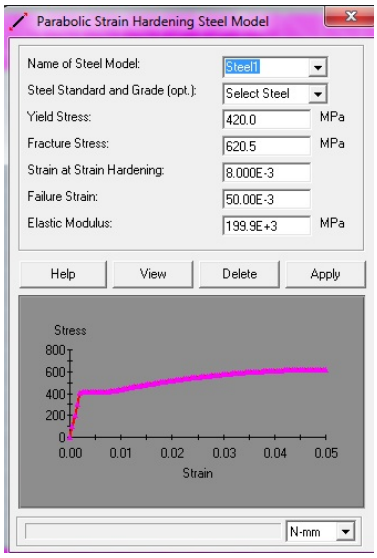

Figure 3.16: Input Parameters for Steel

6. Create a meshing of section as shown in Figure 3.17.

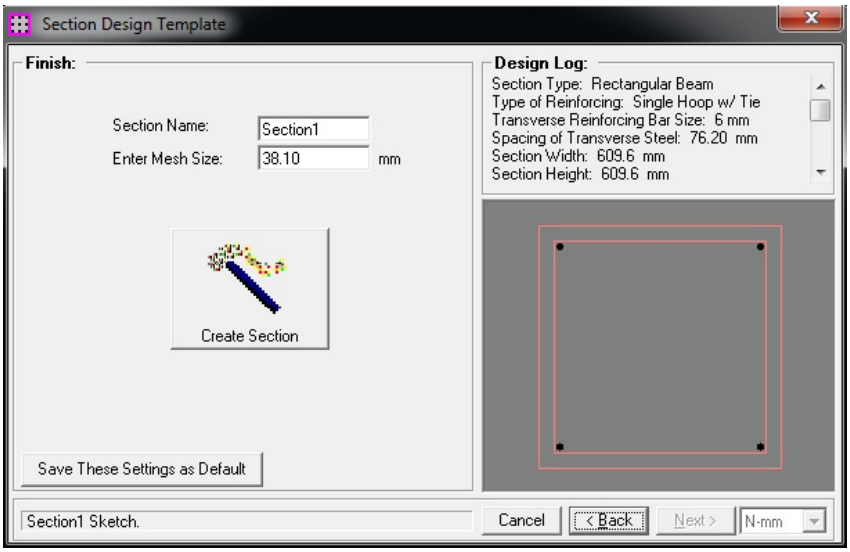

Figure 3.17: Meshing Option for Section

7. Run analysis for Axial Force-Moment Interactions, Moment Curvatures and Moment-Moment Interactions and get the results as shown in Figs. 3.18 and 3.19.

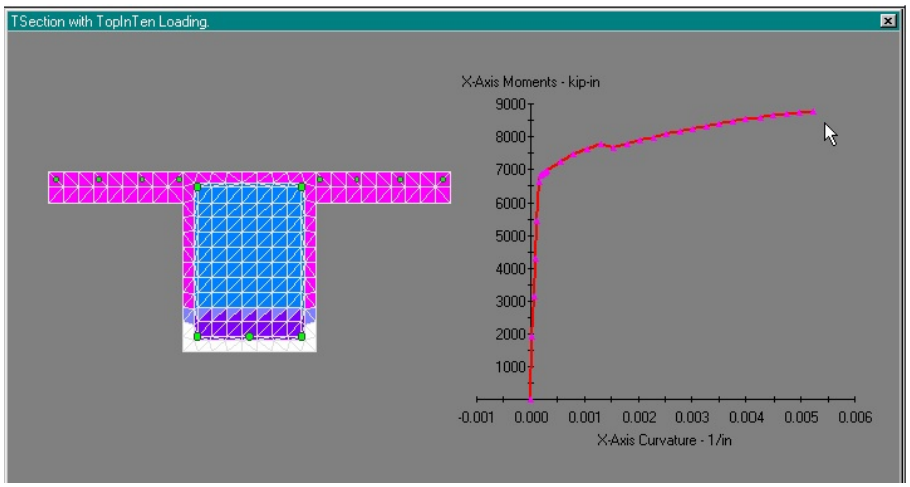

Figure 3.18: Moment Curvature for T-Beam

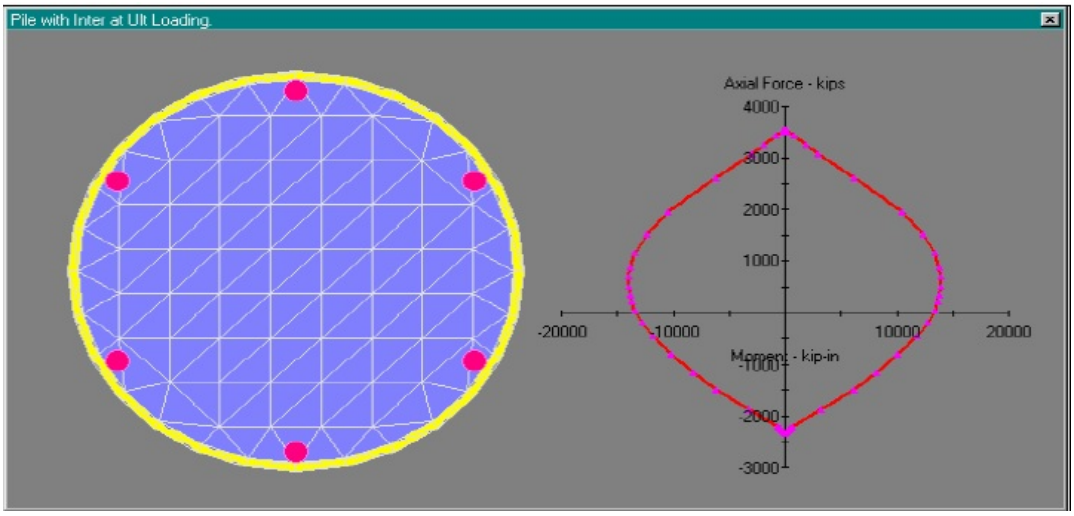

Figure 3.19: Force-Moment Interaction Curve for Circular Column

3.7 Material Models

3.7.1 Mander Concrete Model

Mander et al. developed a stress-strain model for concrete subjected to uniaxial compressive loading and confined by transverse reinforcement [21]. The stress-strain model is illustrated in Figure 3.20. The model is based on an equation suggested by Popovics (1973).The axial stress of confined concrete is given by

$$\sigma_c = \frac{f'_{cc} x r}{r - 1 + x^r} \tag{3.1}$$

f'_{cc} is the confined concrete compressive strength

$$x = \frac{\varepsilon_c}{\varepsilon_{cc}} \tag{3.2}$$

ε_c is the longitudinal compressive concrete strain

$$\varepsilon_{cc} = \varepsilon_{co}\left[1 + 5\left[\frac{f_{cc}^{'}}{f_{co}^{'}} - 1\right]\right] \tag{3.3}$$

as suggested by Richart et al. (1928), where $f_{co}^{'}$ and ε_{co} = the unconfined concrete strength and corresponding strain and

$$r = \frac{E_c}{E_c - E_{\sec}} \tag{3.4}$$

where $E_c = 4700\sqrt{f_{co}^{'}}$ MPa and $E_{sec} = \frac{f_{cc}^{'}}{\varepsilon_{cc}}$

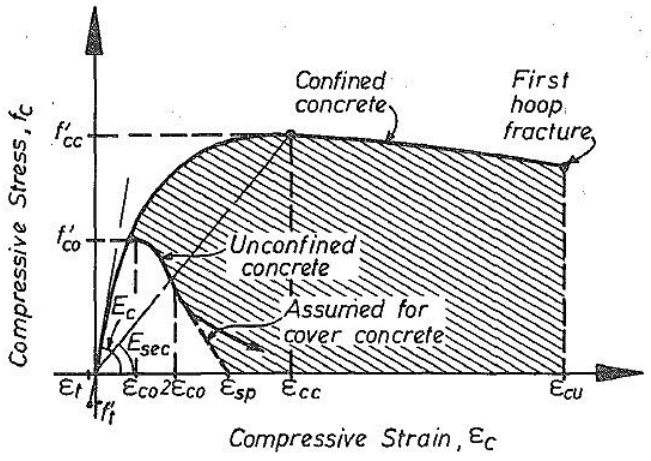

Figure 3.20: Stress-Strain Model of Confined and Unconfined Concrete (Mander et al., 1988)

For circular Section the confined concrete compressive strength is given by

$$f_{cc}^{'} = f_{co}^{'}\left[-1.254 + 2.254\sqrt{1+\frac{7.94 f_l^{'}}{f_{co}^{'}}} - 2\frac{f_l^{'}}{f_{co}^{'}}\right] \tag{3.5}$$

$f_l^{'}$ is the affective lateral confining pressure and is given by

$$f_l^{'} = 0.5 k_e \rho_s f_{yh} \tag{3.6}$$

k_e is the confinement effectiveness coefficient and for circular hoops

$$k_e = \frac{1-\frac{s^{'}}{2d_s}}{1-\rho_{cc}} \tag{3.7}$$

s' and d_s are the vertical clear space between hoops and diameter of hoop as shown in Figure 3.21.

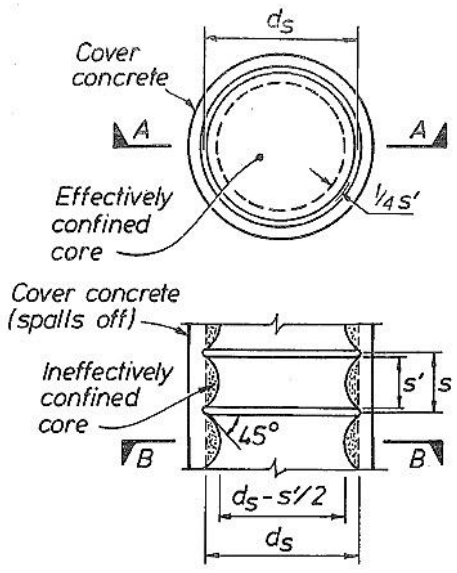

Figure 3.21: Effectively Confined Core for Circular Hoop Reinforcement (Mander et al. ,1988)

For rectangular section the confined concrete compressive strength is given

$$f_{cc}^{'} = f_{co}^{'}\left[-1.254 + 2.254\sqrt{1+\frac{7.94 f_{l}^{'}}{f_{co}^{'}}} - 2\frac{f_{l}^{'}}{f_{co}^{'}}\right] \tag{3.8}$$

The lateral confining stress on the concrete is given in the x direction as

$$f_{lx} = \frac{A_{sx}}{sd_c} f_{yh} = \rho_x f_{yh} \tag{3.9}$$

And in the y direction as

$$f_{ly} = \frac{A_{sy}}{sb_c} f_{yh} = \rho_y f_{yh} \tag{3.10}$$

A_{sx}, A_{sy} and f_{yh} the total area of transverse bars running in the x and y directions and yield strength of the transverse reinforcement respectively.

$$f_{lx}^{'} = k_e \rho_x f_{yh} \tag{3.11}$$

$$f_{lx}^{'} = k_e \rho_x f_{yh} \tag{3.12}$$

$$k_e = \frac{\left(1 - \sum_{i=1}^{n} \frac{\left(w_i^{'}\right)^2}{6b_c d_c}\right)\left(1 - \frac{s^{'}}{2b_c}\right)\left(1 - \frac{s^{'}}{2d_c}\right)}{\left(1 - \rho_{cc}\right)} \tag{3.13}$$

where $w_i^{'}$ is the ith clear distance between adjacent longitudinal bars as shown in Figure 3.22.

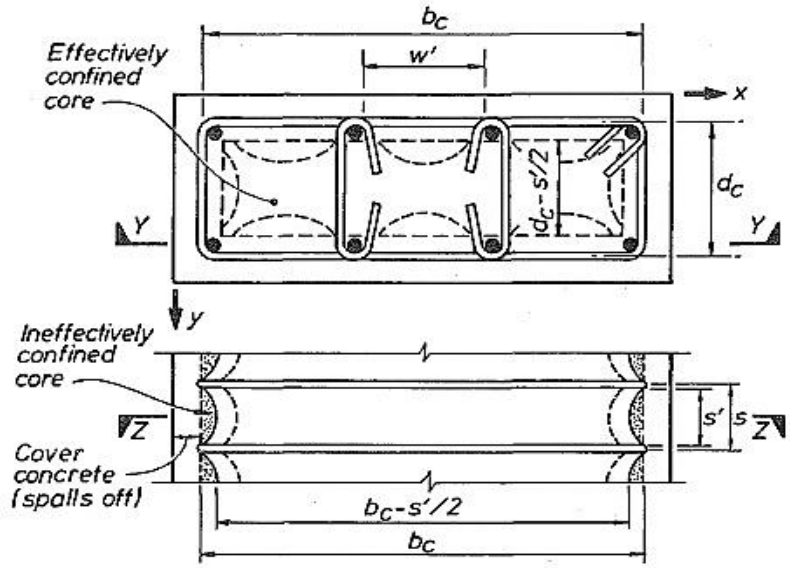

Figure 3.22: Effectively Confined Core for Rectangular Hoop Reinforcement (Mander et al. ,1988)

3.7.2 Kinematic Nonlinear Steel Model

The bilinear with parabolic strain hardening model is utilized for reinforcement having strain hardening 0.01 and ultimate strain capacity 0.05. This model is typically used to describe the stress strain behavior of longitudinal steel in pure tension (or compression). The model is based on an elastic-perfectly plastic, parabolic strain hardening type behavior. The stress-strain model is illustrated in Figure 3.23.

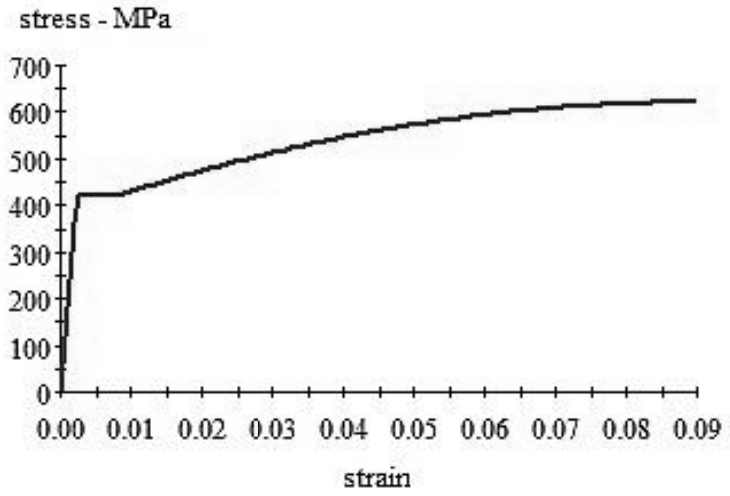

Figure 3.23: Stress Strain Curve for Steel

3.7.3 Lam and Teng's Stress-Strain Model for FRP Confined Concrete

Based on a review of previous models and their large strain database, Lam and Teng (2003b) recently proposed a simple but accurate stress-strain model [22]. Lam and Teng (2003b) established the following stress-strain model for FRP confined concrete

$$f_c = E_c\varepsilon_c - \frac{(E_c - E_2)^2}{4f_c^{'}}\varepsilon_c^2 \qquad \text{for } 0 \le \varepsilon_c \le \varepsilon_t^{'} \tag{3.14}$$

and

$$f_c = f_c^{'} + E_2\varepsilon_c \qquad \text{for } \varepsilon_t^{'} \le \varepsilon_c \le \varepsilon_{ccu} \tag{3.15}$$

Equation defines a stress-strain curve (Figure 3.24) consisting of a parabolic first portion and a linear second portion with a smooth transition at ε_t which is given by

$$\varepsilon_t^{'} = \frac{2f_c^{'}}{(E_c - E_2)} \tag{3.16}$$

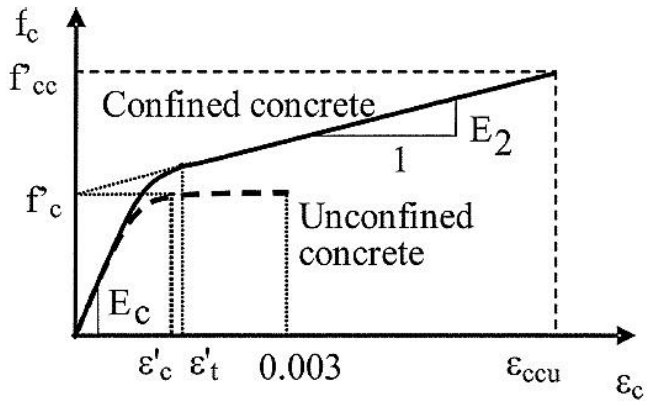

Figure 3.24: Lam and Teng's stress-strain model of FRP –confined concrete (Lam and Teng 2003a)

where E_2 is the slope of the linear second portion, given by

$$E_2 = \frac{f_{cc}^{'} - f_c^{'}}{\varepsilon_{ccu}} \tag{3.17}$$

Eq.3.19 gives the value of $f_{cc}^{'}$ (maximum confined concrete compressive strength) and f_l (maximum confinement pressure) and by adding ψ_f = 0.95 (Lam and Teng 2003).

$$f_{cc}^{'} = f_c^{'} + \psi_f 3.3\kappa_a f_l \tag{3.18}$$

$$f_l = \frac{2E_f n t_f \varepsilon_{fe}}{D} \tag{3.19}$$

where, $f_c^{'}$ = unconfined concrete compressive strength

κ_a = the efficiency factor accounts for the geometry of the section,

D = equivalent circular cross sectional diameter for non-circular section and explained in section 3.7.3.2

In Eq.3.20, the effective strain level in the FRP at failure ε_{fe} is

$$\varepsilon_{fe} = \kappa_{\varepsilon}\varepsilon_{fu} \tag{3.20}$$

κ_{ε}=Premature failure strain efficiency factor for FRP

Minimum value of κ_{ε} is 0.55 and confinement ratio $f_l / f_c^{'}$ is 0.08. These minimum values (that is, $f_{fu} n t_f / f_c^{'} D \geq 0.073$) should be used. It is the minimum level of confinement required to assure a non-descending second branch in the stress-strain performance, as shown by Curve (d) in Figure 3.25.

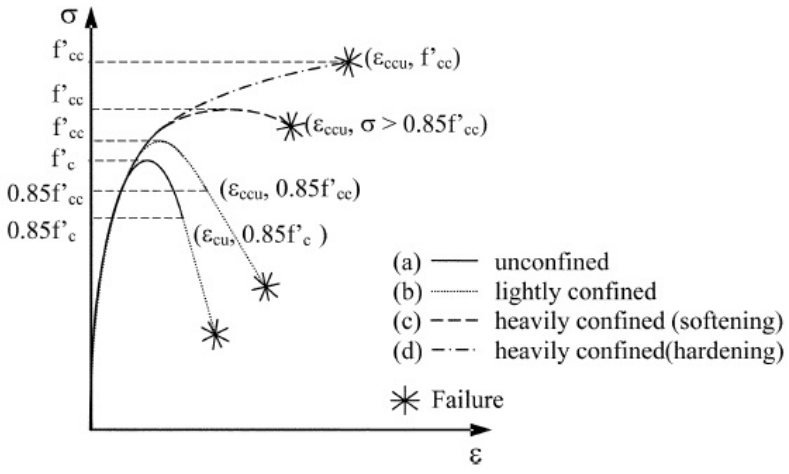

Figure 3.25: Schematic stress-strain behavior of unconfined and confined RC columns

Eq.3.21 gives ε_{ccu} the maximum compressive strain in FRP confined concrete. ε_{ccu} should not be greater than the limit in Eq. 3.22

$$\varepsilon_{ccu} = \varepsilon_c^{'}\left[1.50 + 12\kappa_b \frac{f_l}{f_c^{'}}\left[\frac{\varepsilon_{fe}}{\varepsilon_c^{'}}\right]^{0.45}\right] \tag{3.21}$$

κ_b = the efficiency factor accounts for the geometry of the section

$$\varepsilon_{ccu} \leq 0.01 \tag{3.22}$$

- **FRP Jacketing of Circular Sections**

FRP jackets give more confinement to circular sections. For circular cross sections, the shape factors κ_a and κ_b in Eqs. 3.18 and 3.21, respectively, can be taken as 1.0.

- **FRP Jacketing of Non-circular Sections**

Different studies showed that FRP jacketing increases marginal axial capacity of square and rectangular sections.

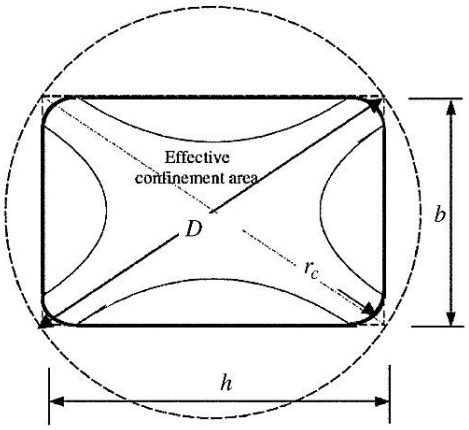

Figure 3.26: Equivalent Circular Cross Section (Lam and Teng 2003b)

$$D = \sqrt{b^2 + h^2} \tag{3.23}$$

The shape factors κ_a and κ_b is obtained using Eqs. 3.24 and 3.25.

$$\kappa_a = \frac{A_e}{A_c}\left[\frac{b}{h}\right]^2 \tag{3.24}$$

A_e = effective confined concrete area

A_c confined concrete area

h/b = side aspect ratio

$$\kappa_b = \frac{A_e}{A_c}\left[\frac{b}{h}\right]^{0.5} \tag{3.25}$$

The generally accepted theoretical approach for the definition of A_e consists of four parabolas within which the concrete is fully confined, and outside of which negligible confinement occurs as shown in Figure 3.26. The shape of the parabolas and the resulting effective confinement area is a function of the dimensions of the column (b and h), the radius of the corners r_c, and the longitudinal steel reinforcement ratio ρ_g, and can be expressed as

$$\frac{A_e}{A_c} = \frac{1 - \dfrac{\left[\left[\dfrac{b}{h}\right](h-2r_c)^2 + \left[\dfrac{h}{b}\right](b-2r_c)^2\right]}{3A_g} - \rho_g}{1-\rho_g} \tag{3.26}$$

where

r_c is the corner radius

A_e is the effective confined area

A_c is the concrete area

ρ_g is the steel ratio

3.8 Shear Wall Modeling

Shear walls are modeled as 3D solid element, 2D shell element or as frame element. Detail of these element models are given in following section [17].

3.8.1 Finite Element Models

Nonlinear solid elements are used to model continuum finite element model available in software as ANSYS, ABAQUS, etc. Concrete is modeled based on the flow theory of plasticity, Von Mises yield criterion, isotropic hardening and associated flow rule.

3.8.2 Multilayer Shell Element Method

The shear wall is modeled using a smeared multi-layer shell elements. The shell element is composed of layers having thickness and each layer has its own properties as shown Figure 3.27.

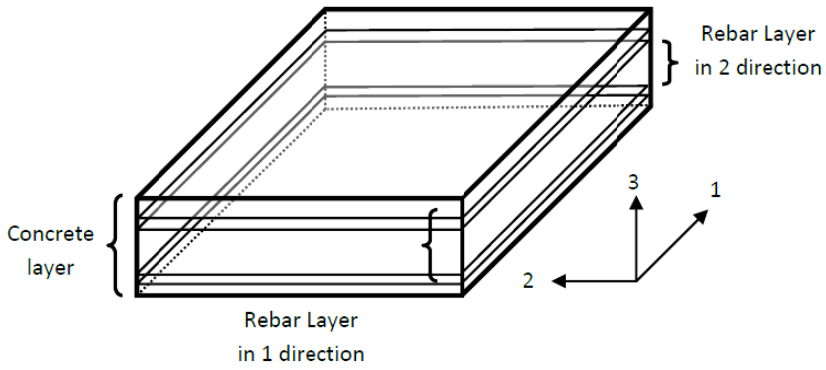

Figure 3.27: Multilayer Shell Elements (Fahjan et al. 2010)

Multilayer shell element is useful to model long and complex shear walls. Shell element has drilling moment problem. This problem is resolved by extending beams to the shell elements as shown in Figure 3.28.

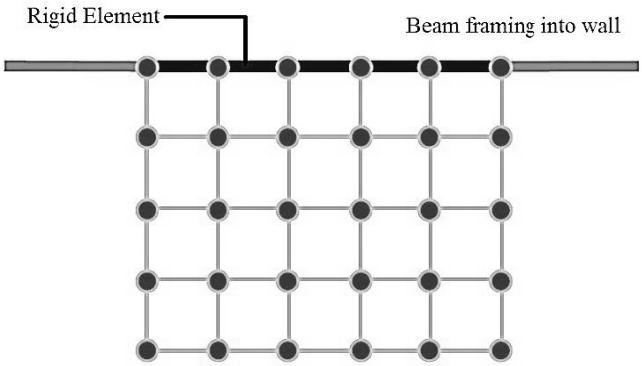

Figure 3.28: Shell Element Model for Shear Wall

3.8.3 Mid-Pier Method

In this approach shear wall is modeled using frame elements. Shear wall is taken as equivalent mid-pier and rigid beams as shown in Figure 3.29. Material properties of shear wall are modeled by having plastic hinge at the ends of mid-pier.

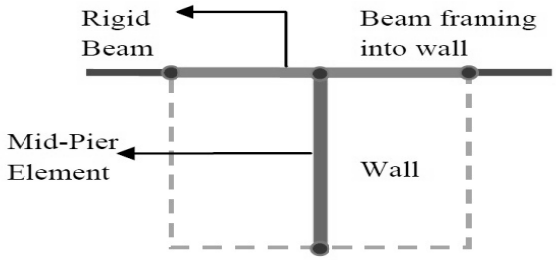

Figure 3.29: Mid pier Model for shear wall

Plastic hinge concept and moment-rotation relationship is considered to model nonlinear behavior of wall as shown in Figure 3.30.In this study Shell element and Mid-Pier approach is utilized to model shear walls.

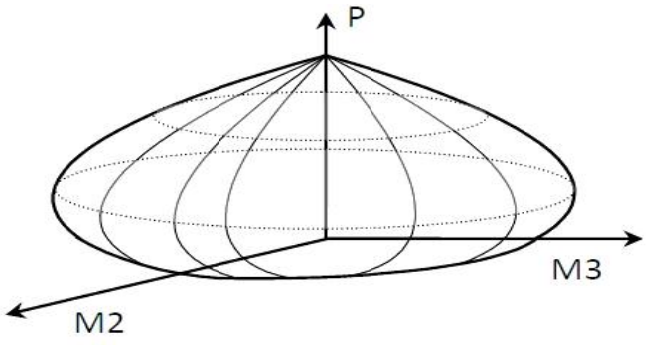

Figure 3.30: Interaction diagram for hinge in shear wall

CHAPTER 4

MODELLING OF EXISTING BUILDING FRAME

WITH SHEAR WALL USING SAP2000

4.1 Description of Building

The structure is an existing building located in Madinah, Saudi Arabia constructed in 1996.The building has eight stories with typical storey height 3.2m for five stories and the rest of three stories height are 4.2m,2.4m and 5m.Plan area of the building is 40 x 40 m. The building has a dome, reinforced concrete frame, elevator shafts and ribbed and flat slab systems at different floor levels. The building was designed according to ACI 318-89 specification. The typical plans of the building are shown in Figure 4.1.

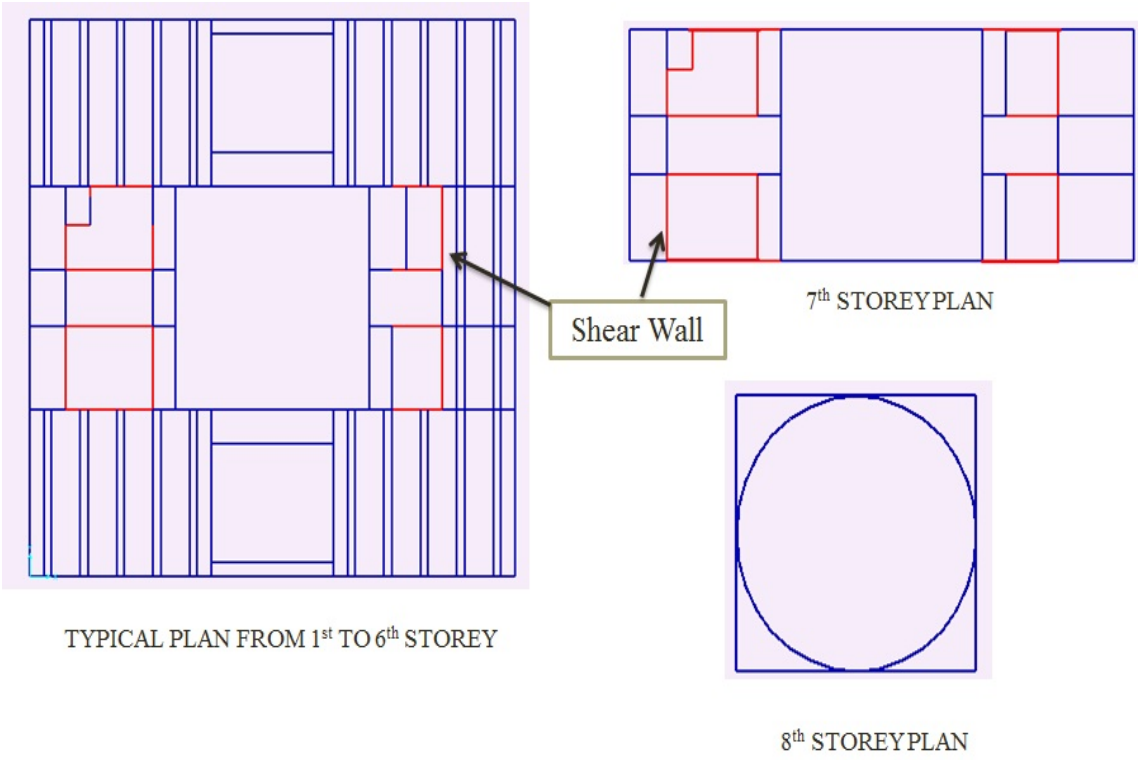

Figure 4.1: Typical Plan of Building

4.2 Frame Selected for Analysis

A typical planar shear wall frame has been selected to study the seismic performance of the building. The frame consists of two shear wall and 7 bays. Each storey has different sections of beams and columns. The Figure 4.2 shows a selected frame of existing building for analysis.

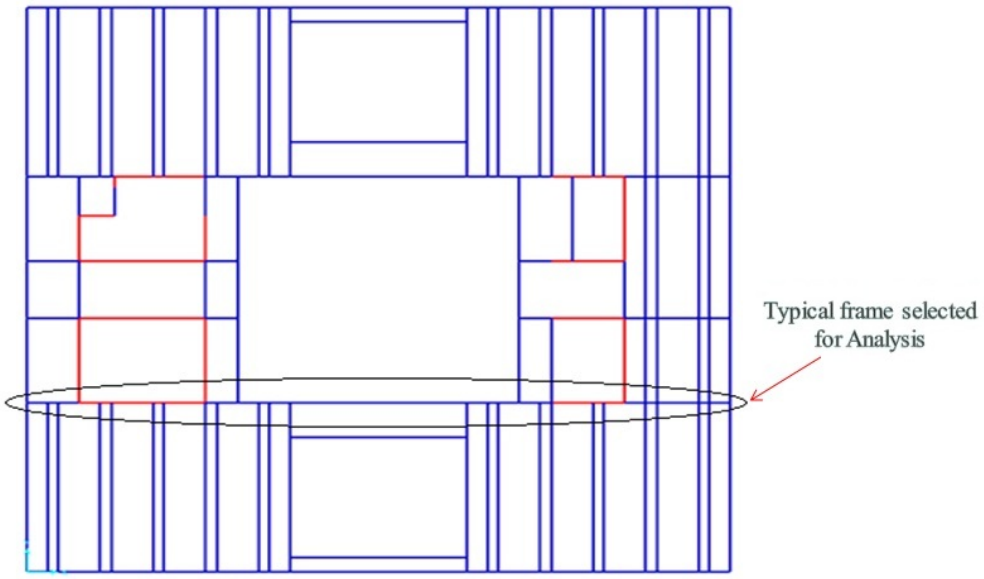

Figure 4.2: Selected Frame for Analysis

Figs. 4.3 and 4.4 shows elevation of the selected frame modeled with Shell Element and Mid-Pier models.

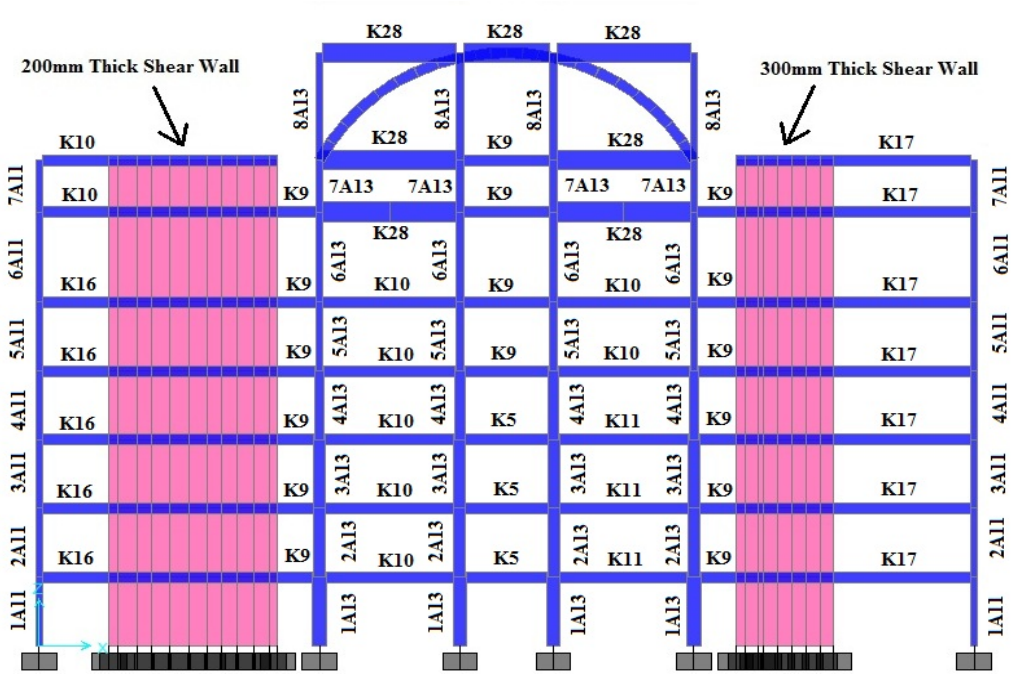

Figure 4.3: Elevation of Selected Frame Modeled Using the Shell Element Method

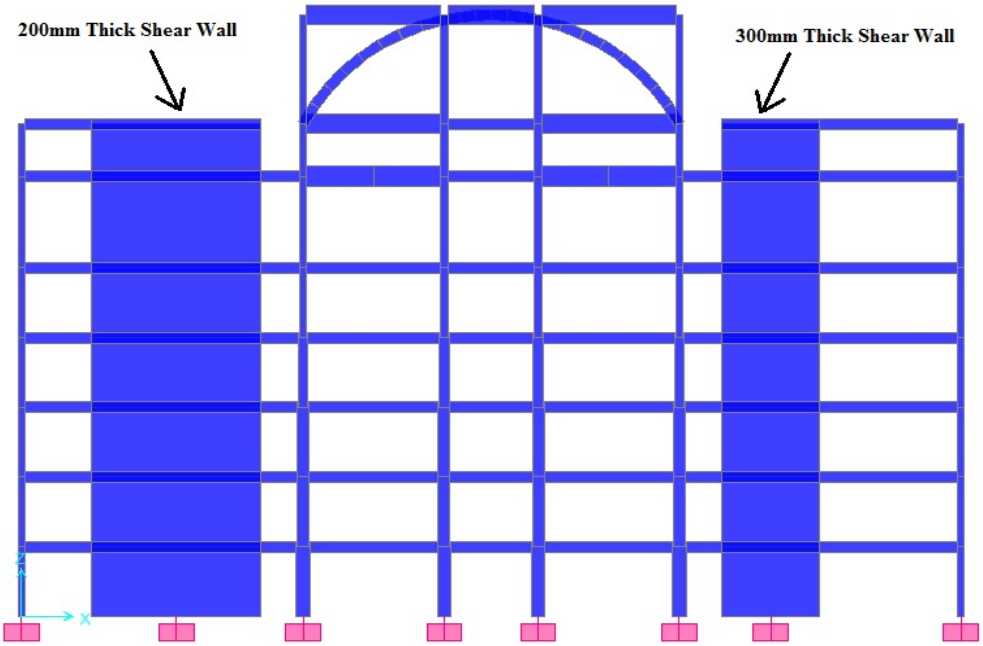

Figure 4.4: Elevation of Selected Frame Modeled Using Mid-Pier Method

4.3 Material Properties

The mechanical properties of reinforcement and concrete used in the design and maintained in the construction phase are shown in Table.4.1

Table 4.1: Material Properties for Structural Elements

Properties	MPa
Compressive Strength of concrete, $f_c^{'}$	30
Modulus of Elasticity of concrete, E_c	25743
Tensile strength of Rebar, f_y	420
Ultimate strength of Rebar, f_u	620
Modulus of Elasticity of steel, E_s	200000

4.4 Dimensions of the Structural Members

The dimension and reinforcements of the structural member sections are shown in Tables 4.2, 4.3 and 4.4.

Table 4.2: Shear Wall Reinforcement Details

Shear Wall	Width (mm)	Length (mm)	Vertical Reinforcement	Horizontal Reinforcement
SW200	200	7200	Φ12 @ 200mm	Φ12 @ 200mm
SW300	300	4200	Φ12 @ 200mm	Φ12 @ 200mm

Table 4.3: Column Dimensions and Reinforcement Details

Column	b (mm)	h (mm)	Longitudinal Reinforcement	Ties
1A13	300	600	14Φ22	3Φ10 @ 142mm
2A13	300	500	12Φ22	3Φ10 @ 142mm
3A13	300	500	12Φ22	3Φ10 @ 142mm
4A13	300	400	10Φ16	2Φ10 @ 167mm
5A13	300	300	8Φ16	2Φ10 @ 200mm
6A13	300	300	8Φ16	2Φ10 @ 200mm
7A13	300	300	8Φ16	2Φ10 @ 200mm
8A13	300	300	8Φ16	2Φ10 @ 200mm
1A11	300	600	14Φ22	2Φ10 @ 167mm
2A11	300	600	14Φ20	2Φ10 @ 167mm
3A11	300	600	14Φ20	2Φ10 @ 167mm
4A11	300	400	10Φ16	2Φ10 @ 167mm
5A11	300	300	8Φ16	2Φ10 @ 200mm
6A11	300	300	8Φ16	2Φ10 @ 200mm
7A11	300	300	8Φ16	2Φ10 @ 200mm

Table 4.4:Beam Dimensions and Reinforcement Details

Beam	b (mm)	h (mm)	Bottom Reinforcement	Top Reinforcement			Stirrups
				Mid span	Left support	Right support	
K5	200	500	3Φ14	3Φ25	3Φ25	3Φ25	Φ8 @ 200mm
K9	300	500	3Φ16	6Φ25	6Φ25	6Φ25	Φ10 @ 150mm
K10	300	500	3Φ25	3Φ16	6Φ25	3Φ22	Φ10 @ 100mm
K11	300	500	3Φ25	3Φ16	3Φ25	6Φ25	Φ10 @ 100mm
K16	500	500	8Φ20	4Φ14	4Φ14	4Φ14	Φ8 @ 100mm
K17	500	500	11Φ25	6Φ20	6Φ20	6Φ20	Φ8 @ 50mm
K28	300	900	4Φ25	4Φ16	4Φ16	4Φ16	Φ8 @ 200mm

4.5 Gravity Loads

The loads on the frame are according to the Saudi Building Code for Loads and Forces Requirements (SBC 301) [23]. Dead and live loads used in the design are summarized in Table 4.5. Dead loads consist of the weight of slabs, flooring for a selected frame, flooring for the roof, internal partitions and electromechanical devices. It should be noted that SAP2000 analysis program automatically estimates the own weight of the structural elements and include it in the elastic analysis.

Table 4.5: Applied load on Structure

Load Description	Load value (KN/m^2)
Slab (0.1 m)	2.375
Flooring for typical floors	0.935
Flooring for the roof	1.425
Super Imposed Load (Includes Partition, electro-mechanical utilities, false ceiling etc.)	0.5
Live loads for typical floors	4.8
Live loads for roof	2.4

Figs. 4.5 and 4.6 show the applied dead load on the typical existing frame for Shell element and Mid-Pier model.

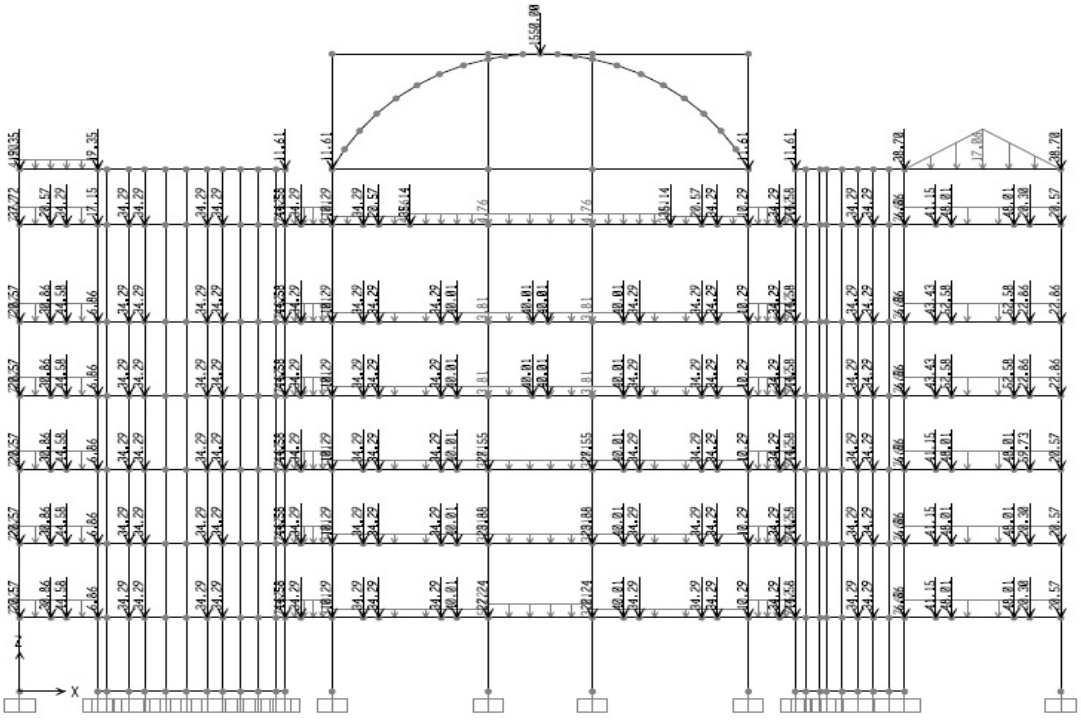

Figure 4.5: The Dead Load Acting on the Frame Modeled Using Shell Element Model

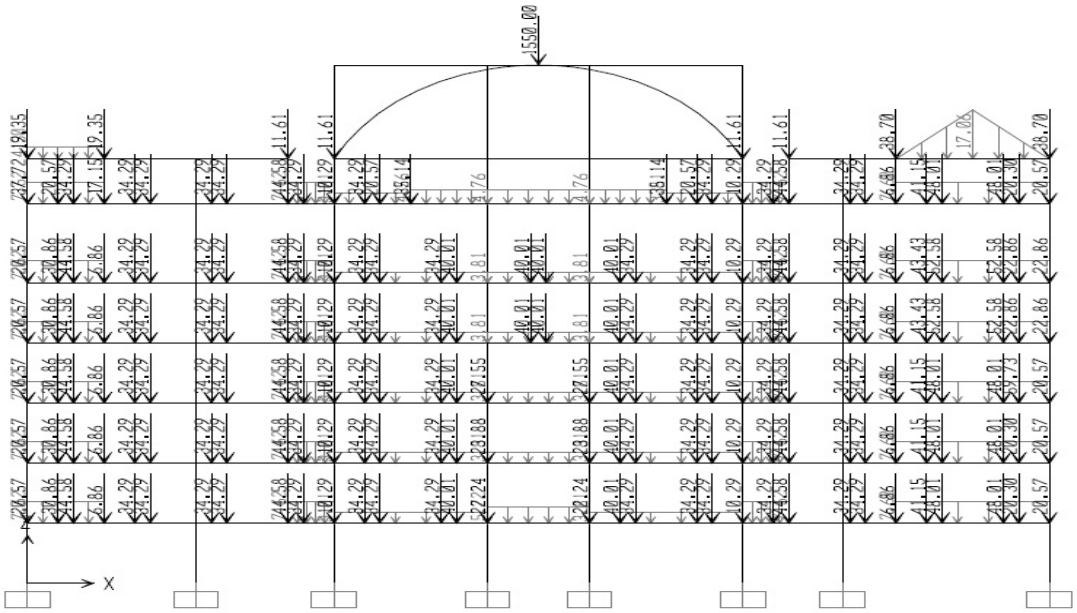

Figure 4.6: The Dead Load Acting on the Frame Modeled Using Mid-Pier Model

Figs. 4.7 and 4.8 show the applied live load on the typical existing frame for Shell element and Mid-Pier model.

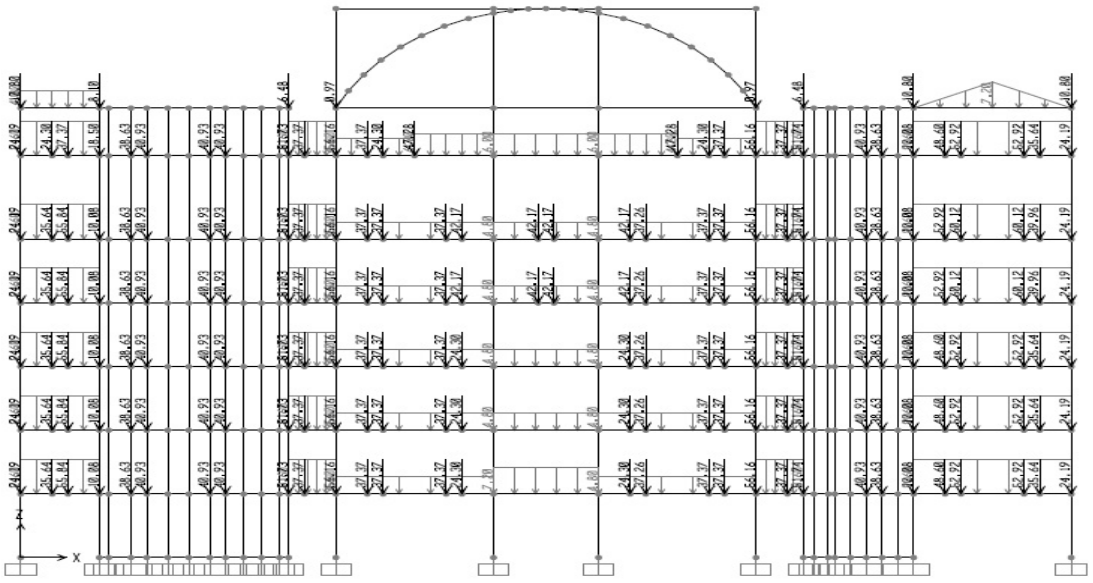

Figure 4.7: Live Load acting on the Frame Modeled Using Shell Element Model

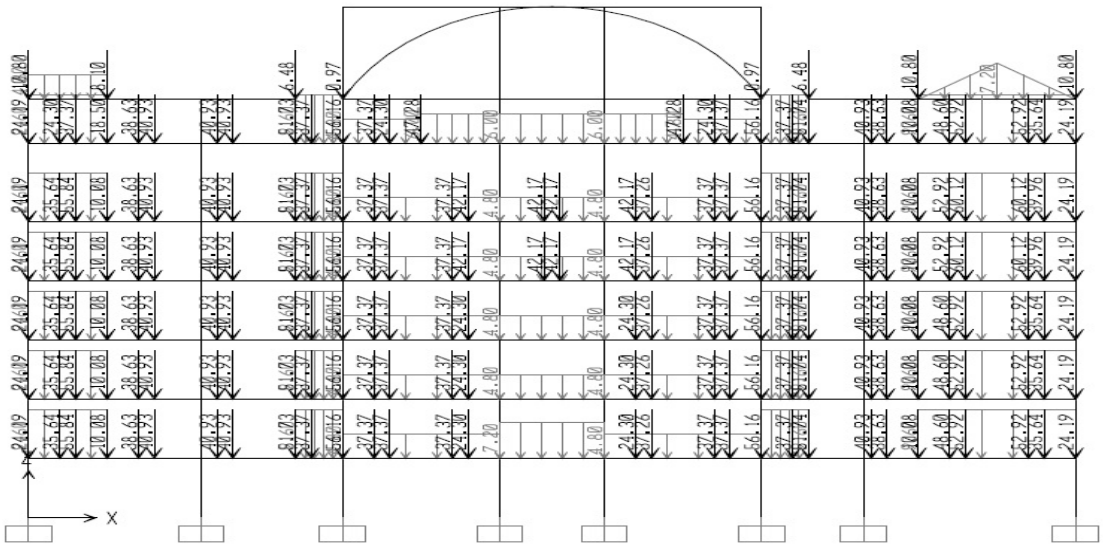

Figure 4.8: Live Load Acting on the Frame Modeled Using Mid-Pier Model

4.6 Fundamental Time Period of Typical Frame

The fundamental time period of the frame is determined by carrying out modal analysis of frame in SAP2000.The time period and frequencies of the first three modes obtained from SAP2000 are shown in Table 4.6.

Table 4.6: Modal Time Period and Frequency for Shell Element and Mid-Pier Model

Modal Properties	Mode		
	1	2	3
Period (sec)	0.612	0.296	0.201
Frequency(rad/sec)	1.634	3.374	4.967

Figs. 4.9, 4.10 and 4.11 shows first three mode shapes of the typical frame for Shell element model.

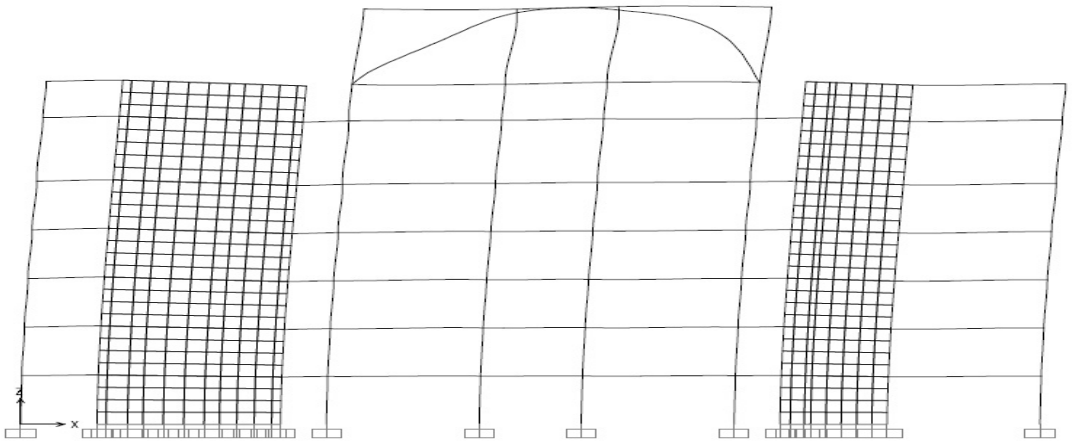

Figure 4.9: 1st Mode Shape of Frame for Shell Element Model

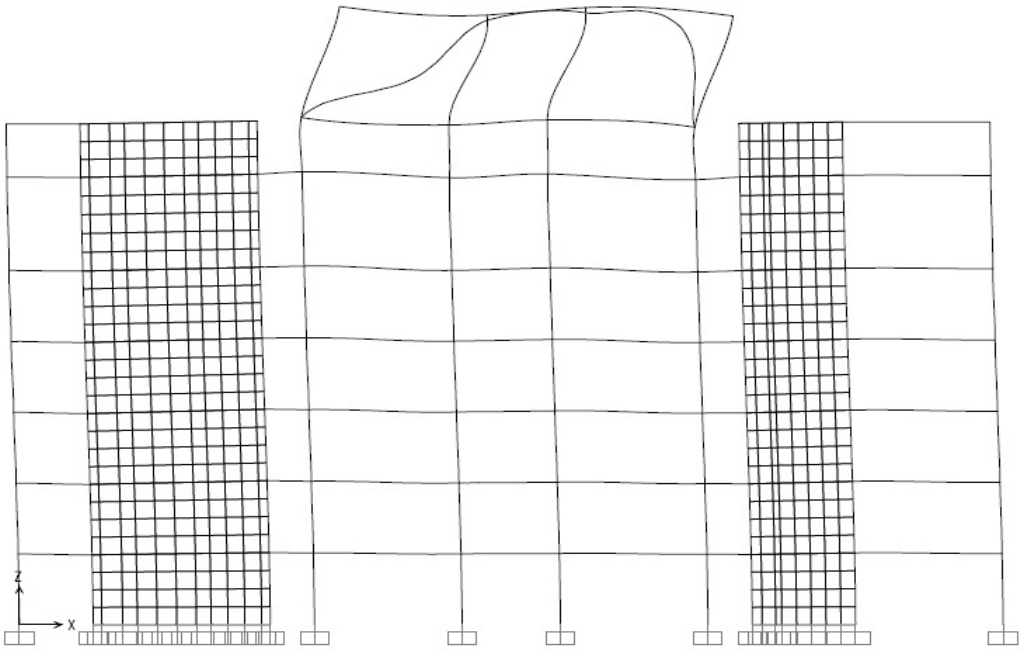

Figure 4.10: 2nd Mode Shape of Frame for Shell Element Model

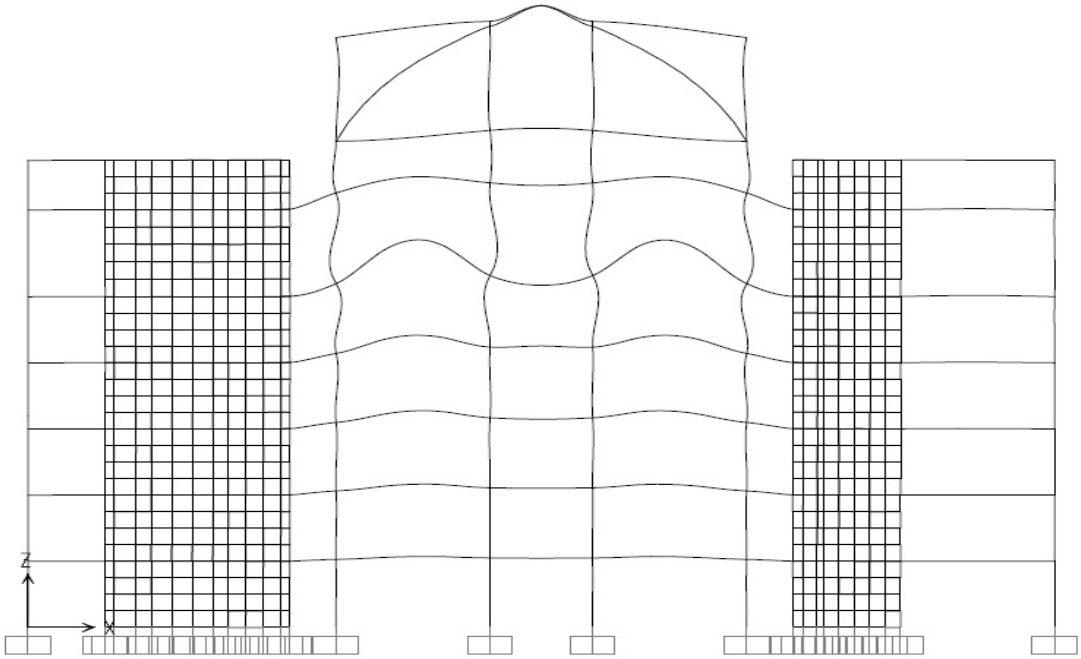

Figure 4.11: 3rd Mode Shape of Frame for Shell Element Model

Figs. 4.12, 4.13 and 4.14 shows first three mode shapes of the typical frame for Mid-Pier model.

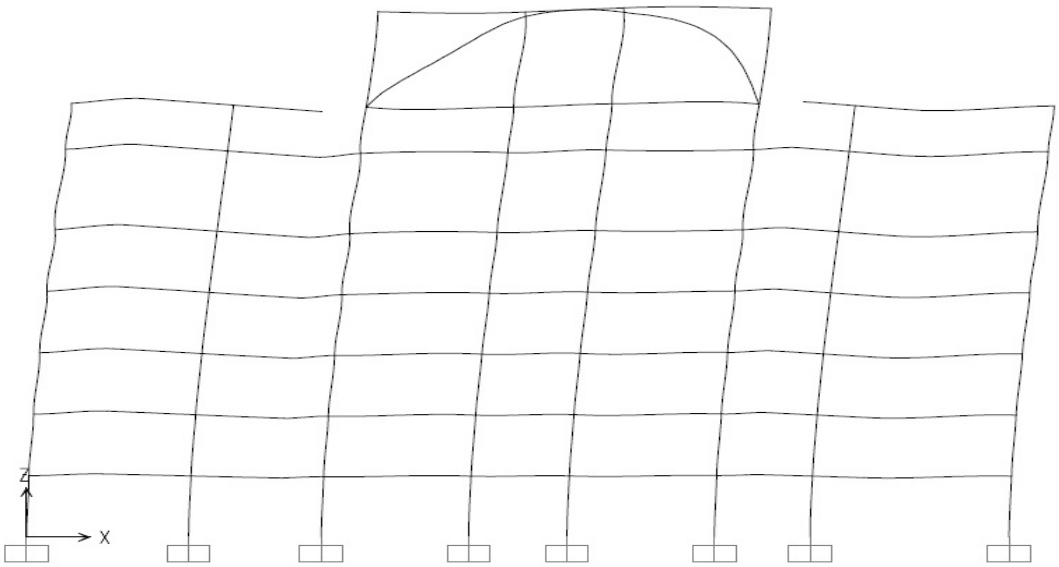

Figure 4.12: 1st mode shape of frame for Mid-Pier model

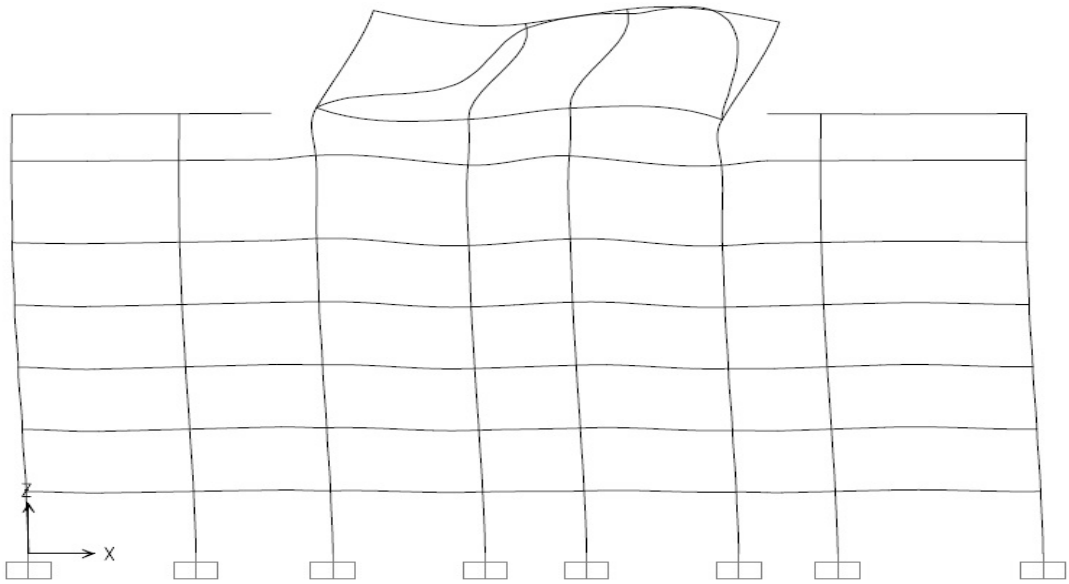

Figure 4.13: 2nd Mode Shape of Frame for Mid-Pier Model

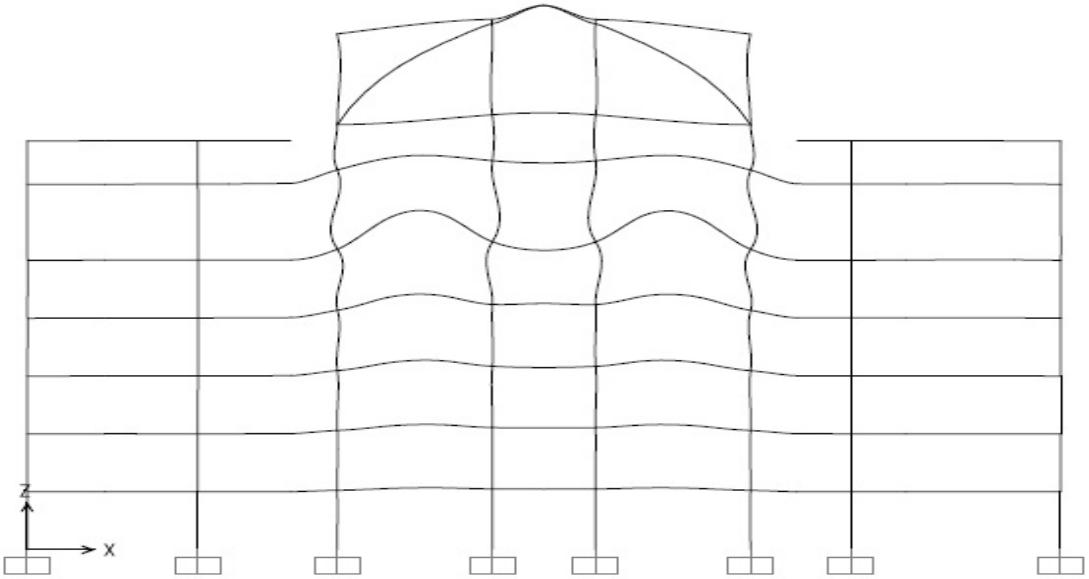

Figure 4.14: 3rd Mode Shape of Frame for Mid-Pier Model

4.7 Response Spectrum

According to SBC 301 the response spectrum curve shall be developed as indicated in Figure 4.15 [23].

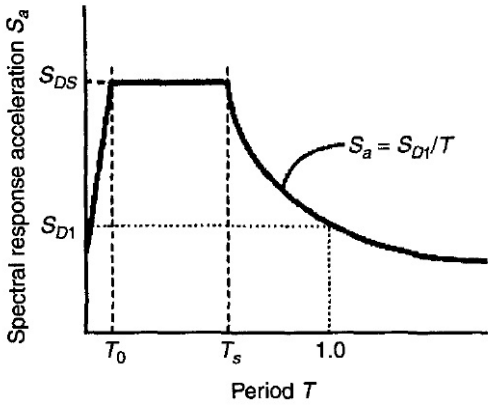

Figure 4.15: Response Spectrum Curve

Following are the steps involved to determine the response spectrum [23]:

1. For periods less than or equal to T_o, the design spectral response acceleration, S_a, shall be taken as given by Eq.4.1.

$$S_a = S_{DS}\left(0.4 + 0.6\frac{T}{T_o}\right) \tag{4.1}$$

2. For periods greater than or equal to T_o and less than or equal to T_s, the design spectral response acceleration, S_a, shall be taken as equal to S_{DS}.
3. For periods greater than T_s, the design spectral response acceleration, S_a, is given by Eq.4.3.

$$T_o = 0.2\ S_{D1}/S_{DS} \tag{4.2}$$

$$T_s = S_{D1}/S_{DS} \tag{4.3}$$

S_{DS}= the design spectral response acceleration at short periods

S_{D1} = the design spectral response acceleration at 1-sec period, in units of g-sec

T = the fundamental period of the structure (sec)

4. Spectral response acceleration at short periods, S_{DS} and at 1-sec period are determined from Eqs.4.4 and 4.5

$$S_{DS} = \frac{2}{3} S_{MS} \tag{4.4}$$

$$S_{D1} = \frac{2}{3} S_{M1} \tag{4.5}$$

where

S_{MS} and S_{M1} are the maximum considered earthquake spectral response acceleration for short periods and at 1-sec.S_{MS} and S_{S1} are determined by Eqs.4.6 and 4.7

$$S_{MS} = F_a S_s \tag{4.6}$$

$$S_{M1} = F_v S_1 \tag{4.7}$$

where

S_s and S_1 are the mapped maximum considered earthquake spectral response acceleration at short periods and at 1-sec and for Madinah S_s and S_1 are 0.3 and 0.11. F_a and F_v are defined in Tables 4.7 and 4.8 [23]. Values of F_a and F_v for intermediate values of S_s and S_1 are determined by straight-line interpolation.

Table 4.7: Values of F_a Function of Site Class and Mapped Short Period Maximum Considered Earthquake Spectral Acceleration

Site Class	Mapped Maximum Considered Earthquake Spectral Response Acceleration at Short Periods				
	$S_s \leq 0.25$	$S_s = 0.5$	$S_s = 0.75$	$S_s = 1.0$	$S_s \geq 1.25$
A	0.8	0.8	0.8	0.8	0.8
B	1.0	1.0	1.0	1.0	1.0
C	1.2	1.2	1.1	1.0	1.0
D	1.6	1.4	1.2	1.1	1.0

Table 4.8: Values of F_v Function of Site Class and Mapped 1-Second Period Maximum Considered Earthquake Spectral Acceleration

Site Class	Mapped Maximum Considered Earthquake Spectral Response Acceleration at 1-Second Periods				
	$S_1 \leq 0.1$	$S_1 = 0.2$	$S_1 = 0.3$	$S_1 = 0.4$	$S_1 \geq 0.5$
A	0.8	0.8	0.8	0.8	0.8
B	1.0	1.0	1.0	1.0	1.0
C	1.7	1.6	1.5	1.4	1.3
D	2.4	2.0	1.8	1.6	1.5

By following all these steps the response spectrum for the structure is developed and shown in Figure 4.16.

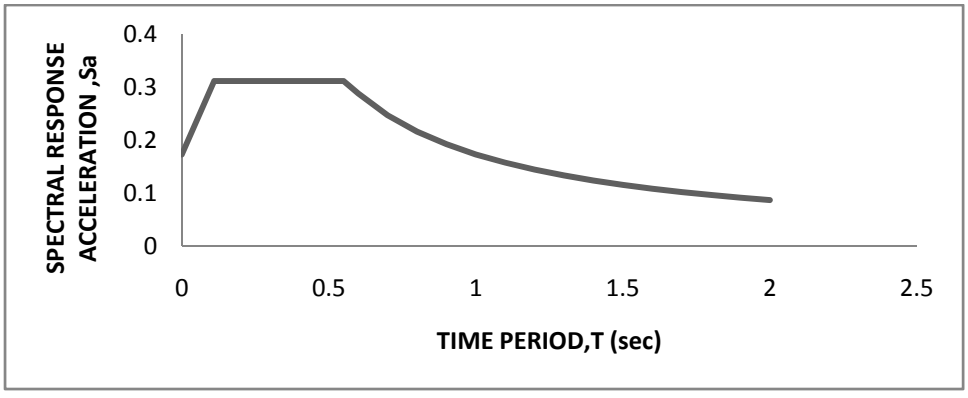

Figure 4.16: Design Response Spectrum for Structure

4.8 Seismic Loads

The seismic loads on the existing frame are determined according to SBC 301. The equivalent static approach is applied on the frame. Hence, a brief description for the procedure in code will be discussed in this section followed by the ratio of the base shears relative to the total weight of the frame.

4.8.1 Seismic Load Parameters

Earthquake characteristics of the existing building frame according to Saudi Building Code (SBC 301) and Uniform Building Code (UBC-1997) are shown in the Table 4.9.

Table 4.9: Seismic Parameters for Frame

Description	**SBC301**	**UBC-1997**
Seismic Zone	Region 3	2B
Building Importance factor, I	1.25	1.25
Local Site class	D(Stiff soil)	D(Stiff soil)
Structural behavior response factor, R	6.5	8.5
Live load participation factor, n	0.25	0.25

4.8.2 Seismic Weight

The Seismic weight of the whole building is the sum of the seismic weights of all the floors. The seismic weight of frame is shown in Table 4.10.

Table 4.10: Seismic Weight Acting On Each Storey

Storey	Floor height (m)	Dead load (kN)	25% Reduced Live Load (kN)	Seismic weight (kN)
8	27.6	1871.258	0	1871.26
7	22.6	800.3979	27.3699	827.77
6	20.2	1653.672	386.2197	2039.90
5	16	1795.328	448.4151	2243.74
4	12.8	1793.562	448.5132	2242.10
3	9.6	1814.556	405.5454	2220.10
2	6.4	1785.911	405.5454	2191.46
1	3.2	1799.252	408.2922	2207.54
				$\sum W_i$= 15843.84

4.8.3 Base Shear Calculation

According to SBC 301 the seismic base shear (V) in a given direction shall be determined in accordance with the Eq.4.8 [23].

$$V = C_s W \tag{4.8}$$

where

Cs = the seismic response coefficient

W = the total dead load

When the fundamental period of the structure is computed, the seismic design coefficient (C_s) shall be determined in accordance with the following Eq.4.9.

$$C_s = \frac{S_{DS}}{R/I} \tag{4.9}$$

S_{DS} = 0.312(from response spectrum)

$$C_s = \frac{0.312}{6.5/1.25} = 0.06$$

The value of the seismic response coefficient, (*Cs*), need not be greater than the Eq.4.10.

$$C_s = \frac{S_{D1}}{T(R/I)} \tag{4.10}$$

S_{D1} = 0.173 (from response spectrum)

$$C_s = \frac{0.173}{0.612(6.5/1.25)} = 0.054 \text{ (Governs)}$$

but shall not be taken less than

$$Cs = 0.044 S_{DS} I \tag{4.11}$$

$$C_s = 0.044\text{x}0.312\text{x}1.25 = 0.01716$$

The base shear V acting on the frame in the earthquake direction considered is determined by Eq.4.8.

$$V = 0.054\text{x}15843.84 = 861.3 \text{ kN}$$

4.8.4 Vertical Distribution of Seismic Forces

The lateral seismic force (F_x) induced at any level shall be determined from the following Eqs.4.12 and 4.13 [23].

$$F_x = C_{vx} V \tag{4.12}$$

$$C_{vx} = \frac{w_x h_x^k}{\sum_{i=1}^{n} w_x h_i^k} \tag{4.13}$$

where

C_{vx} = vertical distribution factor

V = base shear(kN)

w_i and w_x= gravity load applied to level i or x

h_i and h_x= the height (m) upto level i or x

k = an exponent related to the structure period as follows:

for period of 0.5 sec or less, k = 1

for period of 2.5 sec or more, $k = 2$

for period between 0.5 and 2.5 seconds

By interpolation the value of k determined is 1.056.Using Eqs. 4.12 and 4.13 the seismic loads acting on each floor level of the frame is calculated and are shown in Table 4.11.

Table 4.11: Seismic Load Acting at Each Floor Level

Storey	**Seismic weight W(kN)**	**Height h(m)**	**$h^{1.056}$ (m)**	**W x $h^{1.056}$ (kN-m)**	**Loads F_x(kN)**
8	1871.25	5	5.47	10238.73	156.05
7	827.76	2.4	2.52	2086.48	31.80
6	2039.89	4.2	4.55	9284.50	141.50
5	2243.74	3.2	3.42	7663.22	116.80
4	2242.07	3.2	3.42	7657.53	116.71
3	2220.10	3.2	3.42	7582.50	115.56
2	2191.45	3.2	3.42	7484.64	114.07
1	2207.54	3.2	3.42	7539.60	114.91
	$\sum W_i$ =15843.83			$\sum_{i=1}^{n} w_x h_i^k$ =59537.15	

Figs. 4.17 and 4.18 shows the seismic loads acting on the typical existing frame modeled by shell element and Mid-Pier approach.

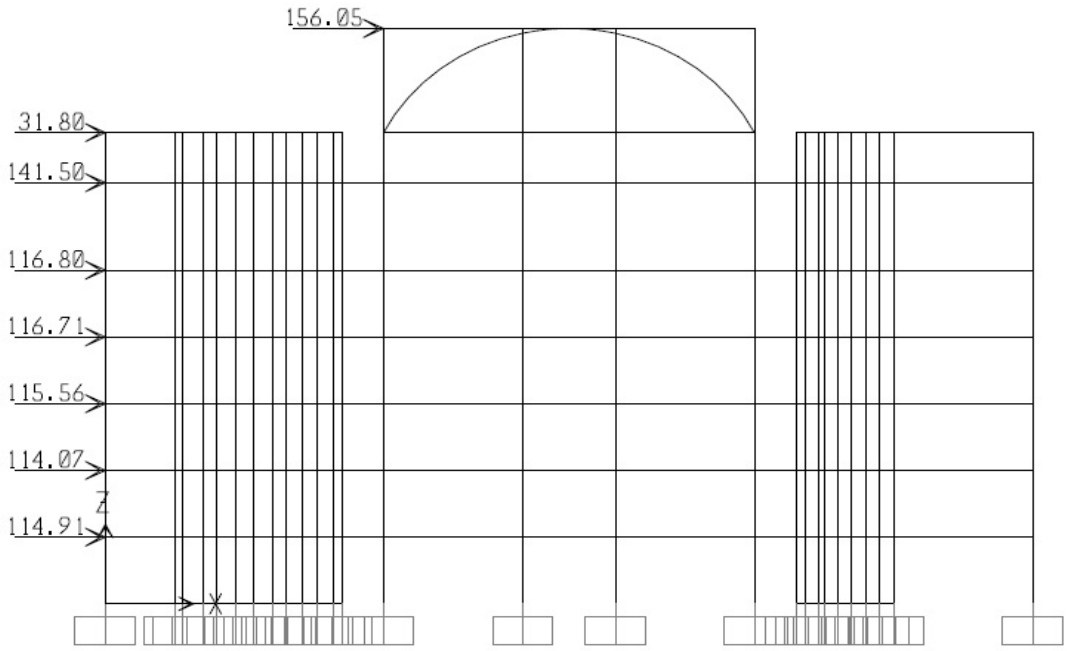

Figure 4.17: The Seismic Load acting on the Frame Modeled Using Shell Element Approach

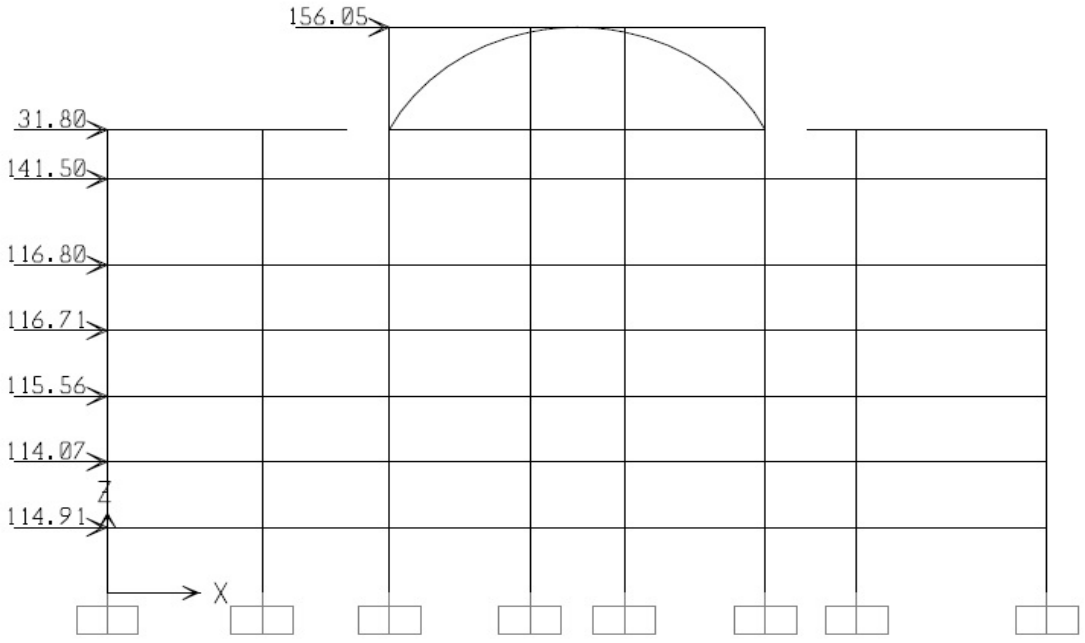

Figure 4.18: The Seismic Load acting on the Frame Modeled Using Mid-Pier Approach

CHAPTER 5

NONLINEAR STATIC PUSHOVER ANALYSIS OF THE SHEAR WALL FRAME

5.1 Introduction

Nonlinear static pushover analysis is a special procedure used in performance based design for seismic loading in order to demonstrate how building really work by identifying modes of failure and potential for progressive collapse. It will be helpful to understand how structures will behave when subjected to earthquakes, where it is assumed that the elastic capacity of the structure will be exceeded.

To evaluate the performance of the typical existing frame, nonlinear static pushover analysis is used which includes the capacity spectrum method (CSM) that uses the intersection of the capacity (pushover) curve and a reduced response spectrum to estimate maximum displacement.

To obtain the pushover curves of the existing frame, SAP2000 structural analysis program is utilized. In pushover analysis of the structure, the plastic hinges hypotheses

are taken into consideration. In that hypothesis, plastic deformations are considered to gather at critical sections called plastic hinge zone and other parts behave linear elastic.

5.2 Effective Flexural Stiffness of Frame Element

According to ATC-40, FEMA-256 and ASCE-2006, the effective flexural stiffness concerning the cracked section of the structural members will be used in Pushover analysis. A non-linear static analysis will be performed using the flexural stiffness of the uncracked sections by considering the vertical loads compatible with storey lumped mass (1D+0.025L). The axial loads obtained from this analysis will be used for calculating the effective flexural stiffness values of beams, columns and walls.

According to ASCE 2006 effective flexural stiffness for different members can be determined as shown in the Table 5.1 [24].

Table 5.1: Effective Stiffness Values

Component	**Flexural Rigidity**	**Shear Rigidity**	**Axial Rigidity**
Beams Nonprestressed	0.3 E_cI_g	$0.4E_cA_w$	-
Beams pre-stressed	E_cI_g	$0.4E_cA_w$	-
Columns $P_u \geq 0.5\ A_g f_c^{'}$	0.7 E_cI_g	$0.4E_cA_w$	E_cA_g
Columns $P_u \leq 0.1\ A_g f_c^{'}$ or with tension	0.3 E_cI_g	$0.4E_cA_w$	E_cA_g

The effective stiffness values for columns are calculated by the linear interpolation method. These values are given in Table 5.2.

Table 5.2: Effective Flexural Stiffness Values Concerning the Crack Section of the Columns

Section	Axial load P(kN)	A_g (mm)	P/($A_c f_c^{'}$)	Effective Flexural Rigidity $(EI)_e$
1A13	1590.92	180000	0.29	0.494
2A13	1415.64	150000	0.31	0.515
3A13	1246.48	150000	0.28	0.477
4A13	1074.22	120000	0.30	0.498
5A13	869.091	90000	0.32	0.521
6A13	665.76	90000	0.25	0.447
7A13	554.161	90000	0.21	0.405
8A13	528.94	90000	0.20	0.396
1A11	1230.35	180000	0.23	0.428
2A11	1042.92	180000	0.19	0.393
3A11	852.85	180000	0.16	0.358
4A11	632.95	120000	0.18	0.376
5A11	441.61	90000	0.16	0.364
6A11	260.031	90000	0.10	0.30
7A11	90.41	90000	0.03	0.30

5.3 Definitions of Plastic Hinges

The maximum strain values of concrete 0.003 and steel 0.05 (considering strain hardening) according to FEMA 356 and ASCE 2006 are used for the definition of the interaction curves of plastic hinges at the member ends.

5.3.1 Definition of Plastic Hinges at Beam

The plastic moment values are calculated by using XTRACT software to define the internal force deformation co-relation. For Beam K28, the cross-section details are given in Figure 5.1, Mander unconfined concrete model is used at the outer zone from the transverse reinforcement and Mander confined concrete model is used for the core material. The stress-strain curves obtained from Mander unconfined and confined concrete model for beam K28 are shown in Figs. 5.2 and 5.3. Hardening of steel material is considered and typical stress-strain curve for steel is shown in Figure 5.4.

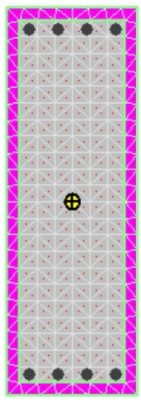

Figure 5.1: Beam K28 Cross sectional Detail

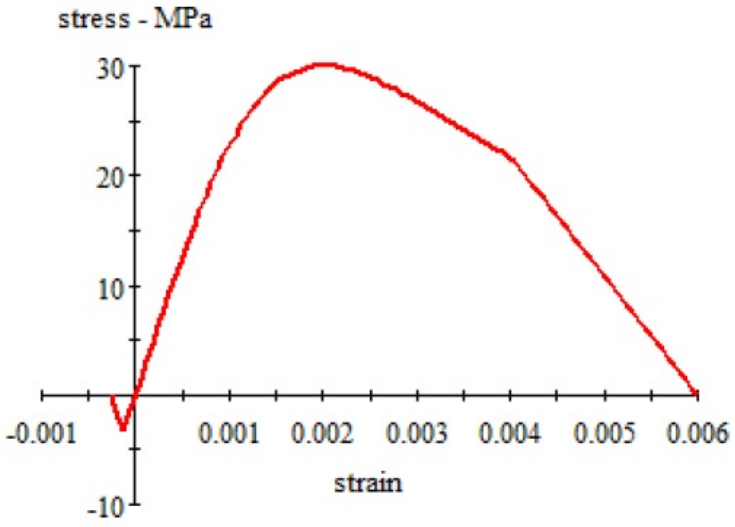

Figure 5.2: Mander Unconfined Concrete Model for Beam K28

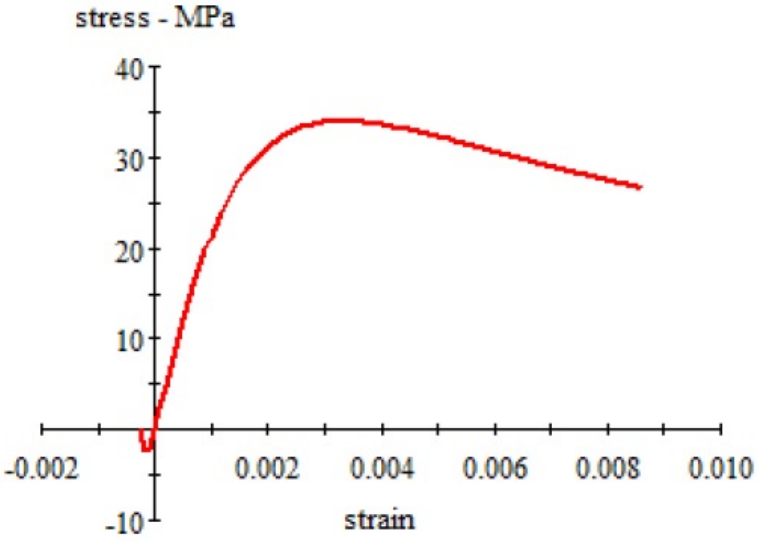

Figure 5.3: Mander Confined Concrete Model for Beam K28

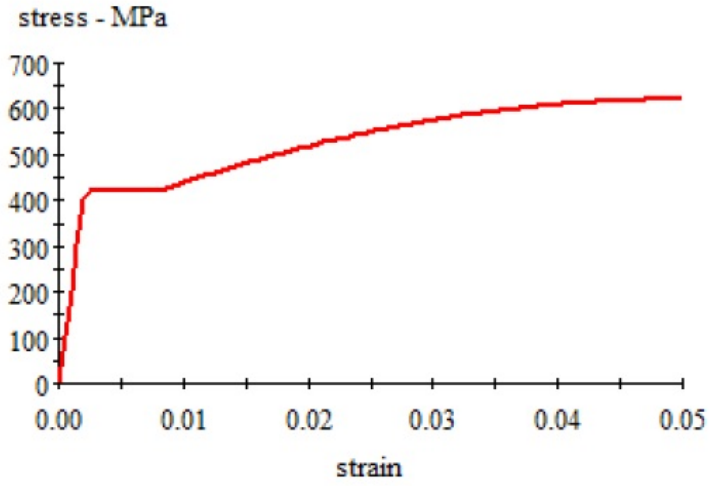

Figure 5.4: Steel Stress-Strain Curve for Beam K28

Internal force – deformation relation can be seen from Figure 5.5.

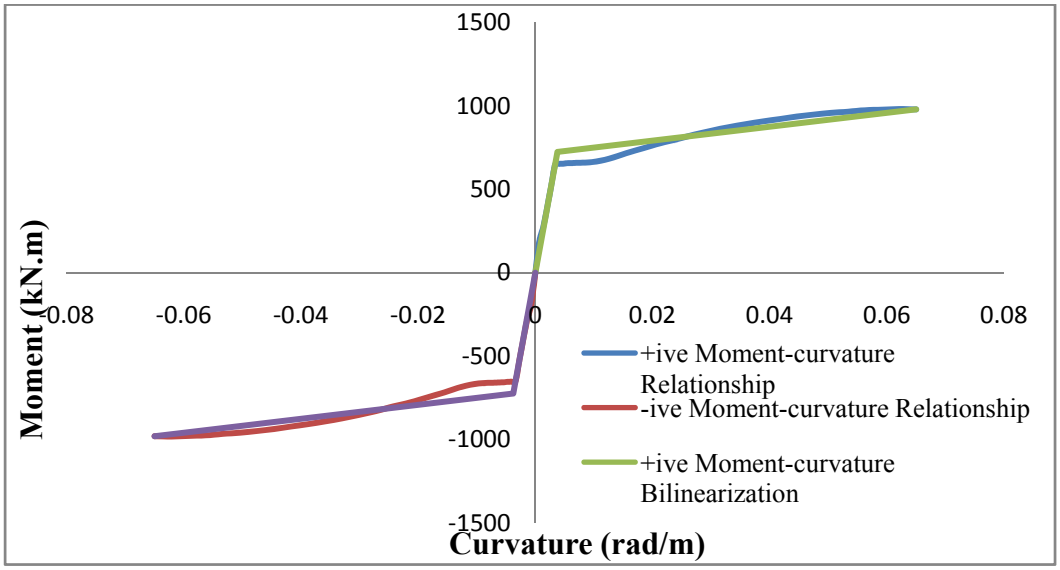

Figure 5.5: Beam K28 Moment-Curvature Graph

The moment-curvature obtained from XTRACT is converted into idealized moment-plastic rotation by using Eqs.5.1 and 5.2.

$$\phi_p = \phi_u - \phi_y \quad (5.1)$$

$$\theta_p = \phi_p . L_p \quad (5.2)$$

ϕ_p = Plastic Curvature

ϕ_u =Ultimate Curvature

ϕ_y =Yield Curvature

θ_p =Plastic hinge rotation

L_p =Plastic hinge length (L_p =0.5 times depth of the section)

The moment-rotation relation is introduced to the structural analysis program SAP200 which will perform the pushover analysis. Figure 5.6 shows the idealized moment rotation graph for beam K28.

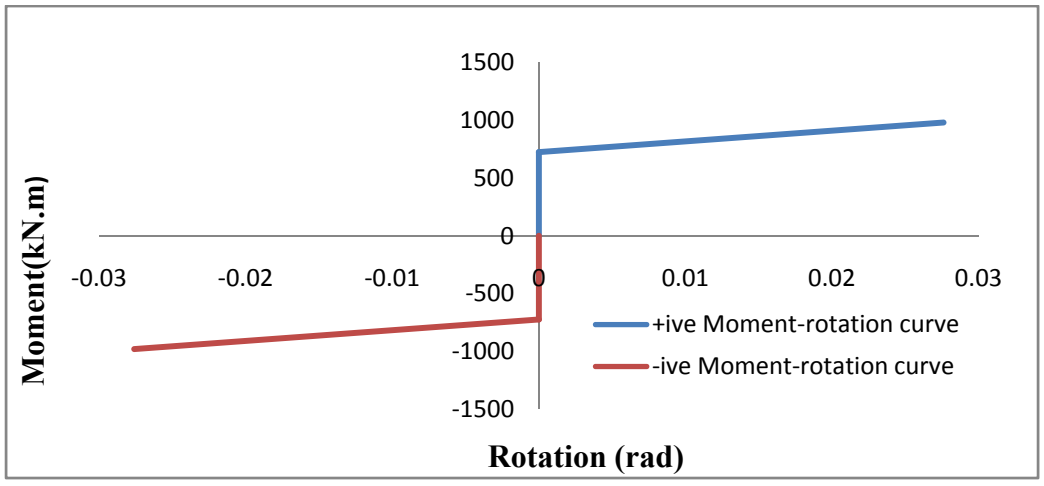

Figure 5.6: Beam K28 Moment-Rotation Idealized curve

5.3.2 Definition of Plastic Hinge at the Columns

Plastic cross-section surfaces are created by XTRACT cross-section analysis software program. For Column 1A13, the cross-section details are given in Figure 5.7, Mander unconfined concrete model is used at the outer zone from the transverse reinforcement and Mander confined concrete model is used for the core material. The stress-strain curves obtained from Mander unconfined and confined concrete model for column 1A13 are shown in Figs. 5.8 and 5.9. Hardening of steel material is considered and typical stress-strain curve for steel is shown in Figure 5.10.

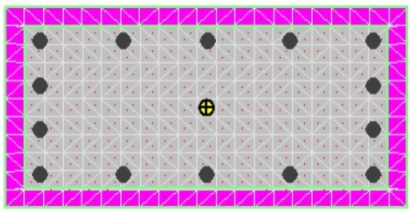

Figure 5.7: Column 1A13 Cross sectional Detail

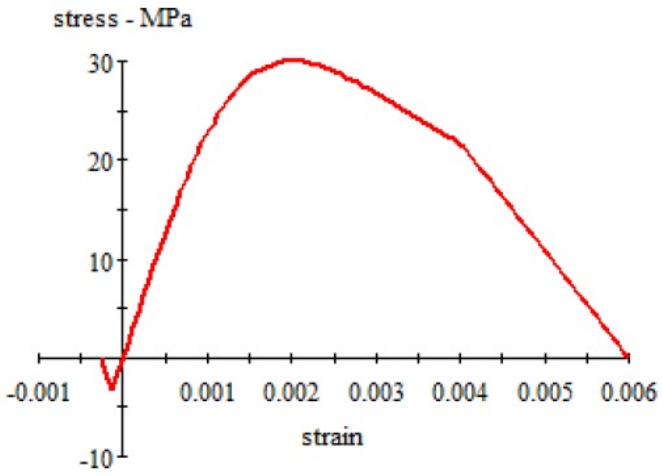

Figure 5.8: Mander Unconfined Concrete Model for Column 1A13

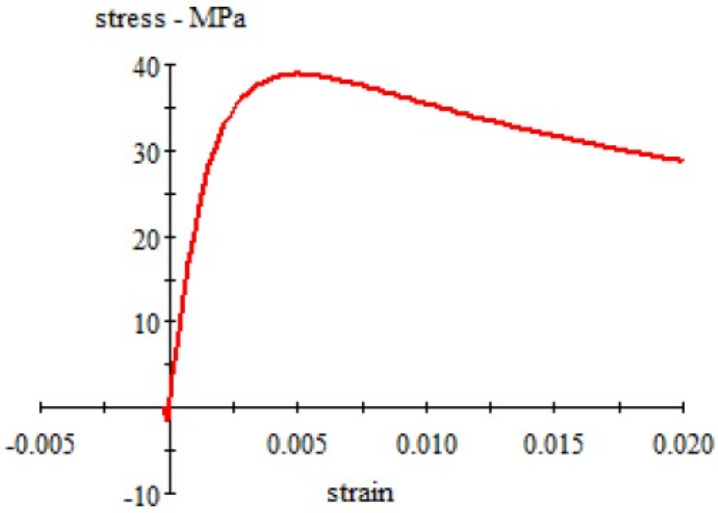

Figure 5.9: Mander Confined Concrete Model for Column 1A13

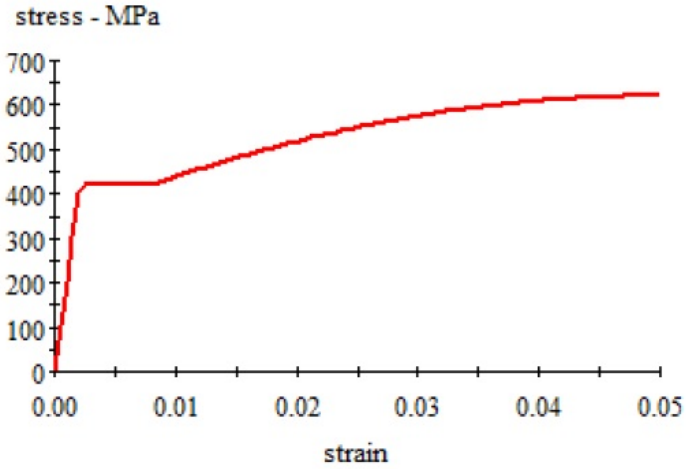

Figure 5.10: Steel Stress-Strain Curve for Column 1A13

The bending moment and axial force interaction curve which is obtained from cross-section analysis is shown in Figure 5.11. An interaction surface is created for 0º, 45º 90º and 135º and entered to the structural analysis program SAP2000.

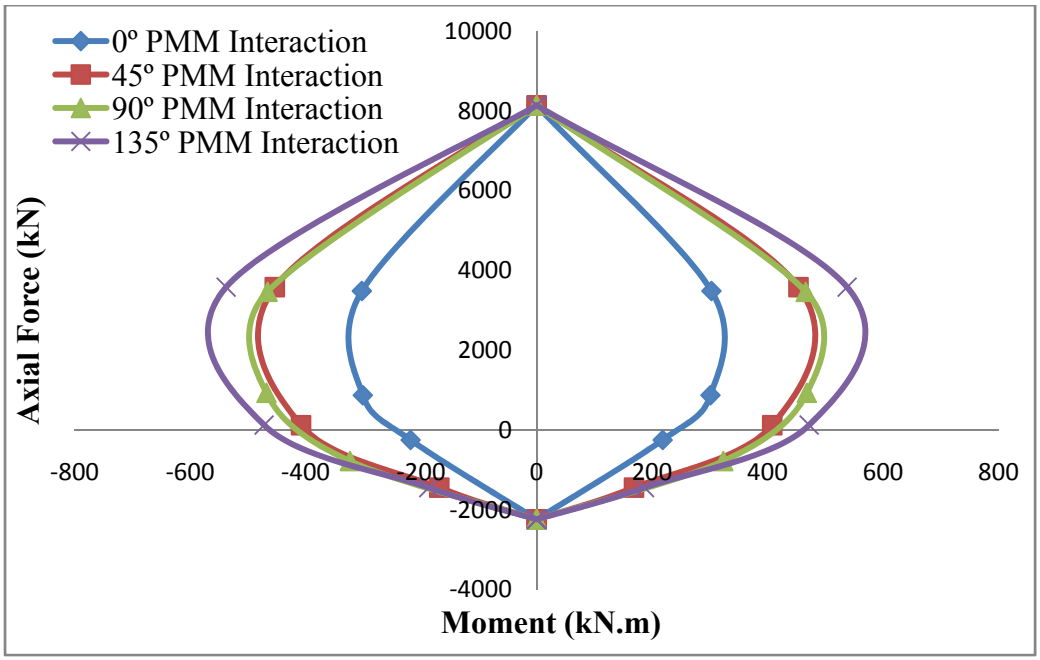

Figure 5.11: Column 1A13 PMM Interaction Curve

5.3.3 Definition of Plastic Hinge at the Shear Wall for the Mid - Pier Model

Plastic cross-section surfaces are created by XTRACT cross-section analysis software program. For shear wall SW200, the cross-section details are given in Figure 5.12, Mander unconfined concrete model is used at the outer zone from the transverse reinforcement and the Mander confined concrete model is used for the core material. The stress-strain curves obtained from Mander unconfined and confined concrete model for shear wall SW200 are shown in Figs. 5.13 and 5.14. Hardening of steel material is considered and typical stress-strain curve for steel is shown in Figure 5.15.

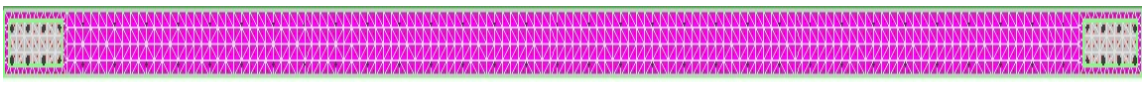

Figure 5.12: Shear Wall SW200 Cross Sectional Detail

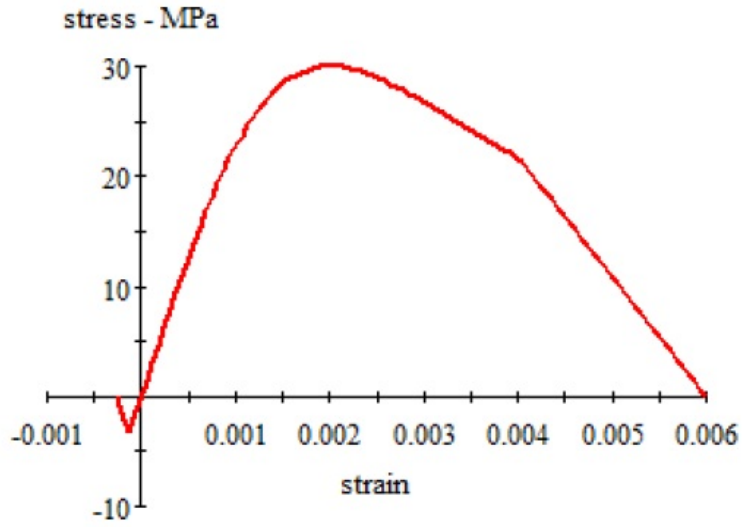

Figure 5.13: Mander Unconfined Concrete Model for Shear Wall SW200

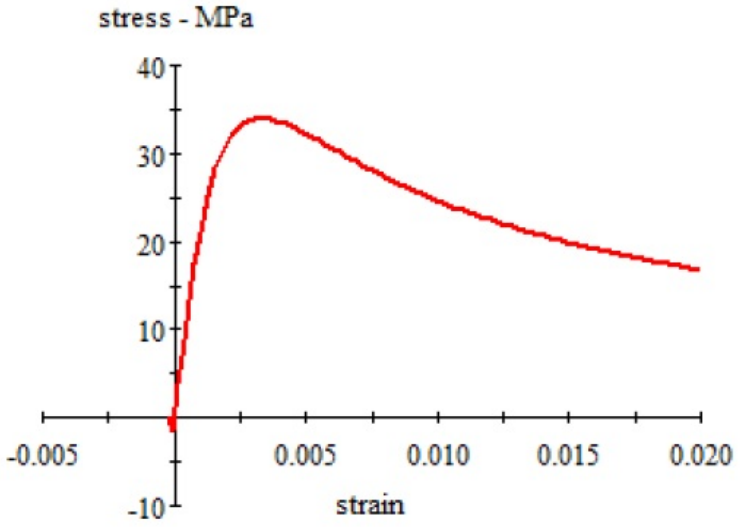

Figure 5.14: Mander Confined Concrete Model for Shear Wall SW200

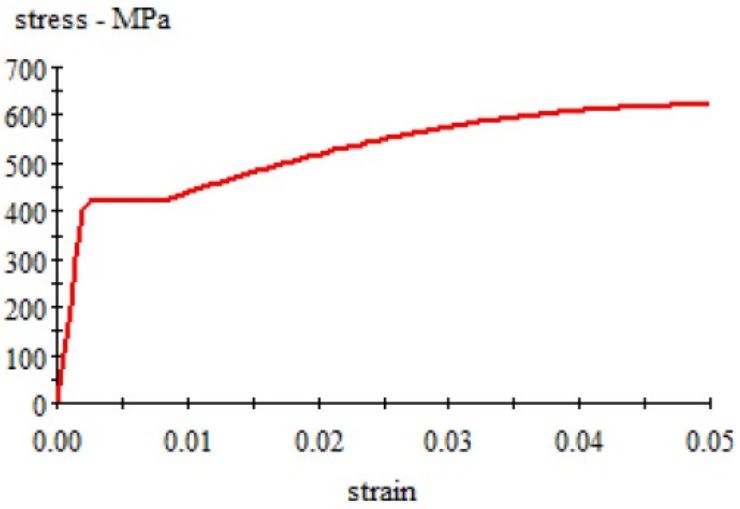

Figure 5.15: Steel Stress-Strain Curve for Shear Wall SW200

The bending moment and axial force interaction curve which is obtained from cross-section analysis is shown in Figure 5.16. An interaction surface is created for 0º, 45º 90º and 135º and entered to the structural analysis program SAP2000.

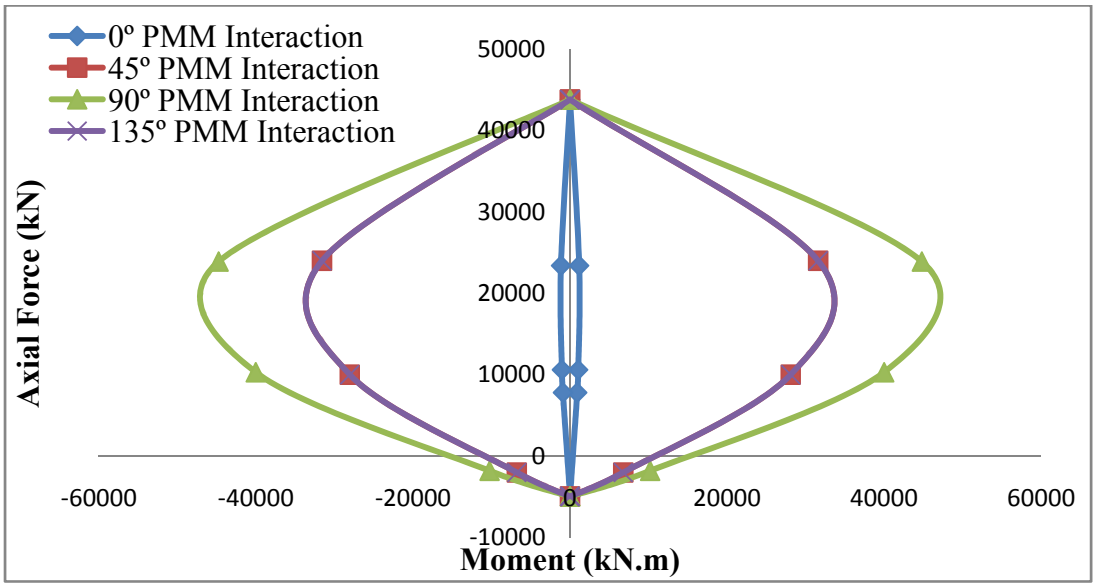

Figure 5.16: Shear Wall SW200 PMM Interaction Curve

5.4 Pushover Analysis of Existing Typical Shear Wall Frame Modeled With Shell Elements

For a nonlinear analysis of the frame plastic hinges are defined at every column and beam end points where a plastic hinge may develop. Plastic hinges defined at the ends of beams and columns are shown in Figure 5.17. For beams moment rotation relationship was entered to SAP 2000 using user defined hinge property. For columns PMM interacting diagram was entered at the angle of 0, 45, 90, 135, 180, 225, 270, 315 degrees to SAP2000 using user defined hinge property. Shear walls are modeled using shell elements. Automatic mesh area option is utilized for meshing of the shear wall.

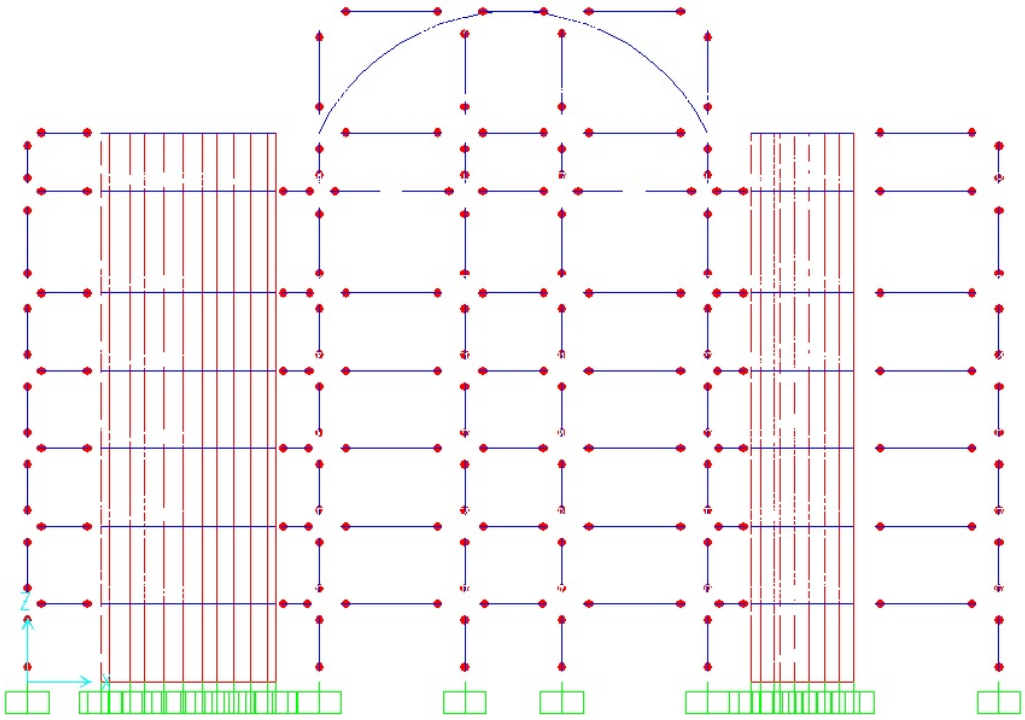

Figure 5.17: Plastic Hinges Defined at the Ends of Beam and Column for Shell Model

Before carrying out pushover analysis nonlinear gravity analysis is carried out by considering 1D+0.25L load. Then frame is pushed up in both direction i.e. positive and negative x upto predefined displacement under constant gravity loads and monotonically increasing equivalent seismic loads. The base shear and control node displacements values for positive and negative x-directions are shown in Tables 5.3 and 5.4.Pushover curves for positive and negative x-directions are shown in Figure 5.18.

Table 5.3: Pushover Curve in Positive x-Direction

Step	Displacement (m)	Base Force (kN)
0	0.001	0
1	0.011	1036.723
2	0.024	2108.739
3	0.045	3115.042
4	0.065	3741.301
5	0.086	4215.070
6	0.106	4572.749
7	0.127	4869.421
8	0.148	5074.804
9	0.168	5228.949
10	0.194	5344.348
11	0.207	5390.756

Table 5.4: Pushover Curve in Negative x-Direction

Step	Displacement (m)	Base Force (kN)
0	0.001	0
1	-0.021	-2083.221
2	-0.026	-2444.417
3	-0.047	-3387.052
4	-0.069	-4060.09
5	-0.090	-4535.301
6	-0.111	-4830.36
7	-0.133	-5055.981
8	-0.155	-5232.018
9	-0.176	-5368.113
10	-0.198	-5455.132
11	-0.210	-5480.712
12	-0.214	-5483.870

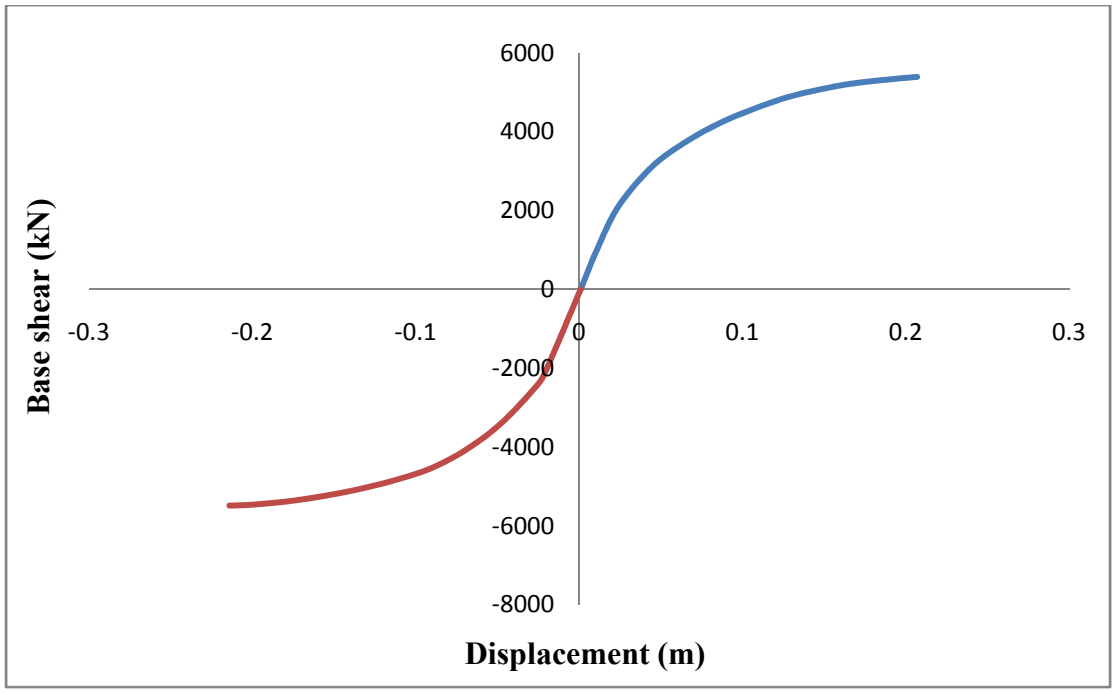

Figure 5.18: Pushover Curves for positive and negative x-directions

5.5 Pushover Analysis of Existing Typical Shear Wall Frame Modeled With the Mid - Pier Model

In this approach shear walls are modeled using the Mid-pier model. To carry a nonlinear analysis of the typical frame, plastic hinges are defined at every column and beam end points where a plastic hinge may develop. Plastic hinges defined at the ends of beams, columns and shear walls are shown in Figure 5.19. For beams moment rotation relationship was entered to SAP 2000 using user defined hinge property. For columns and shear walls PMM interacting diagram was entered at the angle of 0, 45, 90, 135, 180, 225, 270, 315 degrees to SAP2000 using user defined hinge property.

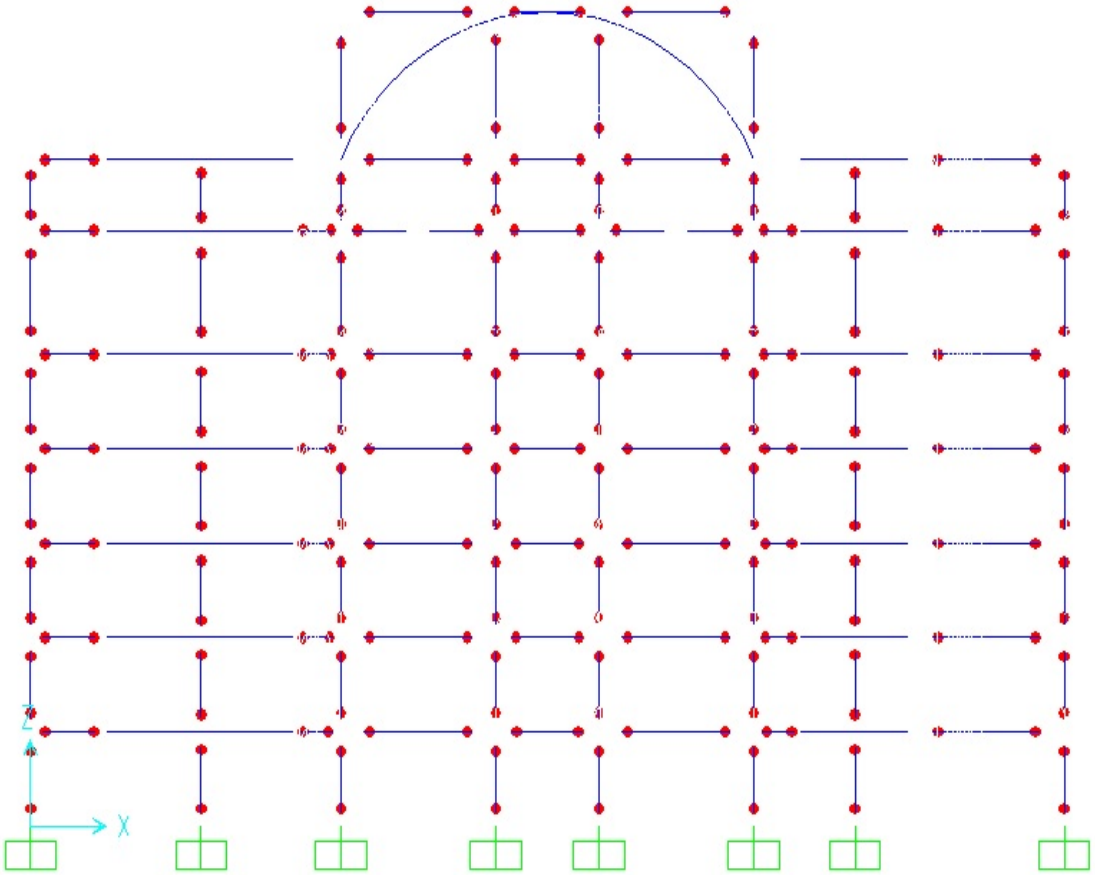

Figure 5.19: Plastic Hinges Defined At the Ends of Beams, Columns, and Shear Wall for Mid-Pier Model

Before carrying out pushover analysis nonlinear gravity analysis is carried out by considering 1D+0.25L load. Then frame is pushed up in both direction i.e. positive and negative x upto predefined displacement under constant gravity loads and monotonically increasing equivalent seismic loads. The base shear and control node displacements values for positive and negative x-directions are shown in Tables 5.5 and 5.6.Pushover curves for positive and negative x-directions are shown in Figure 5.20.

Table 5.5: Pushover Curve in Positive x-Direction

Step	Displacement (m)	Base Force (kN)
0	0.002	0
1	0.022	1502.101
2	0.043	2965.326
3	0.048	3303.443
4	0.058	3730.646
5	0.079	4141.193
6	0.099	4468.342
7	0.119	4694.095
8	0.141	4823.918
9	0.161	4920.371
10	0.182	4999.535
11	0.203	5055.868
12	0.207	5066.867

Table 5.6:Pushover Curve in Negative x-Direction

Step	Displacement (m)	Base Force (kN)
0	0.002	0
1	-0.019	-1567.378
2	-0.041	-3093.273
3	-0.052	-3826.383
4	-0.054	-3989.307
5	-0.083	-4566.563
6	-0.104	-4906.26
7	-0.126	-5159.323
8	-0.137	-5263.461
9	-0.147	-5328.6
10	-0.169	-5402.71
11	-0.190	-5463.534
12	-0.212	-5514.694
13	-0.214	-5519.188

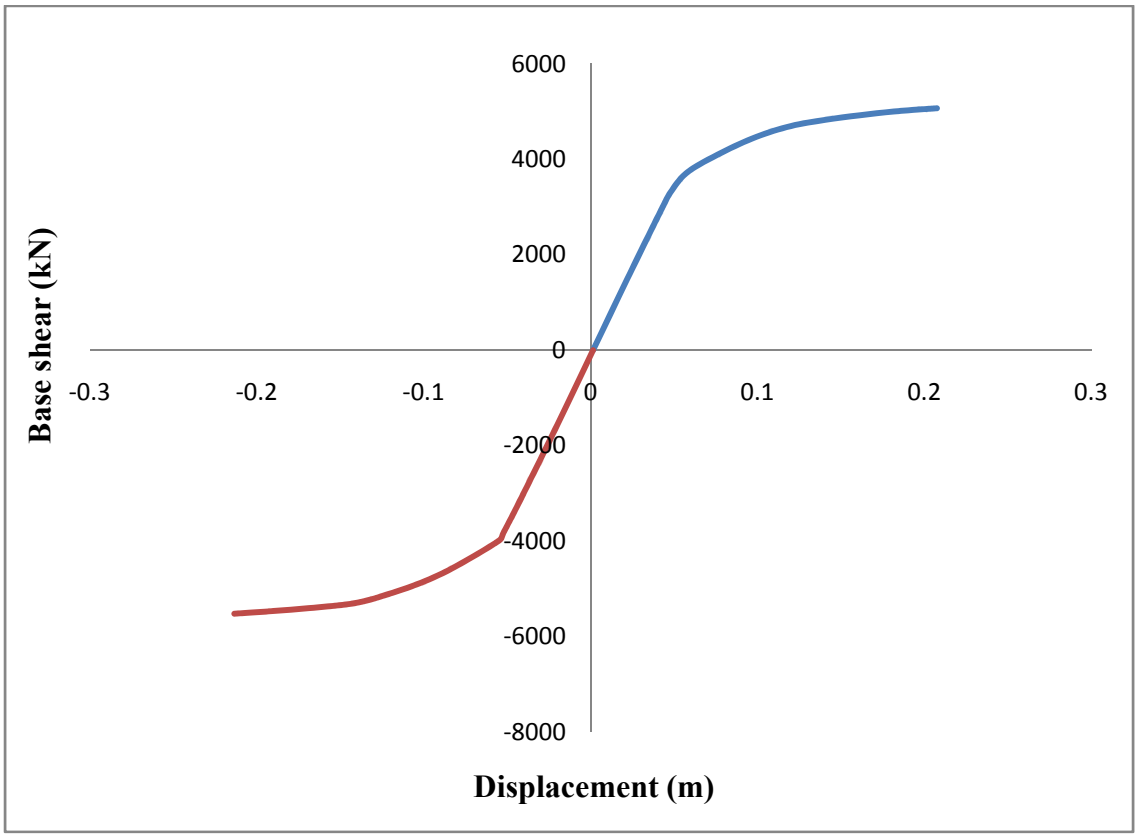

Figure 5.20: Pushover Curves for positive and negative x-directions

5.6 Comparison of Pushover Curves of Existing Frame Modeled With Shell Element and Mid-Pier Approach

Comparison of pushover curves of existing frame modeled with shell element and mid-pier approach is shown in Figure 5.21.

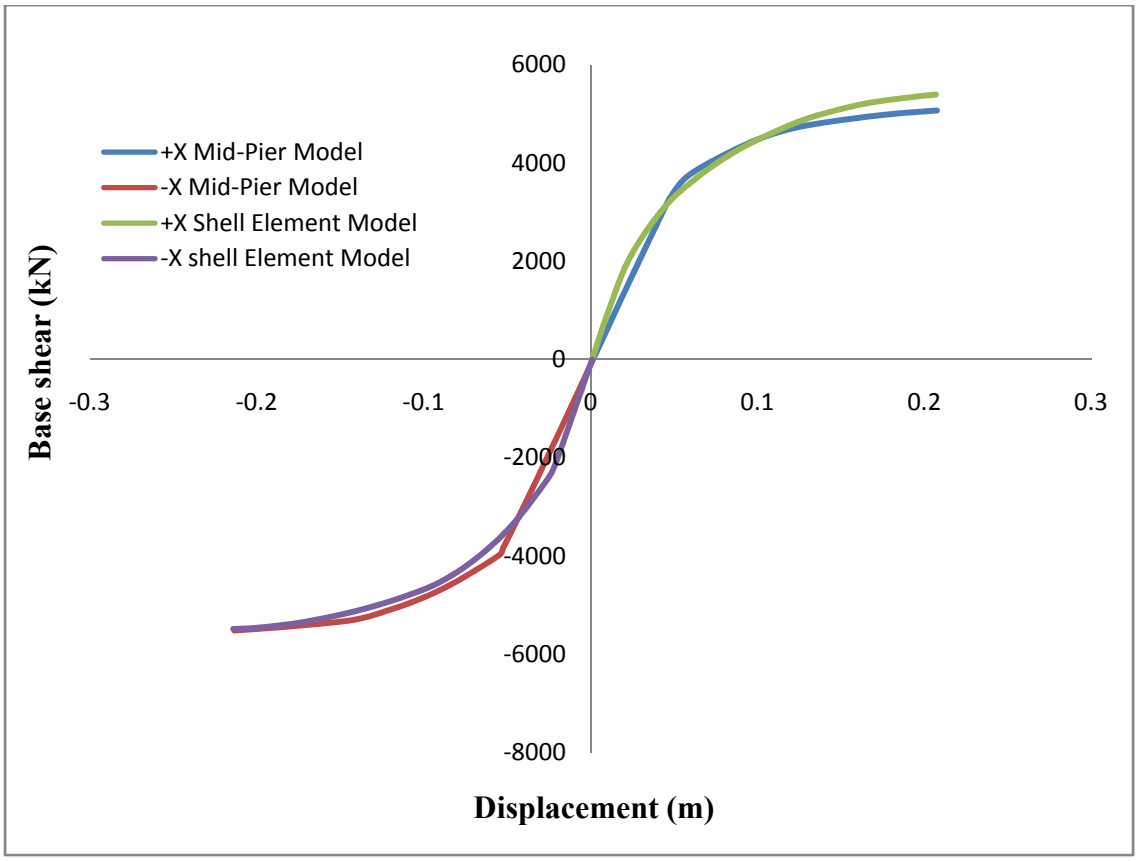

Figure 5.21: Pushover Curves for Shell Element and Mid-Pier Mode

Figure 5.21 shows that the mid-pier approach gives approximately very close results to the shell element approach.

5.7 Capacity Curve

Capacity Curve (modal displacement vs modal acceleration), which is obtained from the pushover curve with coordinate conversions, can be sketched with the following procedure:

The modal acceleration of the fundamental period at i-th step a_1^{ω} can be calculated as follows:

$$a_1^{\omega} = \frac{V_{x1}^{(i)}}{M_{x1}} \tag{5.3}$$

Where $V_{x1}^{(i)}$ is base shear at i-th step in x direction, and M_{x1} is the participated mass at the fundamental period in x direction.

Modal displacement of the fundamental period at i-th step $d_1^{(i)}$ can be calculated as follows:

$$d_1^{(i)} = \frac{u_{xN1}^{(i)}}{\phi_{xN1}\Gamma_{x1}} \tag{5.4}$$

Γ_{x1} is the modal participation factor of the fundamental period in x direction, and ϕ_{xN1} represents the modal shape of N-th storey at the fundamental period of x direction. $u_{xN1}^{(i)}$ is the top displacement value in x direction, obtained from i-th step of the push-over analysis.

By using these equations, the spectral accelerations and displacements are calculated for both models, which are the coordinates of the capacity spectrum in ADRS format. Tables 5.7 and 5.8 shows the capacity spectrum values in positive and negative x-directions for a shell element model of the existing frame. Figs 5.22 and 5.23 shows the capacity curves for existing frame model with shell element approach. Tables 5.9 and 5.10 shows the capacity spectrum values in positive and negative x-directions for a mid-pier model of the

existing frame. Figs. 5.24 and 5.25 shows the capacity curves for the existing frame model with the mid - pier approach.

Table 5.7: Capacity Spectrum Values in Positive x-Direction for Shell Element Model

Step	S_d Capacity (m)	S_a Capacity
0	0	0
1	0.006	0.093
2	0.014	0.183
3	0.028	0.256
4	0.042	0.298
5	0.056	0.331
6	0.071	0.356
7	0.085	0.378
8	0.100	0.392
9	0.114	0.402
10	0.133	0.409
11	0.142	0.411

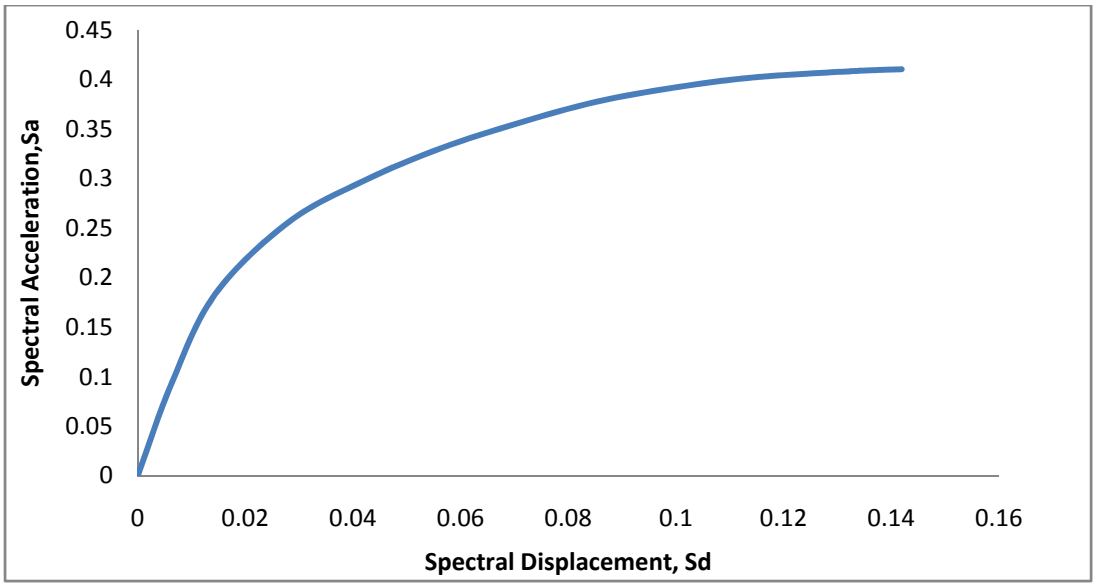

Figure 5.22: Capacity Spectrum Curve in positive x-direction for Shell Element model

Table 5.8: Capacity Spectrum Values in Negative x-Direction for Shell Element Model

Step	S_d Capacity (m)	S_a Capacity
0	0	0
1	0.013	0.185
2	0.017	0.212
3	0.031	0.276
4	0.046	0.321
5	0.061	0.355
6	0.076	0.375
7	0.091	0.390
8	0.106	0.401
9	0.121	0.410
10	0.137	0.415
11	0.145	0.416
12	0.148	0.416

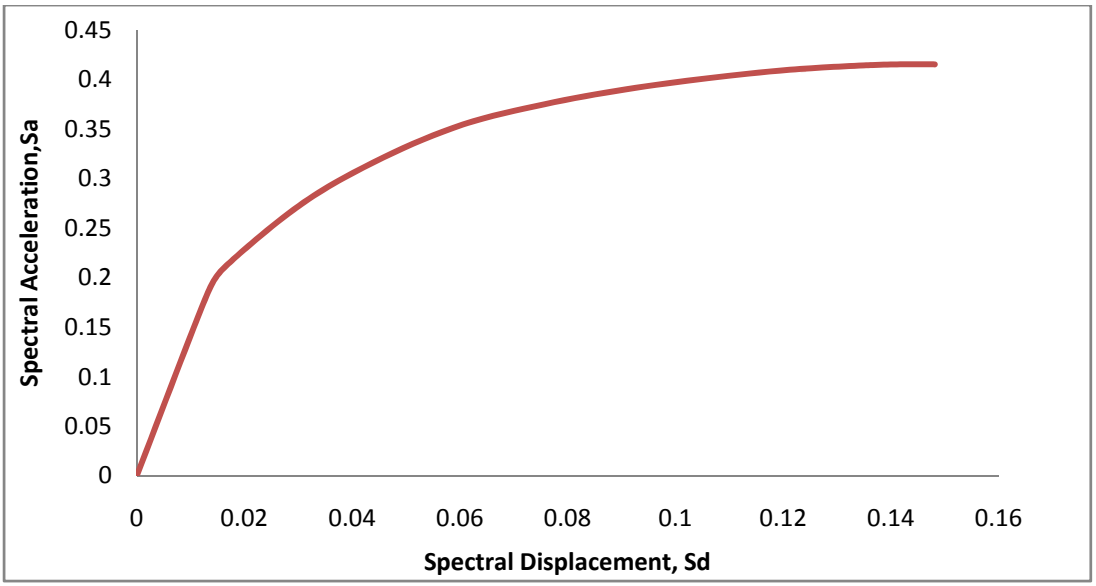

Figure 5.23: Capacity Spectrum Curve in negative x-direction for Shell Element model

Table 5.9: Capacity Spectrum Values in Positive x-Direction for Mid-Pier Model

Step	S_d Capacity (m)	S_a Capacity
0	0	0
1	0.013	0.130
2	0.027	0.257
3	0.030	0.287
4	0.037	0.319
5	0.051	0.338
6	0.066	0.357
7	0.080	0.371
8	0.095	0.378
9	0.110	0.383
10	0.124	0.387
11	0.139	0.390
12	0.143	0.391

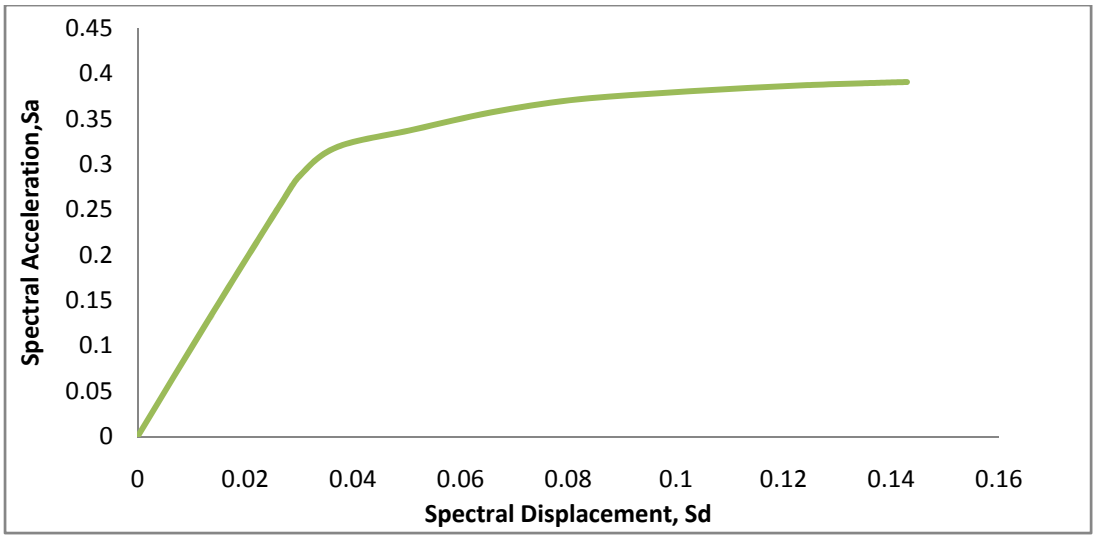

Figure 5.24: Capacity Spectrum Curve in positive x-direction for Mid-Pier Model

Table 5.10: Capacity Spectrum Values in Negative x-Direction for Mid-Pier Model

Step	S_d Capacity (m)	S_a Capacity
0	0	0
1	0.014	0.136
2	0.028	0.269
3	0.035	0.332
4	0.037	0.346
5	0.056	0.372
6	0.071	0.392
7	0.086	0.407
8	0.094	0.413
9	0.101	0.416
10	0.117	0.420
11	0.132	0.422
12	0.148	0.425
13	0.149	0.425

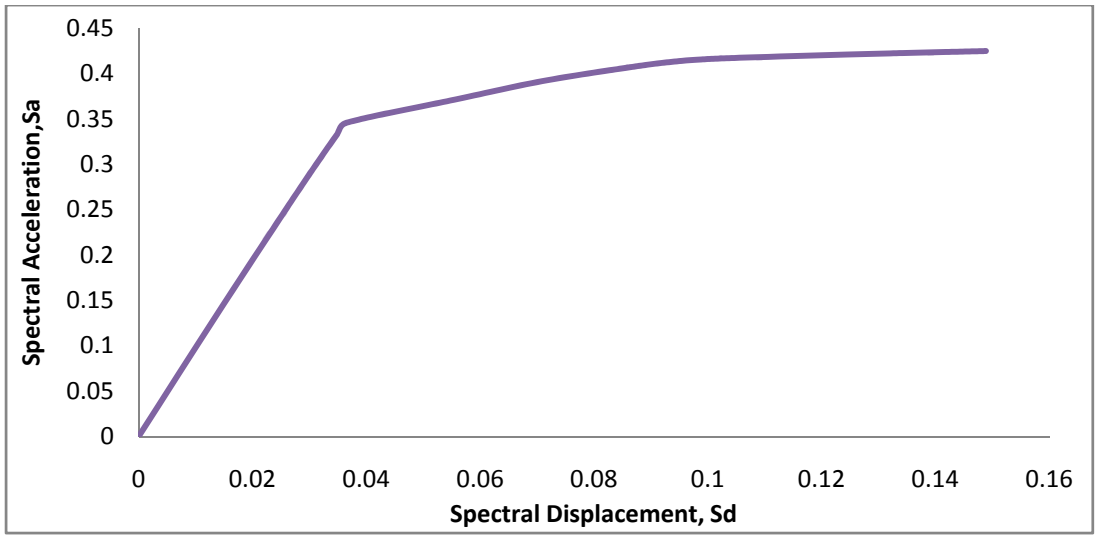

Figure 5.25: Capacity Spectrum Curve in negative x-direction for Mid-Pier Model

5.8 Performance of Existing Frame

Seismic demands for performance evaluation of multistorey buildings are calculated at the state at which the roof displacement is to be evaluated. This performance state is determined by using a graphical procedure implemented for the equivalent SDOF system. In this procedure, the capacity curve of Single Degree of Freedom (SDOF) system is represented by the pushover curve of the multistorey building after proper transformation to the AD format, i.e, spectral acceleration (*Sa*) versus spectral displacement (*Sd*) format. The seismic demand curve of the SDOF system is represented by the inelastic response spectrum established for a given earthquake or the design response spectrum of seismic codes. Now, the intersection of the capacity and demand curves in AD format represents the performance state at which the acceleration and displacement demands of the equivalent SDOF system can be evaluated. Then, this displacement demand is transformed back to determine the corresponding roof displacement of the multistory

building. This roof displacement gives an adequate measure of the target displacement that the building is expected to experience due to the design earthquake excitation. Also, the induced responses and forces at this state are expected to adequately represent the corresponding response quantities of the building due to the design earthquake excitation. In this section the performance point will be estimated for the existing reinforced concrete (RC) frame. A technique based on the Capacity Spectrum Method (CSM) procedure B is adopted to determine the performance point of the existing frame.

Figs. 5.26 and 5.27 show the process of determining the performance points of frame model with Shell element method both in positive and negative x-directions.Figs. 5.28 and 5.29 show the process of determining the performance points of frame model with Mid-Pier method both in positive and negative x-directions

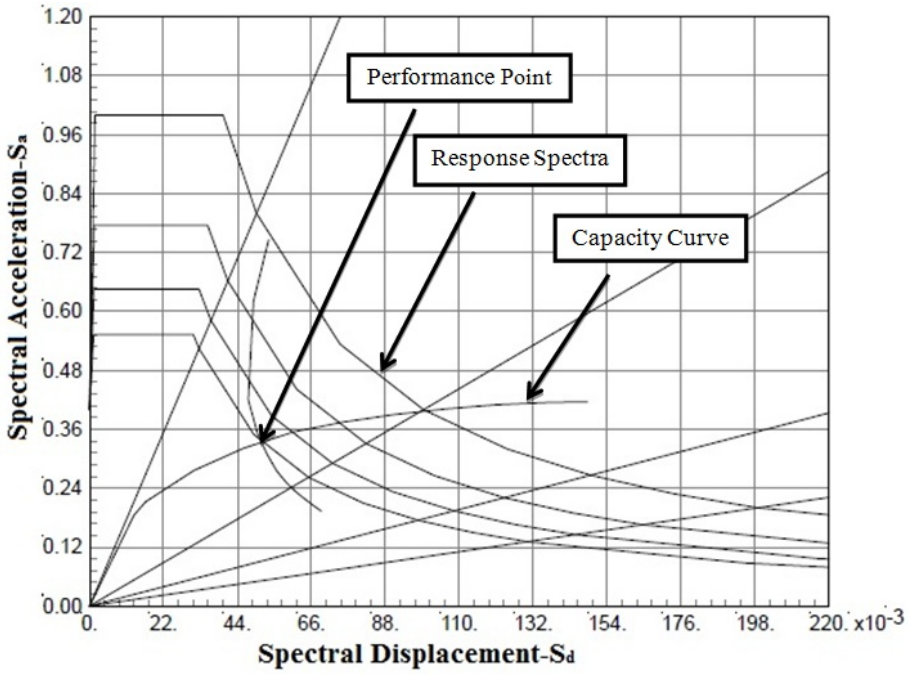

Figure 5.26: Performance Point in positive x-direction for Shell Element Model

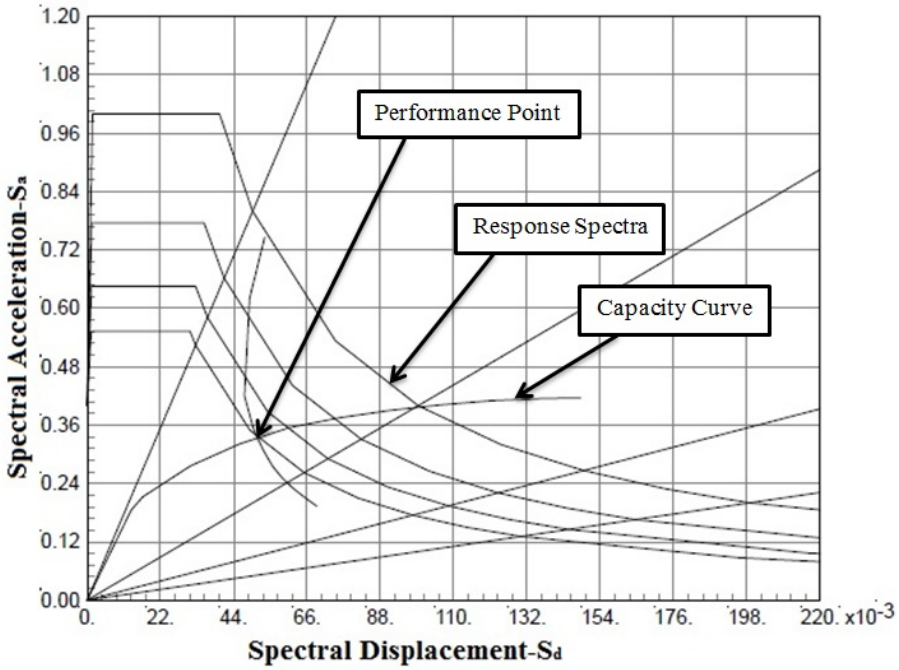

Figure 5.27: Performance Point in negative x-direction for Shell Element Model

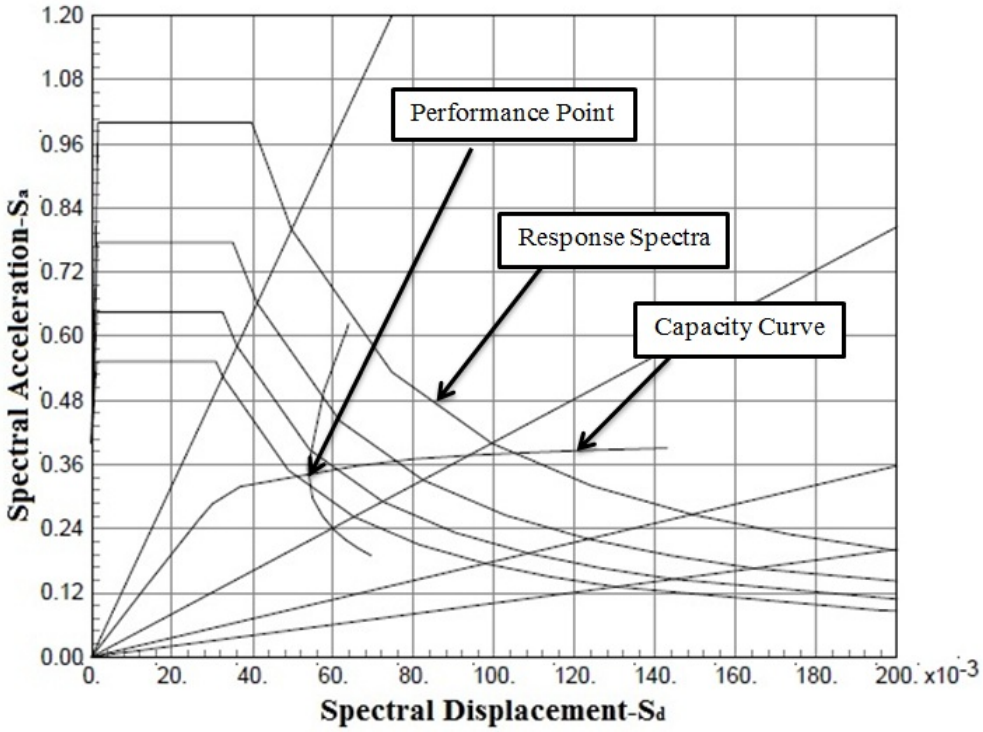

Figure 5.28: Performance Point in positive x-direction for Mid-Pier Model

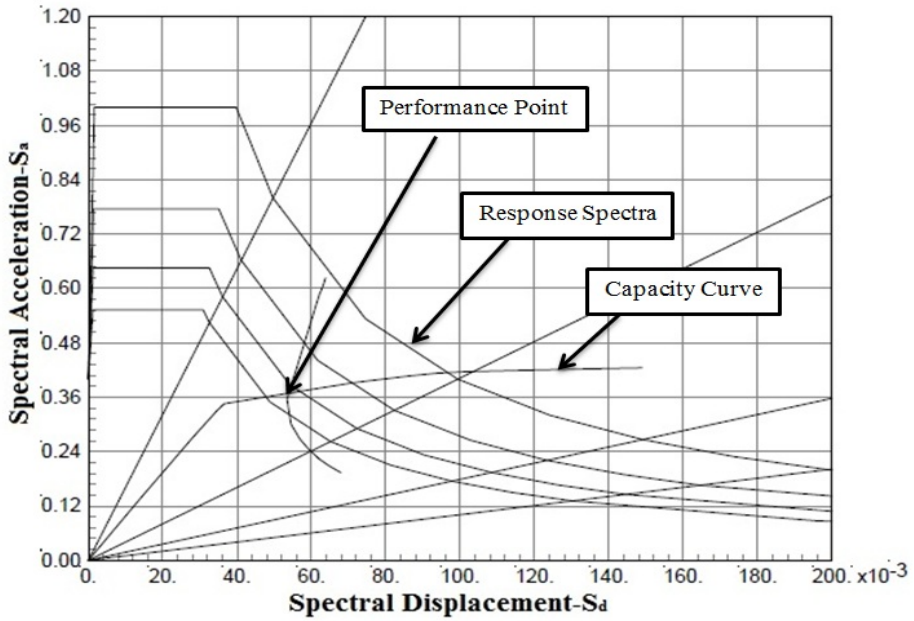

Figure 5.29: Performance Point in negative x-direction for Mid-Pier Model

Table 5.11 shows the base shear and displacement of existing frame model with shell element approach and mid-pier approach at performance point i.e. demand level.

Table 5.11: Performance point of Existing Frame

Frame Model	Direction	Spectral Acceleration S_a	Spectral Displacement S_d	Base Shear (kN)	Displacement (m)
Shell Element	+X	0.321	0.052	4075.3	0.080
Shell Element	-X	0.333	0.051	4227.5	0.077
Mid-Pier	+X	0.342	0.054	4199.7	0.082
Mid-Pier	-X	0.369	0.054	4516.3	0.080

5.9 Acceptance Criteria for Performance and Hinge Formation at Demand Displacement

The ATC-40 and FEMA-356 documents give modeling procedures and acceptance criteria to define force deformation hinge criteria. As shown in Figure 5.30, five points labeled A, B, C, D, and E gives the behavior of the hinge and Immediate Occupancy (IO), Life Safety (LS) and Collapse Prevention (CP) are the acceptance criteria. The Immediate occupancy is in between AB (elastic range) to IO, Life safety is in between IO to and Collapse prevention is in between LS to CP. In SAP2000 these hinges are shown with different colors as shown in Figure 5.30.

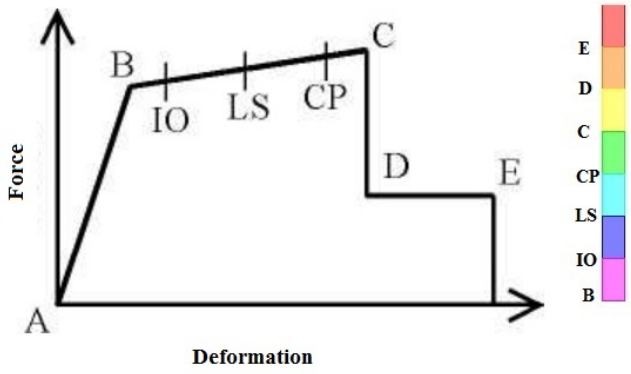

Figure 5.30: Different Stage of Plastic Hinges

The values of these performance levels recommended by ATC-40 for IO, LS and CP are 0.2Δ, $0.5\Delta$and 0.9Δ. Where, Δ is the length of plastic hinge plateau as shown in Figure 5.31.

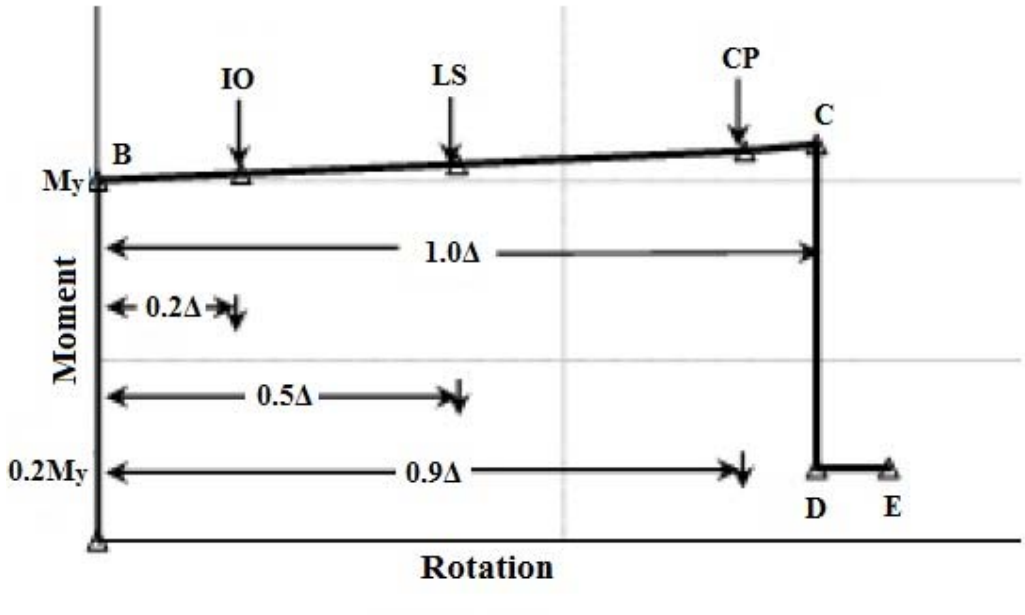

Figure 5.31: Typical Moment and Rotation Curve with Acceptance Criteria

These acceptance criteria are entered in SAP2000 to get the structural performance level of the members. Figs. 5.32 and 5.33 shows the hinges formation in frame modeled with shell element model based on acceptance criteria.

Figs. 5.34 and 5.35 shows the maximum stresses in steel and concrete is formed at the base of shear walls which indicates the hinges formed in shear walls at demand displacement when frame is pushed in positive x-direction.

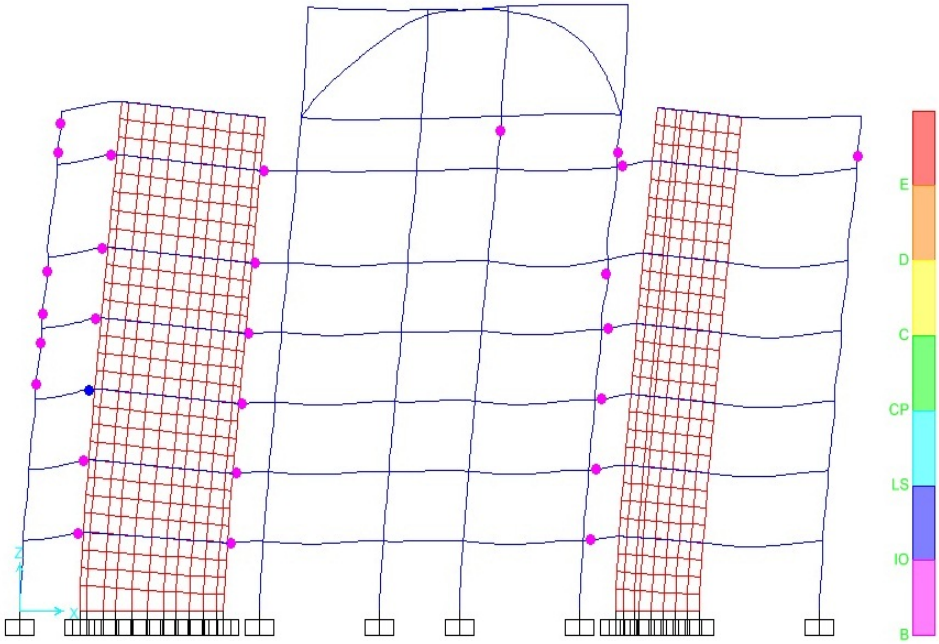

Figure 5.32: Hinge Formation in Frame Modeled with Shell Element in positive x-direction

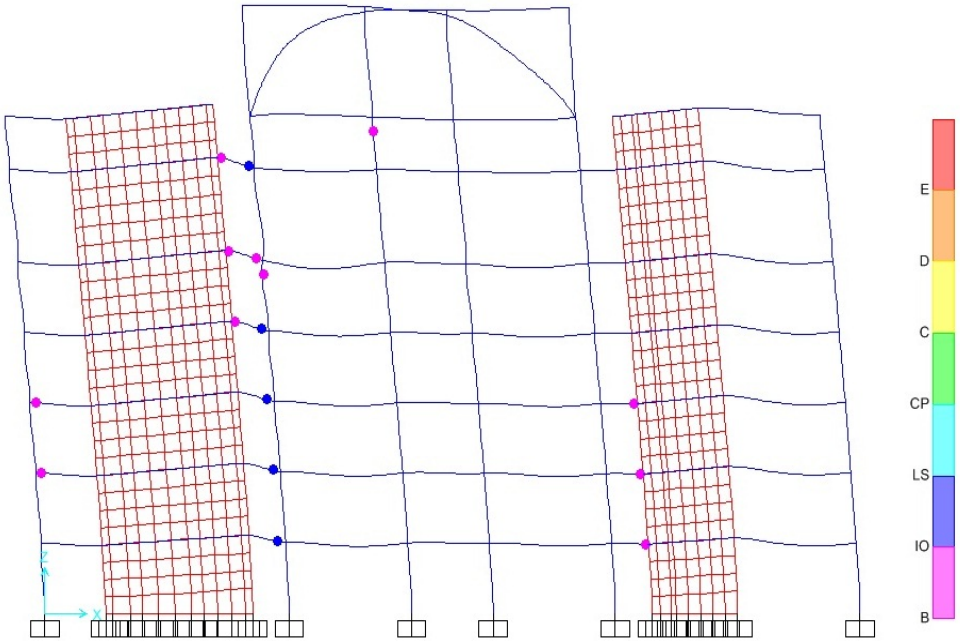

Figure 5.33: Hinge Formation in Frame Modeled with Shell element in negative x-direction

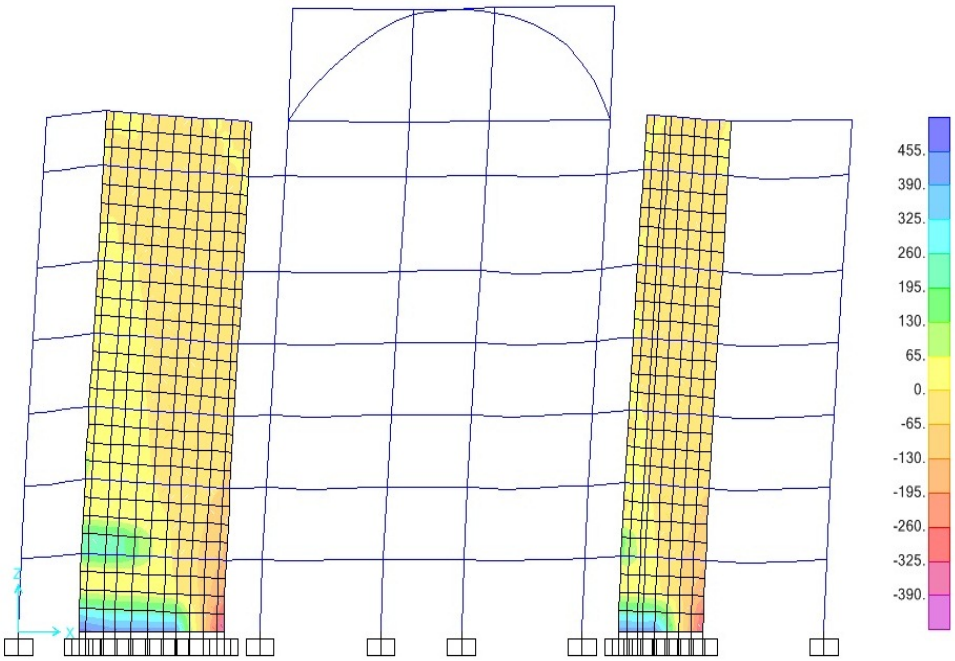

Figure 5.34: Maximum Stresses In Steel at Base of Shear Wall of the Frame Modeled with Shell Element in positive x-direction

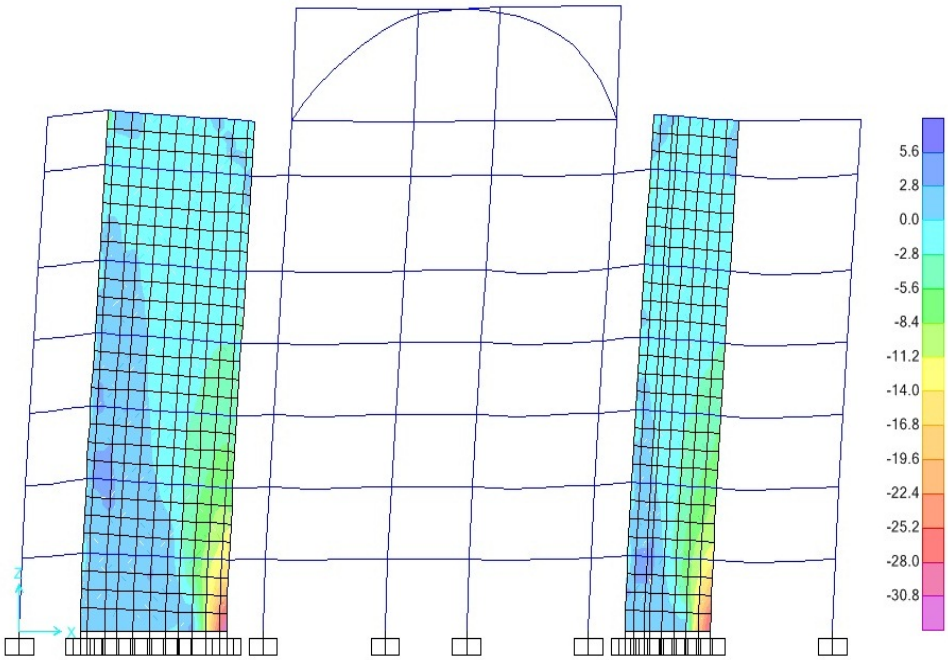

Figure 5.35: Maximum Stresses in Concrete at Base of Shear Wall of the Frame Modeled with Shell Element in positive x-direction

Figs. 5.36 and 5.37 shows the maximum stresses in steel and concrete is formed at the base of shear walls which indicates the hinges formed in shear walls at demand displacement when frame is pushed in negative x-direction.

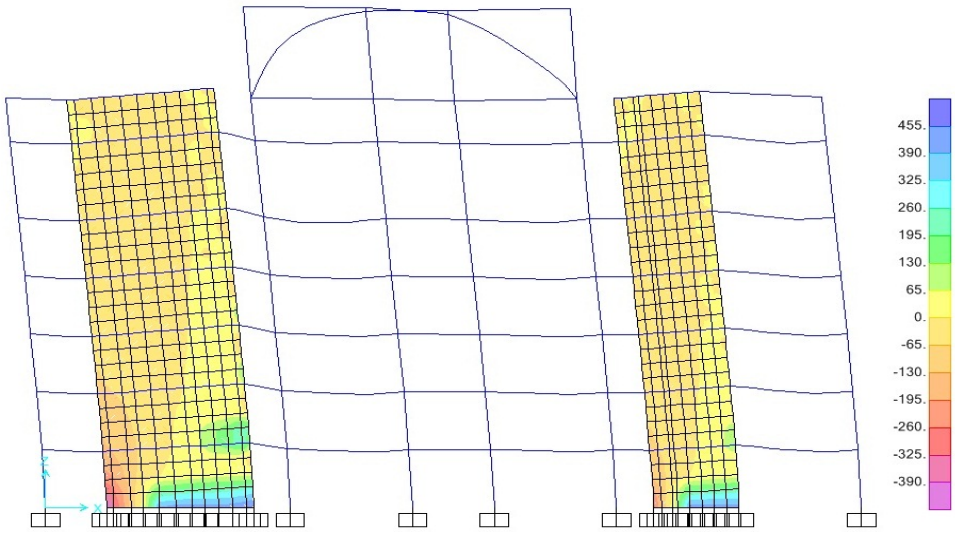

Figure 5.36: Maximum Stresses in Steel at Base of Shear Wall of the Frame Modeled with Shell Element in negative x-direction

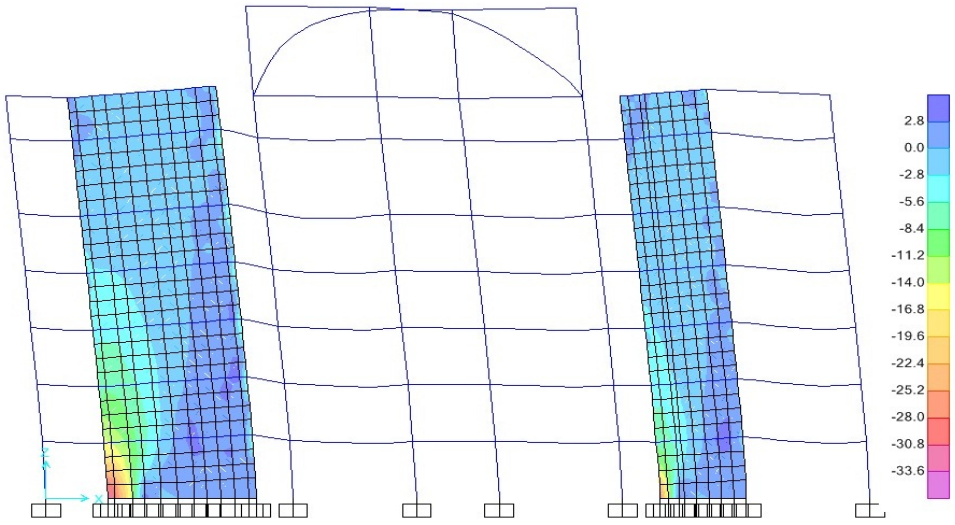

Figure 5.37: Maximum Stresses in Concrete at Base of Shear Wall of the Frame Modeled with Shell Element in negative x-direction

Figs. 5.38 and 5.39 shows the hinges formation in frame modeled with Mid-Pier model based on acceptance criteria.

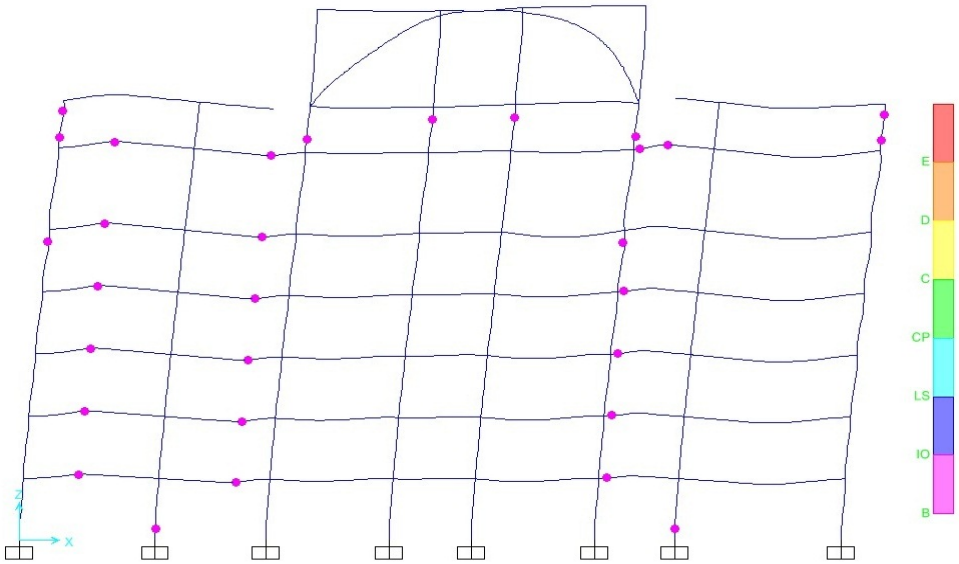

Figure 5.38: Hinge Formation in Frame Modeled with Mid-Pier positive x-direction

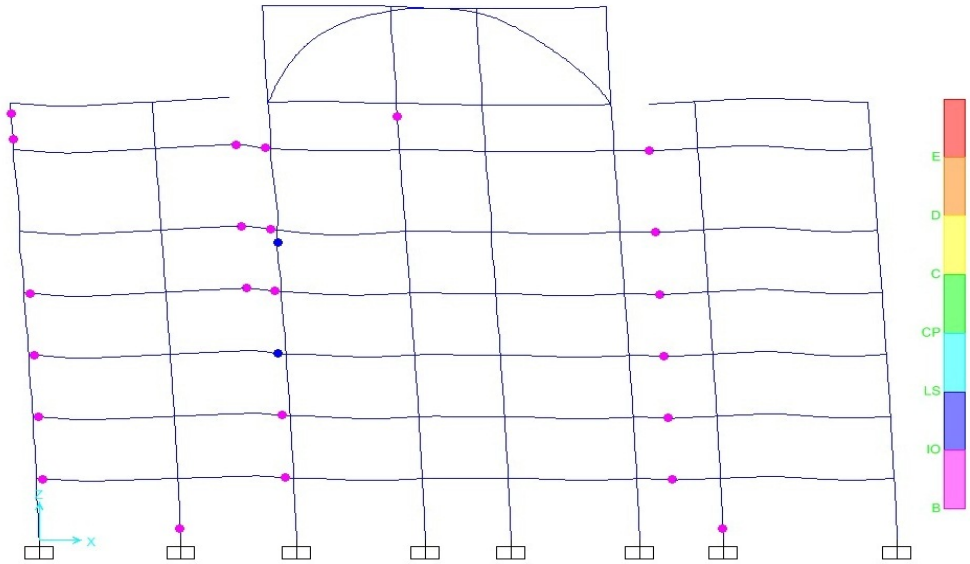

Figure 5.39: Hinge Formation in Frame Modeled with Mid-Pier negative x-direction

5.10 Inter Storey Drift Ratio (IDR)

During earthquake building will experience reversed cyclic loading. It has been seen in past earthquake that most of the damages in structures are due to inter-storey drift. Larger inter storey drift may cause huge damage to structure as well as structural members. Most of the building collapse during earthquake due to weak storey mechanism which is caused by inter-storey drift. Earthquake induced deformations may be quantified by the roof displacement Δ_{roof} as well as the inter-storey displacement Δ_i as shown in Figure 5.40.

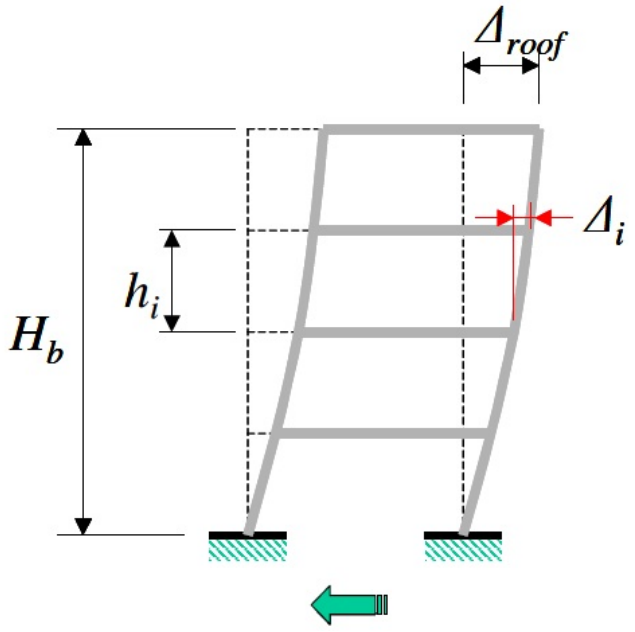

Figure 5.40: Roof Displacement and inter-storey displacement

Inter-storey drift ratio at the i^{th} floor can be defined as given in Eq.5.5.

$$\theta_i = \frac{\Delta_i}{h_i} \tag{5.5}$$

where h_i is the storey height.

Δ_i is the relative floor displacement

Using Eq.5.5 inter-storey drift ratio for existing frame is calculated. Figure 5.41 shows the inter-storey drift ratio for the existing frame model with Shell element and Mid-Pier approach in positive and negative x-directions at demand displacement. Figure 5.42 the total storey drift for the existing frame model with Shell and Mid-Pier approach in positive and negative x-directions at demand displacement.

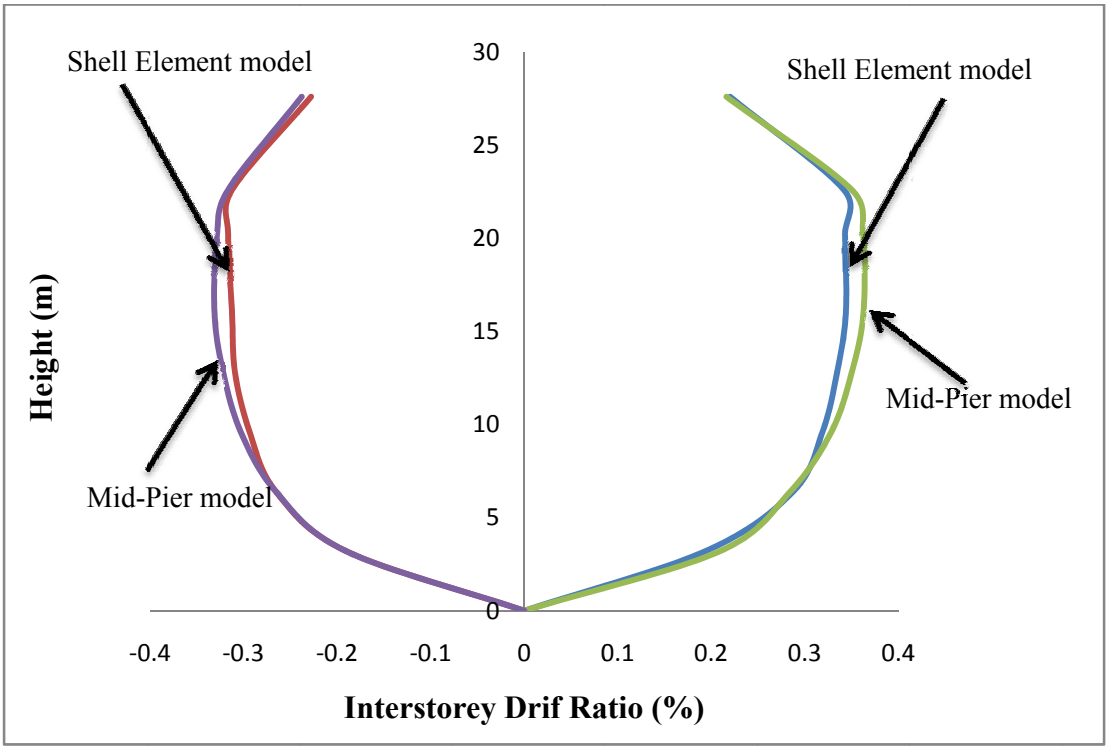

Figure 5.41: Inter-storey drift ratio (IDR) for existing frame at demand displacement

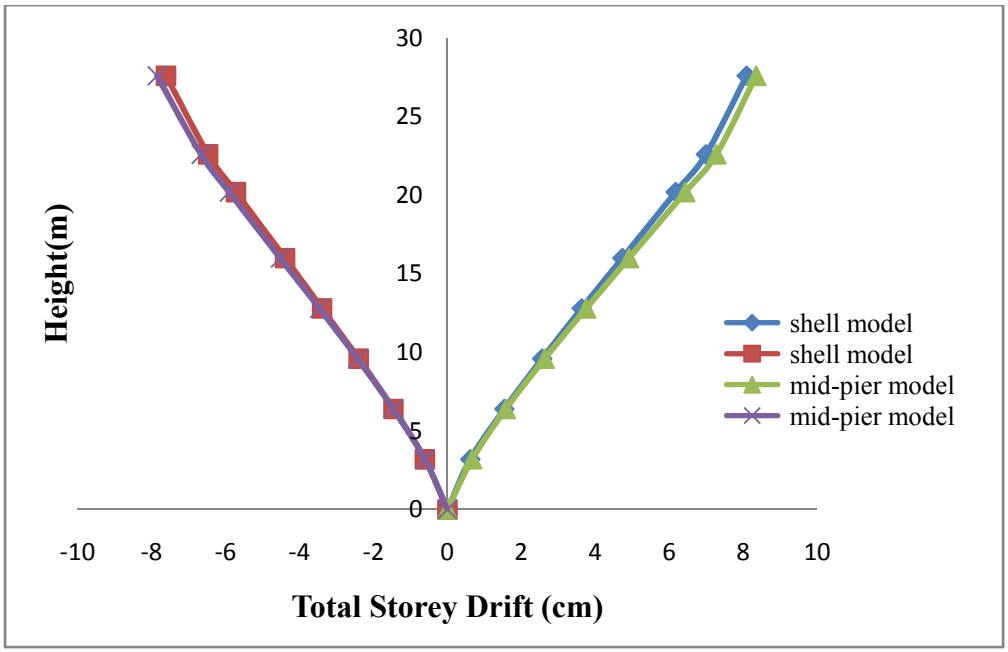

Figure 5.42: Total storey drift for existing frame at demand displacement

CHAPTER 6

PUSHOVER ANALYSIS OF RETROFITTED SHEAR WALL FRAME

6.1 Introduction

After carrying out pushover analysis of existing typical frame of Madinah building it is cleared at demand displacement top story members are failing as well as shear walls are failing due to crushing of concrete and yielding of steel. So retrofitting of these structural members are required so that in case of seismic activity these members can sustain high lateral loads. For this different retrofitting schemes were selected. After application of these retrofitting strategy pushover analysis were carried out and results of retrofitted frame were obtained and presented in this chapter.

6.2 Retrofitting Schemes for Structural Members

Strengthening of structural members is done by many techniques. These techniques include strengthening of members by reinforced or prestressed concrete jacketing, steel jacketing and/or addition of external steel elements, and fiber-reinforced polymer (FRP) composite applications. To retrofit the existing frame different schemes were selected

based on the available techniques. Following are the strategies selected for strengthening of existing frame.

1. Additional shear walls made of high strength concrete and retrofitting of top columns by High Strength Reinforced Concrete (HSRC) jacketing.
2. Additional shear walls made of high strength concrete and retrofitting of top columns by steel jacketing.
3. Additional shear walls made of high strength concrete and retrofitting of top columns by CFRP jacketing.

In all these strategies shear walls have a common scheme for retrofitting whereas for columns different retrofitting schemes have been used to see the response of these techniques. These schemes are shown in Fig. 6.1.

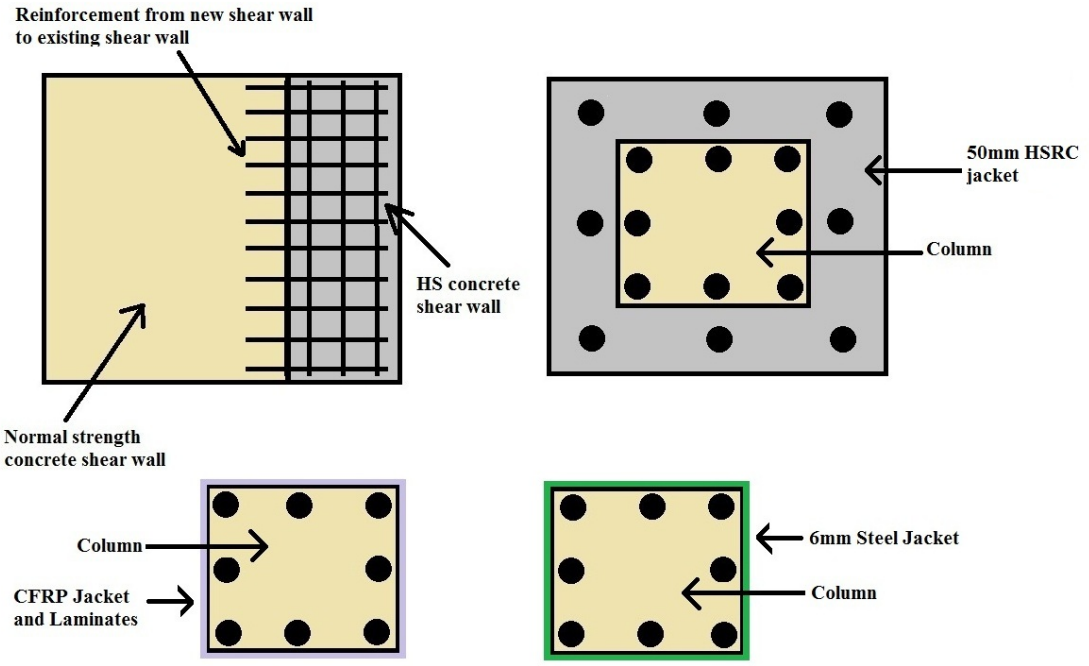

Figure 6.1: Retrofitting Schemes for Strengthening

6.3 Retrofitted Frame

The existing frame is model again by different schemes explained in section 6.2. Figs.6.2 and 6.3 show the retrofitted frame model with shell element and mid-pier methods.

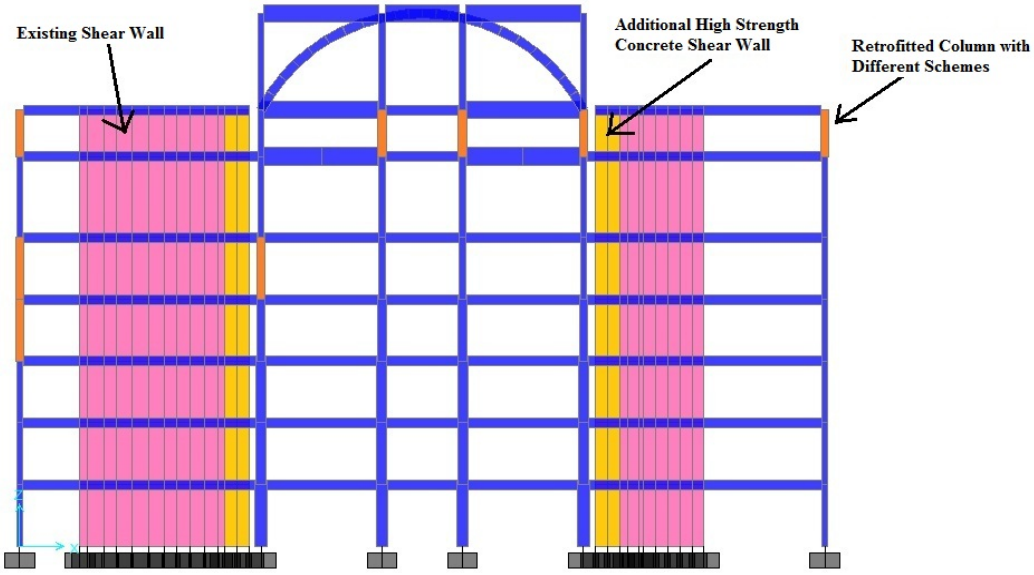

Figure 6.2: Retrofitted Frame Model with Shell Element Method

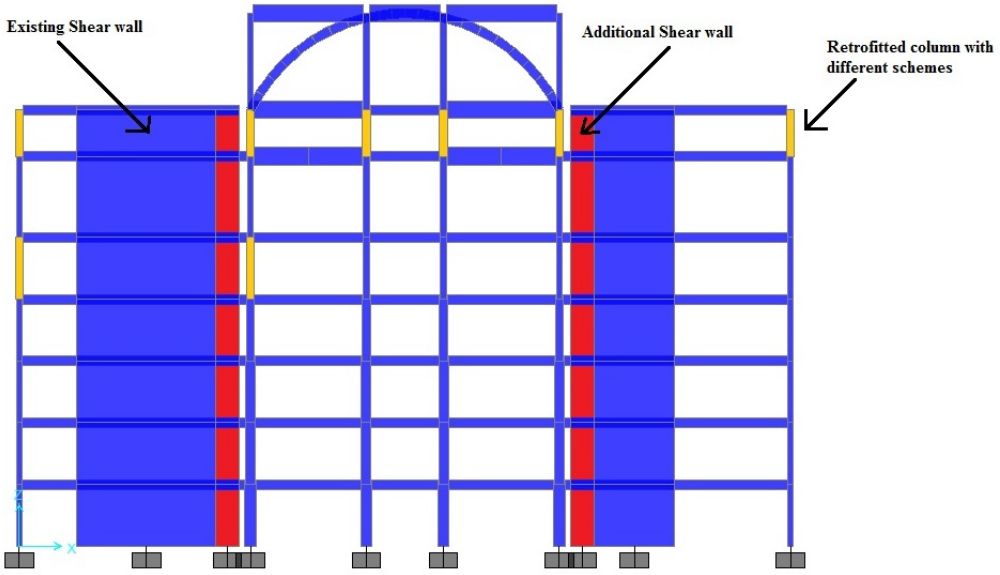

Figure 6.3: Retrofitted Frame Model with Mid-Pier Method

6.4 Plastic Hinges Properties for Retrofitted Frame

Hinge properties for retrofitted frame were obtained using XTRACT (2007). Hinge properties were calculated for only those members which were retrofitted and the remaining members have same hinge properties as assigned during analysis of the existing frame.

6.4.1 Column Retrofitted by HSRC Jacket

For column 5A13 plastic cross-section surfaces are created by XTRACT cross-section analysis software program as shown in Figure 6.4. The high strength RC jacket is utilized to strengthen the column. Properties of High strength (HS) RC jacketed are given Table 6.1. The Mander unconfined concrete model is used at the outer zone from the transverse reinforcement and the Mander confined concrete model is used for the core material. The stress-strain curves obtained from Mander unconfined and confined concrete model for column 5A13 are shown in Fig.6.5 and Fig. 6.6. Hardening of steel material is considered and typical stress-strain curve for steel is shown in Fig. 6.7.

Table 6.1: Properties of High Strength RC Jackets

HSRC Jacket	Compressive Strength of concrete, $f_c^{'}$ (MPa)	Diameter of Rebar (mm)	Tensile strength of Rebar, f_y (MPa)
50 x50 mm	45	16	420

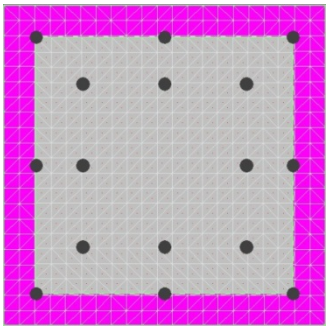

Figure 6.4: HSRC Jacketed Column 5A13 Cross Sectional Detail

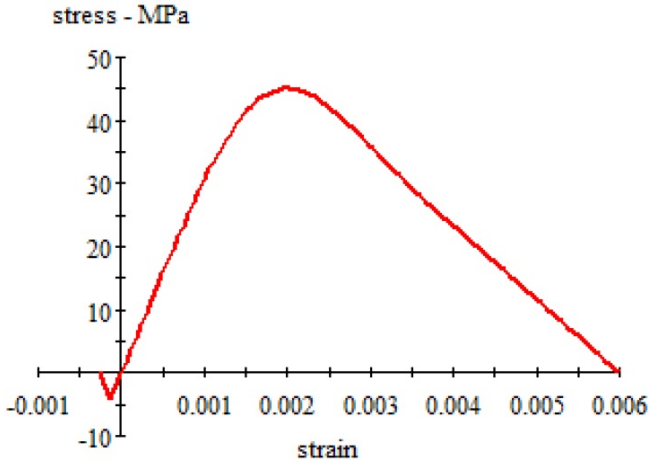

Figure 6.5: Mander Unconfined Concrete Model for Column 5A13

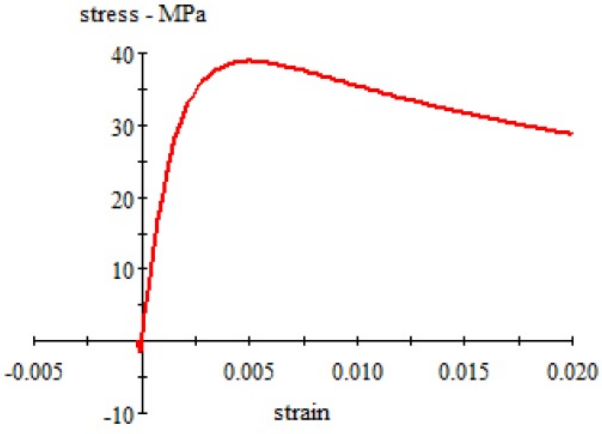

Figure 6.6: Mander Confined Concrete Model for Column 5A13

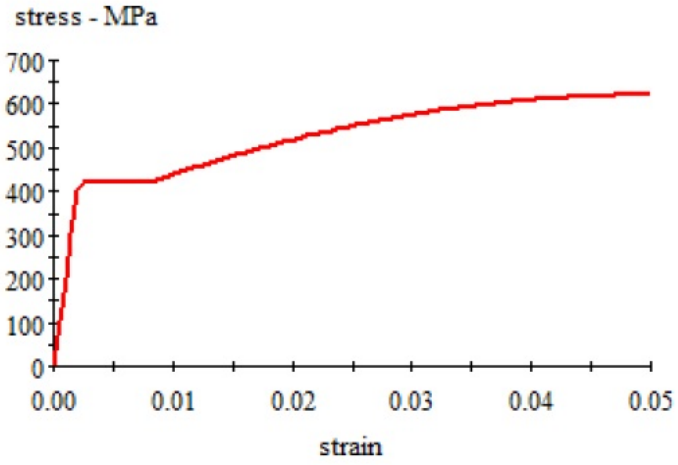

Figure 6.7: Steel Stress-Strain Curve for Column 5A13

The bending moment and axial force interaction curve which is obtained from cross-section analysis is shown in Figure 6.8. An interaction surface is created and entered to the structural analysis program as input file after a moment-axial force interaction curves performed for 0º, 45º 90º and 135º.

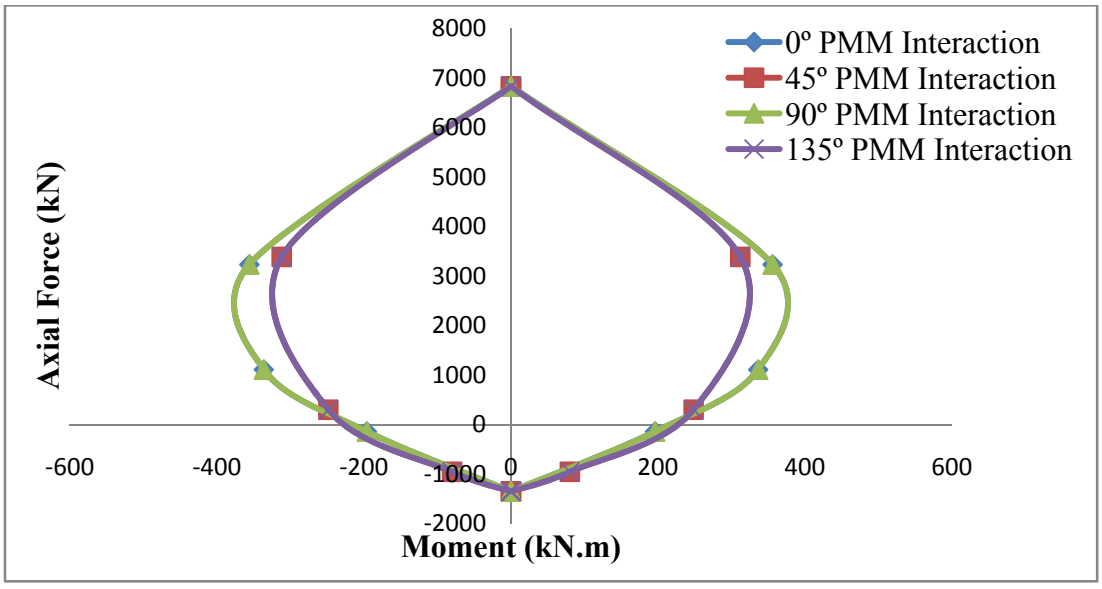

Figure 6.8: HSRC Retrofitted Column 5A13 PMM Interaction Curve

6.4.2 Column Retrofitted by Steel Jacket

For column 5A13 plastic cross-section surfaces are created by XTRACT cross-section analysis software program as shown in Figure 6.9. The steel jacket is utilized to strengthen the column. The properties of steel jacket are given Table 6.2. The Mander confined concrete model is used for the confinement of concrete. The stress-strain curves obtained from the Mander confined concrete model for column 5A13 is shown in Figure 6.10. Hardening of steel rebar and steel jacket is considered and typical stress-strain curve for steel rebar and steel jacket are shown in Figs. 6.11 and 6.12.

Table 6.2: Properties of Steel Jacket

Steel Jacket	**Tensile strength of steel jacket, f_y (MPa)**	**Ultimate strength of steel jacket, f_u (MPa)**	**Modulus of Elasticity (MPa)**
6 mm thick	250	480	200,000

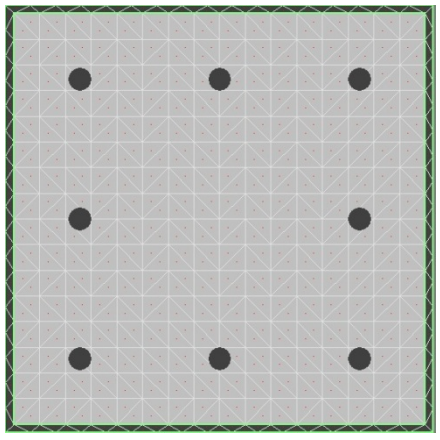

Figure 6.9: Steel Jacketed Column 5A13 Cross Sectional Detail

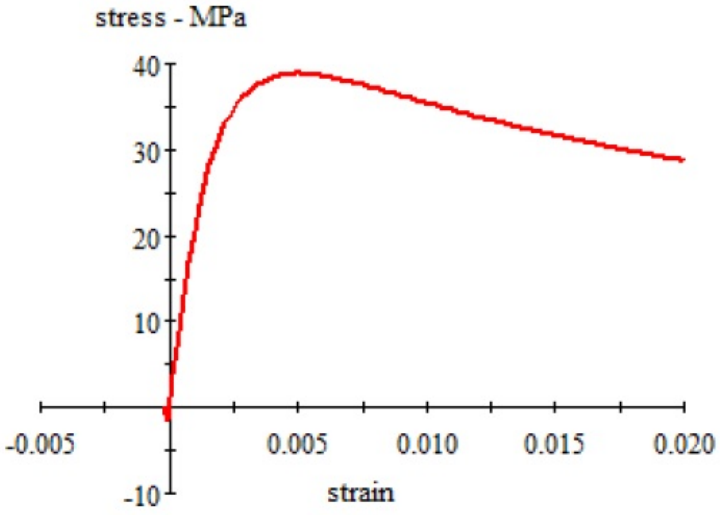

Figure 6.10: Mander Confined Concrete Model for Column 5A13

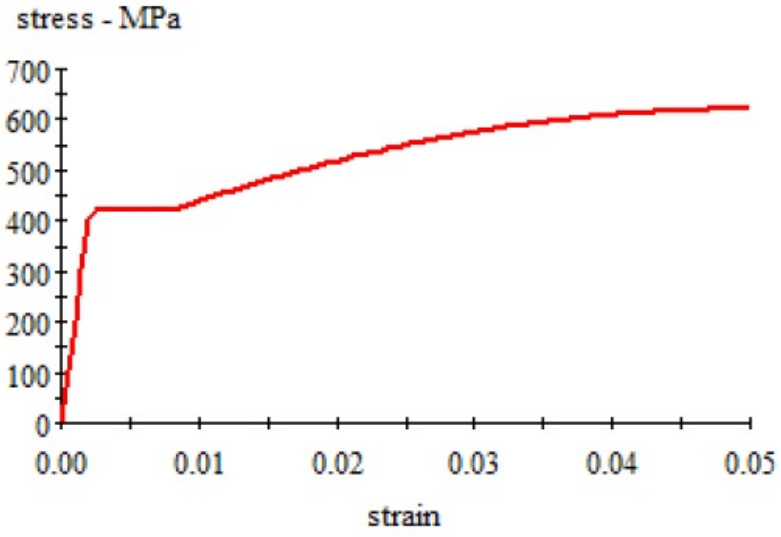

Figure 6.11: Steel Rebar Stress-Strain Curve for Column 5A13

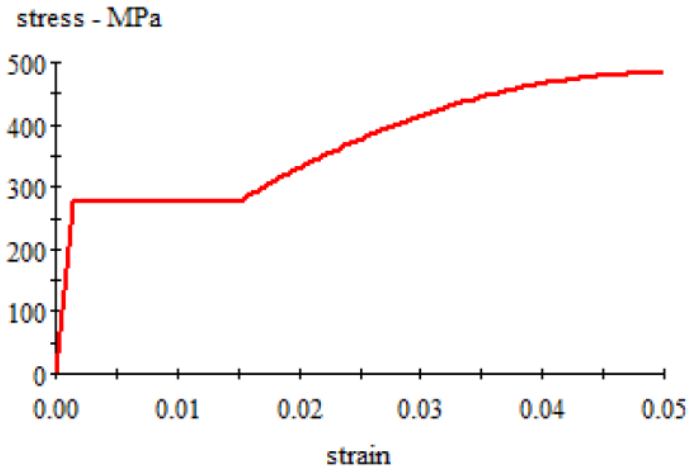

Figure 6.12: Steel Jacket Stress-Strain Curve for Column 5A13

The bending moment and axial force interaction curve which is obtained from cross-section analysis is shown in Figure 6.13. An interaction surface is created and entered to the structural analysis program as input file after a moment-axial force interaction curves performed for 0º, 45º 90º and 135º.

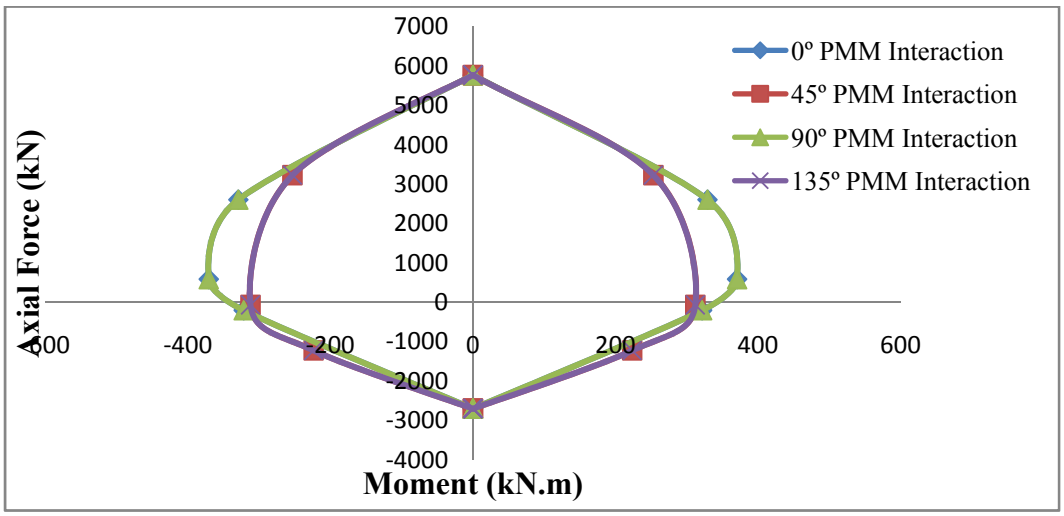

Figure 6.13: Steel Jacketed Retrofitted Column 5A13 PMM Interaction Curve

6.4.3 Column Retrofitted By CFRP Jacket

For column 5A13 plastic cross-section surfaces are created by XTRACT cross-section analysis software program as shown in Figure 6.14. The CFRP jacket is utilized to strengthen the column. The properties of CFRP jacket are given Table 6.3. The Lam and Teng confined concrete model is used for the confinement of concrete. The stress-strain curves obtained from the Lam and Teng confined concrete model for column 5A13 is shown in Figure 6.15. Hardening of steel rebar is considered. The typical stress-strain curve for steel rebar and CFRP are shown in Figs. 6.16 and 6.17.

Table 6.3: Properties of CFRP Jacket

CFRP Jacket and Laminate	**Ultimate strength of CFRP jacket and laminates, f_u (MPa)**	**Ultimate Stain (%)**	**Modulus of Elasticity (MPa)**	**Thickness (mm)**
MBRACE Fibre C1-23	4900	2.10	230,000	0.111

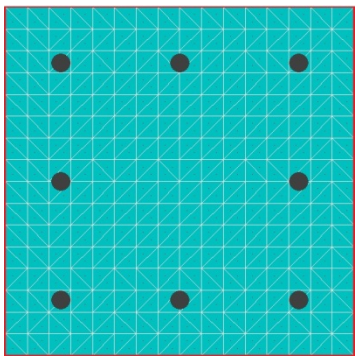

Figure 6.14: CFRP Jacketed Column 5A13 Cross Sectional Detail

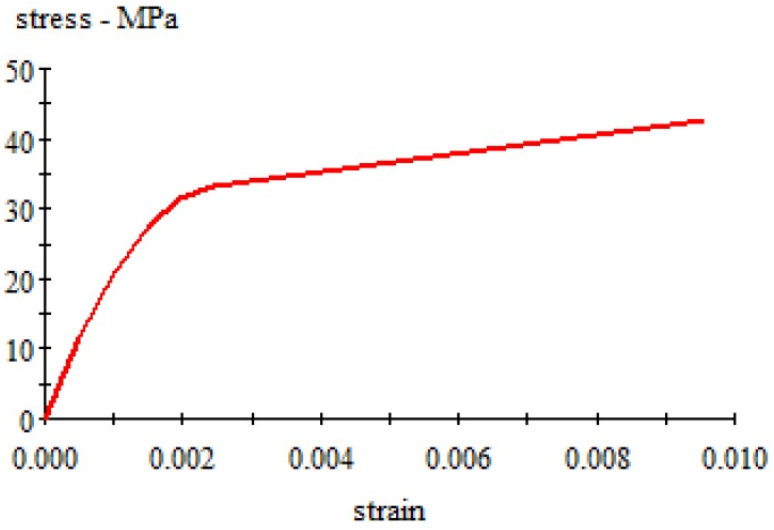

Figure 6.15: Lam and Teng Confined Concrete Model for Column 5A13

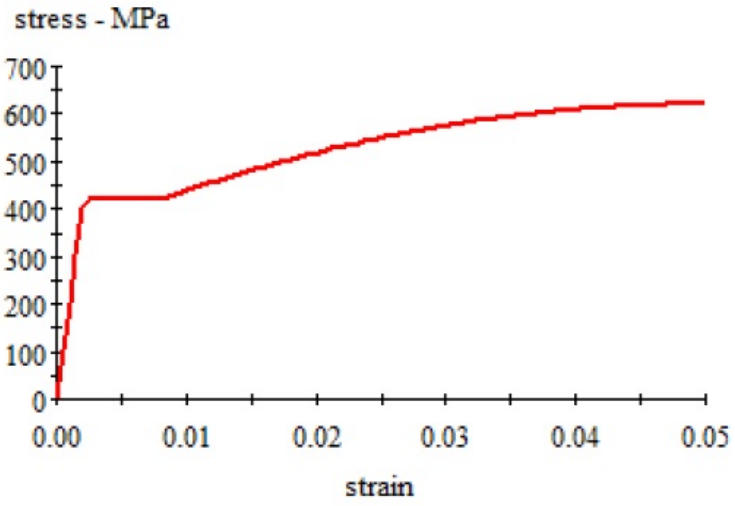

Figure 6.16: Steel Rebar Stress-Strain Curve for Column 5A13

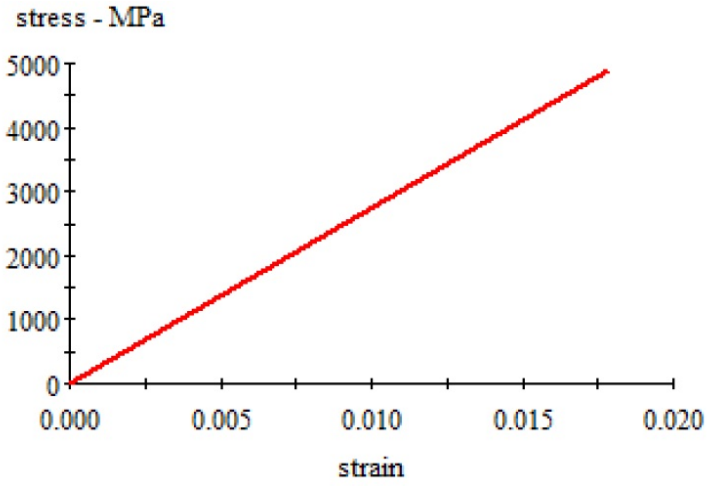

Figure 6.17: CFRP Stress-Strain Curve for Column 5A13

The bending moment and axial force interaction curve which is obtained from cross-section analysis is shown in Figure 6.18. An interaction surface is created and entered to the structural analysis program as input file after a moment-axial force interaction curves performed for 0º, 45º 90º and 135º.

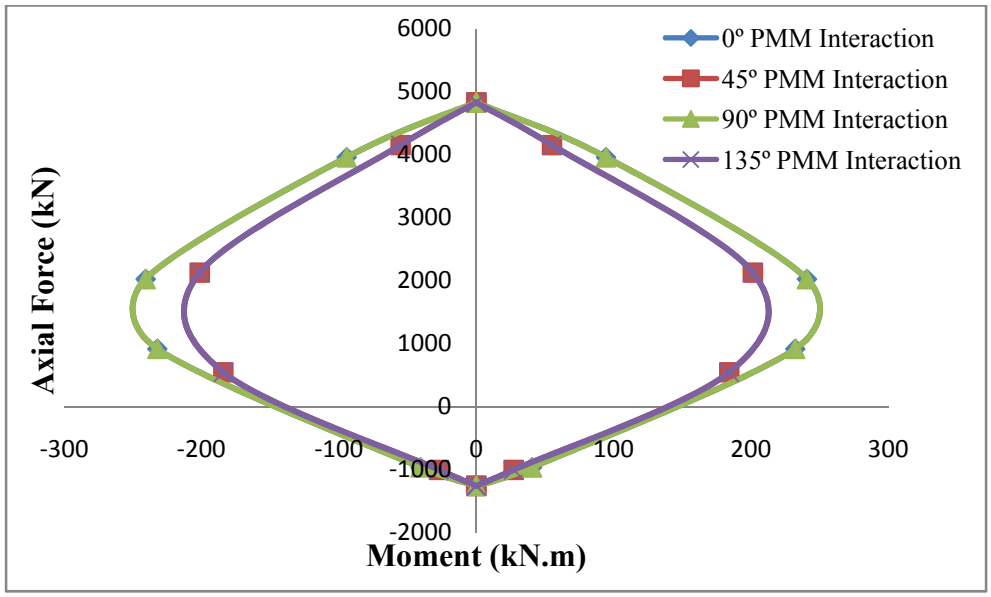

Figure 6.18: CFRP Jacketed Retrofitted Column 5A13 PMM Interaction Curve

6.4.4 Plastic Hinge at the End of Additional Shear Wall for the Mid - Pier Model

For additional shear wall SW200 made of high strength RC plastic cross-section surfaces are created by XTRACT cross-section analysis software program is shown in Figure 6.19. The Mander unconfined concrete model is used at the outer zone from the transverse reinforcement and the Mander confined concrete model is used for the core material. The stress-strain curves obtained from the Mander unconfined and confined concrete model for SW200 are shown in Figs .6.20 and 6.21. Hardening of steel material is considered and typical stress-strain curve for steel is shown in Figure 6.22.

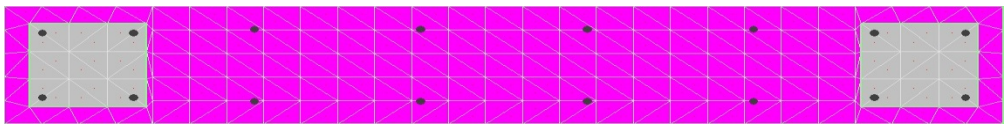

Figure 6.19: HSRC Additional Shear Wall SW200 Cross Sectional Detail

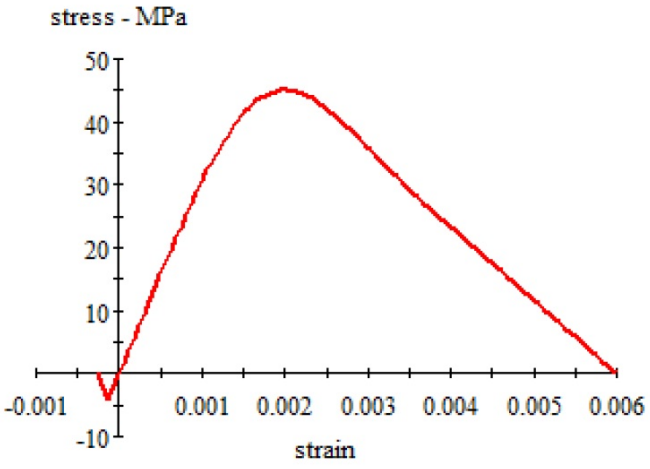

Figure 6.20: Mander Unconfined concrete model for shear wall SW200

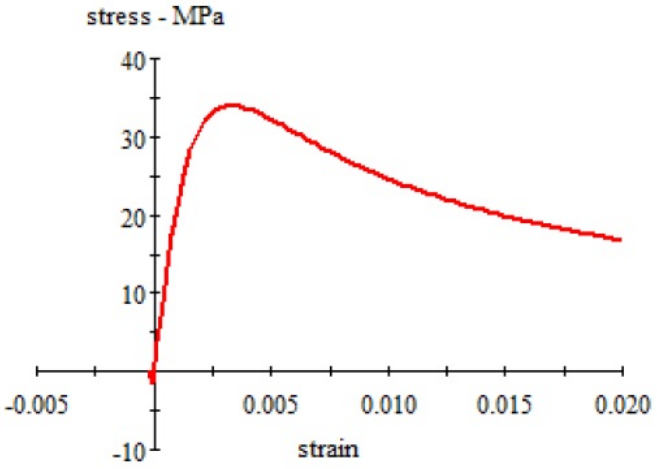

Figure 6.21: Mander Confined Concrete Model for Shear Wall SW200

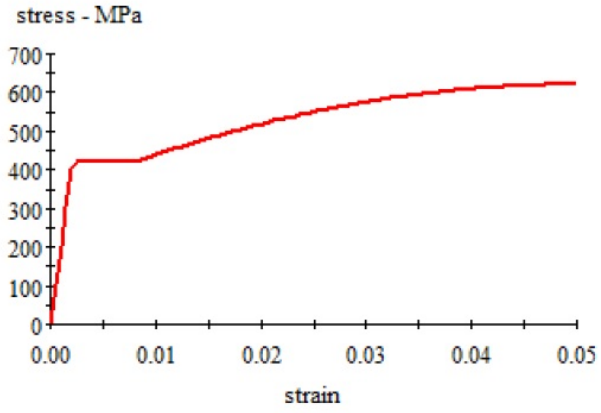

Figure 6.22: Steel Stress-Strain Curve for Shear Wall SW200

The bending moment and axial force interaction curve which is obtained from cross-section analysis is shown in Figure 6.23. An interaction surface is created and entered to the structural analysis program as input file after a moment-axial force interaction curves performed for 0º, 45º 90º and 135º.

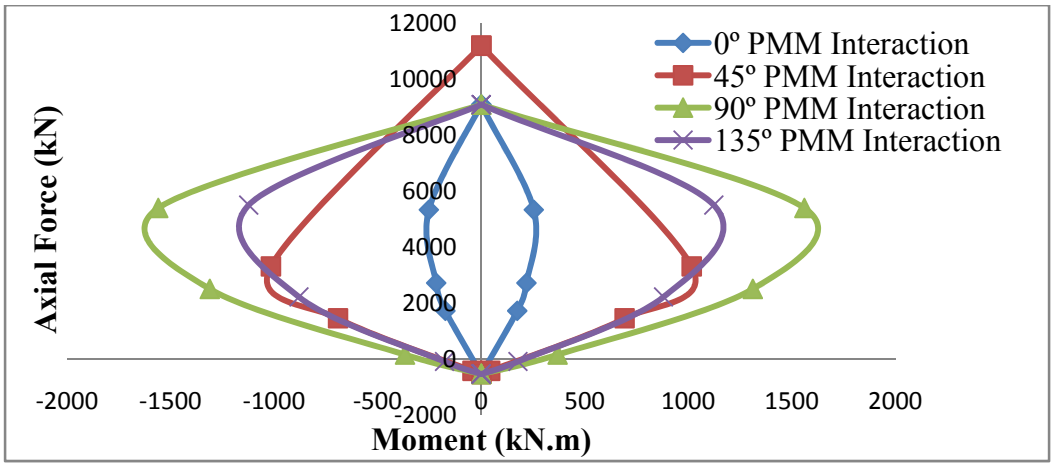

Figure 6.23: HSRC Additional Shear Wall SW200 PMM Interaction Curve

6.5 Pushover Analysis of Frame Retrofitted with High Strength Reinforced Concrete (HSRC) Jacketing

Non-linear analysis of HSRC jacketed retrofitted frame is carried out for shell element and Mid-Pier approach. Plastic hinges are defined at every column, beam end points and shear wall for Mid-Pier approach where a plastic hinge may develop. For beams moment rotation relationship was entered to SAP 2000 using user defined hinge property. For columns and shear walls PMM interacting diagram was entered at the angle of 0, 45, 90, 135, 180, 225, 270, 315 degrees to SAP2000 using user defined hinge property. For Shell element approach shear walls are modeled using shell elements. Automatic mesh area option is utilized for meshing of the shear wall.

Before carrying out pushover analysis of retrofitted frame nonlinear gravity analysis is carried out by considering 1D+0.25L load. Then retrofitted frame is pushed in both direction i.e. positive and negative x upto predefined displacement under constant gravity

loads and monotonically increasing equivalent seismic loads. Figure 6.24 shows the pushover curves for retrofitted frame.

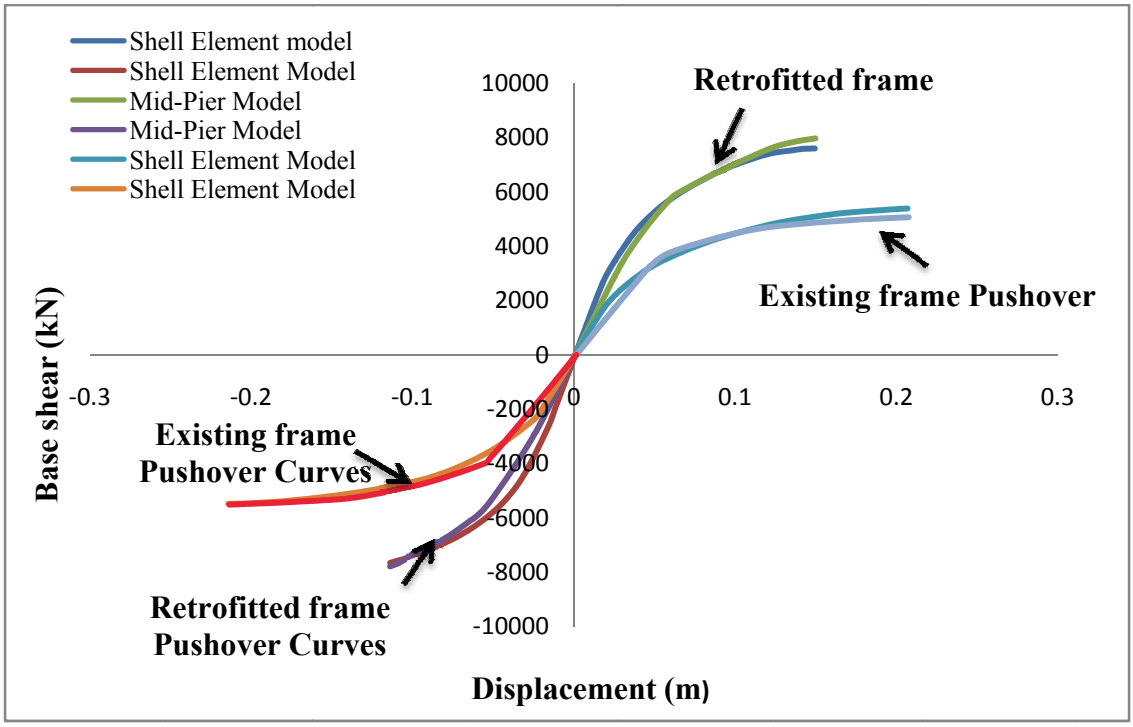

Figure 6.24: Pushover Curves for HSRC Jacketed Retrofitted Frame and Existing Frame

6.6 Pushover Analysis of Frame Retrofitted with Steel Jacketing

Non-linear analysis of Steel jacketed retrofitted frame is carried out for shell element and Mid-Pier approach. Plastic hinges are defined at every column, beam end points and shear wall for Mid-Pier approach where a plastic hinge may develop. For beams moment rotation relationship was entered to SAP 2000 using user defined hinge property. For columns and shear walls PMM interacting diagram was entered at the angle of 0, 45, 90, 135, 180, 225, 270, 315 degrees to SAP2000 using user defined hinge property. For Shell

element approach shear walls are modeled using shell elements. Automatic mesh area option is utilized for meshing of the shear wall.

Before carrying out pushover analysis of retrofitted frame nonlinear gravity analysis is carried out by considering 1D+0.25L load. Then retrofitted frame is pushed in both direction i.e. positive and negative x upto predefined displacement under constant gravity loads and monotonically increasing equivalent seismic loads. Figure 6.25 shows the pushover curves for retrofitted frame.

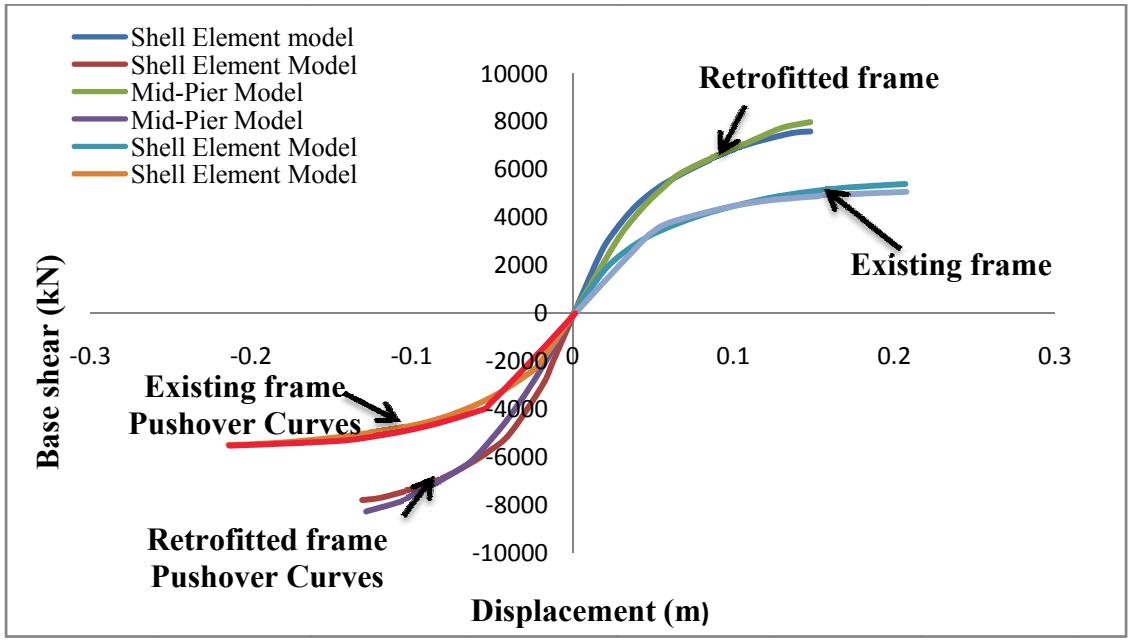

Figure 6.25: Pushover Curves for Steel Jacketed Retrofitted Frame and Existing Frame

6.7 Pushover Analysis of Frame Retrofitted with CFRP Jacketing

Non-linear analysis of CFRP jacketed retrofitted frame is carried out for shell element and Mid-Pier approach. Plastic hinges are defined at every column, beam end points and

shear wall for Mid-Pier approach where a plastic hinge may develop. For beams moment rotation relationship was entered to SAP 2000 using user defined hinge property. For columns and shear walls PMM interacting diagram was entered at the angle of 0, 45, 90, 135, 180, 225, 270, 315 degrees to SAP2000 using user defined hinge property. For Shell element approach shear walls are modeled using shell elements. Automatic mesh area option is utilized for meshing of the shear wall.

Before carrying out pushover analysis of retrofitted frame nonlinear gravity analysis is carried out by considering 1D+0.25L load. Then retrofitted frame is pushed in both direction i.e. positive and negative x upto predefined displacement under constant gravity loads and monotonically increasing equivalent seismic loads. Figure 6.26 shows the pushover curves for retrofitted frame.

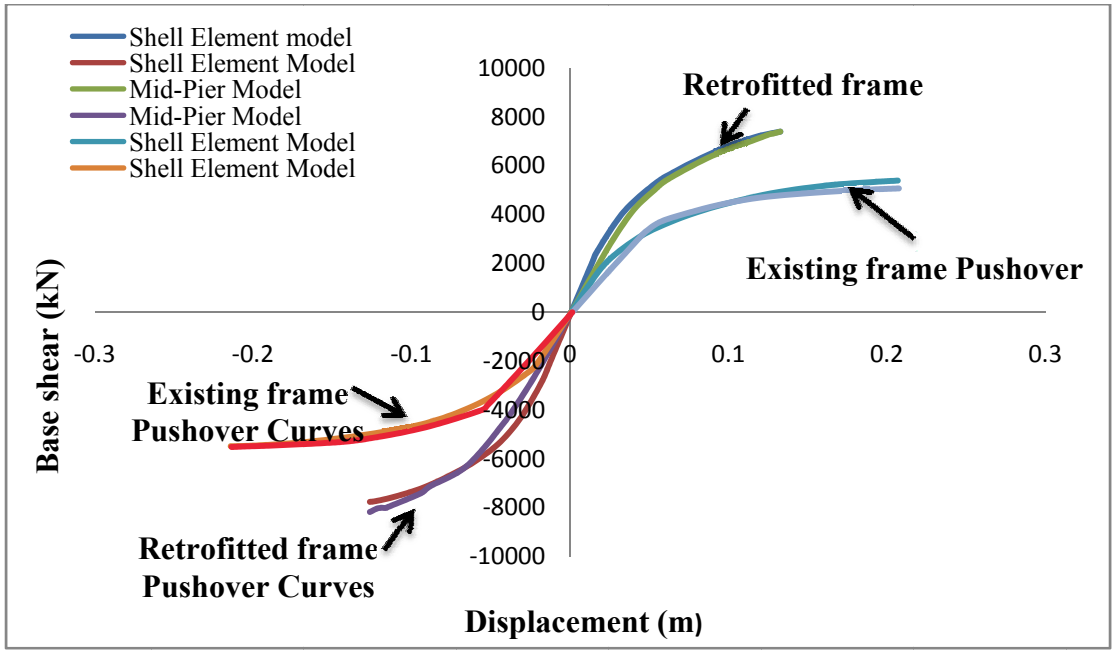

Figure 6.26: Pushover Curves for CFRP Jacketed Retrofitted Frame and Existing Frame

6.8 Comparison of Retrofitting Schemes

Comparison of different retrofitting schemes was carried out based on pushover curves. Figs. 6.27 and 6.28 shows pushover curves of retrofitted and existing frame model with Shell element and Mid-Pier models for different retrofitting schemes.

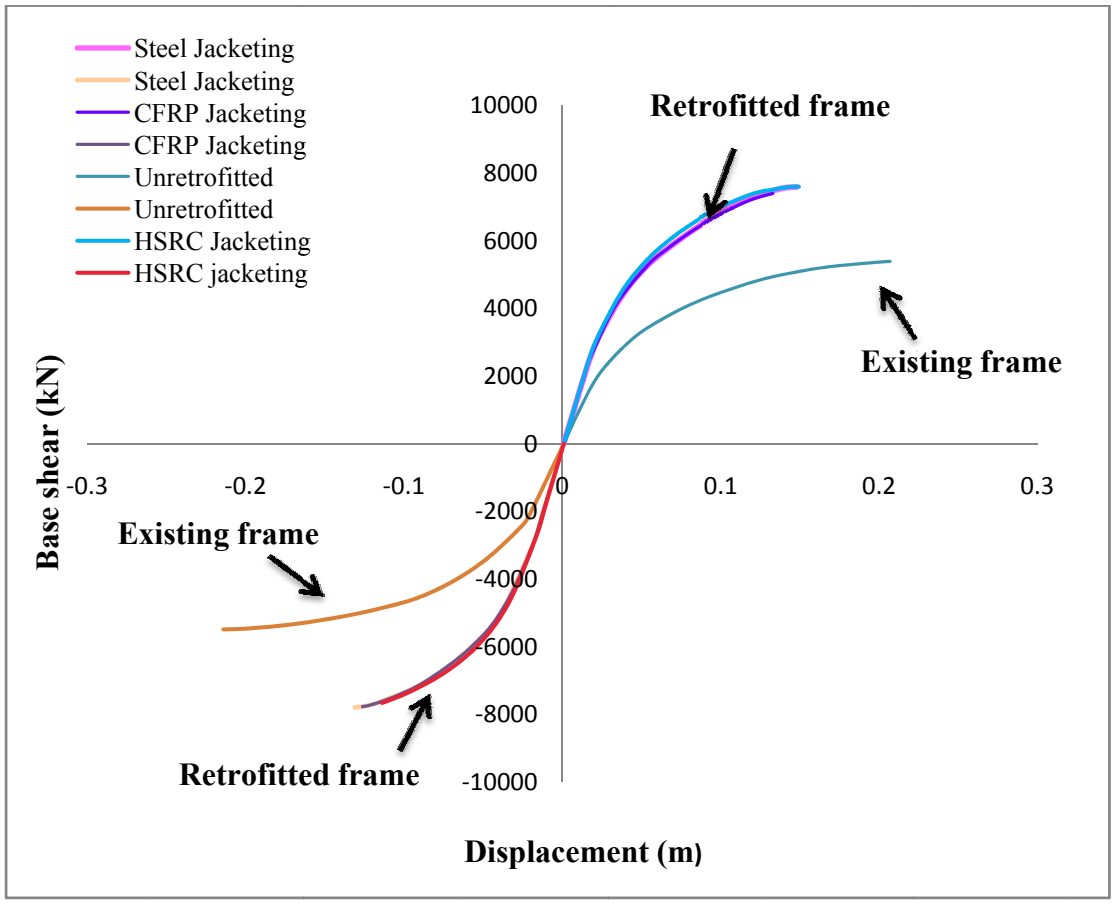

Figure 6.27: Pushover Curves of Retrofitted and Existing Frame Model with Shell Element Approach for Different Retrofitting Schemes

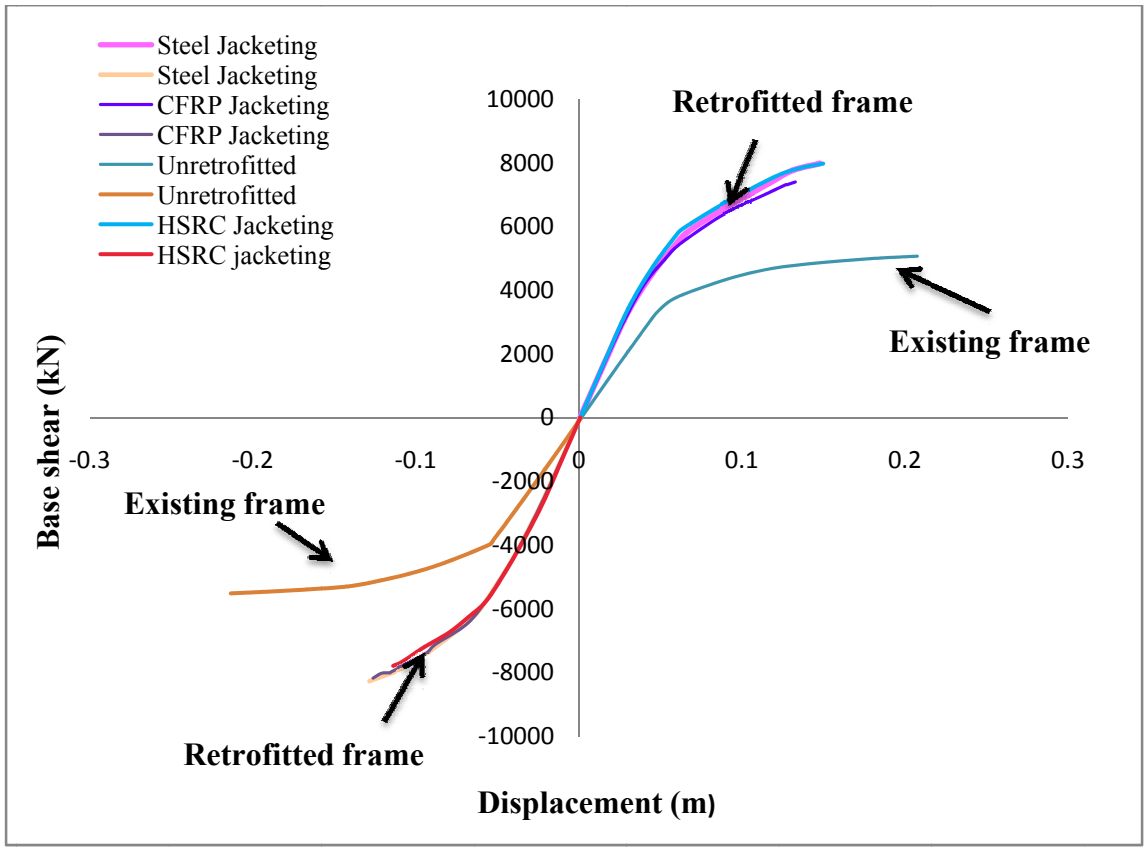

Figure 6.28: Pushover Curves of Retrofitted and Existing Frame Model with Mid-Pier Approach for Different Retrofitting Schemes

6.9 Performance of Retrofitted Frame

In this section the performance point will be estimated for the Retrofitted RC frame. Capacity Spectrum Method (CSM) procedure B is adopted which were explained in section 5.8 to determine the performance point of the existing frame. The typical graphs for calculation of performance point of HSRC retrofitted frame model with shell element are shown in Figure 6.29.The performance point of retrofitted frame model with Shell element and Mid-Pier approaches for different retrofitting schemes are given in Tables 6.4 and 6.5.

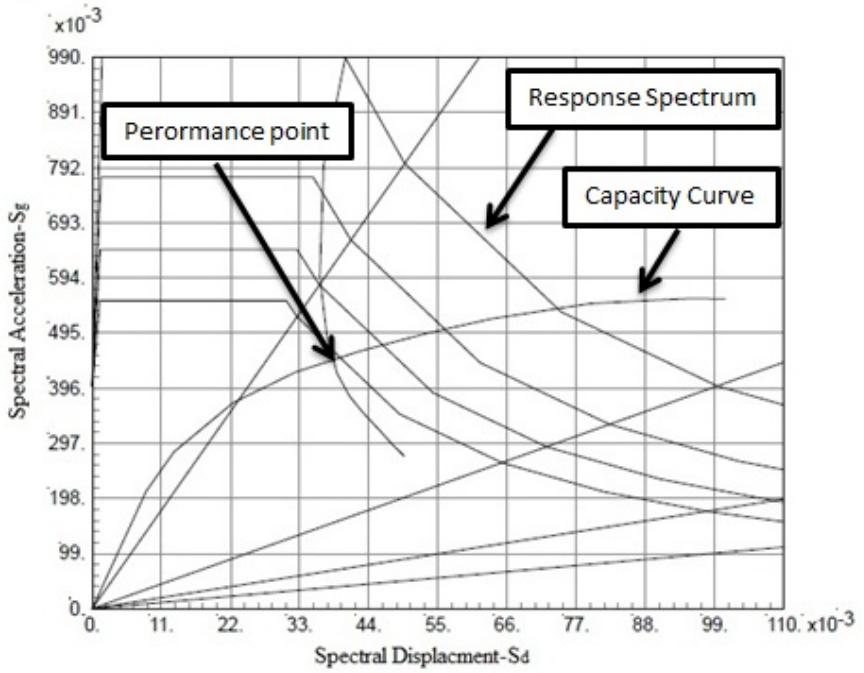

a) positive x-direction

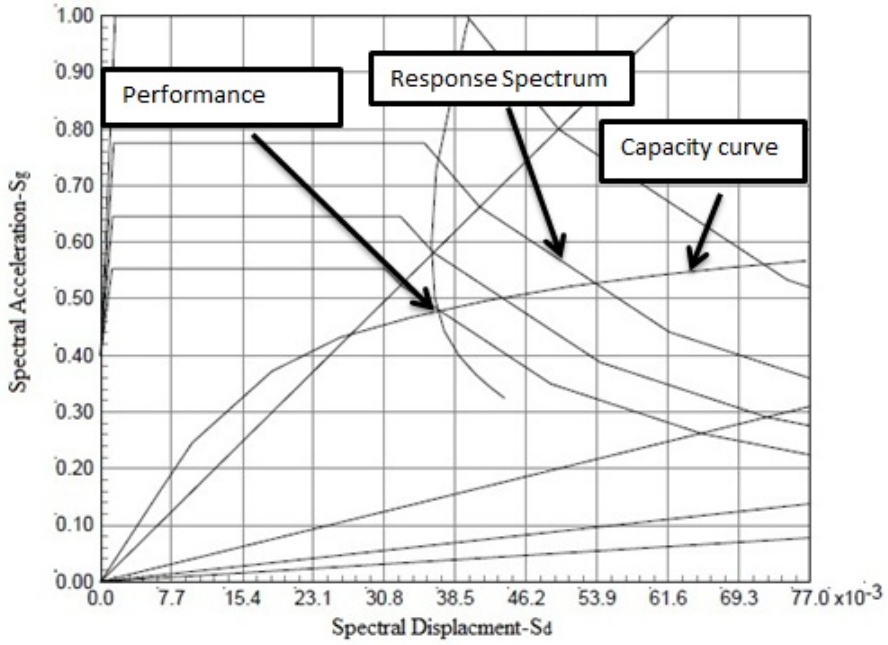

b) negative x-direction

Figure 6.29: Performance Point of HSRC Retrofitted Frame Model with Shell Element Approach

Table 6.4: Performance Point of Retrofitted Frame Model with Shell Element Approach

Retrofitted Schemes	Axis	Spectral Acceleration S_a	Spectral Displacement S_d	Base Shear (kN)	Displacement (m)
HSRC jacketed	+X	0.447	0.038	5767.8	0.061
HSRC jacketed	-X	0.478	0.037	6137.2	0.058
Steel Jacketed	+X	0.435	0.039	5578.5	0.062
Steel Jacketed	-X	0.473	0.037	6017.7	0.058
CFRP Jacketed	+X	0.436	0.039	5595.4	0.062
CFRP Jacketed	-X	0.472	0.037	6013.4	0.058

Table 6.5: Performance Point Of Retrofitted Frame Model With Mid-Pier Approach

Retrofitted Schemes	Axis	Spectral Acceleration S_a	Spectral Displacement S_d	Base Shear (kN)	Displacement (m)
HSRC jacketed	+X	0.497	0.044	6083.6	0.069
HSRC jacketed	-X	0.515	0.044	6255.4	0.068
Steel Jacketed	+X	0.049	0.045	5926.5	0.07
Steel Jacketed	-X	0.542	0.045	6448.9	0.069
CFRP Jacketed	+X	0.466	0.044	5680	0.068
CFRP Jacketed	-X	0.547	0.045	6502.9	0.069

6.10 Acceptance Criteria for Performance and Hinge Formation at Demand Displacement

The ATC-40 acceptance criteria for performance is utilized get the performance level of retrofitted frame for different retrofitting schemes. The values of these performance levels recommended by ATC-40 are explained in section 5.9. In SAP2000 ATC-40 acceptance criteria were entered to get the structural performance level of the retrofitted frame. Figs. 6.30 and 6.31 shows the hinge formation in retrofitted frame modeled with Shell element approach for different retrofitting strategies in positive and negative x-directions.

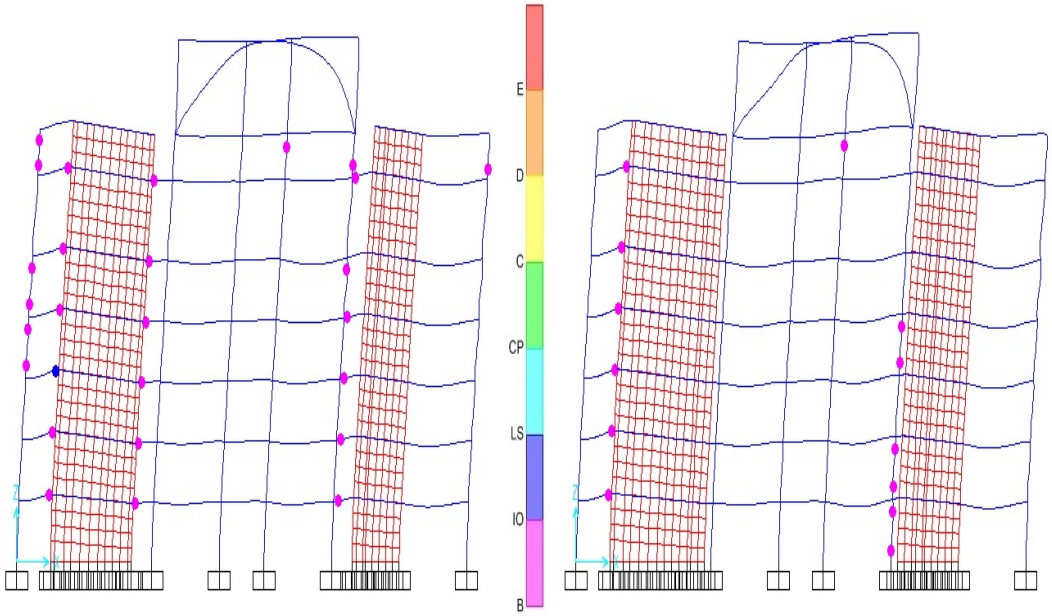

a) Existing Frame b) HSRC Jacketed Retrofitted Frame

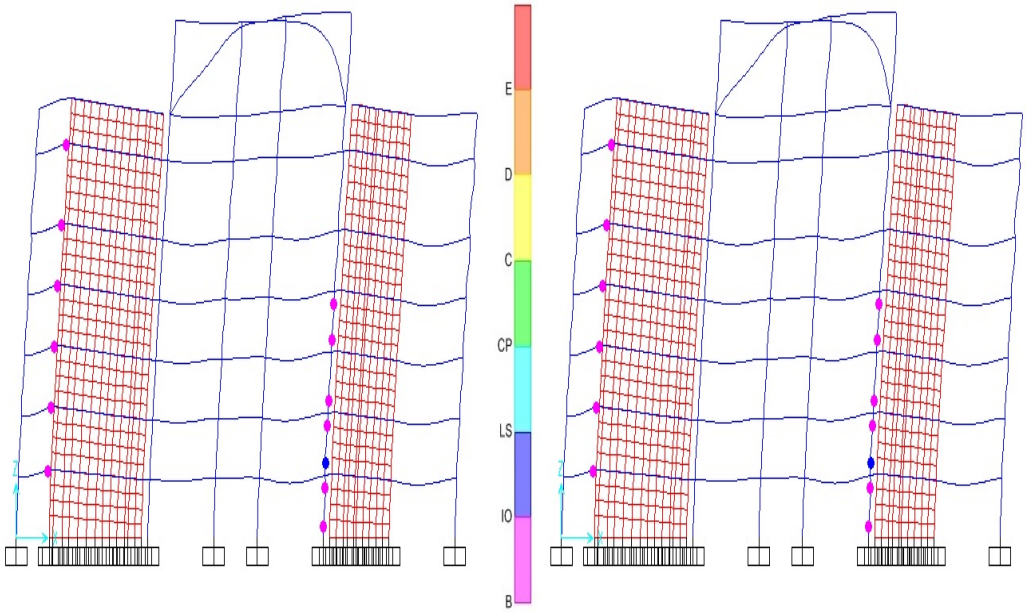

c) Steel Jacketed Retrofitted frame d) CFRP Jacketed Retrofitted Frame

Figure 6.30: Hinge Formation in Existing and Retrofitted Frame In positive x-direction

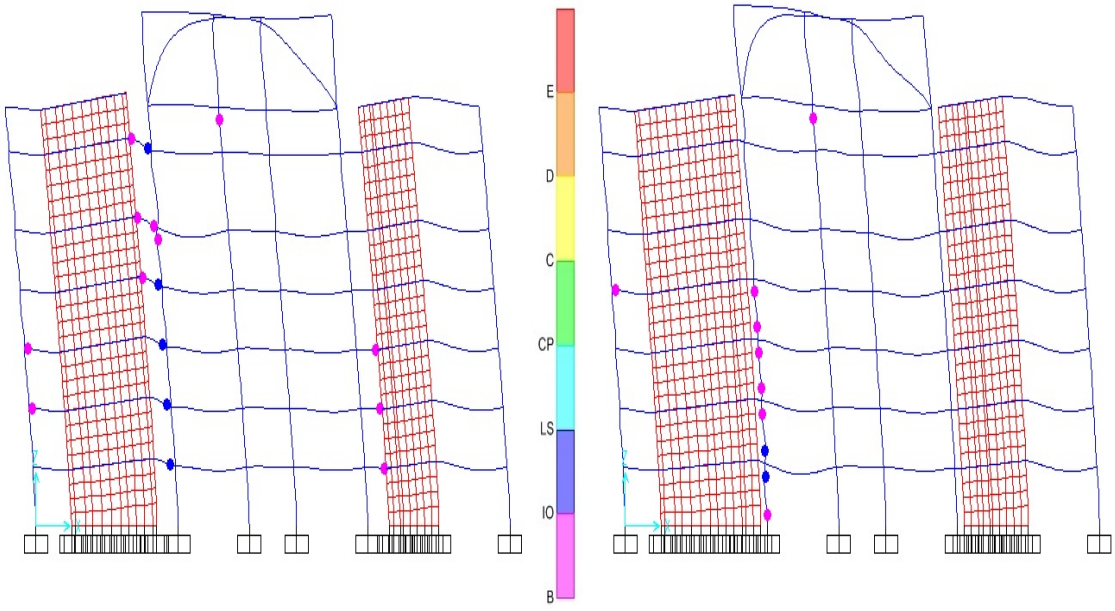

a) Existing Frame b) HSRC Jacketed Retrofitted Frame

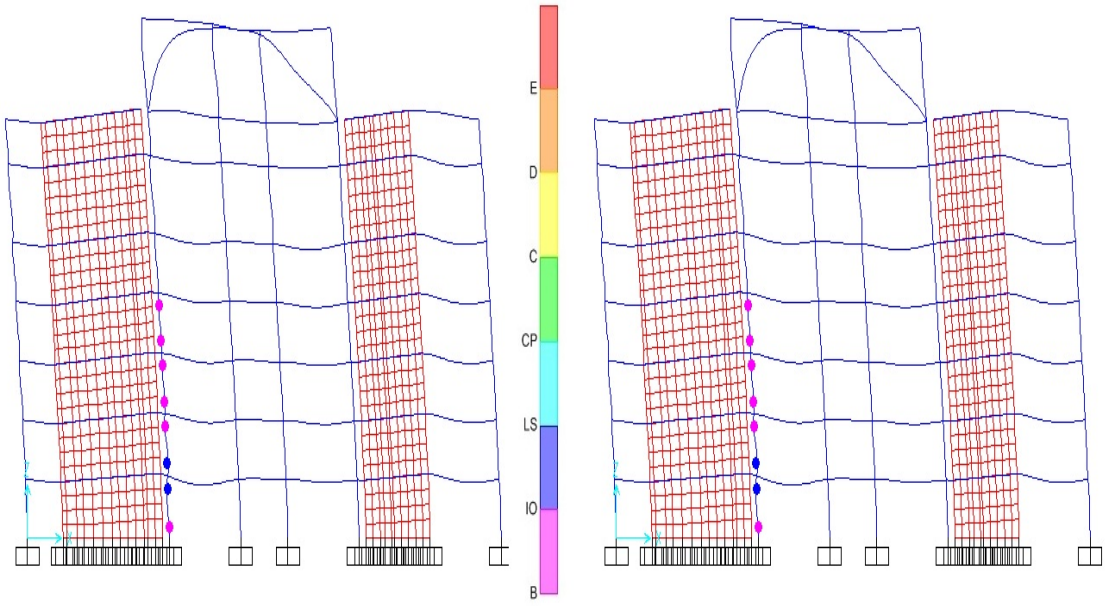

c) Steel Jacketed Retrofitted frame d) CFRP Jacketed Retrofitted Frame

Figure 6.31: Hinge Formation in Existing and Retrofitted Frame in negative x-direction

Figs.6.32 and 6.33 shows the maximum stresses in steel at the base of shear wall in retrofitted frame modeled with Shell element approach for different retrofitting strategies in positive and negative x-directions.

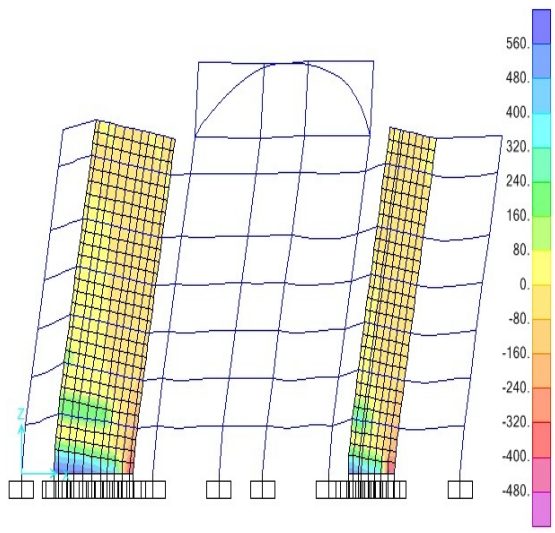

a) Existing Frame

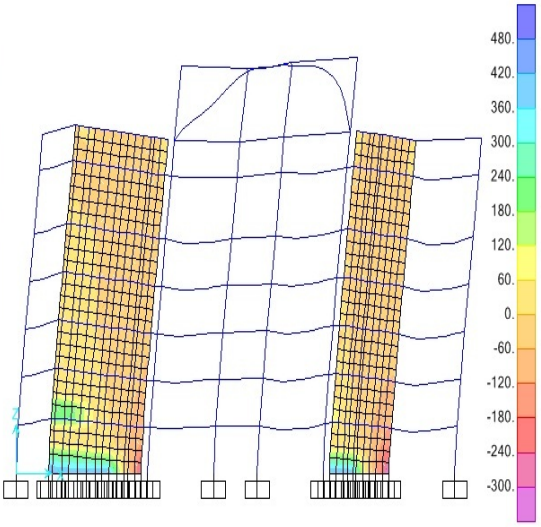

b) HSRC Jacketed Retrofitted Frame

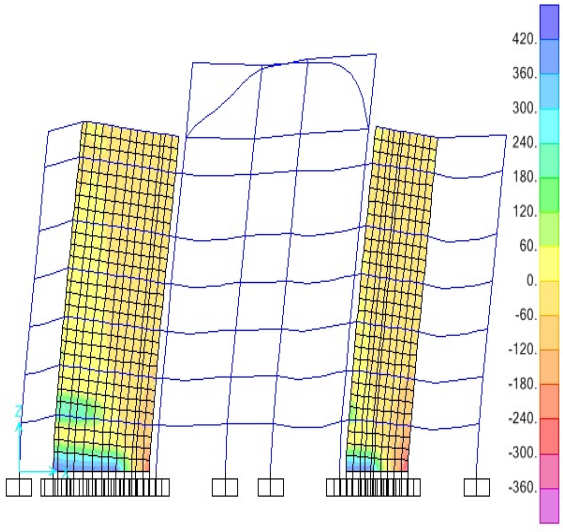

c) Steel Jacketed Retrofitted frame

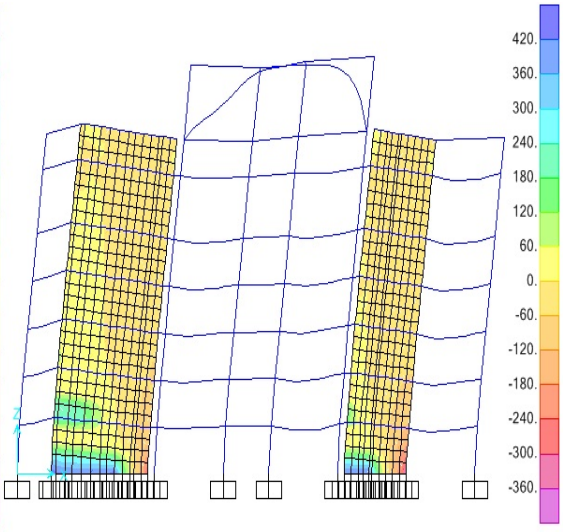

d) CFRP Jacketed Retrofitted Frame

Figure 6.32: Maximum Stresses in Steel at the Base of Shear Wall in Existing and Retrofitted Frame in positive x-direction

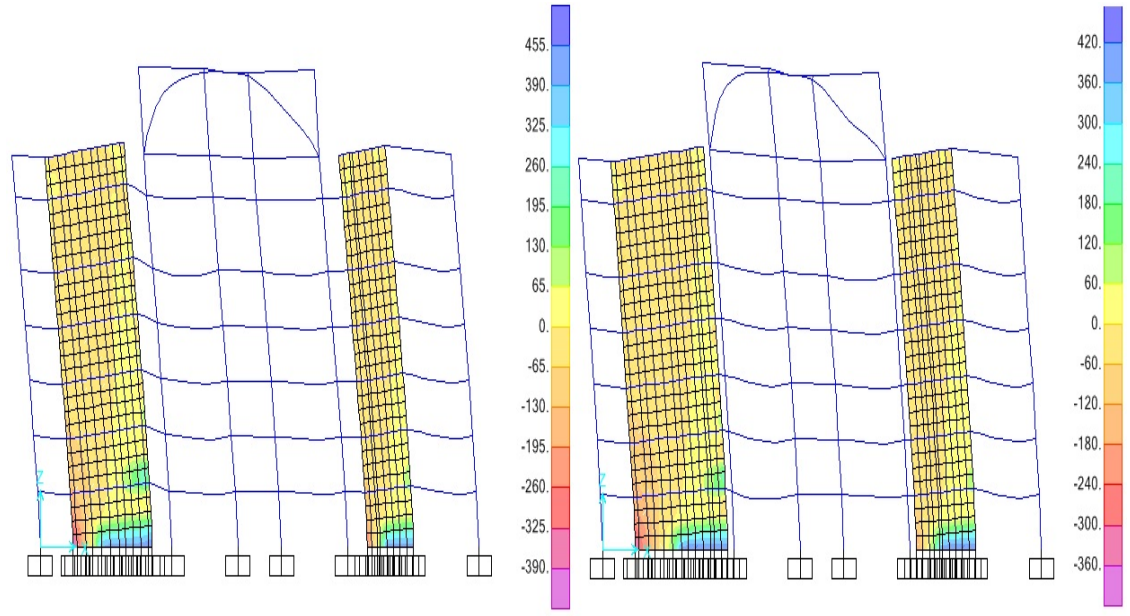

a) Existing Frame b) HSRC Jacketed Retrofitted Frame

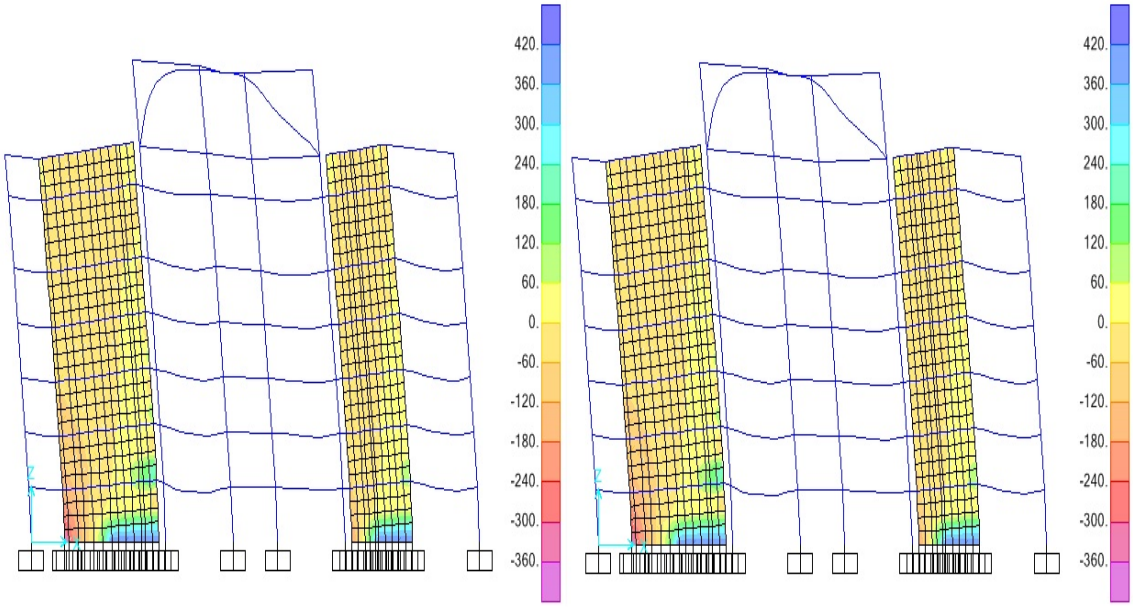

c) Steel Jacketed Retrofitted frame d) CFRP Jacketed Retrofitted Frame

Figure 6.33: Maximum Stresses in Steel at the Base of Shear Wall in Existing and Retrofitted Frame in negative x-direction

Figs.6.34 and 6.35 shows the maximum stresses in concrete at the base of shear wall in retrofitted frame modeled with Shell element approach for different retrofitting strategies in positive and negative x-directions.

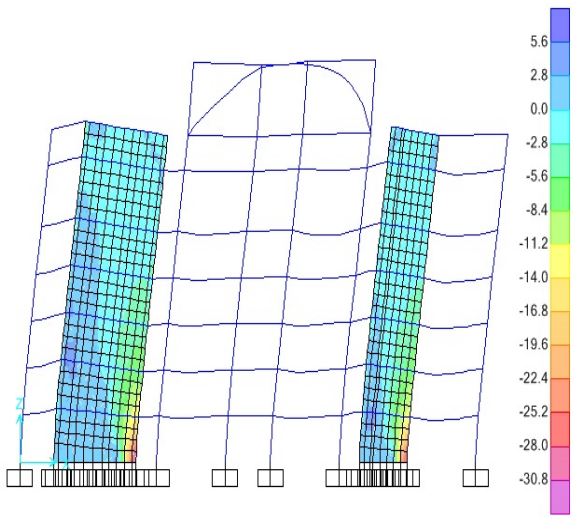

a) Existing Frame

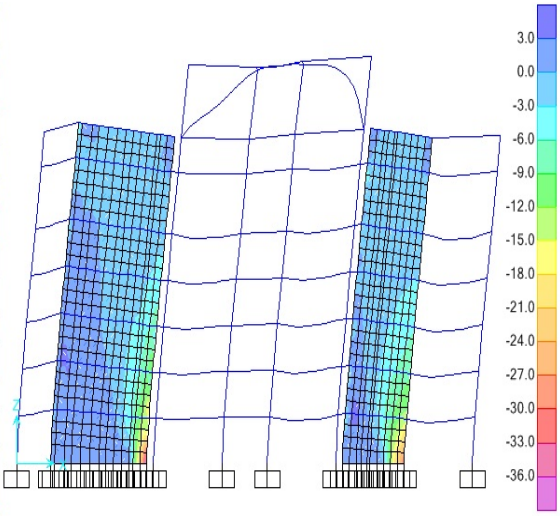

b) HSRC Jacketed Retrofitted Frame

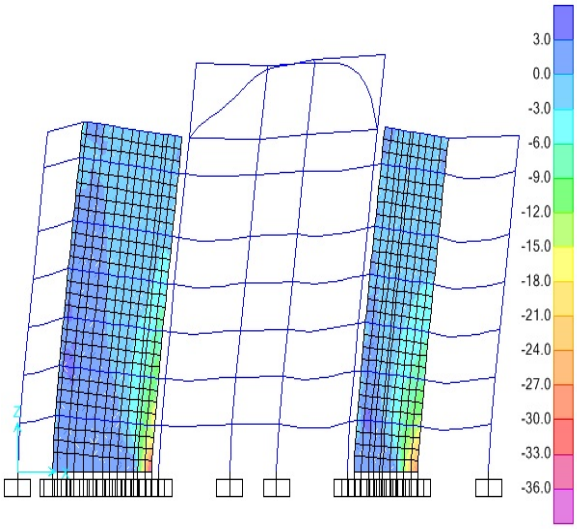

c) Steel Jacketed Retrofitted frame

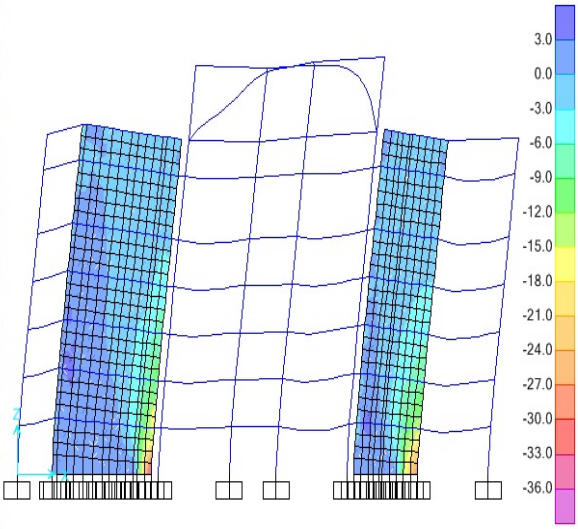

d) CFRP Jacketed Retrofitted Frame

Figure 6.34: Maximum Stresses in Concrete at the Base of Shear Wall in Existing and Retrofitted Frame in positive x-direction

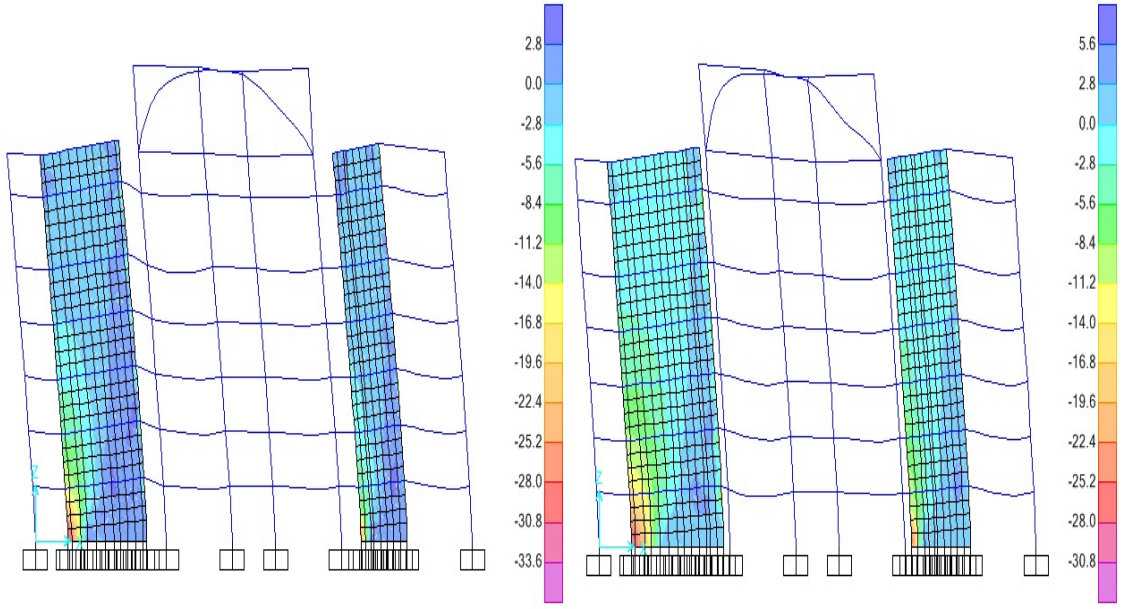

a) Existing Frame

b) HSRC Jacketed Retrofitted Frame

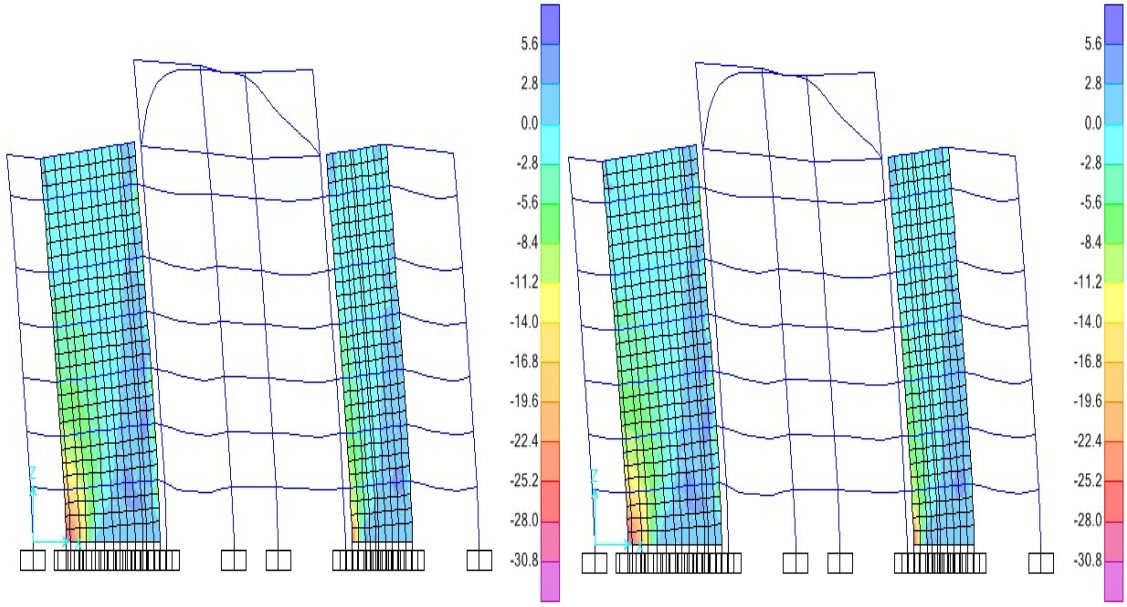

c) Steel Jacketed Retrofitted frame

d) CFRP Jacketed Retrofitted Frame

Figure 6.35: Maximum Stresses in Concrete at the Base of Shear Wall in Existing and Retrofitted Frame in negative x-direction

Figs.6.36 and 6.37 shows the hinge formation in retrofitted frame modeled with Mid-Pier approach for different retrofitting strategies in positive and negative x-directions.

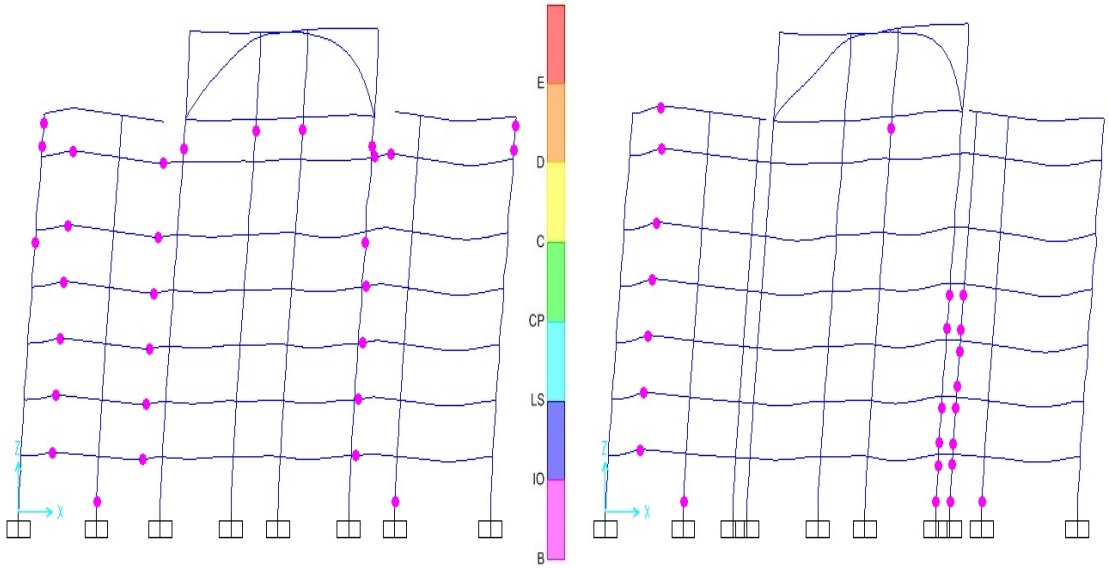

a) Existing Frame b) HSRC Jacketed Retrofitted Frame

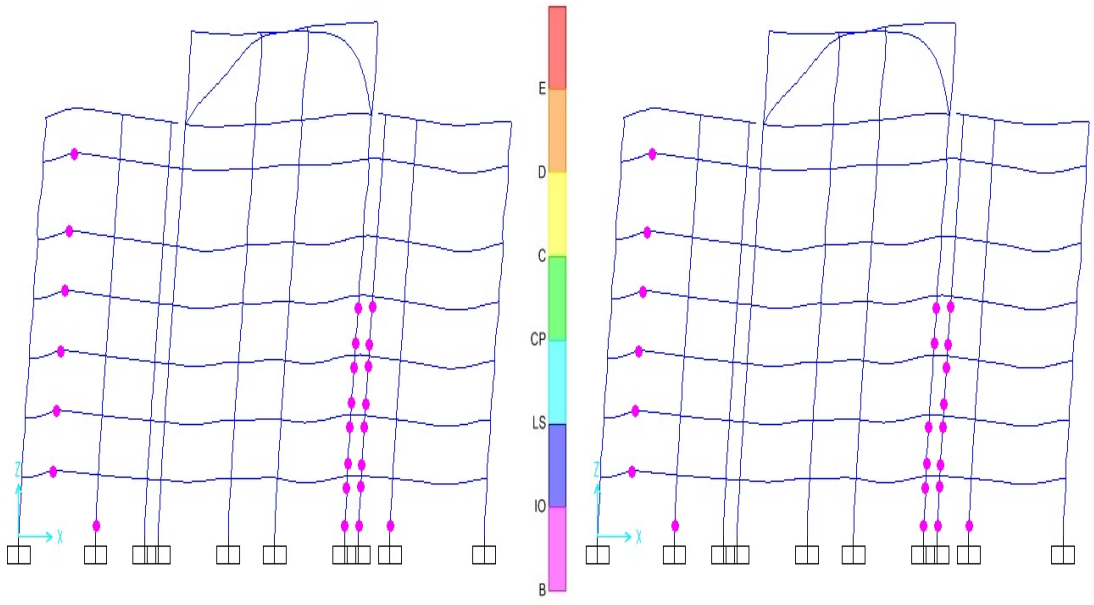

c) Steel Jacketed Retrofitted frame d) CFRP Jacketed Retrofitted Frame

Figure 6.36: Hinge Formation in Existing and Retrofitted Frame in positive x-direction

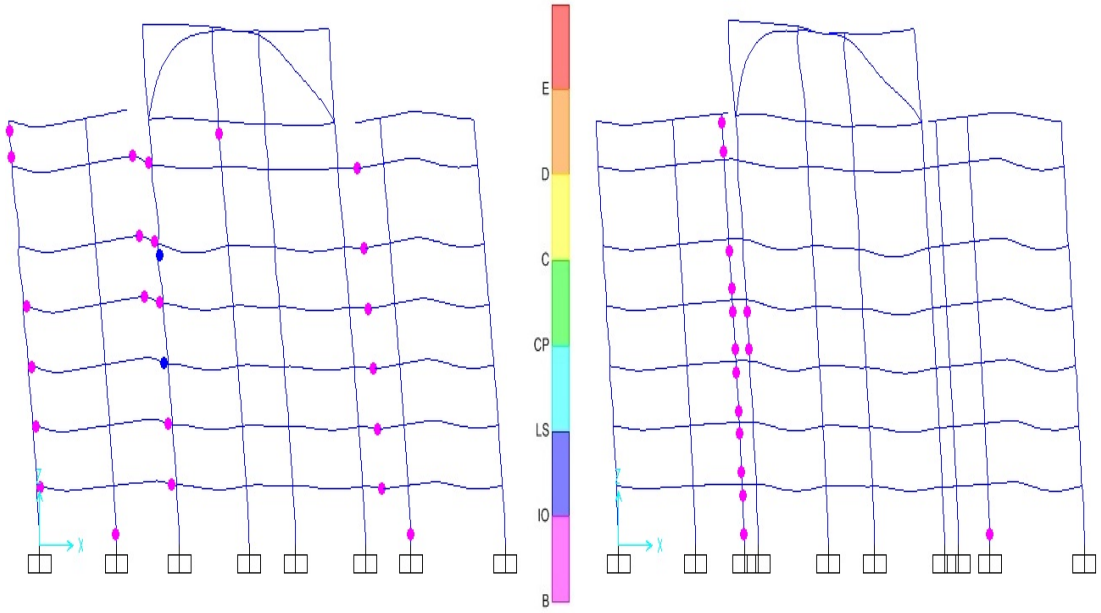

a) Existing Frame

b) HSRC Jacketed Retrofitted Frame

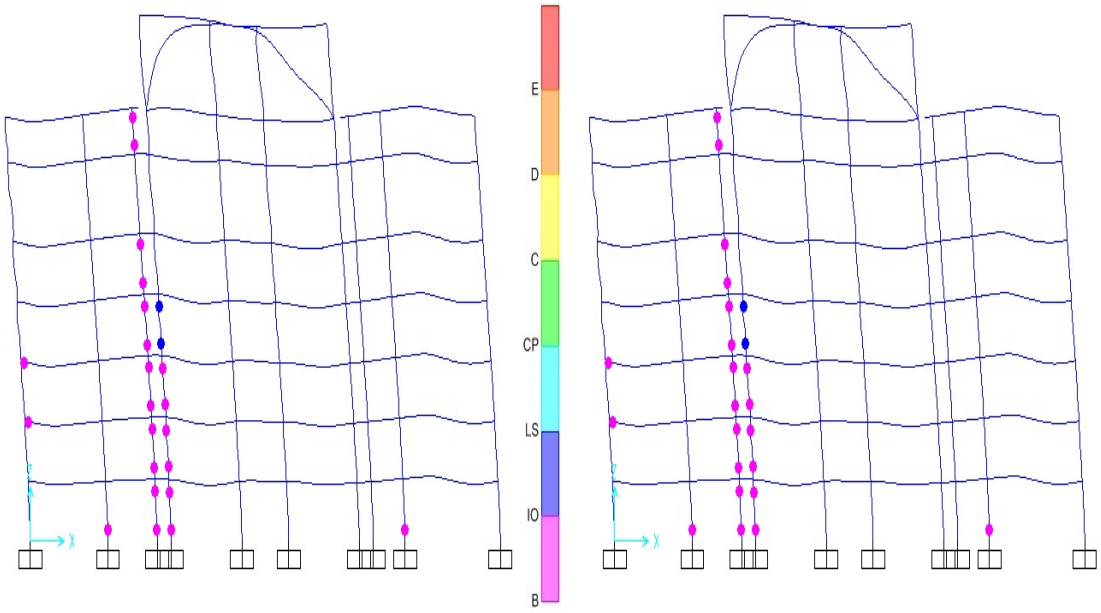

c) Steel Jacketed Retrofitted frame

d) CFRP Jacketed Retrofitted Frame

Figure 6.37: Hinge Formation in Existing and Retrofitted Frame in negative x-direction

6.11 Storey Drifts

Inter-storey drift ratio and total storeys drift is computed for retrofitted frame and compared with the existing frame. Figs. 6.38 and 6.39 show the inter-storey drift ratio of retrofitted frame and existing frame model with shell element and mid-pier approach for different retrofitting schemes. Figs. 6.40 and 6.41 show total storeys drift of retrofitted frame and existing frame model with shell element and mid-pier approach for different retrofitting schemes.

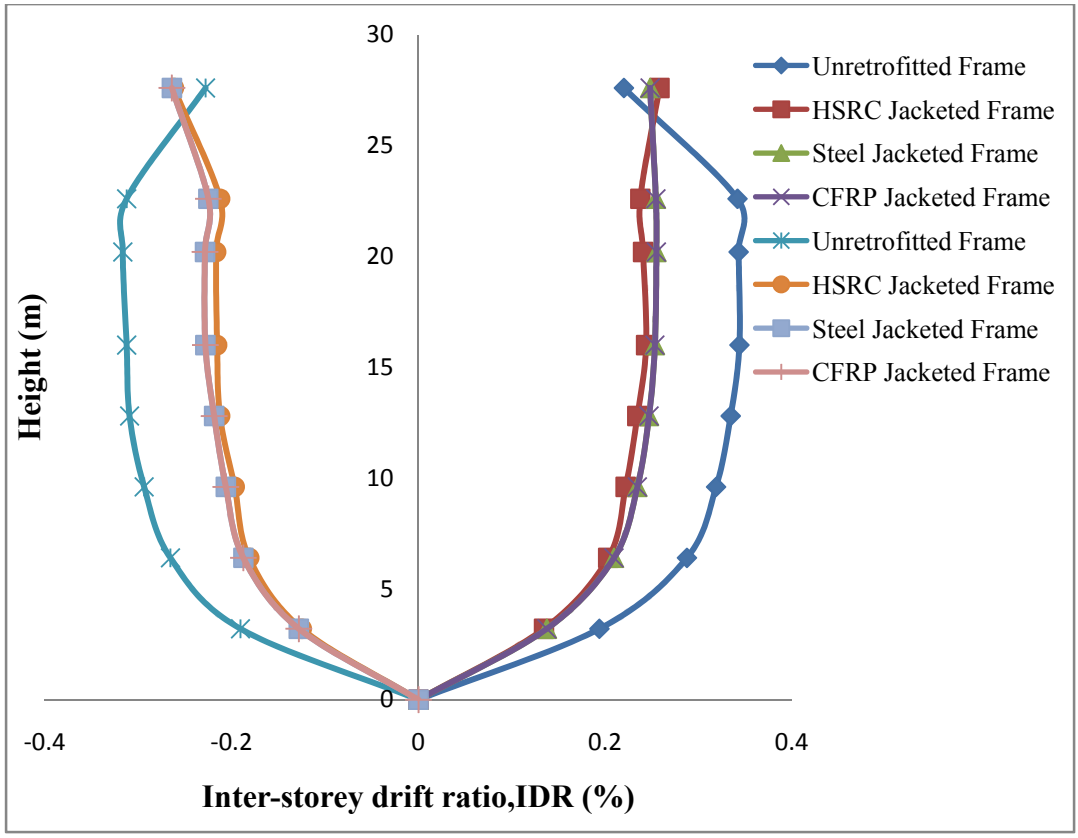

Figure 6.38: Inter-storey drift Ratio for existing and retrofitted frame model using shell approach

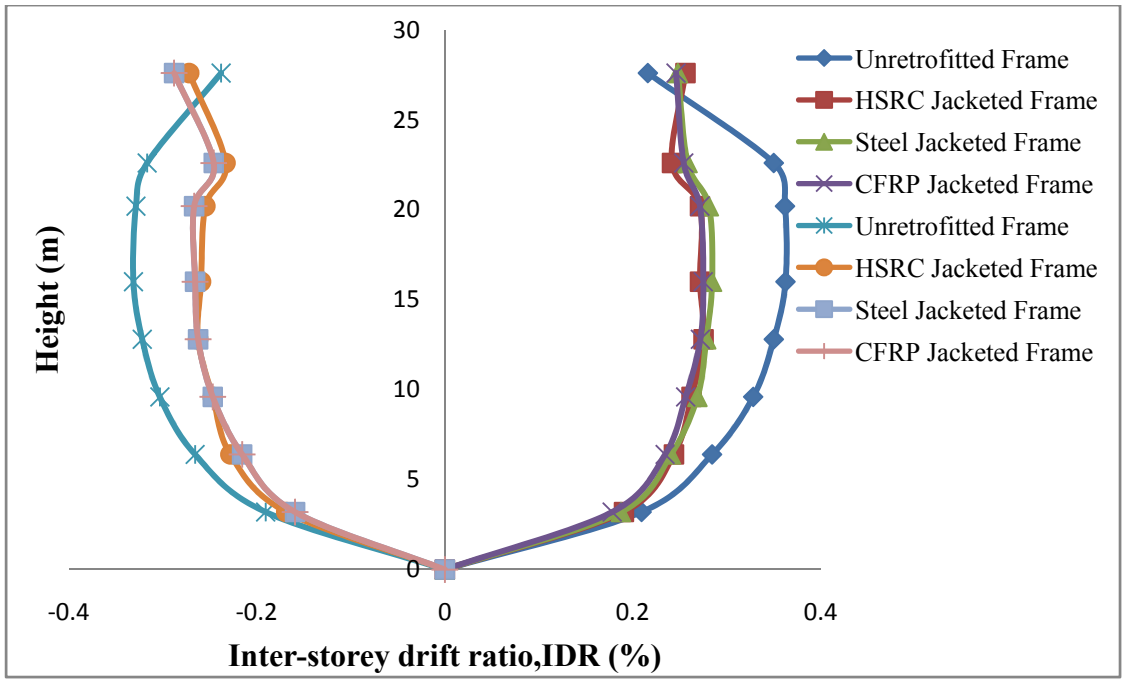

Figure 6.39: Inter-storey drift ratio for existing and retrofitted frame model using Mid-Pier Approach

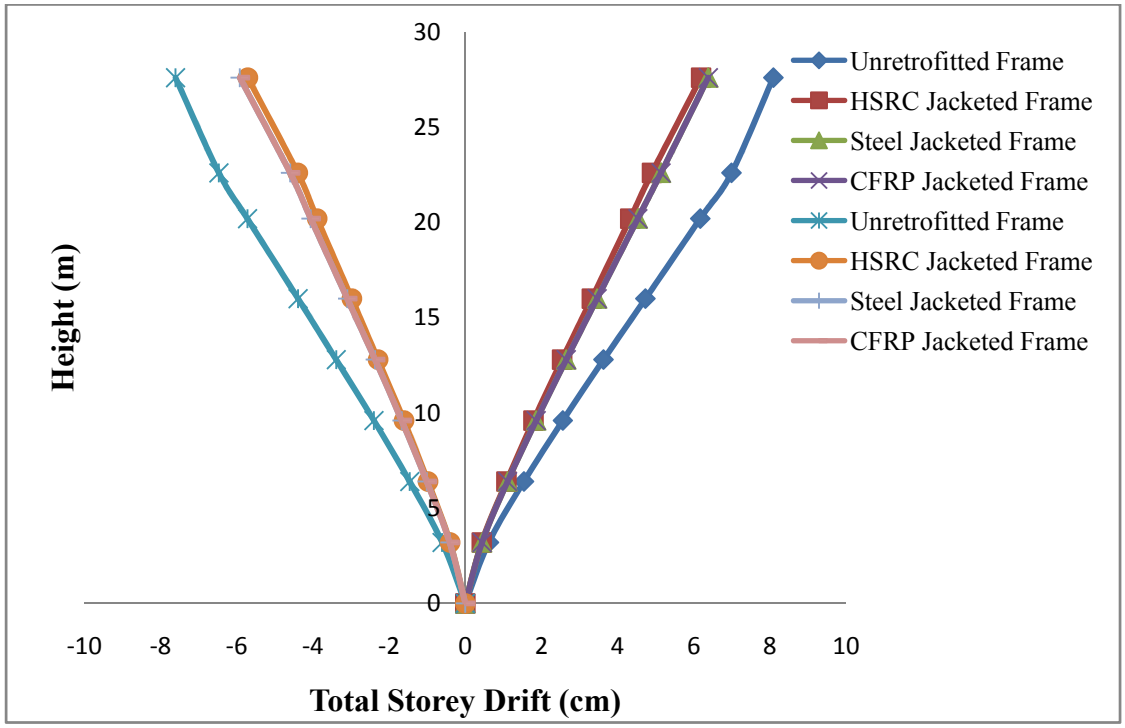

Figure 6.40: Total Storey drift of existing and retrofitted frame model with shell element approach at demand displacement

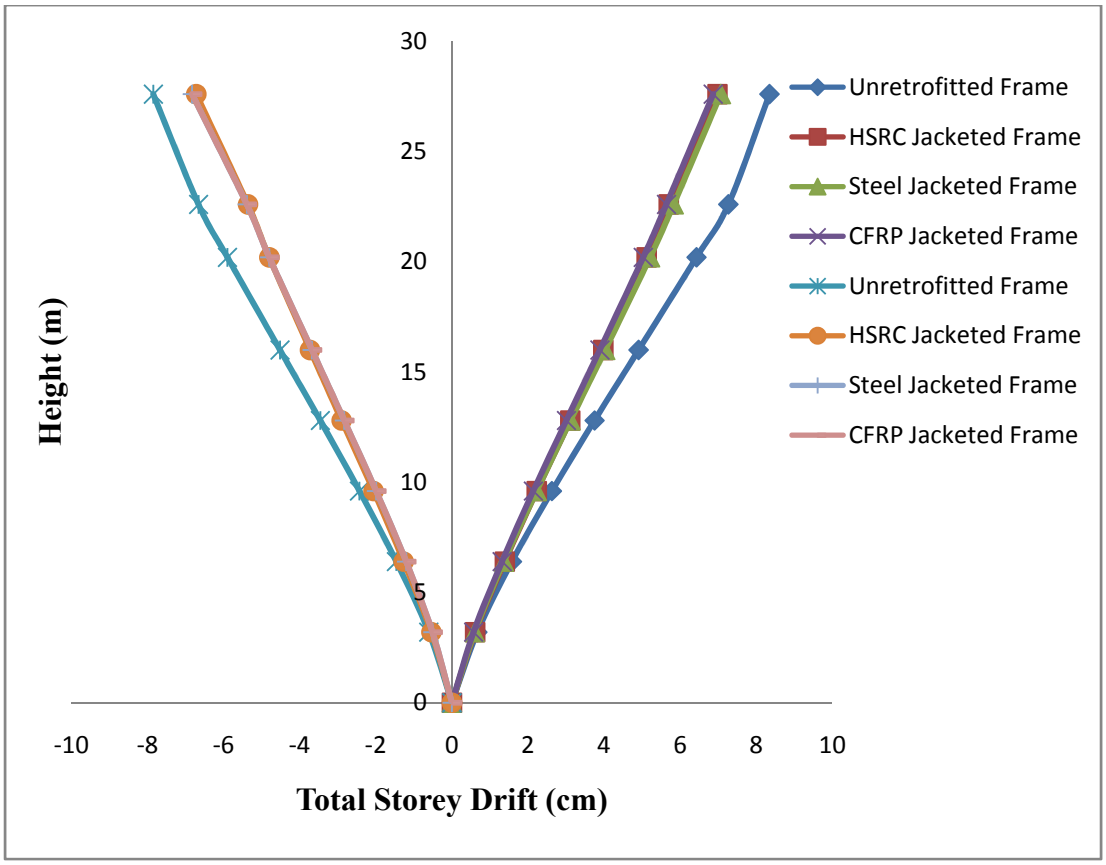

Figure 6.41: Total Storey drift of existing and retrofitted frame model with shell mid-pier approach at demand displacement

CHAPTER 7

CONCLUSIONS AND RECOMMENDATIONS

7.1 Conclusions

In this study, a nonlinear static analysis of a typical existing frame in a eight-storey reinforced concrete building with shear wall was carried out before and after retrofitting the columns with different retrofitting schemes and by increasing the length of existing shear walls using high strength concrete. Retrofitting of the existing frame is done based on the demand displacement of the existing frame obtained from Applied Technology Council (ATC-40) Response Spectra for Zone 2B as per UBC 1997. The seismic displacement response of the existing and the retrofitted frame are obtained using the method of pushover analysis. In addition two approaches are utilized to model shear walls i.e. shell element approach and mid-pier approach. Comparisons of both the approaches were also done. Based on this study following conclusions are made.

1. Pushover analysis of existing frame of Madinah building showed the building is deficient to resist seismic loading. From the pushover analysis of existing frame it is clear that at performance point the shear walls are failing due to crushing of concrete and hinges are formed in top storey columns.

2. Hinges formation clearly shows that the members of building are designed purely for gravity loads as with the small increment of displacement most of the members start yielding.

3. The hinge status of Shell Element and Mid Pier method at maximum displacement provide almost the same pattern. Mid Pier method overestimate base shear because of rigid beam rigidity, so appropriate rigidity must be selected.

4. Retrofitting of existing shear wall frame by the extension of shear walls using high strength concrete and jacketing of the columns with different retrofitting schemes result in significant increase in lateral load capacity of the frame.

5. No flexural hinges are found in top storey columns which were originally failing at demand displacement calculated based on ATC-40 response spectra for different damping ratio.

6. After strengthening there is no crushing of concrete and yielding of steel observed at the base of shear wall model with shell element approach whereas Mid-pier approach indicates the hinge formation at the base of shear walls.

7. Inter-storey drift ratio and total storey drift of the retrofitted shear wall frame is significantly reduced decreasing the seismic vulnerability.

8. The accuracy of these numerical results is acceptable for everyday design purposes, especially the base shear capacity, roof drift and inter-storey drifts of the building. Several international seismic codes and guidelines concerned with performance-based seismic engineering have recently implemented pushover

techniques as practical alternative for nonlinear time-history analysis. On the other hand, the current Saudi Building Code of practice related to earthquake-resistant design incorporate almost none of these modern techniques. Thus, the present study supports the implementation of performance-based concepts in future editions of the local seismic codes by demonstrating the application of the recent pushover techniques for evaluating the performance of multistory buildings due to seismic actions.

7.2 Recommendations for Future Research

The following recommendations can be made for further research in this area.

1. Future research can be carried out on 3-D model of Madinah Building by the application of Pushover and time history analysis.
2. Inclusion of effects of higher modes in multi-storey buildings.
3. Incorporation of torsion effects for unsymmetrical buildings.

References

[1]. Krawinkler, H. and Seneviratna G. D. P. K., "Pros and Cons of a Pushover Analysis of Seismic Performance Evaluation", *J. of Engineering Structures,* 1998.

[2] FEMA, NEHRP, "Improvement of Nonlinear Static Seismic Analysis Procedures (FEMA-440)", *Department of Homeland Security, Federal Emergency Management Agency,* Redwood City, CA. 2005.

[3] FEMA, NEHRP, "Pre-standard and Commentary for the Seismic Rehabilitation of Buildings (FEMA-356*)", American Society of Civil Engineers (ASCE):* Reston, VA., 2000.

[4] ATC, "Evaluation and Improvement of Inelastic Seismic Analysis Procedures (ATC-55)", *Applied Technology Council:* Redwood City, CA. 2001.

[5]. ATC, "Seismic Evaluation and Retrofit of Concrete Buildings (ATC-40)". *Applied Technology* Council: Redwood City, CA.1997.

[6] Elnashai, A.S., "Advanced Inelastic Static (Pushover) Analysis for Earthquake Applications", *J. of Structural Engineering and Mechanics*, 2001.

[7] Kalkan, E. and Kunnath, S.K., "Method of Modal Combinations for Pushover Analysis of Buildings"*, 13th World Conference on Earthquake Engineering*, Vancouver, B.C., Canada, 2004.

[8] Antoniou, S. and Pinho, R., "Advantages and Limitations of Adaptive and Non-adaptive Force-Based Pushover Procedure", *J. of Earthquake Engineering*, 2004.

[9] Menjivar, M.A.L. 3D,"Pushover of Irregular Reinforced Concrete Building", *Master Thesis,* Rose School, Italy. 2003.

[10] Menjivar, M.A.L.,"A Review of Existing Pushover Methods for 2D Reinforced Concrete Building", *PhD Thesis,* Rose School, Italy. 2004.

[11] Barros, R.C. and Almeida, R., "Pushover Analysis of Asymmetric Three-Dimensional Building Frames"*,J. of Civil Engineering and Management,* 2005.

[12] Aschheim, M. Tjhin, T. and Hernandez-Montes E., "Observations on the Reliability of Alternative Multiple-Mode Pushover Analysis Methods ", *J. of Structural Engineering*, 2006.

[13] Park, H.G., Eom, T. and Lee, H., "Factored Modal Combination for Evaluation of Earthquake Load Profiles" , *Journal of Structural Engineering,* 2007.

[14] R. Rana, L.Jin and A. Zekioglu, "Pushover Analysis of a 19 Story Concrete Shear Wall Building", *13th World Conference on Earthquake Engineering*, Canada, 2004.

[15] C. Goksu, C. Demir, K. Darilmaz ,A. Ilki and N. Kumbasar, " Static Nonlinear Analysis of a Retrofitted Typical Reinforced Concrete Building in Turkey", *8th U.S. National Conference on Earthquake Engineering*, California, USA,2006.

[16] R. Pinho,R. Bento and C. Bhatt, "Assessing the 3D Irregular Spear Building with Nonlinear Static Procedures", *14th World Conference on Earthquake Engineering*, Beijing, China, 2008.

[17] Y.M. Fahjan ,J. Kubin and M. T. Tan, "Nonlinear Analysis Methods for reinforced Concrete Building with Shear walls",*14th European Conference on Earthquake Engineering ,*Ohrid, Republic of Macedonia,2010.

[18] ACI 440.2R-08, "Guide for the Design and Construction of Externally Bonded FRP Systems for Strengthening Concrete Structures", *American Concrete Institute, USA,* 2008.

[19] CSI SAP2000,"Static and Dynamic Finite Element Analysis of Structures V14.0", *Computers and Structures, Inc*., Berkeley, California, 2009.

[20] XTRACT, "Cross Section Analysis Program for Structural Engineers", *IMBSEN & Associates Inc***.**, USA, 2007.

[21] J.B Mander, M.J.N Priestley and R Park, "Theoretical Stress–Strain Model for Confined Concrete", *Journal of the Structural,* ASCE, 1988.

[22] L. Lam and J.G. Teng, "Design-oriented Stress-Strain Model for FRP-confined Concrete", *Construction and Building Materials,* 2003.

[23] SBC 301, "Saudi Building Code for Load and Forces Requirements", SBC-301,Saudi Arabia, 2007

[23] Guner, S., and Vecchio, F. J., "Pushover Analysis of Shear-Critical Frames: Formulation," *ACI Structural Journal*, 2010.

[24] ASCE 41-06, "Seismic Rehabilitation of Existing Buildings, *American Society of Civil Engineers (ASCE)*, USA, 2006.

[25] Miao ZW, Lu XZ, Jiang JJ and Ye LP, "Nonlinear FE Model for RC Shear Walls Based on Multi-layer Shell Element and Micro plane Constitutive Model", *Computational Methods in Engineering and Science*, EPMESC X, China, 2006.

[26] Dorninger K and Rammerstorfer FG, "A Layered Composite Shell Element for Elastic and Thermo-elastic Stress and Stability Analysis at Large Deformations", *International Journal for Numerical Methods in Engineering*,1990.

[27] Barros, R.C. and Almeida, R., "Pushover Analysis of Asymmetric Three-Dimensional Building Frames", *J. of Civil Engineering and Management,* 2005.

[28] Bracci, J.M., Reinhorn, A.M. and Mander, J.B., "Seismic Resistance of Reinforced Concrete Frame Structures Designed for Gravity Loads Performance of Structural System", *Structural J.,* 1995.

[29] Chandler, A.M. and Lam, N.T.K., "Performance-Based Design in Earthquake Engineering: a Multidisciplinary Review", *J. of Engineering Structures,* 2001.

[30] Chopra, A.K. and Goel, R.K.,"A Modal Pushover Analysis Procedure to Estimate Seismic Demands for Buildings Theory and Preliminary Evaluation", *Pacific Earthquake Engineering Research Center,* California, USA,2001.

[31] Fajfar, P.,"A Nonlinear Analysis Method for Performance Based Seismic Design", *J. of Earthquake Spectra*,2000.

[32] Ghobarah, A., "Review Article; Performance Based Design in Earthquake Engineering State of Development", *J. of Engineering Structures*, 2001.

[33] Habibullah, A. and Pyle, S., "Practical Three Dimensional Nonlinear Static Pushover Analysis". *Structure Magazine Berkley,* California, USA, 1998.

[34] Hajirasouliha, I. and Moghaddam, H., "Toward More Rational Criteria for Determination of Design Earthquake Forces", *J. of Solids and Structures* 2006.

[35] Kalkan, E. and Kunnath, S.K., "Method of Modal Combinations for Pushover Analysis of Buildings"*, 13th World Conference on Earthquake Engineering*, Canada, 2004.

[36] Kunnath, S.K. and Kalkan, E., "Evaluation Of Seismic Deformation Demands Using Nonlinear Procedures in Multistory Steel and Concrete Moment Frame", *National Science Foundation,* California, USA, 2005.

[37] Moghaddam, A.S. and Tso W.K., "3-D pushover analysis for damage assessment of buildings", *J. of Seismology and Earthquake Engineering,* 2000.

[38] Papanikolaou, V. S., Elnashai, A.S. and Pareja J. F., Limits of Applicability of Conventional and Adaptive Pushover Analysis for Seismic Response Assessment. *Mid-America Earthquake Center,*USA,2005

[39] Turker, K. and Irtem, E., "An Effective Load Increment Method for Multi Modal Adaptive Pushover Analysis of Buildings", *J. of Structural Engineering and Mechanics,*2007.

[40]. Zou, X. "Optimal Seismic Performance-Based Design of Reinforced Concrete Buildings", *PhD Thesis, Hong Kong University of Science and Technology,* Hong Kong,2002.

[41] E.YesimKarci, " Seismic Performance Evaluation of Dual Reinforced Concrete Systems Design According to Turkish Seismic Code, *Master Thesis, Bogazici University*, Turkey, 2007

[42] BahadirAkgul, " Comparison of Linear and Nonlinear Methods for Seismic Evaluation of Existing Reinforced Concrete Buildings in the Turkish Earthquake Code 2007", *Master Thesis, Bogazici University*, Turkey, 2007.

[43] A.E Toprak, "Code-Based Evaluation of Seismic Performance Levels of Reinforced Concrete Buildings with Linear and Non-linear Approaches", *Master Thesis, Istanbul Technical University*, Turkey, 2008.

APPENDIX

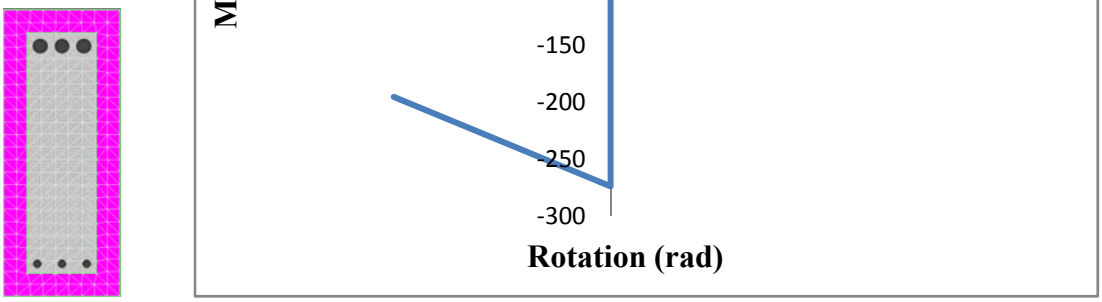

Figure A.1: Beam K5 cross-sectional detail and Bilinear Moment Rotation curve for beam K5

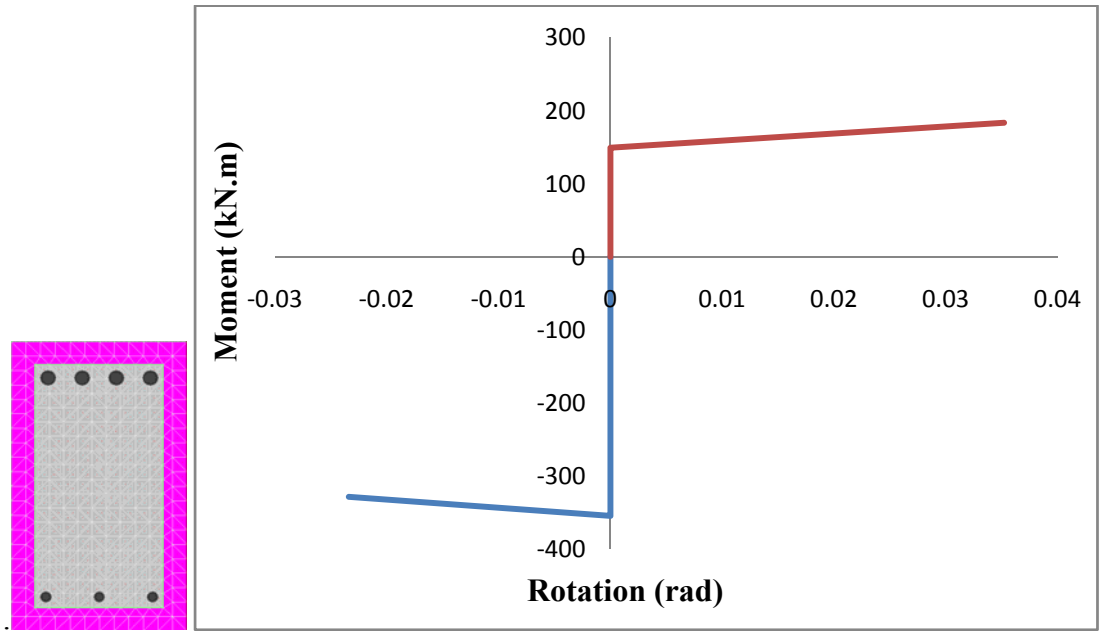

Figure A.2: Beam K9 cross-sectional detail and Bilinear Moment Rotation curve for beam K9

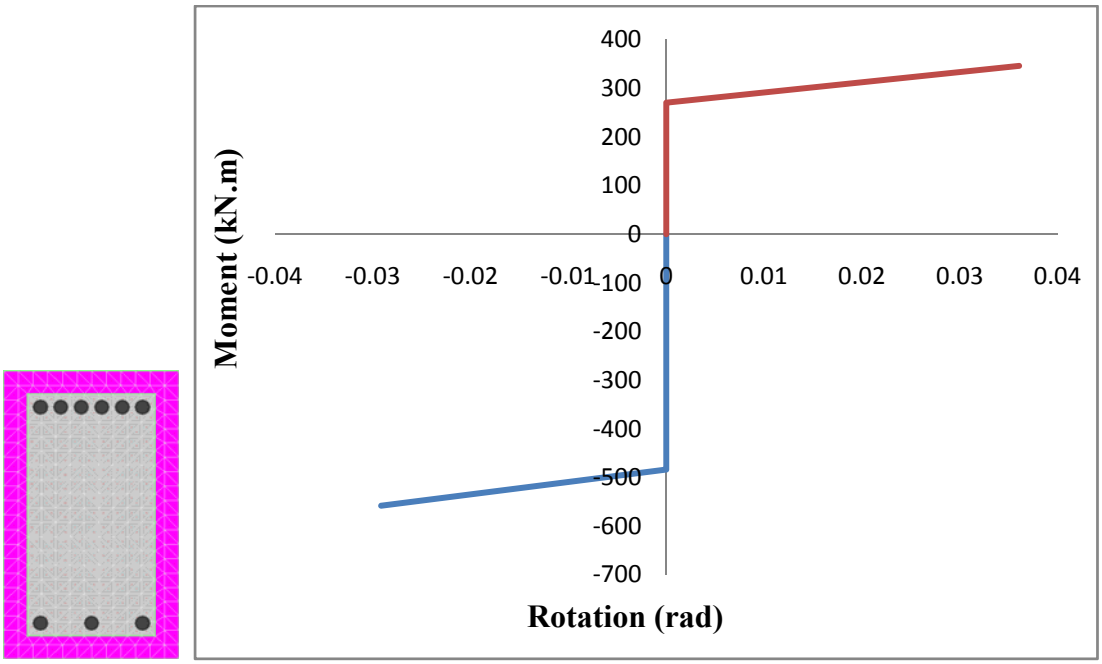

Figure A.3: Beam K10 cross-sectional detail and Bilinear Moment Rotation curve for beam K10 for left support

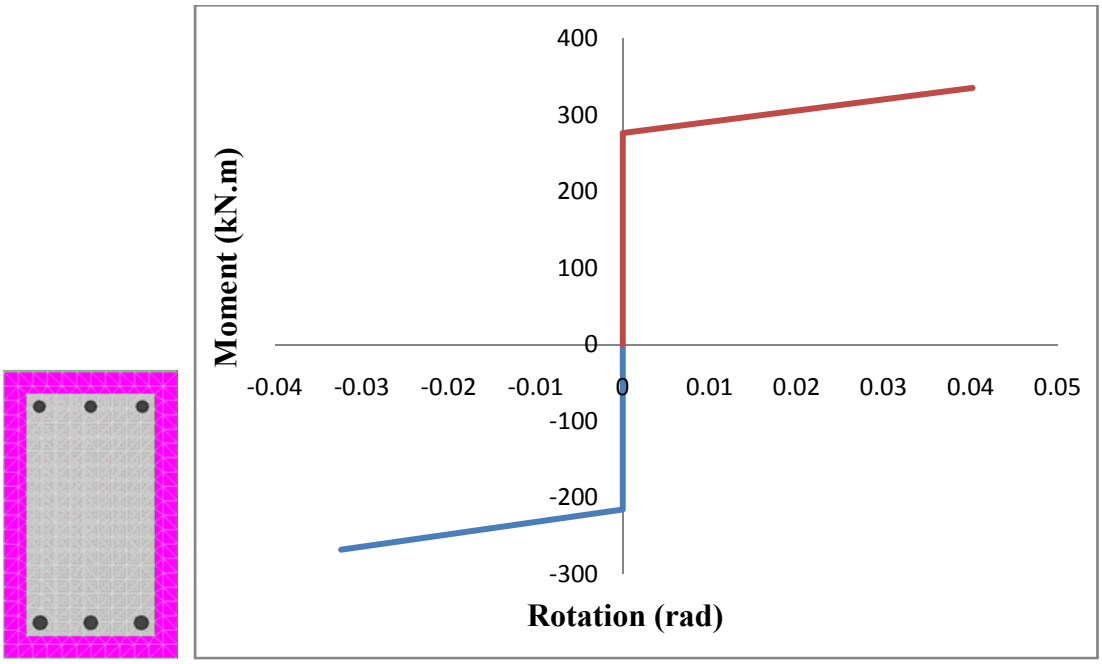

Figure A.4: Beam K10 cross-sectional detail and Bilinear Moment Rotation curve for beam K10 for Right support

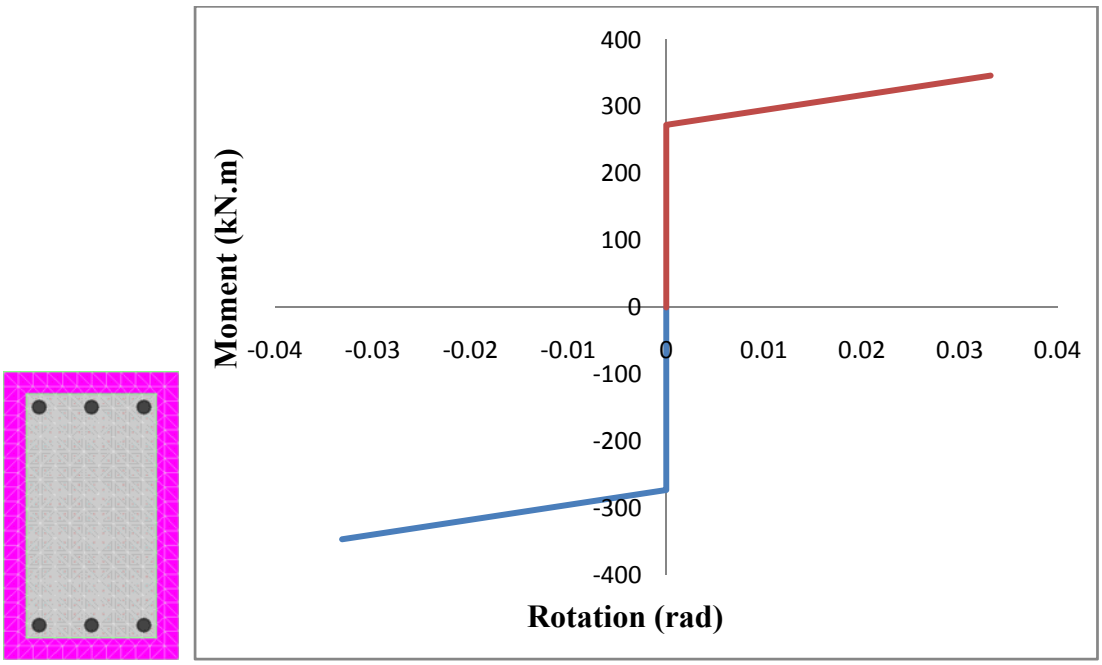

Figure A.5: Beam K11 cross-sectional detail and Bilinear Moment Rotation curve for beam K11 for left support

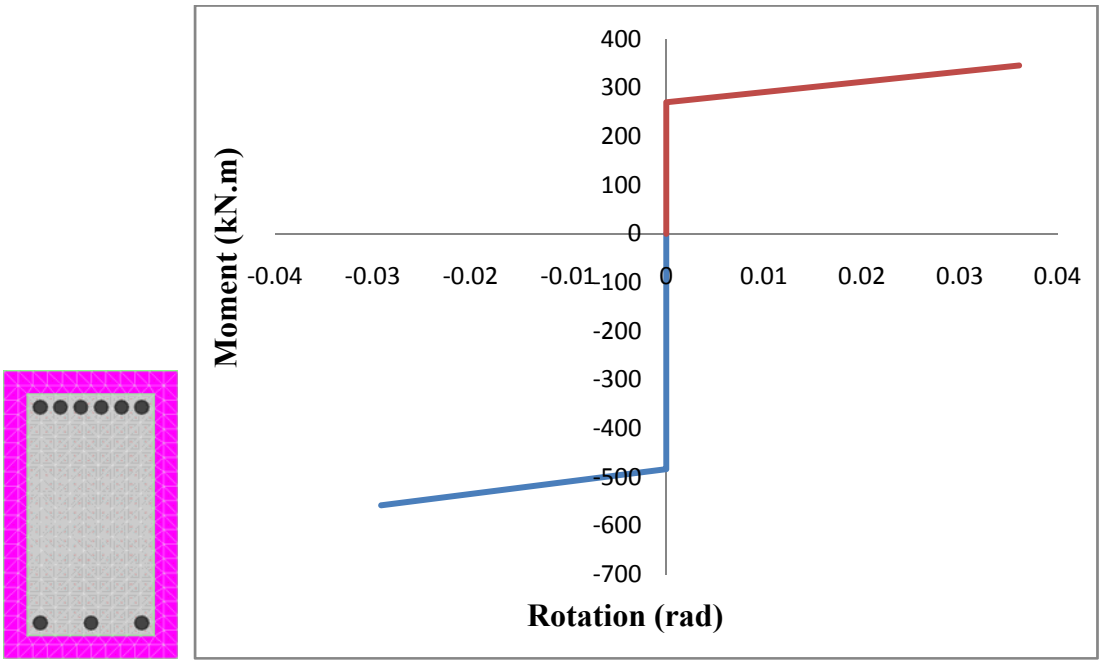

Figure A.6: Beam K11 cross-sectional detail and Bilinear Moment Rotation curve for beam K11 for right support

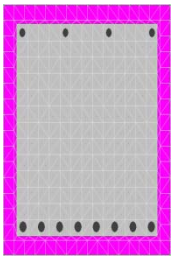

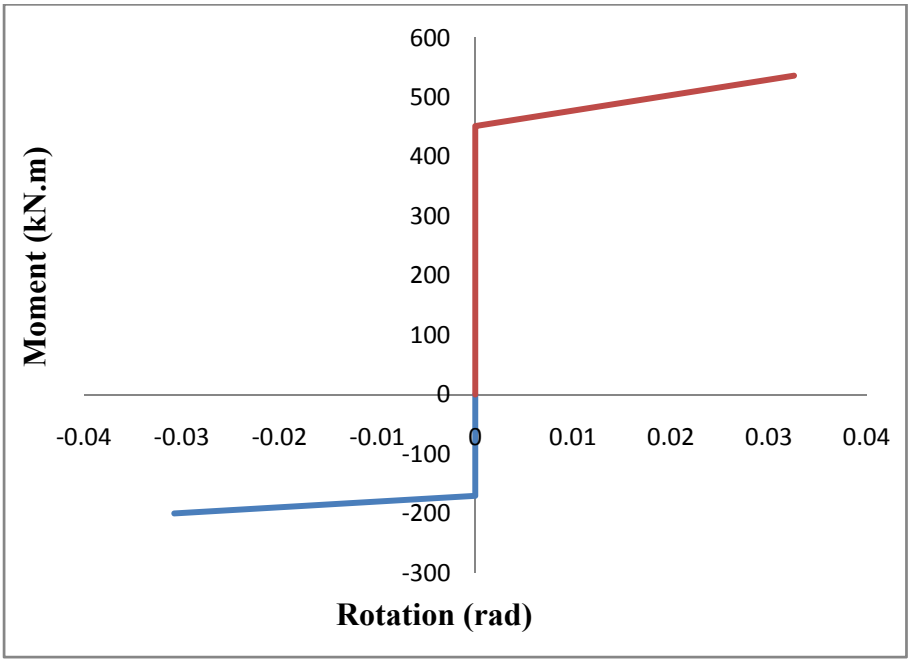

Figure A.7: Beam K16 cross-sectional detail and Bilinear Moment Rotation curve for beam K16

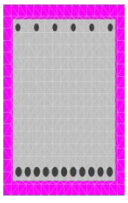

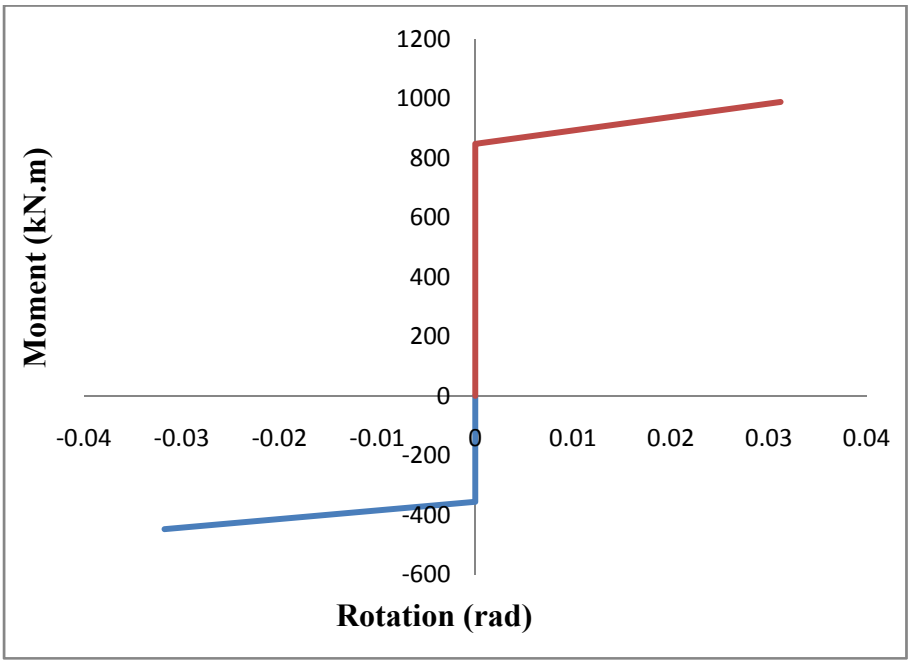

Figure A.8: Beam K17 cross-sectional detail and Bilinear Moment Rotation curve for beam K17

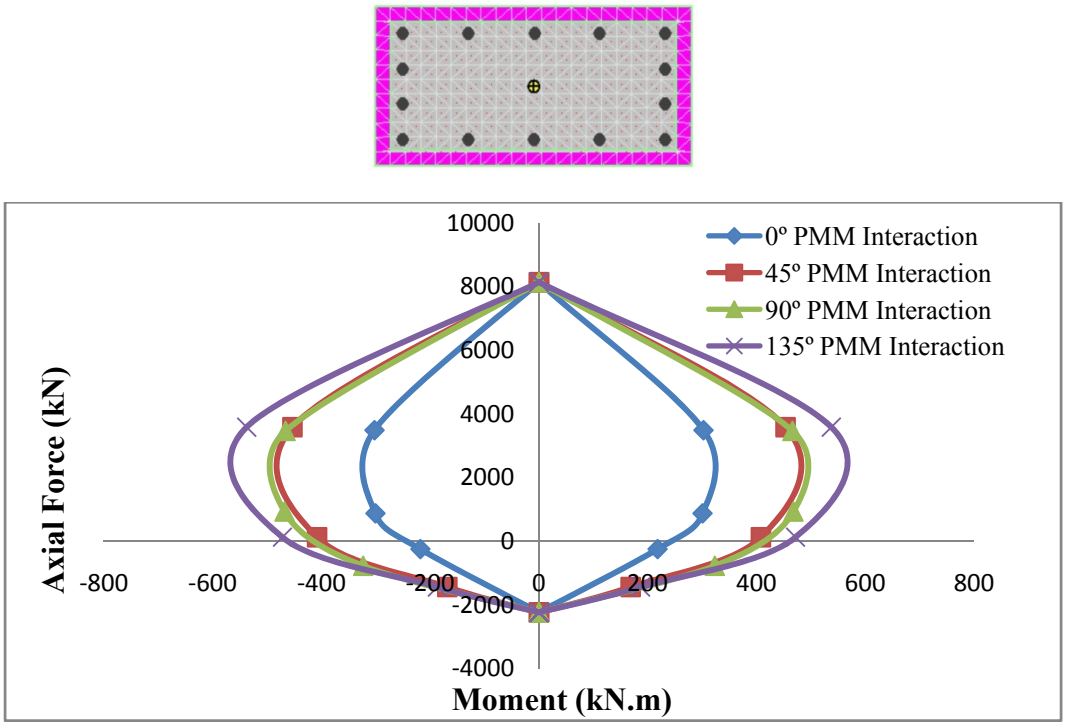

Figure A.9: Column 1A11 cross-sectional detail and PMM interaction diagram

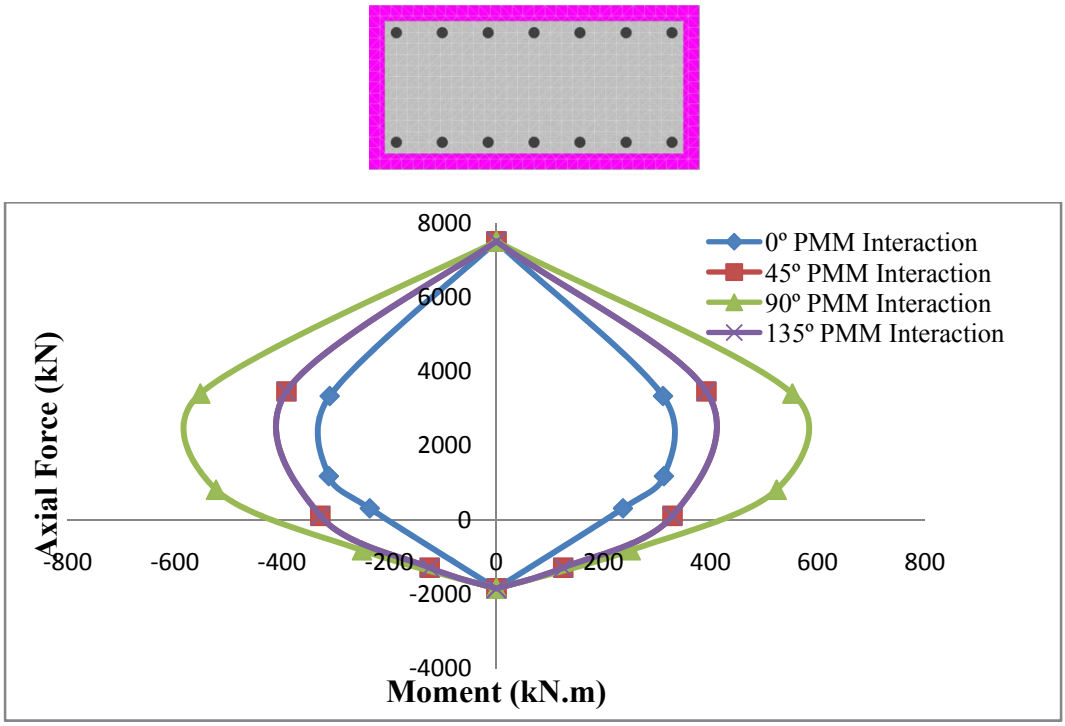

Figure A.10: Columns 2A11 and 3A11 cross-sectional detail and PMM interaction diagram

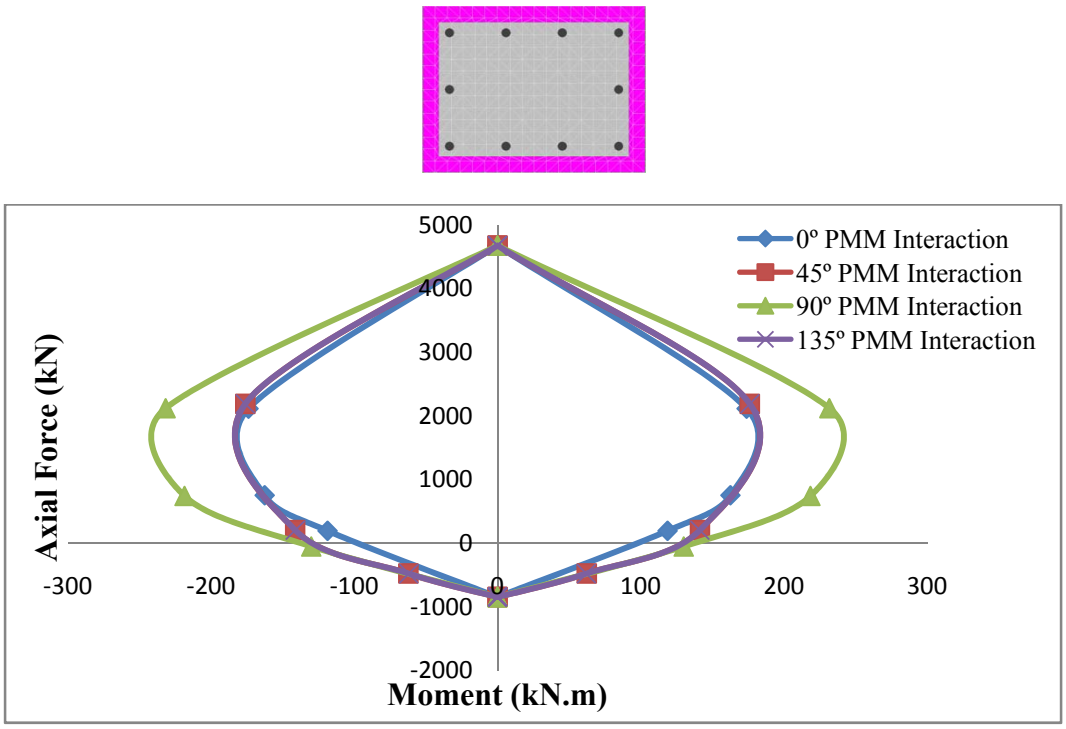

Figure A.11: Column 4A11 cross-sectional detail and PMM interaction diagram

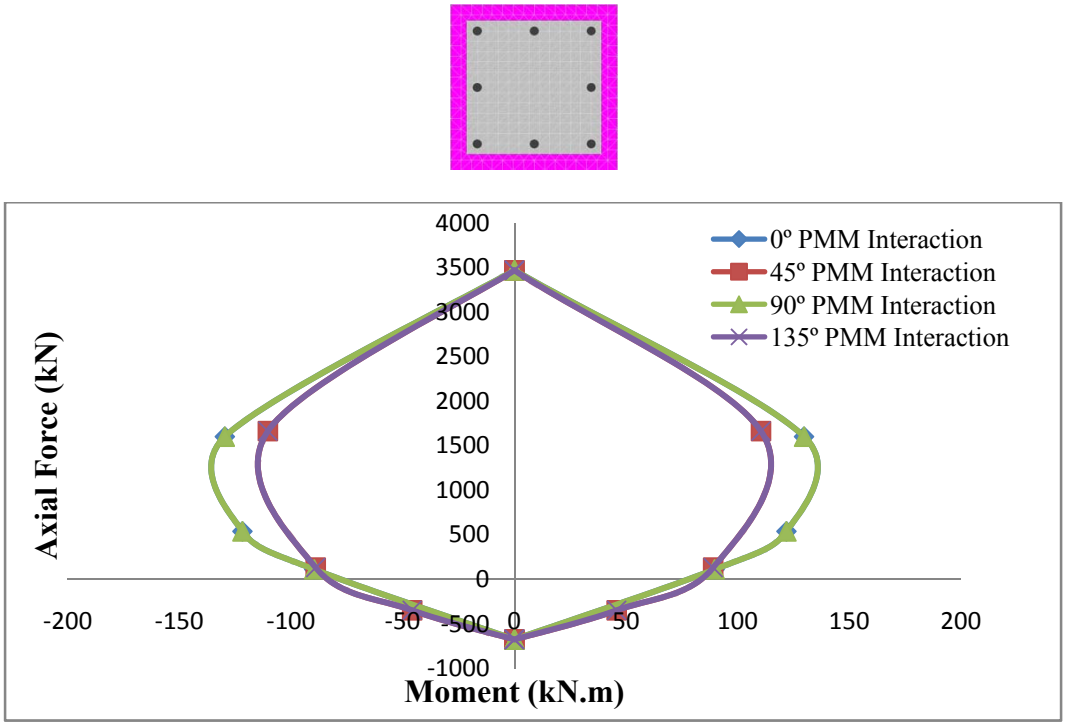

Figure A.12: Columns 5A11, 6A11 and 7A11 cross-sectional detail and PMM interaction diagram

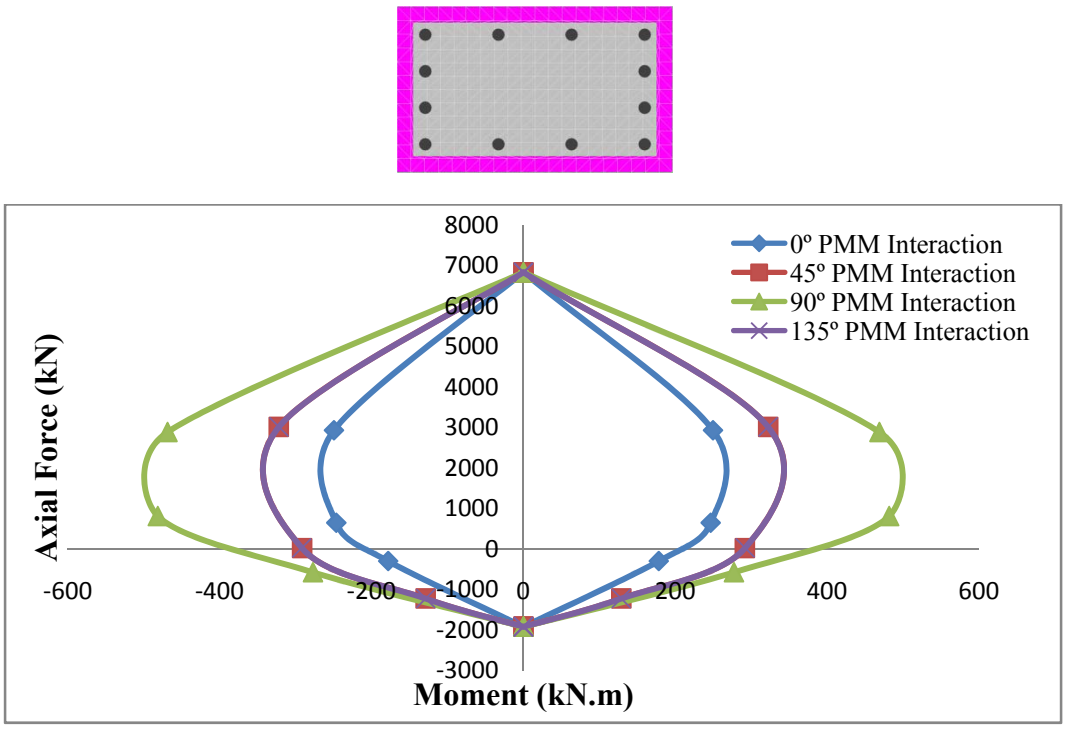

Figure A.13: Columns 2A13 and 3A13 cross-sectional detail and PMM interaction diagram

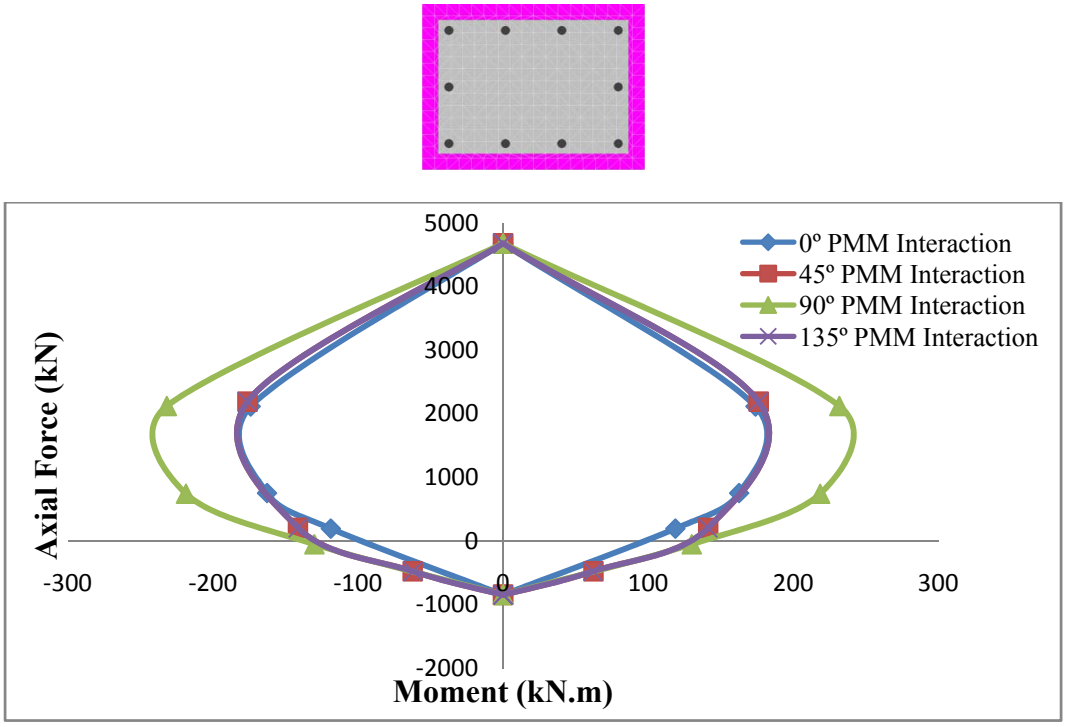

Figure A.14: Column 4A13 cross-sectional detail and PMM interaction diagram

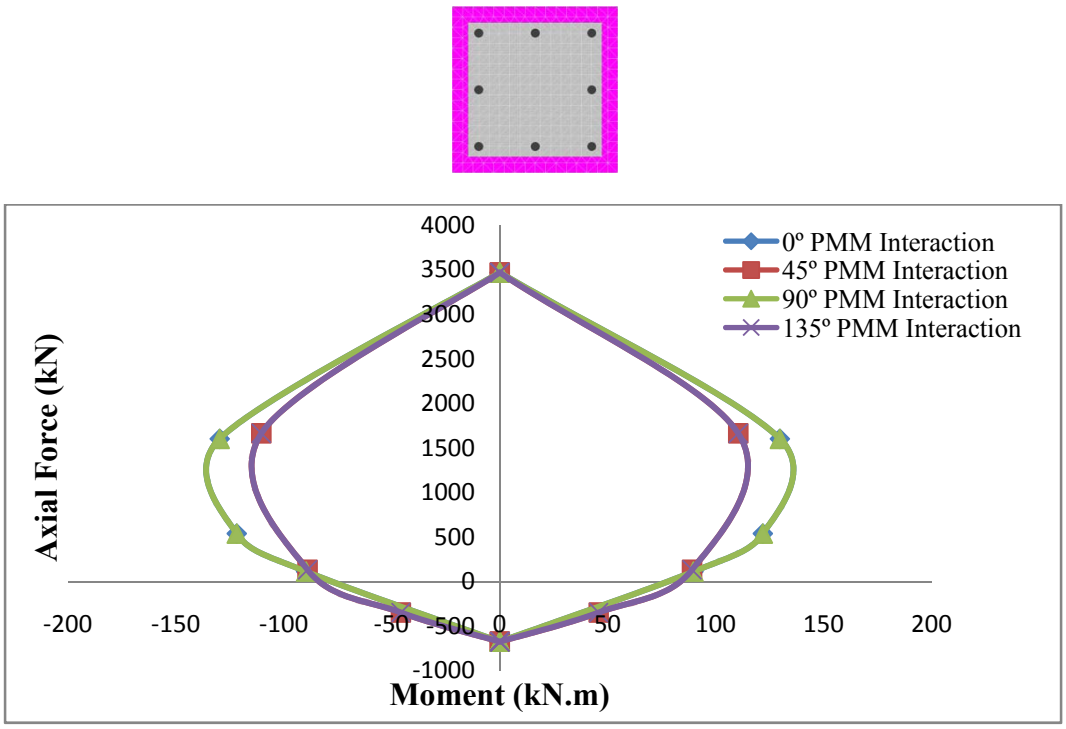

Figure A.15: Columns 5A13, 6A13, 7A13 and 8A13 cross-sectional detail and PMM interaction diagram

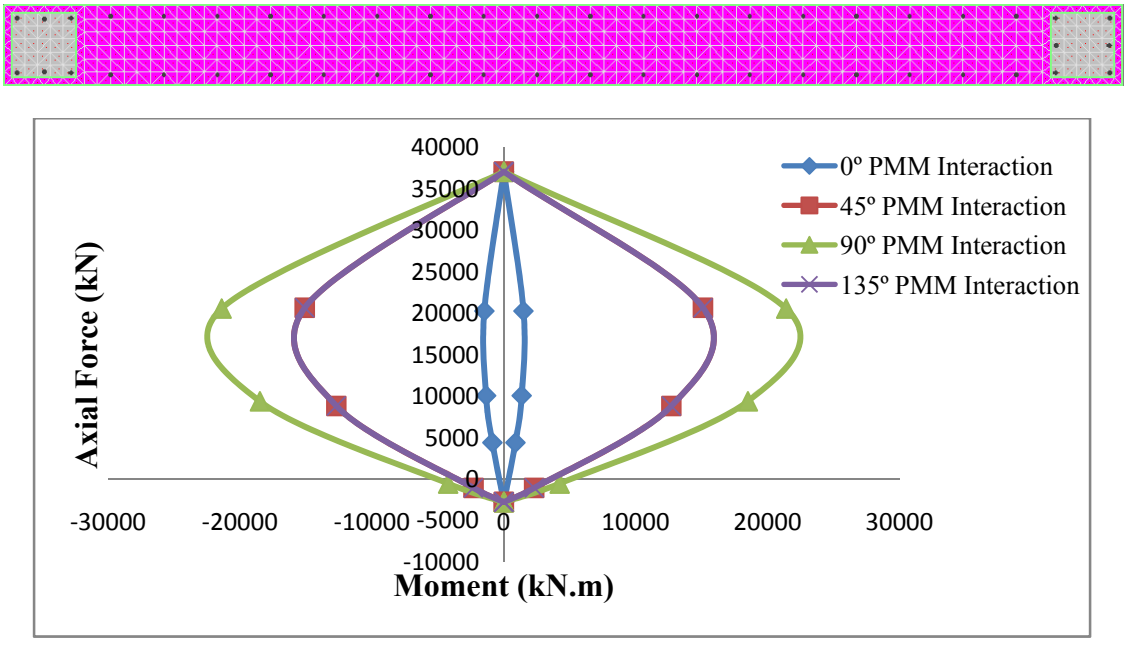

Figure A.16: Shear wall SW300 cross-sectional detail and PMM interaction diagram

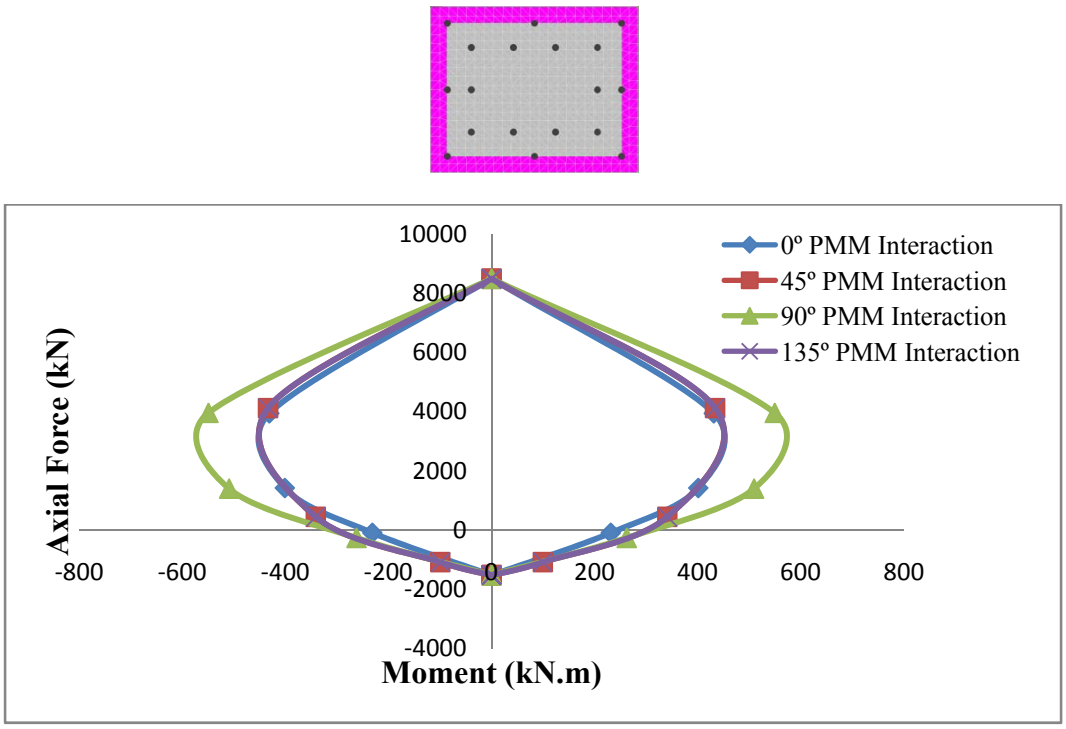

Figure A.17: Columns 4A11 cross-sectional detail Strengthened with HSRC and PMM interaction diagram

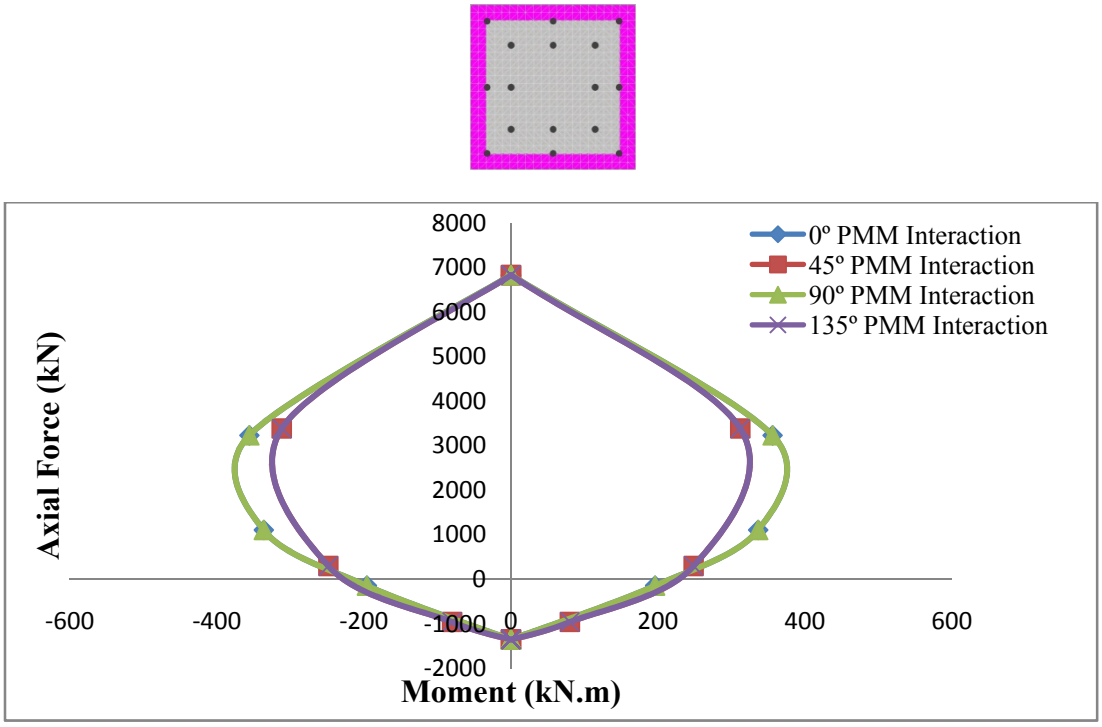

Figure A.18: Columns 5A11 cross-sectional detail Strengthened with HSRC and PMM interaction diagram

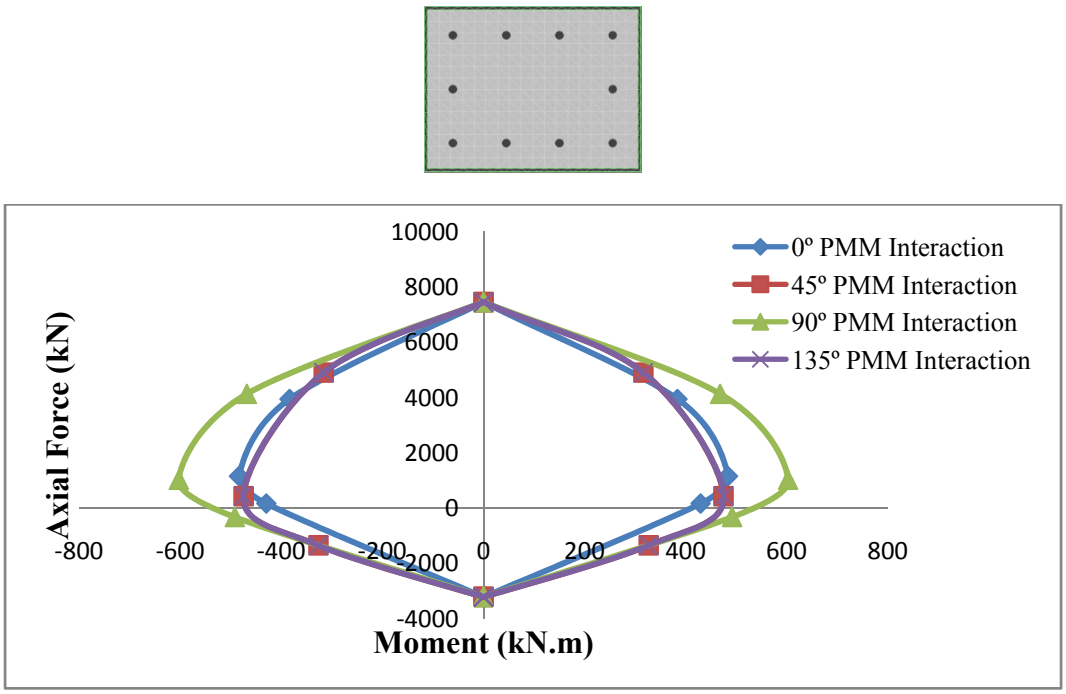

Figure A.19: Columns 4A11 cross-sectional detail Strengthened with Steel jacketing and PMM interaction diagram

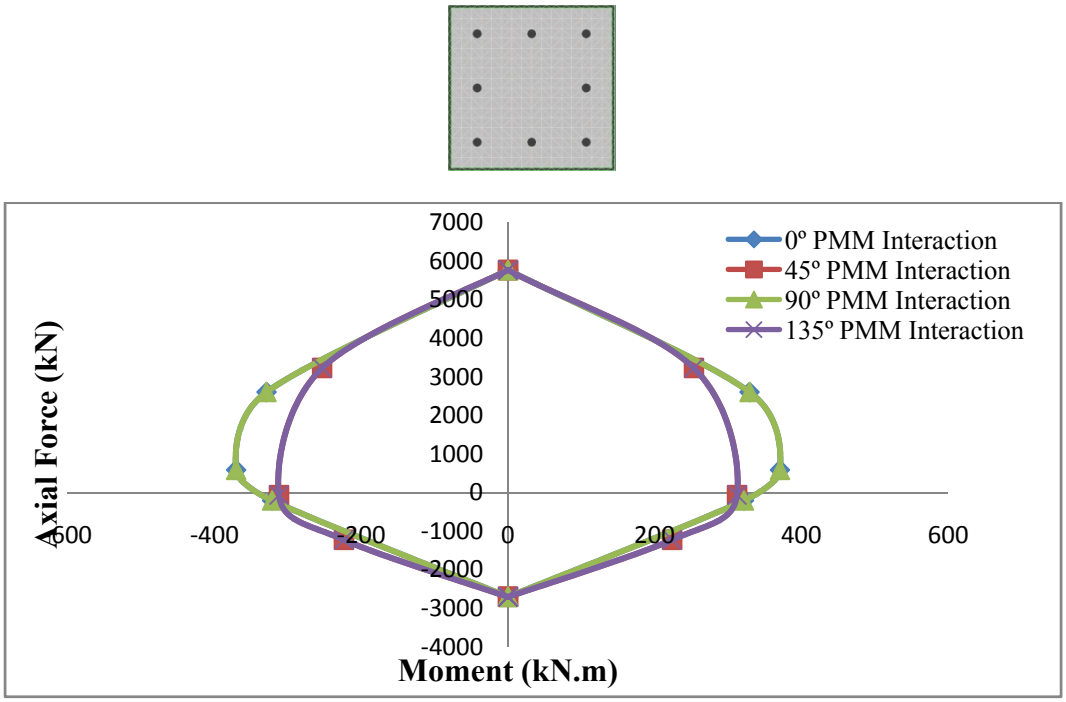

Figure A.20: Columns 5A11 cross-sectional detail Strengthened with Steel Jacketing and PMM interaction diagram

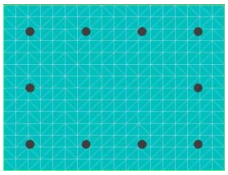

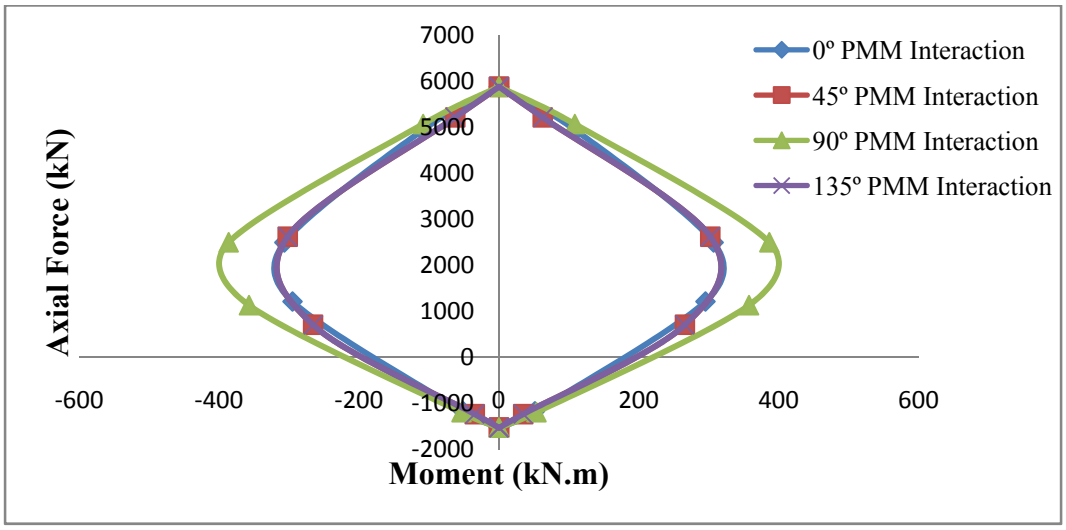

Figure A.21: Columns 4A11 cross-sectional detail Strengthened with CFRP and PMM interaction diagram

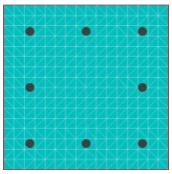

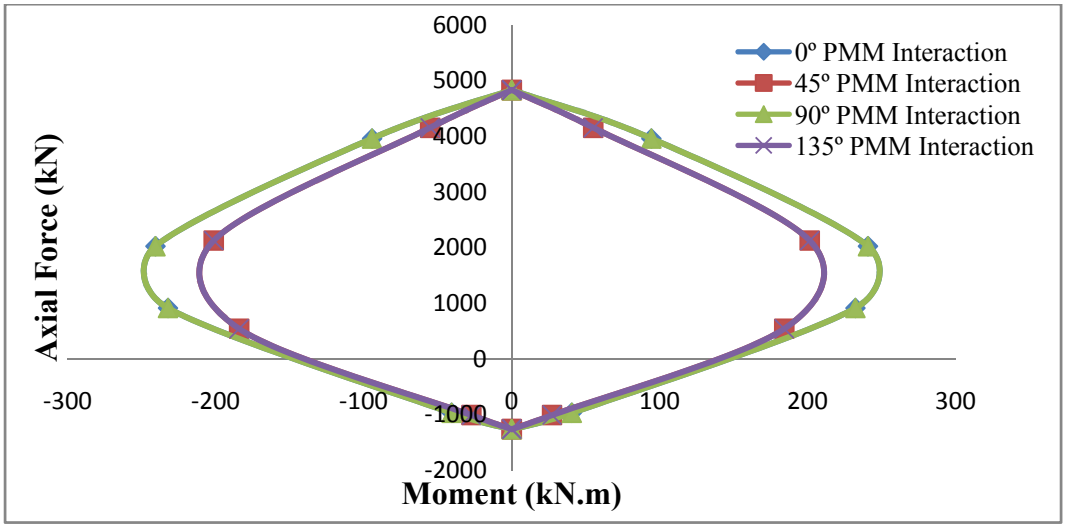

Figure A.22: Columns 5A11 cross-sectional detail Strengthened with CFRP and PMM interaction diagram

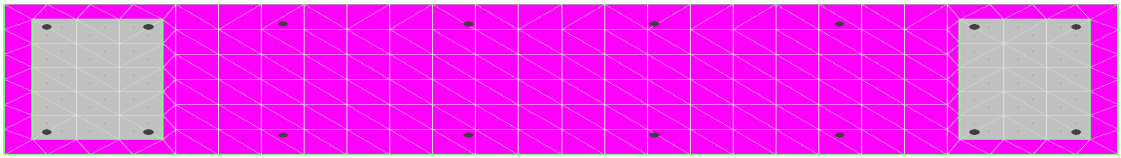

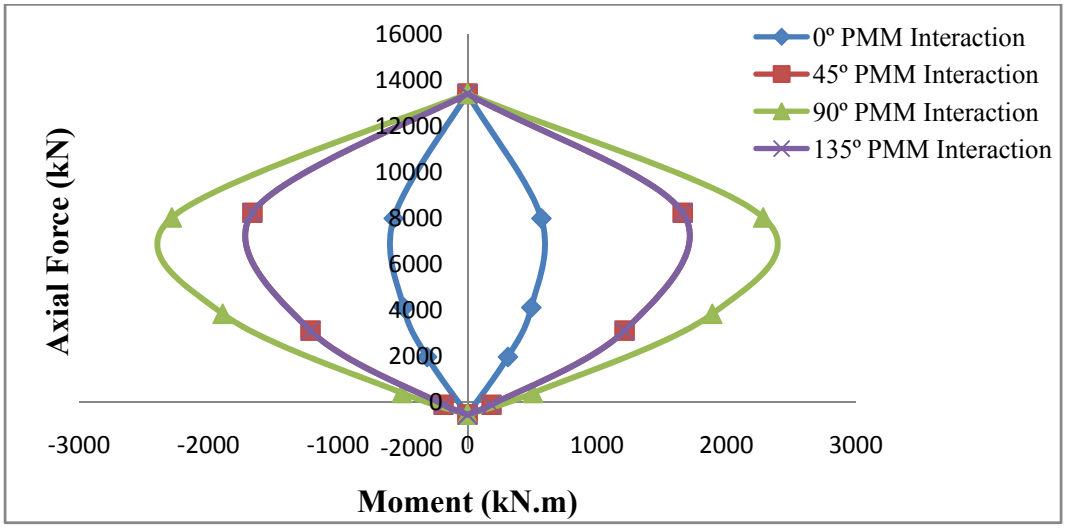

Figure A.23: New High strength Reinforced Concrete shear wall SW300 cross-sectional detail and PMM interaction diagram

Vitae

Name	: Muhammad Ajmal
Nationality	: Pakistani
Date of Birth	: 06/06/1985
Email	: majmal11@hotmail.com
Current Address	: P. O. Box 172, 31411 Dammam Saudi Arabia.
Address	: HNo.8 St. # 2-A Fateh Garh Near Ghani Steel Mill Mughal Pura Lahore, Pakistan.
Academic Background	: Bachelor of Engineering Science, Major Civil Engineering, University Engineering and Technology Lahore, Pakistan, 2009.
	: Master of Science, Major Structural Engineering, King Fahd University of Petroleum & Minerals, Dhahran, Saudi Arabia, 2012.